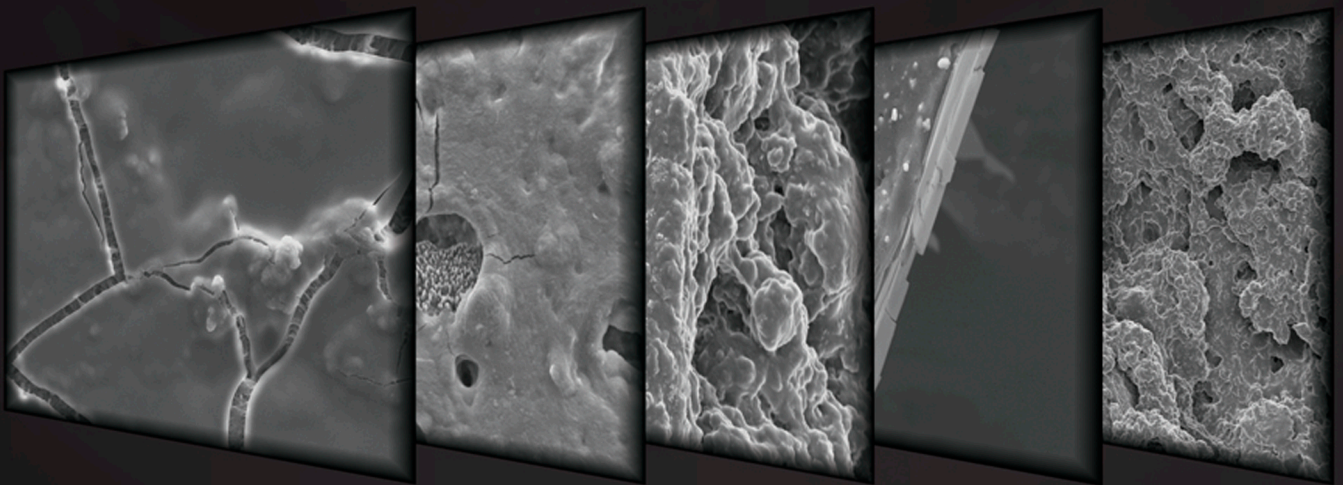


Tribology and sensory attributes of food dispersions



Agnieszka Chojnicka-Paszun

Tribology and sensory attributes of food dispersions

Agnieszka Chojnicka-Paszun



Universiteit Utrecht

ISBN: 978-90-393-5124-6

Cover: Front cover: background- adjusted tribometer for soft contacts; images- Electron Microscopy of the silicone and neoprene rubbers with dried protein aggregate dispersions (experiments done with Hans Meeldijk at Utrecht University, Faculty of Science, Department of Biology, Molecular Cell, Biology Group).

Back cover: commercial tribometer for steel contact.

Design: Dominik Paszun and Tomasz Chojnicki.

Tribology and sensory attributes of food dispersions

Tribologie en sensorische eigenschappen van voedseldispersies

(met een samenvatting in het Nederlands)

Proefschrift

ter verkrijging van de graad van doctor aan de
Universiteit Utrecht op gezag van de rector magnificus,
prof.dr. J.C. Stoof, ingevolge het besluit van het
college voor promoties in het openbaar te verdedigen
op woensdag 16 september 2009 des middags te 4.15
uur

door

Agnieszka Chojnicka-Paszun

geboren op 24 januari 1979
te *Poznań, Polen*

Promotor: Prof.dr. C.G. de Kruif

Co-promotor: Dr. H.H.J. de Jongh

This thesis was accomplished as part of a multidisciplinary research project in TI Food and Nutrition (formerly known as Wageningen Centre for Food Sciences).

To my Family

Table of contents

	Page
Chapter 1 Introduction	1
Chapter 2 Lubrication properties of protein aggregate dispersions in a soft contact	19
Chapter 3 The interactions between oil droplets and gel matrix affect the lubrication properties of sheared emulsion-filled gels	41
Chapter 4 Lubrication, rheology and adsorption of polysaccharide solutions	65
Chapter 5 Sensorial analysis of polysaccharide-protein gel particle dispersions in relation to lubrication and viscosity properties	93
Chapter 6 Friction properties of oral surface analogs and their interaction with polysaccharide/MCC particle dispersions	127
Chapter 7 Sensory perception and friction coefficient of milk with increasing fat content	153
Chapter 8 Future prospects	179
Chapter 9 Concluding remarks and summary	197
Samenvatting	207
Acknowledgements	213
List of publications	217
Curriculum vitae	219
Overview of completed training activities	221

Abstract

The impact of food industry on societal aspects grows dynamically, thereby posing new challenges for food developers to comply to consumer demands. Consumers expect new and more sophisticated products that are tuned to their very specific needs, like health and life-style. This means that food products must be fully programmable to meet these market demands. The taste, smell, and texture perception of food are the most important properties that influence the consumer's experience. To provide control over these features the physics behind them during oral manipulation and structure breakdown must be understood. Most desirably, the physical properties can be tightly linked to attributes of oral perception.

In this thesis the texture of semi-solid and liquid (model) food is studied using Quantitative Descriptive Analysis (QDA). Despite the quantification of sensory scores, it remains difficult to translate these into food physical characteristics in an absolute mode. For that reason, in parallel a physical study is performed using mainly tribology to provide quantitative description of the mechanical processes in the oral environment. For this purpose the experimental setup is adapted such to mimic oral conditions by employing soft surfaces. Next to more complex commercial products, like milk, the samples studied include aqueous dispersions of protein aggregates or polysaccharides, and emulsion filled gels. These components may contribute to fat-feel in low or no-fat dairy products and provide a major uncertainty in predicting the sensorial restraints of the product.

In this thesis we investigate how various factors influence the friction of above-mentioned systems and how this friction can be understood at a more fundamental level. In addition, the surface effects are studied in detail to determine how sensitive the choice of the oral surface analog is on the friction and what the most important surface properties are that are relevant to better predict sensory attributes. Adhesive properties of different food components are investigated using Surface Plasmon Resonance (SPR) and Quartz Crystal Micro Balance Dissipation (QCMD) methods. They provide detailed insight into film formation on a surface thereby complementing friction measurements.

In this thesis we present an overview of correlations obtained between different sensory attributes and frictional data. We show that oral perception can be translated into physical quantities and better programmed using tribological insights. The best correlations are obtained for physical conditions that resemble most the oral environment, i.e. speed below

50 mm/s, shear rate of about 50 s^{-1} and soft, rough surface. Under these conditions a low friction coefficient correlates well with the creamy perception of the consumer. This finding may contribute to develop healthy foods with a full fat creamy taste. We have shown that also the slippery attribute can be well related to friction. Samples with low friction coefficient can be perceived as soft and velvety, while high friction results in rough texture perception. Some attributes, like filmy or slimy, correlate better with viscosity, as their perception is determined by the bulk properties of a sample rather than interaction with oral surfaces. In a few cases the correlation with friction coefficient could not be established, e.g. for sticky or powdery attributes. The latter one, however, shows a good correlation with particles size if they are present in the solution.

This thesis presents a comprehensive picture of the relation between physical quantities and sensory attributes and provides a step forward towards a better control over oral perception of food.

Key words:

Tribology, rheology, friction, oral surfaces, protein aggregates, polysaccharide, protein and polymer gels, particles, emulsions, sensory perception.

Chapter 1

Introduction

1.1 General introduction

Food has always been and will always be crucial for living. It satisfies the most basic demand for energy of all living organisms. Although food consumption is necessary, food can take different forms (from liquids to elastic semi-solids and hard fracturing solids) and provide various experiences. Over centuries people have learned that food can provide pleasure and they have started to prepare more sophisticated products. In the era of globalization products from all over the world are easily available and the demand for very specific customer-designed food properties has grown more than ever. Nowadays people look for very personalized food that fulfills very specific requirements like taste, energy content, smell, or texture. Providing such fine tuned products is a challenge for the food industry. To face this challenge food must be programmable meaning that all its properties should be fully controllable and adjustable according to consumer preferences. This is extremely difficult, as human senses, mostly located in the oral cavity, are not defined in terms of physical principles or quantities. In addition they are very complex and unique for each individual and they vary with age, lifestyle, saliva production etc. [1,2]. Therefore, to successfully target a product to an end-consumer an in-depth understanding of the interaction of the oral environment with a food is necessary. Physical and chemical properties of oral tissues must be well determined and their dependence on external conditions like age or lifestyle well established. Moreover, human perception must be well understood in this context. In particular we should be able to understand and quantify sensations of taste, smell and texture. To program food properties also the physical mechanisms involved in oral processing of food must be understood. Only then a link between the oral perception and physical quantities can be established.

1.2 The primary target

In this thesis the main focus is on mechanical processing of food, in particular those resembling liquids and semi-solids. Therefore tribology was chosen as tool to provide understanding of physics involved in oral processing and perception of textures.

Although friction in relation to oral perception has been studied before [3-6], the experimental setup was limited as at most only one soft surface was used. Therefore the experimental conditions differed significantly from the oral environment. Moreover, different food models were used, making a more general view on the applicability of the technique less clear. In this thesis we use soft-soft contact (see Section 1.5) and explore a

parameter space describing the oral environment as our target is to relate frictional properties obtained in laboratory experiments to human perception of texture during consumption of food products. The obtained relations can be further applied in programming and customization of end-products.

1.3 Oral environment

Food processing that provides sensorial experience occurs in the oral cavity. Products are processed between different surfaces containing various receptors responsible for perception of taste, and texture. The three main surfaces involved are palate, tongue and teeth, where the latter are used mainly to break down food products. The palate is a relatively smooth and hard surface. It does not have taste receptors and is used mainly to smear the partially processed food over the larger area in the mouth. This can provide better taste experience as the product can reach receptors on the tongue responsible for perception of all different tastes. The tongue is rough and a highly flexible muscular tissue. Figure 1.1 shows which areas of the tongue correspond to different taste recognition.

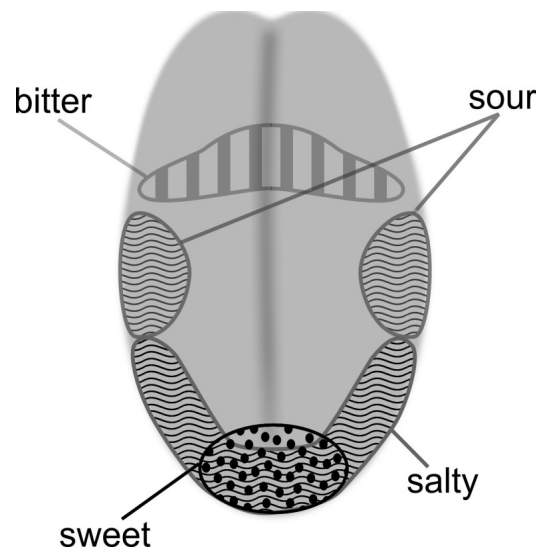


Figure 1.1 Taste receptors on a tongue sensitive to different tastes: sweet, salty, sour and bitter.

Human tongue contains four main types of papillae that differ in size and function [7]. Papillae cover the surface of the tongue and are responsible for the roughness of this surface [8]. The most common are cone-shaped filiform papillae [7] with an approximate size of about 100 μm [8]. They cover almost the entire top surface of the tongue. Although

other papillae (fungi-form, foliate, and circumvallate papillae) are larger, they are far less abundant. These three large papillae are associated with taste buds and are thus believed to be responsible for taste recognition.

The entire oral cavity is covered by a mucus layer that is wetting the surfaces. This layer consists mostly of mucins (glycoproteins) and water, originating from mucin-producing cells and from saliva-depositions [9]. This provides a good lubrication in the oral cavity, as the mucins consists of molecules with a high water binding capacity [10]. Although contact angle measurements of a water droplet on a dry tongue surface disclosed its hydrophobic nature [11], saliva that participates in the lubrication of oral surfaces determines the more hydrophilic character [12-15].

Contact pressure on oral surfaces is rather low, as the tongue under compression is highly deformable. It consists of a complex network of muscles-fibers [16,17]. Their orientation varies within the tongue giving rise to differences in muscular deformability. This results in different elastic moduli depending on the position on the tongue. For instance Pouderoux and Kahrilas [18] showed that the differences in contact pressure depend on the location on the tongue. A contact pressure of about 19 kPa was reported at the anterior part, in the middle it was found to be about 20 kPa and at the posterior area about 11 kPa. A study by Tsuga et al. [19] reveals the differences in pressure during the swallowing of water at the anterior part of the tongue to be 36 kPa and at the posterior to be 24 kPa. Balloon type sensor used by Hayashi et al. [20] demonstrated pressures between 3 and 27 kPa during swallowing.

Next to the contact pressure, another important physical quantity related to mechanical processing is the relative speed that is exerted between the tongue and the palate. Jon Prinz and co-workers (TI Food and Nutrition (TIFN)) developed a method that allows to monitor spatially and to resolve in time the motion of oral surfaces during processing of commercial or model foods. They located a set of sensors inside and outside the mouth of a test-person, who was asked to process different products, varying from liquids to semi-solids. An example of the position of these sensors is shown in Figure 1.2 . The position of the sensors was monitored spatially in three dimensions as a function of time, providing a complete overview of motions involved in the food consumption. Several different types of products were investigated and the speeds involved in processing were shown to be independent on the food sample. Measurements with 5 different testers revealed the

deviation from the mean to be larger than the differences obtained for diverse products (Jon Prinz, personal communication).

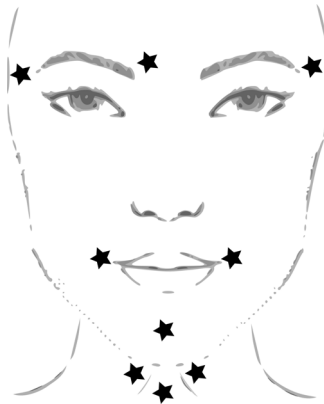


Figure 1.2 Position of motion sensors used to determine speeds of surfaces during oral food processing. Stars indicate location of sensors on a person's face and throat.

The determined speed in the mouth varied between 5 and 60 mm/s depending on several factors like position of a sensor (different surfaces participated differently in the processing) or stage of processing (e.g. different speeds correspond to biting, smearing and swallowing).

During mastication food is processed into smaller particles and it is moved against the palate by the tongue resulting in shear. Therefore shear is considered as another physical parameter that is of importance in the mouth. Many studies have attempted to determine the shear rates that occur between the tongue and the palate. It has been shown that during mastication, the shear rate applied in the mouth varies in between 1 and 1000 s^{-1} depending on the flow behavior of particular food [3]. However, the most common shear rate during oral food processing was determined to be about 50 s^{-1} [21-25].

1.4 Sensorial Evaluation

Before a better control over food properties can be established, sensory perception of products must be defined and quantified. This allows evaluation of consumer experience, which can further be translated into physical quantities. Moreover, the properties that are evaluated must be intuitive and easy to understand for all parties in the supply chain: i.e. the manufacturer, reseller and the end consumer must be able to understand them, which properties are modified and what benefit results from this alterations. Thus sensory

attributes are defined to provide clear and intuitive description of food evaluation experienced during oral processing.

1.4.1 Sensory attributes

The attributes can be classified into several types related to taste/ smell, after-taste, mouth-feel, and after-feel. The first two types are mostly dependent on molecular composition, while the latter two are closely related to physical properties of food processed in the mouth. For this reason our main focus is on mouth-feel and after-feel attributes. An overview of the most important attributes that belong to these two classes is presented in Table 1.1.

Table 1.1 Definitions of different sensory attributes.

Attribute	Type	Description
Thickness	Mouth-feel	Consistency of the product (its density)
Slippery	Mouth-feel	Slippery feeling
Melting	Mouth-feel	Thinning of the product in the mouth
Slimy	Mouth-feel	Thick liquid which stays (in mouth)
Sticky	Mouth-feel	A sticky sensation on palate and between the teeth
Creamy	Mouth-feel	Soft, velvety feeling
Powdery	Mouth-feel	Sensation of particles (powder) in the product
Dry/rough	After-feel	Adsorbing saliva, rough feeling on the tongue and teeth
Film forming	After-feel	Sensation of layer that stays in the mouth after swallowing

The mouth-feel is mostly related to texture perception, and thus related to bulk properties of the product like consistency or lubricity. In the after-feel class the properties of adhesion to the oral cavity (palate or tongue) are highlighted that determine whether the product remains in the mouth or is easily removed during swallowing. Although the relation to physical quantities seems to be straightforward, the attributes indicate strong interrelation with each other (e.g. thickness perception influences perception of other attributes [e.g. 26]).

1.4.2 Evaluation method

Sensory attributes are subjective as they describe oral sensation as experienced by different individuals. Moreover, they reflect human feeling and thus cannot be easily quantified. To overcome these difficulties the score assigned to attributes during

evaluation is expressed in dimensionless units on a scale between 0 and 100 and is relative to a defined reference sample.

The evaluation of products applied in this work is performed by panelists (later also referred to as assessors) trained according to the principles of the Quantitative Descriptive Analysis (QDA) [27]. Although this is a powerful method to evaluate sensory perception and requires only a limited number of panelists (typically 10-12), they must be highly skilled in perceiving and dissecting relevant attributes.

Before each evaluation session panelists are prepared to assess a certain set of attributes. They get familiar with the definitions and evaluation methods for each of the attributes (e.g. specific tongue motion to probe one individual attribute). In addition, the influence of external factors on perception of products is minimized. In some cases a colouring agent and/or artificial sweetener is added to mask the potential differences in color and taste of the tested products and to avoid influence of suggestion on the assessment. Occasionally, samples are provided in covered cups to prevent influence of visual evaluation. Regardless of the precaution method used, all samples are presented to each panelist in a random order. The evaluation was typically performed at room temperature and the panelists were seated individually in sensory booths where proper ventilation was assured.

1.5 Physical counterparts: Tribology

Tactile receptors in the mouth provide texture perception of consumed products. This sensation can be influenced in different ways depending on many properties of food like, fat content, presence of non-dissolved particles etc. The most appropriate physical description of such a system is provided by tribology. The two rubbing surfaces are tongue and palate and the (consumed) food product is treated as a lubricant and depending on desired end-effect its properties are adjusted. Below the general concepts of tribology are presented.

1.5.1 Friction

The friction force is present in all systems where two surfaces are in direct contact and thus it is of great relevance to describe mechanical, oral food processing. The friction force is proportional to the normal load and is given by:

$$F_f = \mu W \tag{1.1}$$

where F is the friction force, μ is a friction coefficient and W is the normal load. This expression is named after Charles-Augustin de Coulomb. Commonly the friction is expressed using the friction coefficient. It describes how the force-load dependence changes with different parameters like temperature, speed, etc. As for oral processing the temperature is predefined and should be fixed at one level, it is common to present speed dependence. Lubricant, depending on the speed of its entrainment, can provide different support for the two rubbing surfaces (due to the pressure it exerts on the two surfaces). This speed dependence is commonly used to describe frictional properties of a lubricant and is called the Stribeck curve [28-30].

1.5.2 Stribeck curve

Liquid lubricant that dynamically enters the contact zone between two rubbing surfaces generates a pressure that provides some support to these surfaces. The faster the entrainment is, the stronger the support and the lower the friction become. In the Stribeck curve three regimes are distinguished depending on the degree of separation of the rubbing planes: the boundary, the mixed, and the hydrodynamic regimes. Figure 1.3 shows a schematic picture of the Stribeck curve marking all three regimes and typical shape of the curve.

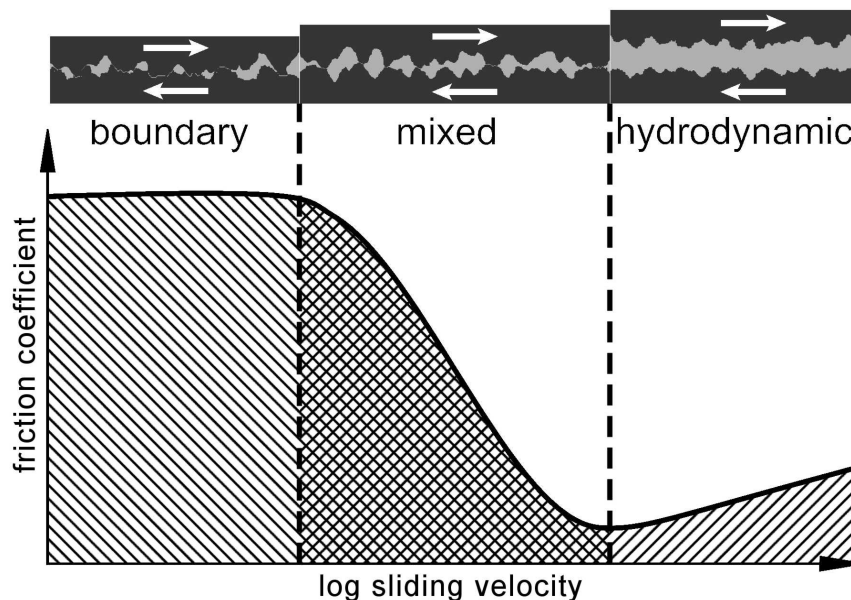


Figure 1.3 The Stribeck curve and three regimes of lubrication: the boundary, the mixed and the hydrodynamic regime. Upper panels show a schematic picture of the asperities separation in each regime.

Boundary lubrication regime

In this regime the two surfaces are in direct contact. The lubricant enters with insufficient speed and the resulting pressure developed cannot lift the upper surface. The friction force is the highest especially in the case of high surface roughness, where asperities can overlap and “lock”. A simple schematic picture of the situation is presented in Figure 1.3 (upper panel). Surface irregularities result in a more extended (towards higher speeds) boundary regime, as larger separation is required to avoid interaction of the asperities. A similar effect to roughness is observed for compliant surfaces (e.g. rubbers). An additional force component appears due to adhesion resulting in an extended boundary regime.

In the boundary regime wearing of the surfaces is a common phenomenon as they are in a direct contact. It leads to degradation of the rubbing surfaces and is an important effect in mechanical engineering. Good lubricants can form a thin boundary film that lowers the wearing efficiency and in some cases can prevent direct contact, although the distance between the surfaces remains lower than the combined size of asperities on both sides.

Mixed lubrication regime

When the entrainment speed increases, additional pressure support develops due to fluid hydrodynamics and the lubrication enters the mixed regime. This is an intermediate stage in which the surfaces are partly supported by the lubricant’s developed pressure, but the separation still remains lower than the sum of the asperities of both surfaces. Therefore, this regime is determined by both the bulk rheological properties of the lubricant and the surface properties. The schematic picture is shown in Figure 1.3 (middle panel). In this case, the friction force decreases with an increasing entrainment speed. The pressure increases, developing more lift and lowering the contact area. In this case the asperities’ overlap decreases and the “locking” effect is suppressed.

Hydrodynamic lubrication regime

Once the entrainment is high enough for the pressure to fully separate the two surfaces, the lubrication enters the hydrodynamic regime (see Figure 1.3). At this point the lubrication is governed by the bulk properties of the lubricant (e.g. viscosity). In the case of laminar flow of a Newtonian fluid the friction force in this regime can be obtained using the Navier-Stokes equation [31]:

$$F_f = \frac{A}{d} \eta v \quad (1.2)$$

where A is the surface area of two parallel plates, d is the thickness of the lubricating layer, η the viscosity of the lubricant, and v is the relative speed of the surfaces. In the laboratory, however, friction is typically measured using a ball on disc setup (see next section). Commonly the hydrodynamic lubrication regime is referred to as elasto-hydrodynamic regime if soft surfaces are investigated (e.g. to simulate oral environment). Esfahanian & Hamrock [32] fitted a wide range of conditions (entrainment speed, viscosity, load, elasticity of soft surfaces and radius of the ball) to obtain an equation describing the central film thickness:

$$h_c \approx 3.2R^{0.76}(\eta U)^{0.66}W^{-0.21}E^{*-0.45} \quad (1.3)$$

where η is the viscosity of the lubricant, U is the entrainment speed, R is the radius of the ball (upper surface), W is the normal load, and E^* is the reduced elasticity modulus of the surfaces (depending on Young's moduli E_i and Poisson ratios ν_i of two rubbing surfaces) given by:

$$E^* = 2 \left(\frac{1-\nu_1^2}{E_1} + \frac{1-\nu_2^2}{E_2} \right)^{-1}. \quad (1.4)$$

1.5.3 Friction measurements (setup overview)

In this thesis the investigation of the friction (tribology) was performed using a Mini Traction Machine (MTM; PCS Instruments). It measures the friction coefficient between a steel ball and a disc submerged in a lubricant moving at different speeds. The manufacturer's design was modified in order to allow the study of friction on compliant surfaces (see Figure 1.4 a and Figure 1.4 b for original and modified setup, respectively). The spherical steel ball was replaced by a device that contained a rubber O-ring and the steel disc was modified such that a variety of rubber specimens could be merged onto the surface. These modifications led to decrease (from GPa to kPa) of the contact pressure between rubbing surfaces allowing us to perform measurements with pressures comparable to those present in the mouth (see section 1.3). Previously, oral conditions have been simulated with tribological equipment that differs from the one used in this study. Initially, one soft surface was introduced in the commercial MTM setup in order to imitate the physical parameters for soft bio-tribological contacts [3,28,29]. The setup with two soft rotating surfaces was introduced by Bongaerts et al. [30]. This further reduced the contact pressure and allowed for better simulation of the oral conditions. However, in their study different geometry and surfaces were used [30]. Moreover, human mouth

environment was also mimicked in the Optical Tribological Configuration setup where the pig's oral tissue with the combination of glass plate was used under oscillatory movements [13]. Another study where oral surrounding was simulated, measured friction in custom-made apparatus between two mucosal surfaces [33,34].

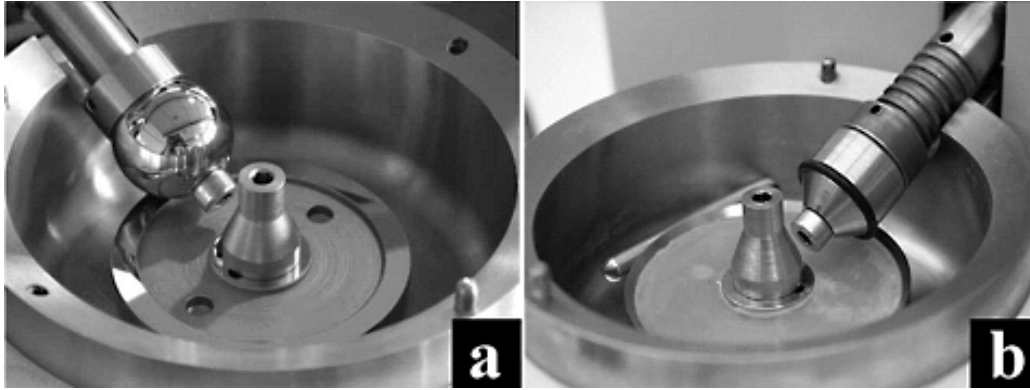


Figure 1.4 Measurement chamber with two rubbing surfaces for original MTM (a) and for modified setup used in this work (b).

The MTM provides control over the type of motion to study rolling friction (for rolling motion), sliding friction (for pure sliding) or any intermediate case [35]. The slide-roll ratio (SRR) is defined as the ratio of the absolute sliding speed $|\vec{U}_{disc} - \vec{U}_{ring}|$ and the entrainment speed $(U_{disc} + U_{ring})/2$, where U_{disc} and U_{ring} are the linear speeds of disc and ring at the point of contact, respectively. In addition, the temperature of the studied sample, the normal load, and the entrainment speed range can be controlled. Every measurement consists of two consecutive steps, where in one the speed decreases from the specified maximum speed to the set minimum speed and in the second step the speed increases back to the maximum speed. The operational ranges of parameters are presented in Table 1.2. Although, presented ranges are wide, the relevant parameter space is much smaller. Firstly, maximum speed is limited to 750 mm/s by strong vibrations of the ring shaft caused by rubber-rubber contact. Secondly, the oral environment equivalent pressure was of interest for this work and thus the investigated pressure varied depending on used rubbers between around 30 and 150 kPa. In addition, the temperature span was limited by the temperatures expected in the oral cavity. Thus the studied range was between ambient (around 20 °C) and human body (37 °C) temperatures.

To investigate surface influence on the friction several different rubbers were studied. They were silicone, neoprene and Teflon discs. To avoid slip between rubber disc and the

steel host the disc was fixed in position using double-sided tape. Due to wear that could occur during experiments both the O-ring and disc were replaced with unprocessed specimens before each measurement.

Table 1.2 Range of operational parameters for MTM as provided by manufacturer (PCS Instruments).

Parameter	Symbol	Operational range	[units]
Slide-roll-ratio	SRR	0 – 200	[%]
Temperature	T	ambient – 150	[°C]
Pressure	P	0 – $1.25 \cdot 10^9$	[Pa]
Speed	U	0 – 5	[m/s]
Load	W	0 – 75	[N]

1.6 Physical counterparts: Rheology

The viscosities of the semi-solid food (model) systems influence to a significant extend their texture perception. In particular, the thickness attribute of a solution is known to be described to a large extend by an apparent viscosity [3, 21-25, 36,37]. In addition, the viscosity of the lubricant plays an important role in the MTM as described by equations: 1.2 and 1.3. Therefore in this thesis, the rheological properties of the food model systems were investigated as well. The viscosity (η) of the solutions primarily was measured using a standard rheometer (AR 2000, TA Instruments, Leatherhead, UK) with double concentric cylinder geometry (see Figure 1.5).

The viscosity is obtained from the ratio of shear-stress to shear-rate [24]. Fluids can present a wide range of different rheological behavior e.g. Newtonian or non-Newtonian. For Newtonian behavior the linear relation between shear stress and rate takes place, which results in viscosity that is independent of the applied shear (see Figure 1.5 b, dashed line). In the case of non-Newtonian behavior, the viscosity changes with the shear-rate. In this thesis most of the solutions show non-Newtonian behavior, where viscosity decreased with the shear rate (see Figure 1.5 b, solid line), indicating shear-thinning effect also known as a pseudo-plastic.

In this thesis flow curves were obtained by measuring the apparent viscosity as a function of increasing shear rate, measured between 0.1 and 1000 s^{-1} .

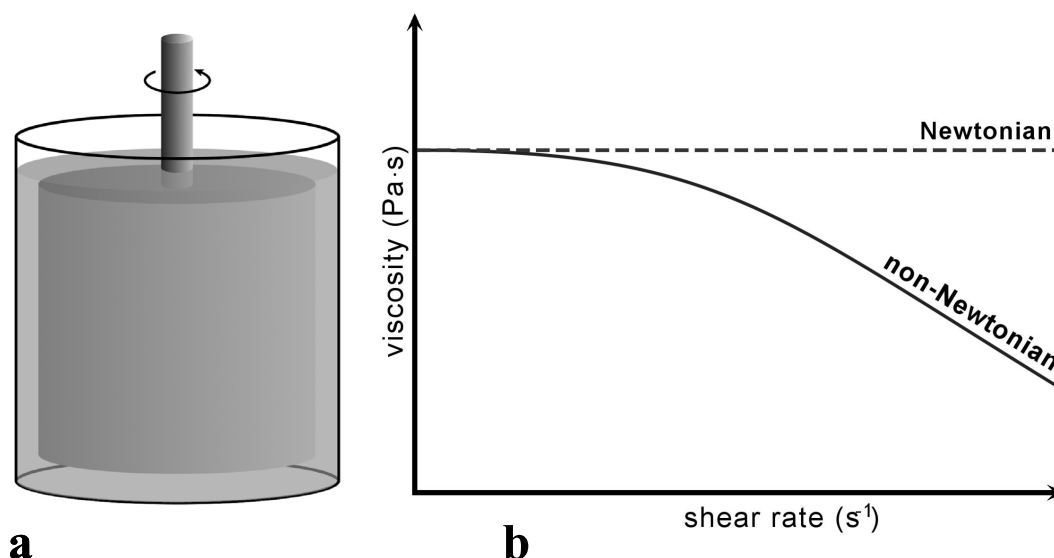


Figure 1.5 Schematic representation of double concentric cylinder geometry (a). The inner cylinder is suspended in a measured solution. Newtonian (dashed line) and non-Newtonian (solid line) behavior of the solution (b). The latter corresponds to the shear thinning and is typically associated with the alignment and disentanglements of the long polymer chains due to shear.

1.7 Food Models

Although controlling real food products is the ultimate goal of food science, achieving it is extremely difficult. Common products contain a large number of additives and agents that influence taste and texture. Therefore, this thesis is focused on some main components of food end-products and their influence on oral perception.

In this thesis the main focus is set to liquid and semi-solid food. Thus the investigated samples are based on protein, polysaccharides and fat, as these are the most common elements of products. Moreover, these individual components are widely used in the food industry in different applications. Thus understanding their influence on oral perception implies a great step towards a good control over the properties of food end-products.

In this thesis we study globular aggregates obtained from whey protein isolate (WPI) and fibrillar aggregates of ovalbumin extracted from egg white. These dispersions are used as models of the semi-solid foods that are structured by a protein network, e.g. yogurt. In addition we investigate a number of polysaccharides that are commonly used in e.g. desserts, soups, sauces, and bakery products. These polysaccharides are: locust bean gum (LBG), pectin, carrageenan, xanthan, gellan, guar, and tara gum. They have a number of applications in the food industry, e.g. thickening agent, stabilizer, water binding, they may provide fat-feel in low or no-fat dairy products. Moreover, these polysaccharides have

neutral or negative charges and different molecular weight. The chemical composition of these biopolymers and their characteristics were previously determined by de Jong and Van de Velde [38]. Detailed characteristics of these polysaccharides are presented in Chapter 4 of this thesis.

Furthermore, fat is of importance for this work, as it has a significant effect on mouth-feel perception [3,5,39,40]. Therefore, in this thesis the role of fat was studied both in real milk products and in filled gels, where emulsion fat droplets were bound or not bound to the matrix. The emulsion filled gels are used as a model of the semi-solid foods that contain emulsified fats and oils e.g. custards, mayonnaise, dressings and different kinds of sauces.

1.8 Outline of this thesis

In the first chapters of this thesis we report on our development of the new tribological methods and apply it to food systems. This is a new approach and therefore required some groundbreaking work. We investigated the tribological properties of different biopolymers (proteins and polysaccharides) and fat. These ingredients are widely used in the food industry and exhibit in the products a variety of forms (e.g. solutions, emulsions, gels or particles). Their unique characteristics provide different sensory perception and therefore it is of importance to describe their physical properties in an oral-environment adequately to allow a more predictive use of these components to direct sensory evaluation of more complex food products.

In Chapter 2 the lubrication and rheological properties of two different protein aggregates in an aqueous dispersion are studied. Their type, shape, size and quantity influenced the bulk viscoelastic properties of the samples and therefore the measured friction. The study on the relative importance of elasticity and roughness of the surfaces used is performed under simulated oral conditions. This was achieved by modification of the commercial tribometer to mimic soft contacts at relevant normal load and entrainment speeds. This chapter shows the applicability of the technique.

Emulsion-filled gels under applied shear are studied in Chapter 3. Gels including emulsion droplets were engineered such that the emulsion droplets were bound or non-bound to the matrix of the filled gel. The relative role of all the different components, their interaction as well as their effect on the frictional properties is investigated. Furthermore, the influence of saliva on the lubrication properties of emulsion-filled gels is studied.

The objective of Chapter 4 is to understand the differences in bulk rheology, lubrication and adsorption film properties of various biopolymer solutions and the more generic mechanism behind these differences. This is done by combination of three techniques: i) the commercial tribometer with soft ball and disc poly(dimethylsiloxane) (PDMS) substrates, ii) high shear viscosity and non-linear viscoelasticity determined up to shear rates of 10^5 s^{-1} using a narrow gap parallel plate geometry and iii) adsorption and interfacial film properties onto soft substrates using Surface Plasmon Resonance (SPR) and Quartz Crystal Microbalance-Dissipation (QCM-D). The combination of these multi-approach study produces a detailed picture of thin film formation, layer deposition and layer stability.

Chapter 5 presents a broad study of the influence of particles (protein spheres and gel particles) on tribological and rheological properties of different types of polysaccharide solutions. More importantly, this experimental work is now complemented by a QDA, a sensory panel study in order to establish a relation between friction data and sensory perception in the oral cavity. Since the thickness perception masked scores of other attributes, all samples were tuned to obtain the same score in sensorial thickness to eliminate its influence.

In Chapter 6 three representative polysaccharide solutions are measured using different rubber discs. How the different surface roughness, deformability and hydrophobicity of the discs influenced lubrication is measured in the tribometer. This parameter study determines how sensitive the tribological measurements are to the properties of the applied surface. Furthermore, this chapter shows the impact of hard microscopic particles on the lubrication properties by mixing the polysaccharide solutions with microcrystalline cellulose particles.

In Chapter 7 the tribological properties of milk with different fat content are studied. Their sensory perception is linked to lubrication and rheological properties. For different entrainment speeds measured in the tribometer the correlation coefficient between attributes and friction was determined. Furthermore, the visualization of the discs in the contact zone after the tribological experiments is provided using the Confocal Laser Scanning Microscope (CLSM).

In Chapter 8 future perspectives are discussed. The preliminary study on relation between slide-to-roll ratio and sensory attributes (like stickiness) are presented. In addition the lubrication effect of two artificial saliva lubricants, the effect of non-dissolved particles in

polysaccharide solutions, and the size of the particles are discussed. Finally the lubrication and rheological properties of commercial dairy products are presented in relation to their fat content.

References

- 1 Mojet, J., Christ-Hazelhof, E. & Heidema J. (2001) Taste perception with age: Generic or specific losses in threshold sensitivity to the five basic tastes, *Chem. Senses*, 26, 845-860.
- 2 Engelen L., van den Keybus P., de Wijk R.A., Veerman E., Amerongen A., Bosman F., Prinz A. & van der Bilt (2007), The effect of saliva composition on texture perception of semi-solids, *Archives of Oral Biology*, 52(6), 518-525
- 3 Malone ME., Apperlqvist, I. A. M. and Norton I. T. Oral behaviour of food hydrocolloids and emulsions. Part 1. Lubrication and deposition considerations, *Food Hydrocolloids* , (2003), 17, 763-773
- 4 De Wijk R.A. and Prinz, J.F. "The role of friction in perceived oral texture". *Food Quality Preference*, (2005), 16, 121-129
- 5 Dresselhuis, D.M., De Hoog, E. H. A, Cohen Stuart M. A., Vingerhoeds, M.H, Van Aken, G. A., "The occurrence of coalescence of emulsion droplets in relation to perception of fat" (2008) *Food Hydrocolloids*, vol 22, Issue 6, 1170-1183.
- 6 Dresselhuis, D. M., De Hoog, E. H. A., Cohen Stuart, M. A., Van Aken, G. A. (2007) Tribology as a tool to study emulsion behaviour in the mouth, *Food Colloids, Self-assembly and Material Science* , 451 – 461
- 7 Toyoda, M., Sakita, S., Kagoura, M., Morohashi, M. (1998). "Electron microscopic characterization of filiform papillae in the normal human tongue". *Archives Of Histology And Cytology*, 61(3), 253- 268.
- 8 Van Aken G.A. "Relating food microstructure to sensory quality", in: D.J. McClements (ed.) "Understanding and controlling the microstructure of complex foods" Woodhead Publishing Limited, year Cambridge, CB21 6AH, England
- 9 Schipper, R. G., Silletti, E., Vingerhoeds, M. H. (2007). Saliva as research material: Biochemical, physicochemical and practical aspects. *Archives of Oral Biology*, 52 (12), 1113-1214.
- 10 Amerongen, A. V. N., Veerman, E. C. I. (2002). Saliva - the defender of the oral cavity. *Oral Diseases*, 8(1), 12-22.
- 11 Mei van der, H. C., White, D. J., Busscher, H. J. (2004). On the wettability of soft tissues in the human oral cavity. *Archives of Oral Biology*, 49(8), 671-673.
- 12 van Aken, G.A., Vingerhoeds, M.H., de Hoog E.H.A. (2005) "Colloidal behaviour of food emulsions under oral conditions" in Dickinson E., *Food Colloids* (2004): Interactions, microstructure and processing. Cambridge, The Royal Society of Chemistry, 356-366
- 13 Dresselhuis, D. M., de Hoog, E.H.A., Cohen Stuart, M.A., van Aken, G.A. "Application of oral tissue in tribological measurements in an emulsion perception context" (2008), *Food Hydrocolloids*, 22(2), 323-335
- 14 Ranc, H., Elkhyat, A., Servais, C., Mac-Mary, S., Launay, B., Humbert, P., (2006). Friction coefficient and wettability of oral mucosal tissue: Changes induced by a salivary layer. *Colloids and Surfaces A: Physicochemical and Engineering Aspects* 276 (1-3), 155.).
- 15 Bongaerts, J.H.H., Rosetti D. and Stokes, J.R. "The Lubricating Properties of Human Whole Saliva", (2007), *Tribology Letters* vol 27, Nr 3, 277-287
- 16 Napadow, V. J., Chen, Q., Wedeen, V. J., Gilbert, R. J. (1999). Intramural mechanics of the human tongue in association with physiological deformations. *Journal of Biomechanics*, 32(1), 1-12

- 17 Gilbert, R. J., Napadow, V. J. (2005). Three-dimensional muscular architecture of the human tongue determined in vivo with diffusion tensor magnetic resonance imaging. *Dysphagia*, 20(1), 1-7
- 18 Pouderouc P. and Kahrilas, P.J. (1995). Deglutitive tongue force modulation by volition, volume, and viscosity in humans. *Gastroenterology* 108, 1418–1426.
- 19 Tsuga, K. Hayashi, R., Sato Y., and Y. Akgawa, (2003). Handy measurement for tongue motion and coordination with laryngeal elevation at swallowing. *J. Oral Rehabil.* 30, 985–989.
- 20 Hayashi R., Tsuga, K., Hosokawa, R., Yoshida M., Sato, Y., Akagawa, Y. (2002) A novel handy probe for tongue pressure measurements. *Int. J. Prosthodont.* 15: 385-388
- 21 Shama and Sherman (1973), *J. Texture Studies* 4(1), 111-118.
- 22 Cutler, A.N., Morris, E.R., & Taylor, L.J. (1983), *J. Texture Studies* 14(4), 377-395.
- 23 Dickie, A.M., & Kokini, J.L. (1983), *J. Food Sci.* 48(1), 57-61.
- 24 Stanley, N.L. & Taylor, L.J. (1993), *Acta Psychologica* 84, 79-92.
- 25 Wood, F. W. (1968), *Psychophysical studies on the consistency of liquid foods. Rheology and texture of foods.* London: Society of Chemical Industry, Monograph 27, 40–49.
- 26 De Wijk, R. A., van Gemert, L. J., Terpstra, M. E. J., & Wilkinson, C. L. (2003). Texture of semi-solids: Sensory and instrumental measurements on vanilla custard desserts. *Food Quality and Preference*, 14, 35–317.
- 27 Stone, H. & Sidel, J. L. (2004). *Sensory evaluation practices.* London: Elsevier Academic Press
- 28 Cassin, G., Heinrich, E. And Spikes H.A., *Tribology Letters* (2001) 11:95-102
- 29 De Vicente, J., Stokes, J.R. and Spikes, H.A. *Tribology International* (2005);38:515–26
- 30 J.H.H. Bongaerts, K. Fourtouni, J.R. Stokes, *Tribology international* (2007); 40:1531-42
- 31 Butt, H.J., Graf, K., Kappl, M., (2003) *Physics and Chemistry of interfaces.* Weinheim: WILEY-VCH Verlag.
- 32 Esfahanian M. & Hamrock, B.J. (1991), Fluid-film lubrication regimes revisited, *Trib. Trans.*, 34 628.
- 33 De Hoog, E. H. A., Prinz, J. F., Huntjens, L., Dresselhuis, D. M., van Aken, G. A. (2006). Lubrication of oral surfaces by food emulsions: the importance of surface characteristics. *Journal of Food Science*, 71(7), E337-E341.
- 34 Prinz, J.F., de Wijk, R.A., Huntjens, L., Load dependency of the coefficient of friction of oral mucosa. *Food Hydrocolloids*, (2007), vol.21(3), 402-408.
- 35 De Vicente, J., Stokes, J.R. and Spikes, H.A. Rolling and sliding friction in compliant, lubricated contact. *Proceedings of the Institution of Mechanical Engineers, Part J: Journal of Engineering Tribology* (2006), vol 220 (2), 55-63
- 36 Richardson, R. K., Morris, E. R., Ross-Murphy, S. B., Taylor, L. J., & Dea, I. C. M. (1989), Characterisation of the perceived texture of thickened systems by dynamic viscosity measurements. *Food Hydrocolloids*, 3(3), 175–191.
- 37 Kokini, J. L., Kadane, J. B., & Cussler, E. L. (1977). Liquid texture perceived in mouth, *Journal of Texture Studies*, 8(2), 195–218.
- 38 De Jong, S. & van de Velde, F., (2007), *Food Hydrocolloids* 21 1172-1187.
- 39 Vingerhoeds, M.H., de Wijk, R.A., Zoet, F.D., Nixdorf, R.R. & Van Aken, G.A., “How emulsion composition and structure affect sensory perception of low-viscosity model emulsions”, (2008), *Food Hydrocoll*, 22, 4, 631-646.
- 40 Van Aken, G.A., Vingerhoeds, M.H., De Hoog, E.H.A. (2009) Oral processing and perception of food emulsions: the relevance for fat reduction in food. In “Designing functional foods”, Ed. D.J. McClements, Woodhead Publishing, Cambridge UK, (2009, in press)

Chapter 2

Lubrication properties of protein aggregate dispersions in a soft contact

A. Chojnicka, S. de Jong, C.G. de Kruif, and R.W. Visschers (2008). Lubrication properties of protein aggregate dispersions in a soft contact. *Journal of Agricultural and Food Chemistry*, 56, 1274-1282.

Abstract

In this chapter, the lubrication, rheological, and molecular properties of two different protein aggregate dispersions were compared: globular aggregates of whey protein isolate (WPI) and fibrillar aggregates of ovalbumin from egg white. These dispersions are models for the lubricating fluid that is present between the tongue and the palate when consuming liquid or gelled products. To simulate oral conditions, a commercial tribometer was modified so that soft rubber surfaces could be used. This allowed us to measure friction at low contact pressures similar to those present between the tongue and palate. Clear correlations were observed between the measured friction coefficients and specific properties of the lubricating fluid such as protein concentration and aggregate size and shape. Furthermore, surface properties like elasticity, surface-surface interactions, and surface roughness had a significant effect on the friction under conditions that are relevant for texture perception. In conclusion in vitro measurements at low contact pressure provide valuable information for understanding and controlling food properties that modulate oral friction.

2.1 Introduction

Sensory perception of food is a complex process that involves all human senses [1,2]. Texture, or perception of food structure, depends on (i) the composition and bulk rheological properties of the food, (ii) the properties of the oral surfaces that take part in the processing of the food, and (iii) the interactions between oral surface and food. Attributes such as creaminess, smoothness, and stickiness that describe the quality of the texture of food are easy to perceive but difficult to characterize physically [3,4]. The microstructure of proteins, fat, and possible networks of other ingredients will affect oral friction, and this will probably influence perception. Relations between texture sensation and microstructure of food have been demonstrated in some cases [5-8] but the relation between microstructure and tribological properties of food have not been studied extensively [9-11].

Frictional behavior of food systems in the gap between palate and tongue is of key relevance to the perceived texture of food. Friction between two sliding surfaces in general depends on (i) the properties of the lubricating substance separating the two surfaces [12], (ii) the force pressing the two surfaces together, and (iii) the roughness of the surfaces in contact. During consumption food acts as a lubricant substance, and therefore frictional forces during the oral processing will depend on the properties of the food material. More precisely, in this chapter the working hypothesis is that the force needed to slide the tongue over the palate depends on food properties and is relevant to the texture of food.

Typically, the oral regime is characterized by a mean low contact pressure and low traction speed during eating. The contact pressure in the mouth is estimated to be approximately 30 kPa [13]. These low pressures cannot be easily achieved with standard tribometers. Steel-steel contacts under normal measuring conditions generate contact pressures in the GPa region. Introduction of different rubber surfaces to a tribometer lowered the measured contact pressure to about 50-100 kPa. Oral friction also depends on the difference between sliding and rolling motions as well as on the shear rate. During mastication it is likely that different sliding and rolling motions are present between the tongue and palate depending on the consumed food. However, how this impacts on friction is not known since no data on in vivo or in vitro measurements are available. It has been shown that during mastication the shear rate applied in the mouth varies in between 1 and 1000 s⁻¹ [5,14].

Roughness of oral surfaces also has a significant effect on the perceived texture of food. It is influenced by the amount of saliva and the amount and properties of the adhered food. Furthermore, the surface roughness can change as a result of abrasion of these layers during oral processing and may be affected by muscular contraction of the tongue muscles. Therefore, it seems particularly relevant to establish the relation between surface roughness and the amount of friction at contact pressure and traction speeds that are relevant for the oral regime [5,12,15,16].

This chapter focuses on the lubrication of protein aggregate dispersion and studies how protein ingredients modulate friction under conditions that are relevant for oral texture perception. These dispersions serve as a model for foods that are structured by a protein network. It was expected that the lubrication properties of the dispersions would vary with composition. Thus two different protein solutions were used: globular aggregates from whey protein isolate (WPI) and fibrillar aggregates from ovalbumin. The shape of the aggregates has a significant effect on the viscoelastic properties of the dispersions, and the aim of this work is to determine its influence on the lubrication properties. To our knowledge, this is the first time that a quantitative measurement is made of lubrication properties of protein aggregate dispersions between soft surfaces. Finally, it should be realized that consumption itself induces changes in the structure of the food [15,17] or the oral tissue that can have an effect on the friction. These types of effects are not explicitly included in this chapter.

2.2 Material and Methods

2.2.1 Characteristics and preparation of the protein aggregates

Lubricants studied in this chapter are dispersions of aggregates of ovalbumin and whey protein isolate (WPI). Ovalbumin was purchased from Sigma (albumin from chicken egg white, grade III, minimum 90% pure by agarose gel electrophoresis, crystallized and lyophilized, batch 074K7011). The second dispersion was made of Bipro, which is a whey protein mixture obtained from Davisco Foods International Inc. (La Sueur, MN). The WPI is mainly composed (based on dry weight) of 74% β -lactoglobulin (β -lg) and 13% α -lactalbumin [18].

Depending on the type of protein heated, different types of aggregate can be formed [18]. In the case of heated WPI, globular protein aggregates are obtained, while ovalbumin aggregates are typically fibrillar in shape. The size and voluminosity of aggregates and

thereby the viscosity can be controlled by heating the solution at a specific concentration. The preparation of soluble WPI and ovalbumin aggregates was done according to Alting et al. and Weijers et al. [19-22].

Both proteins were dissolved in distilled water at ambient temperature to a concentration of 3%, 6%, and 9% for WPI and 2%, 3.5%, and 5.3% for ovalbumin. The pH was adjusted to 7, and in the case of ovalbumin the solutions were filtered through a 0.5 μm filter to remove any unsolubilized material prior to heating. After heating, the dispersions were cooled to room temperature in a water bath. The dispersions were stored at 4 °C and used within 4 days after preparation. According to Alting et al. [21] and Weijers et al. [22] the WPI forms aggregates with a diameter of 30 to 80 nm. The fibrillar aggregates formed during heating are 30 up to 700nm long. For different concentrations of the WPI protein aggregate dispersions the dynamic light scattering technique was used to verify that the hydrodynamic and gyration radii did not change after the MTM experiment.

2.2.2 Rheological measurements

The viscosity data of the different protein aggregate dispersions were recorded at 21 and 31 °C using a standard rheometer (AR2000, TA Instruments, Leatherhead, U.K.) with double concentric cylinder geometry. Flow deformation curves were obtained by measuring the viscosity as a function of increasing shear rate. The measurement consists of three steps (15 min each): a conditioning step where the system is temperature equilibrated, followed by a continuous ramp step with the shear rate increased from 0.006 to 1000 s^{-1} . Finally, a reverse continuous ramp step was performed in order to check if there were any changes in the structure of the protein aggregates as a result of shearing. Each point was measured at a fixed shear rate with a duration time of 12-18 s. Brookfield oils (viscosity standard, Benelux Scientific, Scientific Instrument & Laboratory Equipment) with 10, 50, and 100 mPa were used to calibrate the equipment.

2.2.3 Tribological measurements

A Mini Traction Machine (MTM) (PCS Instrument) was used in the experiments to measure friction. Typically, a rotating steel disc and ball are used in this instrument as the two surfaces. The friction force arises from the ball-disc interaction at the applied speed. The rotating speed of the disc and the ball as well as the load can be adjusted using the instrument software. In order to study low contact pressure, the MTM was modified using

compliant surfaces by introduction of a steel cylinder with an attached neoprene O-ring. In addition, a 3 mm silicone or neoprene sheet was fixed on top of the steel disc. To accommodate the layer of the rubber, the disc was modified (Figure 2.1). Flat surface and fixed position of the rubber on the steel disc was obtained by gluing it using Bison Kit TM Transparent glue. Before experiments were performed all rubbers were cleaned with an ethanol, reverse osmosis water and dried with air. Since all of the results were reproducible and no changes after cleaning the rubbers have been noticed, it is safe to assume that the cleaning procedure does not affect the measurements. The scatter points in the data are a good indication of their accuracy.

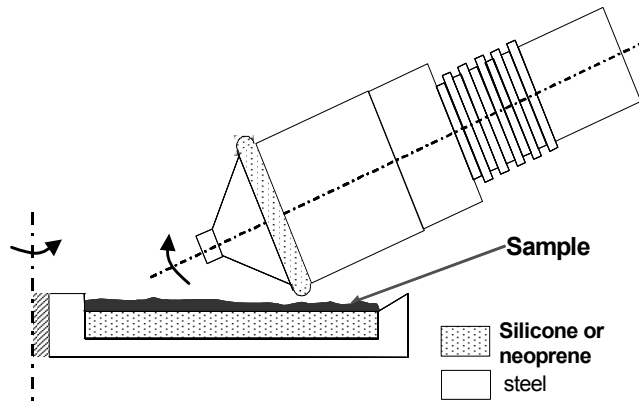


Figure 2.1 Schematic representation of the experimental setup. It consists of two essential parts: a neoprene ring and steel disc with an attached silicone or neoprene sheet on top of it. The dotted area represents the rubber surfaces that are in contact and are the source of friction.

In this study the contact pressure was significantly lowered compared to the steel-steel contact. Table 2.1 shows the calculated pressures for the different materials using:

$$P = \frac{W^{1/3}}{\pi} \left(\frac{4E^*}{3R} \right)^{2/3} \quad (2.1)$$

which is derived from the Hertz theory. W and R are the normal load and reduced radius, respectively. The contact modulus E^* is given in equation 2.5. Although the pressure obtained in this work is higher than the rubber-steel case, it is of the same order as in the rubber-rubber contact. Moreover, the hard steel surface against the rubber causes cracking of the soft surface unlike in the case of the rubber-rubber contact. The latter due to the material flexibility causes weaker damage.

Table 2.1 Comparison of the pressure for contact of different materials. All values were calculated using Hertz theory. In the case of the O-ring the elliptical contact was taken into account.

Contact type	Steel ball-steel	Rubber ball-steel	Rubber ball-rubber	Rubber O-ring-rubber
Pressure (Pa)	$2.16 \cdot 10^8$	$3.78 \cdot 10^4$	$2.33 \cdot 10^4$	$6.11 \cdot 10^4$

The rubber – rubber contact caused strong vibration of the ball-drive shaft at high speeds which could be only partially remedied by gluing the surface to the support. For this reason the upper limit of the speed had to be 600 or 750 mm/s. Due to technical reasons the data at speeds below 5 mm/s are very noisy, and therefore they are removed from the figures. The slide-roll ratio (SRR) is calculated using equation 2.2, where U is the mean tangential velocity of the ball and disc at the point of contact.

$$SRR = \frac{U_{disc} - U_{ball}}{U} \quad (2.2)$$

All measurements were performed at a temperature of 21 or 31 °C ($\pm 1^\circ\text{C}$) using the thermostat of the MTM. Sometimes wear of the material occurred during the measurements as a track became visible on the disc after repeated measurements. For this reason the number of runs with the same surface was limited and verified that wear did not result in significant changes over the period of the measurement.

2.2.4 Elasticity measurements and contact pressure calculation

The configuration where both the soft disc and the rubber ring were used made it possible to measure the relation between the friction coefficient and the entrainment speed at relatively low contact pressure. To estimate the contact pressure, the elasticity of the silicone and neoprene rubbers was measured. Young's modulus is calculated from the slope of the initial linear relation of the stress/strain curve. This relation was obtained using an Instron 5543 (Instron Int., Edegem, Belgium), where the rubber was placed between two parallel plates, which were pressed toward each other. Both rubbers were compressed at 1 mm/s and to 95% strain. The Young modulus for each rubber is a mean value obtained in eight independent measurements.

To calculate pressure in between two surfaces, the contact area has to be determined. In the case of the rubber ring the contact area has an elliptical shape and is described by two semi-axes given by Greenwood et al. [23]:

$$\begin{aligned} a &= \left(\frac{3k^2 \varepsilon W R}{\pi E^*} \right)^{1/3} \\ b &= \left(\frac{3\varepsilon W R}{\pi k E^*} \right)^{1/3} \end{aligned} \quad (2.3)$$

The axis ratio $k=a/b$ can be approximated by $k \approx (1.0339(R_1/R_2))^{0.636}$, while the elliptic integral $\varepsilon \approx 1.0003 + 0.5968(R_2/R_1)$ [23-24], where R_1 and R_2 are radii of the O-ring and its cross section, respectively. The reduced radius R is given by $(1/R_1 + 1/R_2)^{-1}$.

The contact pressure depends on the contact area between rubbers, the normal load applied, and the elasticity modulus of the materials. The elliptical contact area is given by

$$S = \pi ab \quad (2.4)$$

The contact modulus using equation 2.3 is defined as

$$E^* = \left(\frac{1 - \nu_1^2}{E_1} + \frac{1 - \nu_2^2}{E_2} \right)^{-1} \quad (2.5)$$

where the E_i and ν_i are the Young moduli and Poisson ratios of the two rubbers in contact.

The Poisson ratio for rubbers is in good approximation 0.5.

Finally, the contact pressure is calculated:

$$P = \frac{W}{S} \quad (2.6)$$

2.2.5 Contact angle measurements

To estimate the strength of the hydrophobic interactions between the protein aggregate dispersions and the different types of rubber discs the contact angles between samples and the rubbers were measured. The contact angle measurement was done using a conventional goniometer (ERMA contact angle meter G-1). A symmetrical drop of around 0.5 – 0.7 cm radius was deposited on the surface material using a syringe with a constant solution volume of 10 μ L. All rubbers were cleaned with an ethanol, reverse osmosis water and dried with air. The contact angles were collected visually at room temperature from both sides of the drop directly (within 1 min after the drop was applied). Reported contact angles are the average of 10 measurements.

2.2.6 Stereomicroscopy

Stereomicroscopy (Leica Microsystems MZ16 with optical zoom 16) was used to evaluate the surface of the rubbers. The objective lens used was a PL APO type with a numerical aperture of 0.20 and 1.7 μm resolving power. The image roughness was calculated using the method described in [25].

2.3 Results

2.3.1 Rheological measurements

In order to understand the tribological data, the dynamic viscosity of the lubricants has been determined. The WPI and ovalbumin protein aggregate dispersions show non-Newtonian behavior: the viscosity decreased with shear-rate, indicating that shear thinning occurred (Figure 2.2).

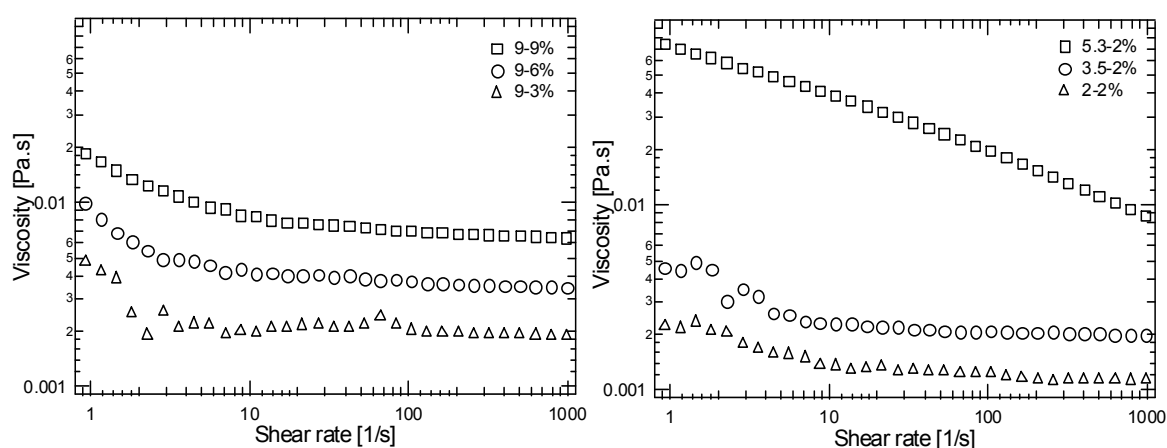


Figure 2.2 Viscosity data for WPI (left) and ovalbumin (right) protein aggregate dispersion. The effect of the protein concentration was shown for WPI where squares correspond to WPI9%; this solution was diluted to 6% (circles) and to 3% (triangles). The effect of the aggregate size was shown for ovalbumin where all of the solutions were diluted to the same ending concentration. Squares correspond to the ovalbumin 5.3-2%, circles to 3.5-2% and triangles to ovalbumin 2%. Measurements were done at 31 °C.

The viscosity increases with concentration and with volume factor. Ovalbumin protein aggregate dispersion had higher overall viscosities compared to WPI on a w/w basis, which is related to the fibrillar shape of the ovalbumin aggregates formed during incubation in the heater bath [22]. Since the length of the fibrils formed is highly dependent on the protein concentration during heating [19], long fibrils and a high viscosity were observed near the critical gel concentration. Both the length of the aggregates and the viscosity decreased drastically when the concentration of the protein

during heating is lowered. The changes in viscosity as a function of the concentration and the aggregate size were less significant in case of WPI, which is known to form more globular-shaped aggregates during heating [18]. It should be noted that no irreversible breakdown of aggregates was apparent in the rheological measurements.

2.3.2 Tribological measurements

Figure 2.3 shows how the friction coefficient changed as a function of traction speed when different solutions (WPI and water) were present as a lubricant.

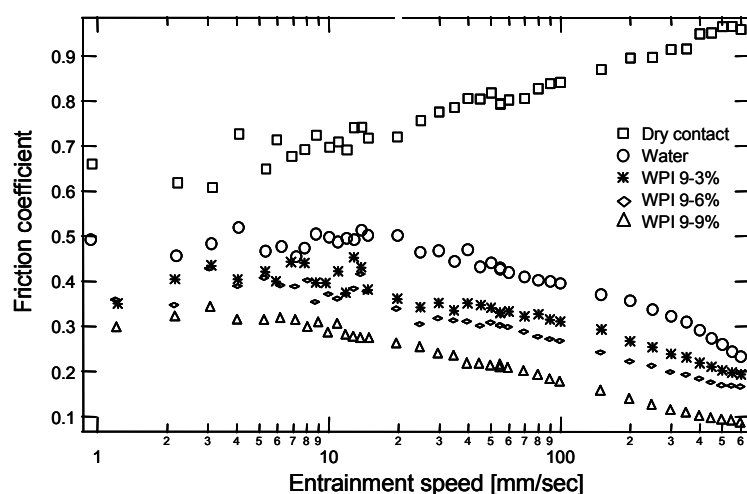


Figure 2.3 Stribeck curves for different lubricants: water (circles), WPI9-3% (asterisk), WPI9-6% (diamond), WPI9% (triangle). The effect of the protein concentration is noticed by diluting the solution with the same aggregate size to lower concentration. Squares correspond to the case where there is no lubricant present and the rubber ring and silicone sheets are in direct contact. Physical parameters: load 5N; $T=30\text{ }^{\circ}\text{C}$, $\text{SRR}=50\%$.

When there is no lubricant present, the friction coefficient increased linearly with increasing speed. When water is introduced as a lubricant, the friction coefficient at very low traction speed is about the same as for the dry contact. A mixed lubrication regime occurs at about 10-15 mm/s for the applied conditions. Figure 2.3 demonstrates that when a small amount of WPI aggregates is present, the lubrication properties improved with respect to water. Both in the boundary as well as in the mixed regime friction is lower and depends on the concentration of the protein. Figure 2.4 shows the concentration dependences of the friction coefficient in the boundary regime (5-10 mm/s) for both WPI and ovalbumin in a neoprene-silicone contact.

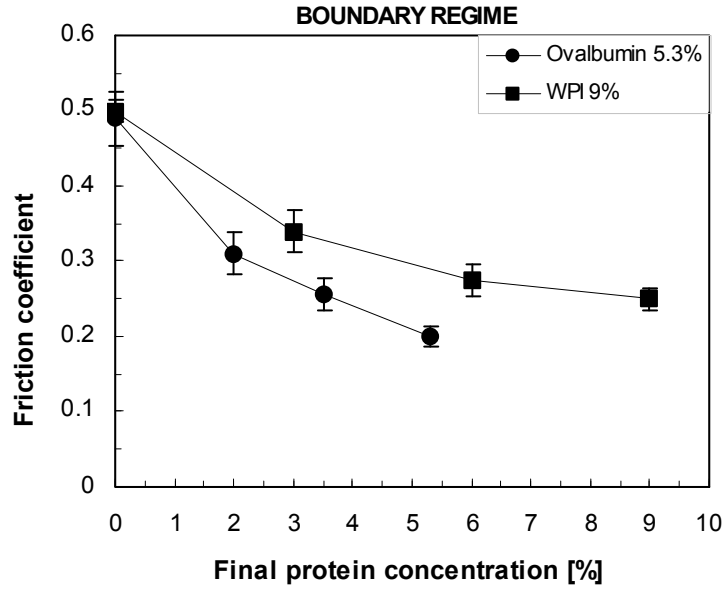


Figure 2.4 Friction coefficient in boundary lubrication regime (5 to 10 mm/s) as a function of protein concentration for WPI and ovalbumin protein aggregate dispersions. The applied load was 5N for neoprene – silicone contact. For WPI a 9% solution was heated and after cooling diluted to the appropriate concentrations. For ovalbumin, the concentration during heating was 5.3%. The measurements were repeated for three times and averaged to give an averaged friction coefficient.

Higher concentrations for both types of protein aggregates yield lower friction coefficients in the boundary regime. The concentration dependence for both protein dispersions was similar and correlated with their viscosity. In most cases the transition from boundary to mixed regime was observed between the 10 -15 mm/s and slightly depended on concentration. In the boundary regime ovalbumin solutions had lower friction coefficients compared to WPI. For WPI, the boundary friction level decreased about 40% when the protein concentration was increased from 0 to 9% (see Table 2.2). For ovalbumin a 50% decrease was observed at a protein concentration of 5.3% relative to water. Also, the dependence of the friction coefficient on the concentration was stronger for ovalbumin than for WPI in the mixed regime. Logarithmic function $\xi(U) = a_0 + a_1 \times \log(U)$ was used in order to be able to compare obtained results more quantitatively and to fit data in the mixed lubrication regime. Measurements of water were better represented by a linear function. Table 2.2 summarizes the estimated boundary friction of the different protein aggregate dispersions and the fitted slope a_1 in the mixed regime as a function of WPI protein concentration.

Table 2.2 Friction coefficient and corresponding speed, obtained in boundary lubrication regime. The slope results from fitting the Stribeck curve in the mixed regime. (Notation: WPI 9-9%: means that during the measurements the concentration of the protein aggregates dispersion were the same as in the heating procedure. In case of WPI9-3% means that initial heated concentration of protein was 9% and after cooling down the aggregate dispersion was diluted to 3% and measured).

Conc. of WPI [%]	Upper limit Boundary plateau		Slope a ₁ in the mixed regime		Conc. of Ovalbumin [%]	Upper limit Boundary Plateau		Slope a ₁ in the mixed regime
	SRR [%]		SRR [%]			SRR [%]		
	50	100	50	100		50	50	
0	0.5 10 mm/s	0.55 20 mm/s	Linear 0.42 ±0.0025	-0.259 ±0.0055	0	0.5 10 mm/s	Linear 0.42 ±0.0025	
3-3	0.4 10 mm/s	0.45 10 mm/s	-0.139 ±0.0029	-0.18 ±0.0034	2-2	0.35 10 mm/s	-0.155 ±0.00439	
6-6	0.33 15 mm/s	0.4 15 mm/s	-0.129 ±0.0032	-0.145 ±0.0016	3.5-3.5	0.33 16 mm/s	-0.103 ±0.0021	
9-9	0.33 8 mm/s	0.35 9 mm/s	-0.121 ±0.002	-0.096 ±0.0032	5.3-5.3	0.22 20 mm/s	-0.087 ±0.0031	

The onset of the mixed regime appeared to shift to somewhat lower speeds when the protein concentration increases. The slope of the Stribeck curves in the mixed regime also depends on the protein concentration. At lower concentrations the friction in the mixed regime dropped faster with increasing speed.

To investigate the effect of aggregate size, the protein concentrations during heating were varied. Subsequently, the samples were diluted to equal concentrations (Figure 2.5), and friction measurements were made at different pressures. This is different from the data presented in Figure 2.4 , where the concentration during heating was the same but the final protein concentrations were different.

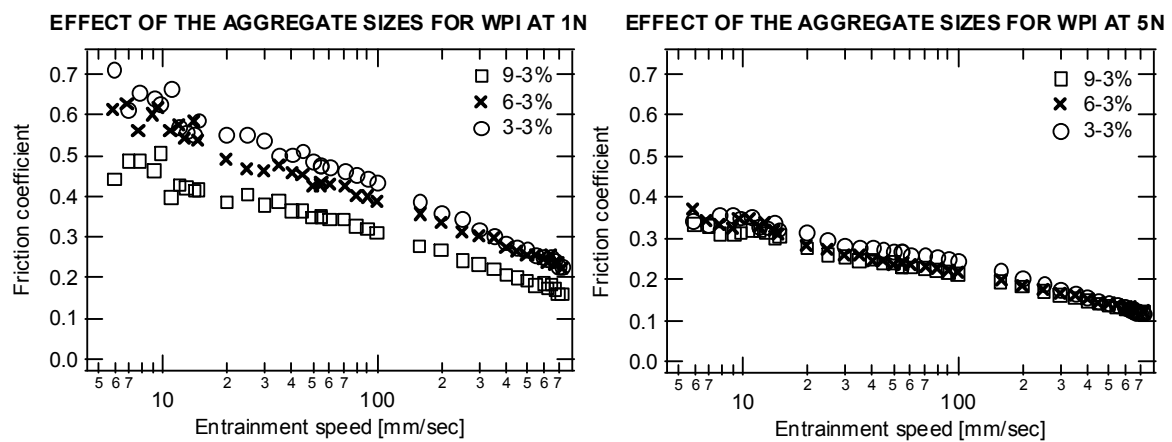


Figure 2.5 Influence of aggregate size on friction for WPI protein dispersion at 1N normal load (left) and 5N (right). The friction coefficient was measured in neoprene – silicone contact.

Bigger aggregates cause a decrease of the friction coefficient in the boundary regime at equal protein concentrations for both types of protein aggregates. This is observed in the boundary regime and mixed regime, and it is more pronounced at low pressure (see below).

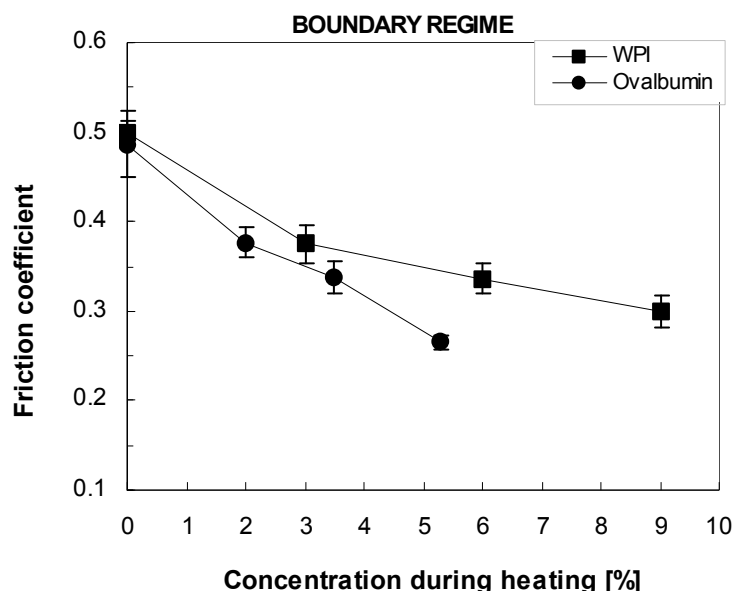


Figure 2.6 Friction coefficient in boundary lubrication regime (average value from 5 to 10 mm/s) as a function of aggregate size for WPI and ovalbumin protein aggregate solutions. The applied load was 5N. The measurements were repeated for three times and averaged to give an averaged friction coefficient.

Figure 2.6 shows the relation between boundary friction and heating concentration for two different types of aggregates. The fact that the curves do not coincide is explained by the actual size of the aggregates. In case of WPI, aggregates have a globular shape, and sizes vary between 30 and 80 nm. Ovalbumin aggregates have a fibrillar shape, and sizes vary between about 40 and 700 nm. The WPI and Ovalbumin aggregates of small sizes (30 and 40 nm, respectively) show very similar friction coefficients (~ 0.38). The trend is continued for larger sizes (80 and 100 nm) and friction decreases for both species to about 0.34 for ovalbumin and 0.3 for WPI. The largest ovalbumin aggregates also showed the lowest friction coefficient (~ 0.2).

Interestingly, when the normal load is increased, the measured friction coefficient decreased for both types of protein aggregates as well as water. The differences in Stribeck curves for WPI protein aggregates dispersions obtained at 1N and 5N are shown in Figure 2.5. Similar behavior was observed for ovalbumin aggregate dispersions. The

results showed that in the case of 5N a lower friction coefficient is measured compared to the low load. According to a simple adhesion theory of friction, the friction coefficient is

$$\mu = \frac{F}{W} = \frac{S\tau}{SP} = \frac{\tau}{P}, \quad (2.7)$$

where τ is shear strength [26]. Thus in the boundary and mixed regimes, where the surfaces are not separated, the friction coefficient decreases with increasing contact pressure. Indeed, the ratio of the friction coefficients determined at different normal loads is close to the ratio of the pressures corresponding to these loads. In the case of the smaller aggregates, however, that ratio shows deviation. The largest difference occurs at high speeds, where the lubrication starts to dominate. In the boundary regime however, smaller aggregates seem to be less efficient lubricants at lower pressures. In the case of the largest aggregate (9-3% WPI) the ratio of the friction coefficients is 1.61 ± 0.09 , while the corresponding pressure ratio is 1.71.

When changing the slide-roll ratio from 50% to 100%, three observations were made (see Table 2.2). First, the boundary friction value measured between 5 and 10 mm/s increased significantly. Second, the onset of the mixed regime occurred at slightly higher speeds, and, finally, the slope in the mixed regime became steeper (especially for the 3% and 6% protein concentrations). The explanation for this behavior can primarily be found in the deformability of the surface material. Soft material like rubber can deform due to the applied force, which results in increased contact area. This in turn causes higher values of boundary friction coefficients (shift upward). This effect is stronger when “more sliding” motion occurs. More sliding motion results in a later onset of the mixed regime, which implies a larger effect of surface asperities, which is in line with the increased mechanical interactions due to the sliding motion.

2.3.3 Influence of surface properties on the friction coefficient

In order to establish the relative importance of elasticity, surface-surface, surface-lubricant and roughness on the friction coefficient the friction for silicone and neoprene rubbers was compared. Figure 2.7 shows Stribeck curves for ovalbumin protein dispersion obtained for neoprene-neoprene contacts and neoprene-silicone contacts. Higher friction coefficients were obtained when neoprene was used for both surfaces, and also a larger influence of protein concentration on friction was observed in this case.

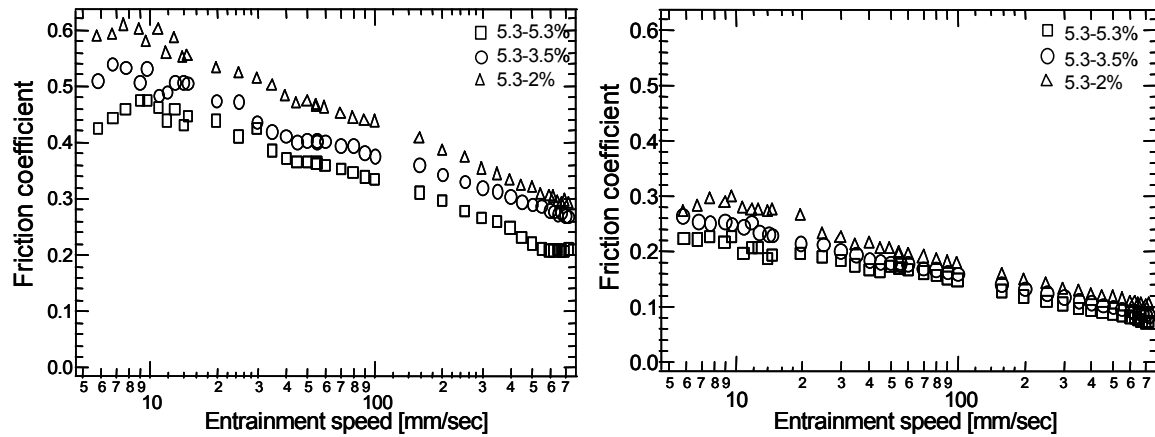


Figure 2.7 Stribeck curves for ovalbumin protein solution obtained for neoprene (left) and silicone (right) rubber at 5N of normal load.

From the stress-strain relation Young's moduli were calculated to be $E_1=0.2$ MPa for the neoprene and $E_2=0.29$ MPa for the silicone discs. Based on these moduli the contact area and the contact pressure between two touching surfaces were calculated at 1N and 5N (Table 2.3 and equation 2.3-2.5). Indeed, the calculations show that the contact area for the soft neoprene-neoprene contact is about 10% larger compared to the neoprene-silicone contact. This results in a lower contact pressure and higher friction coefficient (Figure 2.7). The increase of the friction coefficient however, cannot be explained by the adhesion theory alone, since the ratio of the pressures is 1.1, while the ratio of the friction coefficients is above 2. This implies that at equal loads the observed difference probably originates from differences in surface properties and the adhesion which occurs at the region of contact, as well as on the surface roughness.

Table 2.3 Contact area and contact pressure for a neoprene – silicone and neoprene – neoprene rubbers, calculated for 1 and 5N normal load ^a.

RUBBER	A [m ²] 1N	P [kPa] 1N	A [m ²] 5N	P [kPa] 5N
Neoprene - Silicone	$1.64 \cdot 10^{-5}$	61.1	$4.78 \cdot 10^{-5}$	104.6
Neoprene - Neoprene	$1.83 \cdot 10^{-5}$	54.6	$5.35 \cdot 10^{-5}$	93.4

^a See equation 2.3-2.6. The Poisson ration was assumed to be 0.5 for both rubbers. The radius of the neoprene ring were measured to be $R=9 \times 10^{-3}$ m while the cross section radius was $r=1 \times 10^{-3}$ m. From this the half length and half width of the contact area at $W=5$ N were calculated to be: $a_1= 5.98 \times 10^{-3}$ m and $a_2=2.87 \times 10^{-3}$ m, respectively. While the half length and half width of the contact area at $W=1$ N were calculated to be: $a_1= 3.48 \times 10^{-3}$ m and $a_2=1.67 \times 10^{-3}$ m, respectively.

Contact angle measurements were made in order to investigate the wetting properties of the neoprene and silicone surfaces. This technique was used to characterize the affinity of

water and aqueous solutions like the protein aggregate dispersions to coat the material. The results showed a smaller contact angle for the neoprene, indicating stronger attraction behavior of this rubber compared to the silicone (see Table 2.4).

Table 2.4 Contact angle measurements for silicone and neoprene rubber. The readings were repeated for 10 times and averaged.

RUBBER	WATER	WPI3%	WPI6%	WPI9%
Silicone	96.4	102.2	108.5	109.2
	±2.9	±3.3	±3.8	±4.9
Neoprene	79.5	82.4	88.6	92.8
	±3.2	±4.7	±5.2	±6.3

The effect of wetting is more prominent for neoprene, meaning that the droplets become more spread on top of the neoprene surface than in the case of silicone. This is an indication of a more hydrophilic character of the neoprene. According to Ranc et al [27] using materials that facilitate formation of a water film would lead to a decrease of the observed friction. However, generally a higher friction coefficient was observed for neoprene-neoprene contacts compared to neoprene-silicone. This suggests that in the friction measurements not wetting but another effect dominates over the lubricant–surface interaction. Probably wetting and surface-lubricant interactions are more important at even lower pressures than was applied here.

In an alternative explanation for a system in which metal-rubber contacts were studied [27], it was suggested that less of the lubricant would flow into the contact zone when surfaces attract each other and friction will be higher at equal load [28]. This appears to be more in line with measurements since silicone is more hydrophobic than neoprene and more attraction will occur between the two neoprene surfaces. This would lead to less lubricant flowing into this contact, and indeed a higher friction coefficient for the neoprene–neoprene contact was observed compared to the neoprene - silicone contact at equal load, lubricant, and traction speed.

Surface roughness also differs between silicone and neoprene material. It is likely that surface roughness has an effect on the pressure dependence since multiple contacts at high contact pressure can cause high friction for irregular surfaces (Figure 2.8). The surface roughness of the material was estimated according to a 2D Fourier transform method [25] of the rubber images obtained with a scanning microscope. The asperities of the neoprene

($R_q = 31 \pm 10 \mu\text{m}$) are about three times bigger compared to silicone ($R_q = 9 \pm 4 \mu\text{m}$). This difference in size of the asperities likely contributes significantly to the 3 times higher friction of neoprene compared to silicone when water is used as a lubricant. Figure 2.7 shows that Stribeck curves obtained for different protein concentrations with a neoprene are more separated than with silicone, which might be due to the size of the asperities of the neoprene. Larger protein concentration can provide more material filling voids, which effectively lowers the surface roughness. In the case of silicone rubber that effect is weaker because asperities can be well leveled at lower concentrations.

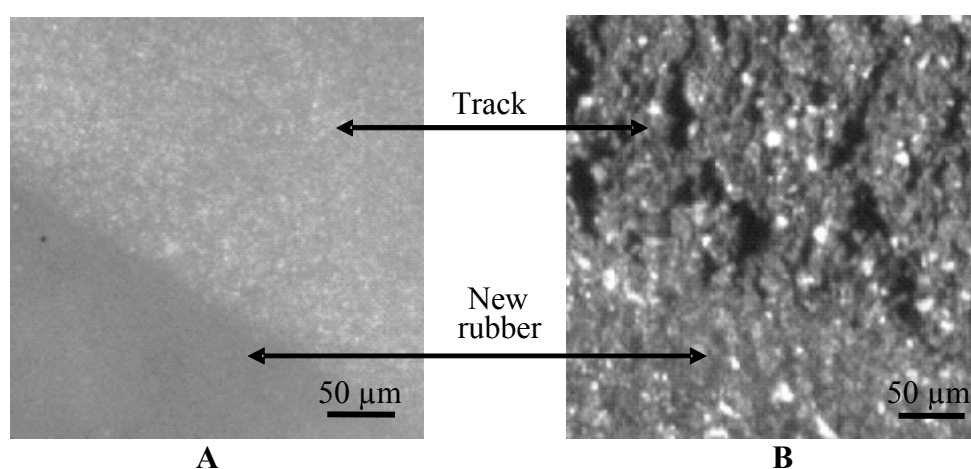


Figure 2.8 Scanning force microscope images obtained for silicone (A) and neoprene (B) rubber. The surface of the rubber before and after measurement is indicated.

2.3.4 Influence of viscosity on the friction coefficient

In the full-film elastohydrodynamic regime the friction coefficient strongly depends on the viscosity of the lubricants as is predicted by elastohydrodynamic (EHL) theory. However, the effect of aggregate size and shape is more complicated. It should be realized that EHL theory [29] confirms that in the tribometer a very high shear rate is applied. It was estimated that in the MTM even at very low velocities shear rates are already above 1000 s^{-1} . Thus tribological measurements occur in the region where the shear rate dependence of the viscosity is probably not so strong. Therefore, an analysis was made an analysis of the viscosity at the highest shear rates measured and the friction measurements at the high speed limit ($\sim 700 \text{ mm/s}$) (Figure 2.9).

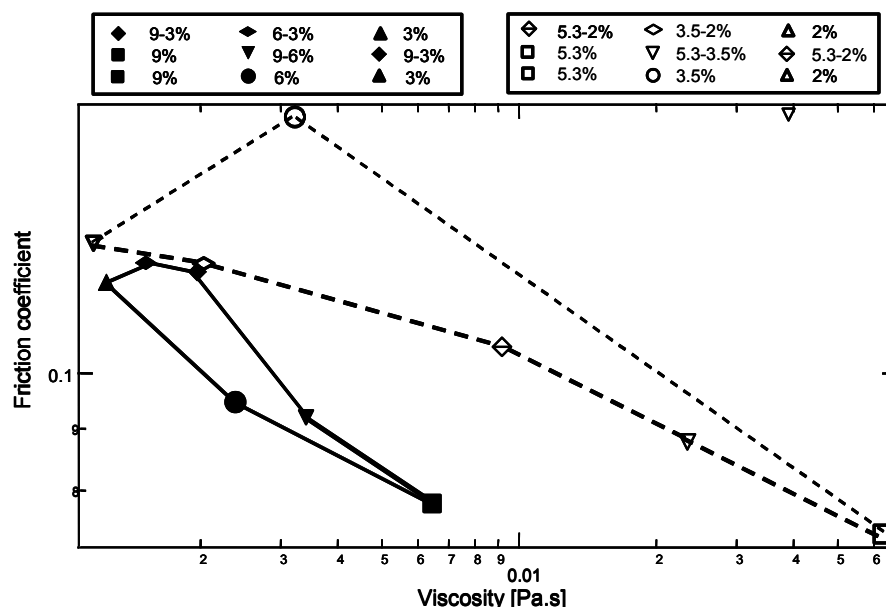


Figure 2.9 Friction coefficient obtained at high mean speed as a function of viscosity measured at high shear rate ($\sim 1000 \text{ s}^{-1}$). The points correspond to data obtained for WPI and ovalbumin protein aggregate dispersion. Filled symbols connected with solid lines and open symbols connected with dashed lines correspond to data obtained for WPI and ovalbumin, respectively.

Figure 2.9 demonstrates that WPI aggregates effectively lower the friction at much lower viscosities than ovalbumin aggregates. Next, it can be noticed that large ovalbumin aggregates are more effective at low concentration. This difference can be due to differences in shape or polymer-surface interactions.

Although in the mixed regime viscosity is not the main factor determining the friction coefficient, an attempt to estimate its contribution was made. In order to do this, a similar dependence of the friction on the viscosity and speed was assumed, as predicted by EHL. The Stribeck curve as a function of the product of the speed and the effective viscosity was investigated. The latter was chosen to be the viscosity measured at shear rate 1000 s^{-1} . It should be noted that this assumption is based on full-film lubrication, while that regime was not fully reached in this work. Figure 2.10 shows the friction coefficient versus the product of the speed and the effective viscosity for two different protein aggregate dispersions. The water curve is shown for comparison.

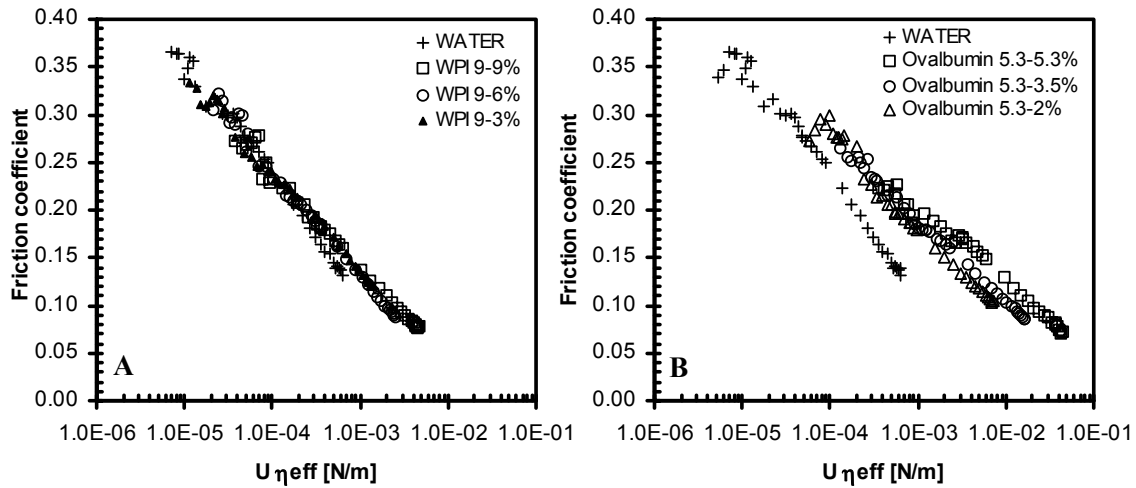


Figure 2.10 Friction coefficient versus effective viscosity (viscosity at shear rate of 1000 s^{-1}) for different concentrations of WPI (left) and ovalbumin (right). As a reference the water curve is also shown.

Different concentration curves of WPI collapse approximately to one line. This suggests that the initial assumption is valid and the decrease in the friction coefficient with concentration is purely from the increase in viscosity of the system. In the case of ovalbumin, however, the concentration data do not collapse, meaning that other effects besides viscosity such as ordering of the fibrillar ovalbumin aggregates also have a significant contribution to the friction.

2.4 Discussion

Lubrication studied in a soft contact

Results obtained in this chapter show that the concentration of protein aggregates as well as their size and shape in the lubricant significantly affects friction in a soft contact at relatively low pressure (50 -100 kPa). A higher concentration of aggregates as well as larger particle size provides better lubrication. The boundary friction is effectively lowered by all of the protein dispersions with respect to water in a concentration dependent manner. This shows that the number density of aggregates is more important at low speed. It can be speculated that the boundary regime is governed by the micro-properties of the aggregate solutions, i.e., number of aggregates, their size, and sample-surface interactions like necking and failure or adhesion properties. The observed differences between ovalbumin and WPI aggregates may be explained by the fibrillar shape of the ovalbumin aggregates, allowing them to more effectively interact with a rough surface due to shear

induced ordering within the contact zone. Interestingly, Vicente et al. have observed that xanthan and guar gum solutions display opposite behavior in a rubber-metal contact, which was much smoother than in this work. Asperity sizes of $R_q \approx 10$ nm for the elastomer and $R_q \approx 800$ nm in the case of steel [28] are over an order of magnitude smaller than the roughness present in this chapter ($31\text{ }\mu\text{m}$ for neoprene and $9\text{ }\mu\text{m}$ for silicone). At low speeds the friction coefficient shows a very strong dependence on the concentration, while at high speeds the concentration becomes less important. At high speed it is the macroscopic properties that determine the flow of the lubricant and friction.

The friction cannot be predicted from the lubricant viscosity properties alone. At low contact pressure the effect of the slide-to-roll ratio on friction is significant as is shown by study. During oral processing, the tongue presses the food against the palate. Since the latter does not move, it is assumed that sliding movements dominate in the mouth. In practice, this process is more complex as far as the mandible movement; teeth squeezing and chewing play a role as well. In general, it is not easy to fully reproduce the process of consumption. Thus, to understand the oral condition better, the effect of changing the ratio of sliding and rolling motion has to be studied in more detail.

Figure 2.10 shows that the difference in the friction coefficient due to concentration is caused mainly by viscosity in the case of WPI. For ovalbumin dispersions the friction is most likely influenced also by other effects. These samples, however, exhibit non-Newtonian behavior, which may affect the choice of the effective viscosity. Moreover the aggregates shape may also have some impact on the friction in the mixed regime. This effect, however, needs to be further investigated.

Deposition of protein material on the surfaces is probably an important issue that needs to be further studied. Higher protein concentration may cause a larger deposition of proteins, leading to formation of thicker adhered layers. Thus, when polymers adsorb on the material, a coating on the hydrophobic surface can occur, resulting in the reduction of the friction coefficient in the boundary regime. Also, deposition of material may explain the difference with the results for polysaccharide solutions as reported by Vicente et al. [28].

It is obvious that oral surfaces are elastic and tend to deform under pressure. However, to what extent this contributes to changes in friction is not clear. For this reason, in this work two different rubber surfaces with different properties were used. Neoprene rubber is more elastic, which causes lower contact pressure for neoprene – neoprene configuration. The rougher neoprene surface shifts the onset of the mixed regime to higher entrainment

speeds (up to 150 mm/s). In the highly concentrated ovalbumin solutions the onset of the mixed regime is again shifted to lower speeds, indicating that roughness is masked by high viscosity under this condition. A hypothesis can be made that, for large enough asperities, the protein aggregate particles can be easily trapped in between them, thus effectively countering the roughness. This implies that adding protein aggregates induces a better lubrication on neoprene compared to silicone, which may explain the difference in concentration dependence observed in Figure 2.7 .

2.5 Concluding Remarks

This chapter has shown that physical parameters such as normal load, elasticity, and slide-roll ratio influence friction at conditions that are relevant for oral processing. At pressures and traction speeds relevant to oral conditions, as applied in current study, the amount of friction is influenced both by the bulk viscosity of the food in the mouth and by the roughness, elasticity, and surface-surface interactions of the oral tissue with the food. This suggests that it may possible to control oral perception by adjusting the friction either by changing concentration or by modulating surface roughness. Lubrication may be improved through the introduction of higher deformability of the surfaces and relatively high viscosity liquids. Surface roughness will counter this effect. The viscosity of the sample can be increased by raising the protein concentration, while the surface roughness on the other hand can be adjusted in the mouth by using material-surface interactions which especially have been noted for fibrillar ovalbumin aggregates.

Clearly, both aspects need to be studied in more detail before they can be applied in real food systems.

Acknowledgements

The authors gratefully acknowledge Jan Klok (NIZO) for assistance with the microscopy measurements, Anne van de Pijpekamp (WCFS and TNO) for experimental assistance, Kyriaki Zinoviadou (WCFS) for advice on the contact angle experiments, and Harmen de Jongh (WCFS) for carefully reading the manuscript.

References

- 1 Tyle, P. *Acta Physiol.* 1993, 84, 111–118.
- 2 Engelen, L.; de Wijk, R.; der Bilt, A.; Prinz, J. F.; Janssen, A. M.; Bosman, F. *Physiol. Behav.* 2005, 86, 111–117.
- 3 Bogue, J.; Sorenson, D.; Delahunty, C. Determination of Consumers' Sensory Preferences for Full-fat and Reduced-fat Dairy Products, Agribusiness Discussion Paper No. 37, 2002.
- 4 Phillips, L. O.; McGiff, M. L.; Barbano, D. M.; Lawless, H. T. The Influence of Fat on the Sensory Properties, Viscosity, and Color of Lowfat Milk. *J. Dairy Sci.* 1995, 78, 1258–1266.
- 5 Malone, E.; Appelqvist, I. A. M.; Norton, I. T. *Food Hydrocolloids*, 2003, 17, 763–773
- 6 Imai, E.; Saito, K.; Hatakeyama, M.; Hatae, K.; Shimada, A. *J. Texture Stud.* 1999, 30, 59–88.
- 7 Langton, M.; Åström, A.; Hermansson, A. M. *Food Hydrocolloids* 1997, 11, 217–230.
- 8 Lawless, H. T.; Heymann, H. *Sensory evaluation of food: principles and practices*; Chapman & Hall: New York, 1998; pp 379–405.
- 9 Kokini, J. L. *J. Food Eng.* 1987, 6, 51–81.
- 10 Giasson, S.; Israelachvili, J.; Yoshizawa, H. *J. Food Sci.* 1997, 62, 640–646.
- 11 Luengo, G.; Tsuchiya, M.; Heuberger, M.; Israelachvili, J. *J. Food Sci.* 1997, 62, 767.
- 12 Cassin, G.; Heinrich, E.; Spikes, H. A. *Tribol. Lett.* 2001, 11.
- 13 Christiansen, J. B. 1979, 5, 335–337.
- 14 Shama and Sherman (1973), *J. Texture Studies* 4(1), 111–118.
- 15 Malone, E.; Appelqvist, I. A. M.; Norton, I. T. *Food Hydrocolloids* 2003, 17, 775–784.
- 16 Lee, S.; Heuberger, M.; Rousset, P.; Spencer, N. D. *Tribol. Lett.* 2004, 16, 239–249.
- 17 De Wijk, R. A.; Prinz, J. F. *Food Qual. Prefer.* 2005, 16, 121–129.
- 18 Alting, A. C.; Weijers, M.; de Hoog, E. H. A.; van de Pijpekamp, A. M.; Stuart, M. C.; Hamer, R. J.; de Kruif, K. G.; Visschers, R. W. *J. Agric. Food Chem.* 2004, 52, 623–631.
- 19 Alting, A. C.; Hamer, R. J.; de Kruif, K. G.; Paques, M.; Visschers, R. W. *Food Hydrocolloids* 2003, 1–11.
- 20 Weijers, M.; Nicolai, T.; Visschers, R. W. *Macromolecules* 2002, 35, 4753–4762.
- 21 Alting, A. C.; Hamer, R. J.; de Kruif, K. G.; Visschers, R. W. *J. Agric. Food Chem.* 2000, 48, 5001–5007.
- 22 Weijers, M.; Barneveld, P. A.; Stuart, M. A. C.; Visschers, R. W. *Protein Sci.* 2003, 12, 2693–2703.
- 23 Greenwood, J. A. Analysis of elliptical Hertzian contacts. *Tribol. Int.* 1997, 30, 235–237.
- 24 Brewe, D. E.; Hamrock, B. J. Simplified solution for elliptical contact deformation between two elastic solids. *ASME, J. Lub. Technol.* 1977, 99, 485–487.
- 25 De Jong, S. & van de Velde, F. Charge density of polysaccharide controls microstructure and large deformation properties of mixed gels. *Food Hydrocolloids* 21 (2007) 1172–1187
- 26 Bowden, F. P.; Tabor, D. Friction, lubrication and wear: a survey of work during the last decade. *Br. J. Appl. Phys.* 1966, 17, 1521–1544.
- 27 Ranc, H.; Elkhyat, C.; Servais, C.; Mac-Mary, S.; Launay, B.; Humbert, P. *Physicochem. Eng. Aspects* 2006, 276, 155–161.
- 28 De Vicente, J.; Stokes, J. R.; Spikes, H. A. *Tribol. Int.* 2005, 38, 515–526.
- 29 De Vincente, J., Stokes, J. R. & Spikes, H. A. (2006) *Food Hydrocolloids*, 20(4), 483–491

Chapter 3

**The interactions between oil droplets and gel matrix
affect the lubrication properties of sheared emulsion-
filled gels**

Abstract

In this chapter the lubrication behaviour of emulsions, gels, and emulsion-filled gels was studied in relation to their composition and structure. It was found that emulsions had much lower friction coefficients than those of their continuous phases. Emulsions with 40 wt % oil had the same friction coefficient as the pure oil. The lubrication properties of the gels, sheared by pressing them through a syringe, strongly depended on the molecular properties of the gelling agent and on the breakdown behaviour of the gel matrix. For each type of emulsion-filled gel, the lubrication behaviour was affected by the interactions between oil droplets and matrix. For gels containing oil droplets bound to the matrix, the friction coefficient gradually decreased with increasing oil concentration. For gels containing oil droplets non-bound to the matrix, the friction coefficient of the filled gels was lower than that of the same gel matrix without oil. However, no effect of the oil concentration on friction was observed. The different effects of the oil concentration on the lubrication behaviour of the various gels were explained by the relation between droplet-matrix interactions and the 'apparent viscosity' of the sheared gels. For gels with bound droplets, increasing the oil concentration resulted in an increase of the 'apparent viscosity' of the sheared gel. For gels with unbound droplets, the oil concentration did not affect the 'apparent viscosity'. Confocal Laser Scanning Microscopy (CLSM) observations of both emulsions and filled gels did not reveal coalescence of the oil droplets as a result of the shear treatment inherent to friction measurements.

3.1 Introduction

During oral processing food products are confined to thin films between the oral tissues. Tribology studies the mechanics of friction, lubrication and wear of interacting surfaces that are in relative motion. Tribology and thin-film rheology allow to mimic in-mouth conditions (forces and surfaces) and are used to study the lubrication properties of food. Oral friction is influenced by: (i) the type of food consumed and its lubrication properties, (ii) the interactions between the lubricants and the surfaces, (iii) the properties of the oral tissues, and (iv) physical parameters like the sliding to rolling motion between the tongue and palate as well as the force applied during food consumption. Thin-film rheological properties of foods have been related to the sensory perceptions of mouth-feel, texture and taste [1].

The behaviour of a lubricant between two rubbing surfaces is characterised in the form of a so-called Stribeck curve. In this curve the friction coefficient, defined as $\mu = F_f/W$ (where F_f and W are a friction force and normal load, respectively), is given as a function of the entrainment speed. The friction behaviour can be classified into three separate regimes that are distinguishable in the Stribeck curve. The boundary lubrication regime is present at low speeds, where the friction is affected by both the surface-surface interaction dominated by the asperities and ability of the lubricant to form a boundary interfacial film. In the hydrodynamic regime, present at the high speeds, the surfaces are fully separated and the lubrication is governed by bulk rheological properties of the lubricant. Between those two regimes a mixed regime can be recognised, where the pressure of the fluid carries only part of the load, while the other part is sustained by the surface asperities. In this case the two surfaces are not fully separated [1,2]. The pattern of the Stribeck curves strongly depends on the properties of lubricant and rotating materials, as well as on the experimental conditions applied during measurement.

For semi-solid foods containing emulsified fats and oils, an attempt was made to correlate the sensory attributes generated by a panel to rheological and friction measurements [3-5]. For custards, the mouth-feel attribute *creamy* was not correlated to small deformation measurements (dynamic stress and frequency sweep) or large deformation properties (flow curves and steady shear rate behaviour). The oral perception of these foods was reported to be related to their lubrication properties [6] measured with a friction tester with a metal-rubber configuration. Increasing the fat content resulted in a decrease of the friction coefficient as well as in an increase of creaminess of the products.

The decrease of friction observed as a result of the structure breakdown by α -amylase in starch containing products was explained with a surfacing mechanism of the oil droplets released from the starch matrix. The presence of particles caused on the other hand astringent sensations and higher friction. Similar results were found by Malone et al. for polymer solutions, emulsions and different types of milk [7].

The lubrication properties of gels have not been studied extensively and those of sheared gels have not been reported. Chen et al. [8] measured the surface friction of WPI gels and studied the relation between speed and friction. Chen et al. also investigated the influence of the surface roughness of the gel on the surface friction.

The rheological properties and the breakdown behaviour of gels filled with emulsions droplets can be varied by changing the interactions between oil droplets and gel matrix, the oil content and the oil droplet size [9-11]. In previous studies it was shown that the interactions between the oil droplets and the gel matrix in gelatine, κ -carrageenan and cold-set acid-induced whey protein isolates (WPI) gels could be varied by changing the emulsifying agent used for emulsion preparation [12-14]. The oil droplets were bound to the matrix in gelatine gels containing emulsions stabilised by WPI, in κ -carrageenan containing emulsions stabilised by lactoferrin and in WPI gels containing emulsions stabilised by WPI aggregates. This resulted for all gels in an increase of the gel modulus and a decrease of the fracture strain with increasing oil concentration. In gelatine and κ -carrageenan gels with bound droplets the fracture stress decreased, whereas in WPI gels it increased. The oil droplets were not bound to the matrix in gelatine gels containing Tween 20-stabilised emulsions and in κ -carrageenan containing emulsions stabilised by WPI. This gave a decrease in gel modulus and fracture stress with increasing oil concentration. The fracture strain also decreased, but less than in gels with bound droplets.

In an explorative study on the sensory properties of emulsion-filled gels with different matrices, gels with unbound droplets or melting in the mouth were evaluated as more creamy [15]. Therefore, it was hypothesised that for emulsion-filled gels the perception of mouth-feel attributes related to the presence of oil droplets could be mediated by the release of the droplets from the gel matrix upon oral processing. A following study on the relation between oil droplets release and sensory perception revealed that the release of the oil droplets is not the only mechanism explaining the perception of creaminess and fattiness in emulsion-filled gels [16].

We hypothesised that the lubrication behaviour of emulsion-filled gels might be another factor involved in their sensory perception. Therefore, in this chapter we investigate the effect of the individual components of emulsion-filled gels on their lubrication properties by using a tribometer modified to obtain a low contact pressure. Our simulated environment mimics in that respect oral conditions. The effect of saliva on friction is also studied. The chosen systems are gelatine, κ -carrageenan and cold-set, acid-induced WPI gels, containing both bound and unbound oil droplets.

3.2 Materials and methods

3.2.1 Materials

Porcine skin gelatine PBG 07 (bloom 280, isoelectric point 8-9) was kindly provided by PB gelatines (Vilvoorde, Belgium). Kappa-carrageenan was kindly donated by CP Kelco (Lille Skensved, Denmark). The κ -carrageenan sample consisted of 93% mol κ -units and 7% mol ι -units, as determined by NMR spectrometry [17]. Powdered whey protein isolate (WPI, BiproTM) was obtained from Davisco International Inc. (La Sueur, MN, USA). Tween 20 (Polyoxyethylene sorbitan monolaurate, in the text referred to as Tween) was obtained from Sigma (Sigma-Aldrich Chemie BV, Zwijndrecht, The Netherlands). Sodium-caseinate and lactoferrin were kindly donated by DMV International, (Veghel, The Netherlands). Medium Chain Triglycerides (MCT) MIGLYOL 812N oil was purchased from Internatio BN (Mechelen, Belgium). Potassium chloride (p.a.) was obtained from Merck (Darmstadt, Germany). Glucono- δ -lactone (GDL) was kindly donated by Purac (Gorinchem, The Netherlands). All materials were used without further purification. All solutions were prepared with demineralised water.

3.2.2 Sample preparation

Emulsions

WPI solutions were prepared by adding the protein to the required amount of demineralised water. Subsequently, the solutions were gently stirred for 2 hours. Stock emulsions, consisting of 40 wt% MCT oil and 60 wt% aqueous phase containing 1 wt% WPI, were prepared by pre-homogenising the ingredients using an Ultra Turrax (Polytron, Kinematica AG, Lucerne, Switzerland) homogeniser. Pre-emulsions were further processed using a laboratory homogeniser (Ariete, Model NS1001L 2K – Panda 2K, Niro Soavi S.p.A, Parma, Italy). The same procedure was used for the preparation of the

emulsions stabilised with Tween and lactoferrin, except that the emulsifying agent concentration in the aqueous phase was 2 wt%. WPI-stabilised emulsions were used for the preparation of filled gelatine and κ -carrageenan gels. Tween-stabilised emulsions were used for the preparation of filled gelatine gels and lactoferrin-stabilised emulsions for the preparation of filled κ -carrageenan gels. KCl was added to the emulsions used for the preparation of κ -carrageenan gels, up to a concentration of 30 mM in the aqueous phase.

Emulsions stabilised with WPI aggregates were prepared as described above, but using a 3 wt% WPI aggregates dispersion as continuous phase. This dispersion was prepared by heating a 9 wt% WPI solution at 68.5°C for 2 hours and subsequent cooling to room temperature with tap water and subsequent dilution to 3 wt% with demineralised water. WPI aggregates-stabilised emulsions were used for the preparation of filled WPI gels.

The droplet size distribution of the obtained emulsions was measured using a Malvern Mastersizer 2000 (Malvern Instruments Ltd., Malvern, UK). The homogenisation pressure, the droplet volume-surface average or Sauter diameter ($d_{3,2}$) and the pH of the emulsions used for the preparation of the filled gels are reported in Table 3.1.

Table 3.1 Homogenisation pressure (1 pass), volume-surface average diameter (Sauter diameter) (\pm standard error) and pH (\pm standard error) of the emulsions used for the preparation of the filled gels.

Emulsifier in the water phase	Homogenisation pressure (bar)	$d_{3,2}$ (μm)	pH
1 wt% WPI	400	1.15 \pm 0.05	7.06 \pm 0.02
2 wt% Tween	50	0.10 \pm 0.05	4.30 \pm 0.02
2 wt% Lactoferrin	400	1.85 \pm 0.05	5.10 \pm 0.02
3 wt% WPI aggregates	500	1.45 \pm 0.05	6.64 \pm 0.02

Gels

Gelatine (4 wt%) and WPI (3 wt%) gels were prepared in demineralised water. Kappa-carrageenan (0.6 wt%) gels were prepared in a 30 mM KCl solution. Samples were prepared without emulsion and with different oil concentrations (5, 10 and 20 wt%). In all samples the concentration of the gelling agent in the aqueous phase was kept constant.

To obtain efficient dissolution of κ -carrageenan and gelatine, the gelling agent was first allowed to hydrate for 2 hours under gentle stirring at room temperature. The samples were subsequently dissolved by heating at 80°C for 30 minutes and cooled to 45°C. For κ -

carrageenan gels, prior to emulsion addition the emulsion was heated to 45°C before mixing. For gelatine gels, the gelling agent solution was allowed to cool to 20°C prior to mixing with the emulsion. This procedure was applied to prevent depletion flocculation of the emulsion droplets before gel formation (Sala et al. 2007). After mixing, the samples were stirred for 1 minute by a magnetic stirrer. Subsequently they were allowed to gel at room temperatures in 60 ml plastic syringes (internal diameter 26.4 mm).

Gelation of the WPI gels was induced by addition of GDL (0.22 wt% in the case of WPI aggregates dispersion with a concentration of 3 wt%) to the WPI dispersion and to the WPI dispersion/emulsion mix and incubation at 25°C for 17 hours. The final pH of the gels was about 4.8. The WPI dispersion was prepared as described above.

3.2.3 Friction measurements

The lubrication properties of emulsifier solutions, emulsions and sheared gels were measured between two rotating surfaces in a Mini Traction Machine (MTM, PCS Instruments, London). A low contact pressure was assured by the selection of deformable materials: a neoprene ring and a silicone disc (see Chapter 2 [18]). In Chapter 2, Figure 2.1 a schematic representation of the MTM tribometer was shown.

Relevant physical parameters for friction measurements are the normal load (the force pressing the rubber ring against the disc), the temperature of the system, the tangential (entrainment) speed of the two rotating surfaces at the contact point and the slide-to-roll

ratio, defined as $SRR = \frac{U_{disc} - U_{ring}}{U}$, where the U_{disc} is the mean tangential speed of the disc, U_{ring} that of the ring and U the mean tangential speed at the contact between the surfaces. These physical parameters can be varied in the MTM tribometer.

The friction was then measured as a function of the applied entrainment speed. In order to mimic oral relevant conditions, the mean speed of the ring and the disc was kept in a range between 10 and 100 mm/s. As commonly used in literature, the SRR of 50 % was applied, which corresponds to a mixed rolling-sliding contact. This type of contact was chosen to minimise possible wear damage of the soft surfaces. The temperature was set to 37°C ($\pm 1^\circ\text{C}$), as in the human mouth, while the normal load was chosen to be 3 and 5 N. Since only a part of the Stribeck curve was recorded, the results will be referred to as friction curves. For gelatine gels, friction measurements were also carried out at 20°C. Before each experiment all the rubbers were cleaned with an ethanol, demineralised water

and dried with compressed air. For each measurement, a new neoprene ring and a new silicone disc were used.

For all systems studied the tribometer reservoir was completely filled to assure that the lubricant was present between the rotating surfaces. Measurements were carried out in triplicate. The gels (typical weight of the specimens: 55 g) were prepared in syringes with a capacity of 60 ml. Prior to friction measurement, the emulsion-filled gels systems were destroyed by pushing them out of the syringe in which they were prepared.

For emulsions and gels, the friction measurements were also carried out after addition of 7 wt% water or saliva. Stimulated saliva was collected from 3 healthy, non-medicated donors that refrained from eating and drinking, with the exception of water, for two hours before donation. The donors collected the produced saliva in ice-chilled containers. The collected saliva of all donors was mixed and added to a weighed amount of emulsion or broken gels prior to application to the reservoir of the tribometer. The mix sample/ water or saliva was accurately stirred with a spatula. The saliva percentage was chosen as a good approximation of the ratio between saliva and food during bolus formation (A. Janssen, personal communication).

3.2.4 Rheological measurements

The ‘apparent viscosity’ of the gels sheared by forcing them out of the syringe in which they were prepared was measured at 37°C using a rheometer (AR 2000, TA Instruments, Leatherhead, UK) with a vane geometry. For gelatine gels also measurements at 20°C were carried out. The vane had four blades, a diameter of 28 mm, a height of 42 mm and was used in combination with a cylindrical shaped cup with a diameter of 70 mm. After lowering the vane into the sheared gel, rotating movements were applied. The ‘apparent viscosity’ was measured at steady shear rate as a function of time. The experiments were done with two steps. First, a step at a shear rate of 10 s⁻¹ was applied for 2 minutes. Then a step at a shear rate of 100 s⁻¹ followed for 5 minutes. The data collected at a shear rate of 100 s⁻¹ were used for analysis. Measurements were carried out in duplicate.

3.2.5 Confocal Laser Scanning Microscopy (CLSM)

The microstructure of the emulsion-filled gels was visualised with confocal laser scanning microscopy. Observations were made on the gels before and after friction measurements as well as on the silicone rubber used. A combination of Fluorescein isothiocyanate with

Nile Blue (FITC/NB) was used to stain the protein and oil phases, respectively. Nile Blue was chosen as a staining agent of the oil droplets in order to specifically reveal possible coalescence or aggregation. CLSM-images were recorded on a LEICA TCS SP Confocal Scanning Laser Microscope (Leica Microsystems CMS GmbH., Mannheim, Germany), equipped with an inverted microscope (model Leica DM IRBE), used in the single photon mode with an Ar/Kr visible light laser. A Leica objective lens (63x/UV/1.25NA/water immersion/PL APO) was used. The excitation wavelength was set at 488 nm. Digital image files were acquired in tagged image file format and at 1024x1024 pixel resolution.

3.3 Results

The aim of this chapter was to establish the link between the lubrication properties of emulsion-filled gels and their composition and structure. To achieve this goal, the contribution of all components of the gels to their lubrication properties was studied. Therefore, lubrication measurements were carried out on the individual components of the gel. For both the emulsions and the gels, the effect of the oil concentration on lubrication properties was studied. Furthermore, in order to simulate the lubrication properties under oral conditions the effect of saliva on the lubrication behaviour of all systems was studied as well.

3.3.1 *Lubrication properties of the emulsions*

Figure 3.1 shows the friction coefficient of the WPI stabilised emulsion and its components as a function of the entrainment speed. A mixed lubrication regime was observed for water, the WPI solution and the 10 wt% emulsions for the whole range of the speeds measured. The friction coefficient of the solution of the emulsifying agent was about 0.2 lower than that of water. Ten wt% oil in the emulsion remarkably improved the lubrication properties compared to the emulsifying agent. An increase of the oil concentration up to 40 wt% led to only a slight decrease of the friction coefficient. At this oil concentration the hydrodynamic regime appeared to dominate over the whole speed range. In the hydrodynamic regime the lubrication properties are determined by the oil droplets entering the contact zone. When MCT oil was used as a lubricant the lubrication behaviour was about the same as that measured for the emulsion with 40 wt% oil. For the other emulsifying agents the friction curves of their solutions and of the emulsions were comparable to those shown in Figure 3.1 (results not shown).

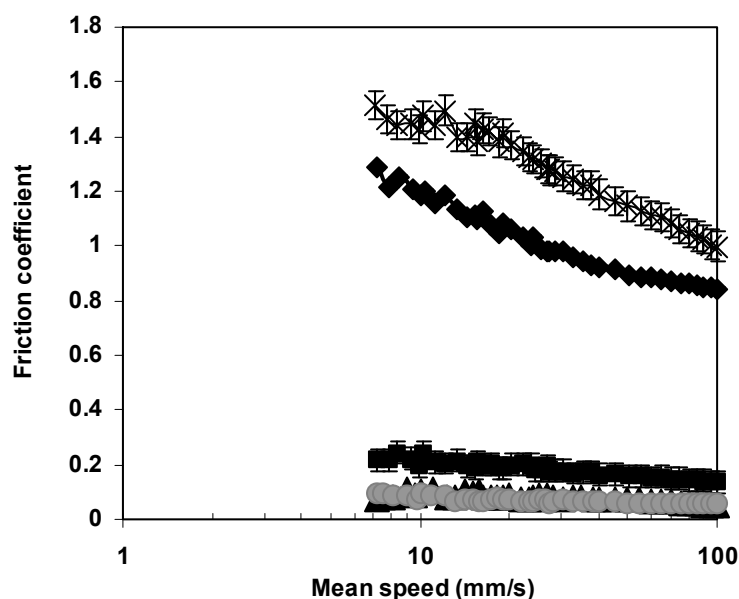


Figure 3.1 Friction curves of components of WPI stabilised emulsions (X: water; ◆: solution 1 wt% WPI; ■ emulsion with 10 wt% oil ▲: emulsion with 40 wt% oil; ●: MCT oil; Load: 3 N).

In Figures 3.2A and B the friction coefficients for the different emulsions are plotted as a function of the oil concentration at the entrainment speeds of 10 and 100 mm/s, respectively. For all emulsions the emulsifying agent solutions had higher friction coefficients compared with the emulsions in which they were used (Figure 3.2). Solutions of Tween 20 showed lower friction coefficient than protein solutions. Increasing the oil content in the emulsions up to 1 wt% led to large decrease of the friction coefficient (~ 0.5 for the emulsions stabilised by protein, ~ 0.18 for the emulsions stabilised by Tween 20). For all types of emulsion, a further increase of the oil concentrations up to 40 wt% gave lower values of the friction coefficient, comparable to that obtained for MCT oil. The lubrication properties of the emulsion at low oil concentration appear to be determined by both the emulsifying agent and the oil droplets concentration. On the other hand, at high oil concentration these properties appear to be affected by the oil droplets. For both speeds a similar behaviour was observed. Friction was lower at higher velocity as is expected for a mixed lubrication regime.

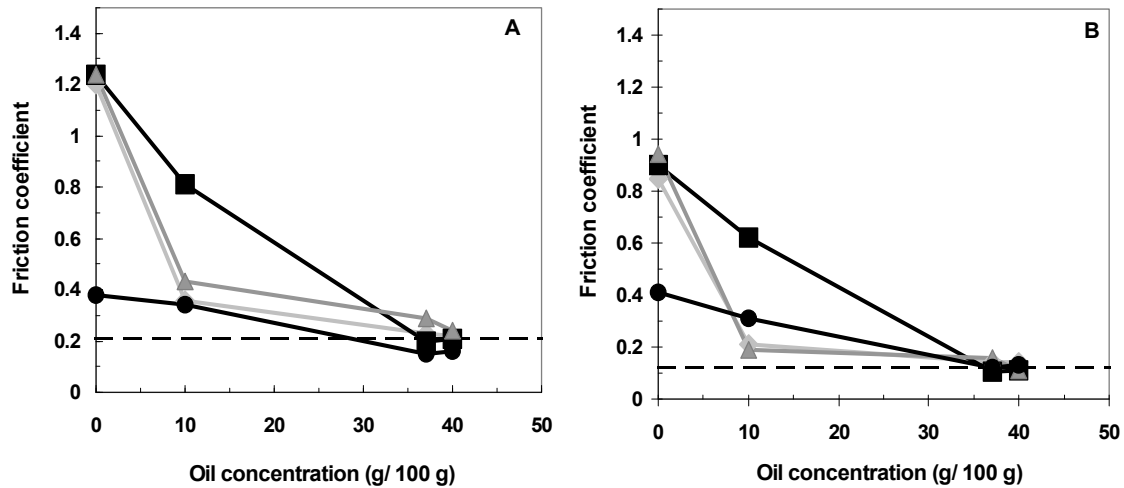


Figure 3.2 Friction coefficient vs. oil concentration for emulsions stabilised by different emulsifying agents and for MCT oil (◆: 1 wt% WPI; ■: 3 wt% WPI aggregates; ▲: 1 wt% lactoferrin; ●: 2 wt% Tween 20. The dashed line represents the friction coefficient of pure MCT oil. Load: 3 N. A: Entrainment speed= 10 mm/s; B: Entrainment speed= 100 mm/s).

Table 3.2 shows the effect of the saliva on the friction coefficient of the four different emulsions with 40 wt% oil, stabilised by different emulsifying agents at 10 and 100 mm/s. Differences in friction coefficient between the emulsions could be only observed at low speed. No significant differences were observed between the systems with 7 wt% water and those with the same amount of saliva. It seems evident that saliva does not affect friction. An exception was the lactoferrin-stabilised emulsion, for which the friction coefficient with saliva was 30% lower compared to that for the emulsions with added water. In this case complexation between lactoferrin, which is positively charged at the pH of the emulsion, and the negatively charged mucins present in saliva might occur. This can lead to aggregation of emulsion droplets caused by saliva addition, as reported by [19]. Aggregation of oil droplets could decrease friction by two different mechanisms. It could either result in an increase of the effective viscosity of the emulsion or facilitate the entrance of the oil droplets into the contact zone between disc and ring.

Table 3.2 Effect of water and saliva on friction coefficient (\pm standard deviation) in emulsions with 40 wt% oil and stabilised by different emulsifying agents (entrainment speeds: 10 and 100 mm/s).

Emulsifying agent	Entrainment speed			
	10 mm/s		100 mm/s	
	7 wt% water	7 wt% saliva	7 wt% water	7 wt% saliva
1 % WPI	0.23 \pm 0.02	0.25 \pm 0.02	0.14 \pm 0.05	0.15 \pm 0.03
3 % WPI	0.20 \pm 0.02	0.21 \pm 0.01	0.11 \pm 0.04	0.12 \pm 0.02
1 % lactoferrin	0.29 \pm 0.07	0.19 \pm 0.05	0.16 \pm 0.03	0.10 \pm 0.02
2 % Tween	0.15 \pm 0.02	0.19 \pm 0.02	0.12 \pm 0.04	0.16 \pm 0.06

3.3.2 Lubrication properties of the gels without oil

In a preliminary phase of the study, the gels were allowed to gel on top of the silicone disc. Following this procedure only 5 ml of the sample could be used for measurement. In this case the gelled samples were destroyed by the rotating surfaces within a few seconds from the beginning of the measurements. The destruction of the gels was uncontrolled and part of the samples fell out of the disc. As a consequence, the rotating surfaces were not constantly in contact with the lubricant. Therefore, a previously described technique to break the gel in a controlled way by means of a Texture Analyzer was applied [16]. This technique was subsequently compared to manually squeezing the gels out of the syringes. No effect of the breakdown technique was observed on the friction properties of the gels. Therefore, the manual procedure was applied for the measurements. The absence of effect of the breakdown procedure on friction properties was confirmed by the good reproducibility of the results for gels manually squeezed out of different syringes. The sheared gels consisted of thick, viscous, pourable fluids. The homogeneity of these fluids was only visually evaluated and varied with the type of gel matrix. Before starting the friction measurements the destroyed gel was spread on the top of the silicone disc placed in the tribometer.

The friction curves of the three gel matrices without oil droplets are shown in Figure 3.3. The friction curve of gelatine was lower than those of κ -carrageenan and WPI. The temperature of 37°C was applied during these measurements to mimic oral conditions. Since at this temperature gelatine gels were molten, for these gels friction measurements were carried out also at 20°C, at which they were not molten. For gelatine gels, the friction coefficient measured at 20°C was only slightly lower than that measured at 37°C. At 20°C gelatine gels broke down into a highly homogeneous material. Consequently, the lubrication behaviour of gelatine gels without oil droplets is only

partially related to their physical state (molten/gelled). The molecular properties of the gelling agents are likely to play an important role. The sheared κ -carrageenan and WPI gels were not homogenous, resulting in a large variation in the size of the gel particles. The latter sample (WPI) broke down into large pieces and a serum phase was released. In this sample, the lubrication properties were probably dominated by the exuded water phase with small pieces of broken down gel, whereas large gel particles were not entering the contact zone between the two rotating parts. As a result, WPI gels had the highest friction coefficient compared to the two other systems. Compared to WPI, the κ -carrageenan gels broke down into more defined and homogenous structures, which may explain the lower friction coefficient.

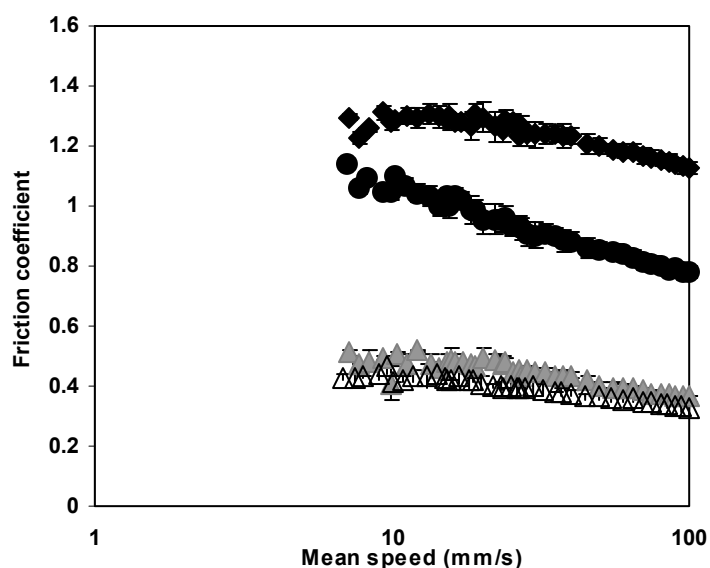


Figure 3.3 Friction curves of the three gel matrices studied (\blacklozenge : WPI; \blacktriangle : gelatine 37°C; \triangle : gelatine 20°C; \bullet κ -carrageenan; Load: 3 N).

3.3.3 Lubrication properties of the filled gels

The presence of oil droplets in the gel matrix remarkably affected the lubrication behaviour of the gels. For gelatine gels, the effect of the oil droplets on lubrication properties was temperature-dependent. At 37°C, gelatine gels containing unbound oil droplets (Tween-stabilised emulsions) had a lower friction coefficient than that of gels without oil, as measured at 100 mm/s (Figure 3.4). For these gels, the friction coefficient decreased to 0.15 at 5 wt% oil and remained approximately constant with a further increase of the oil content. At 37°C, no effect of the presence of oil droplets was observed

for the gelatine gels containing bound droplets (WPI-stabilised emulsions). At the temperature of the measurement gelatine gels, both with bound and unbound droplets, were molten, resulting in a homogenous, emulsions-like fluids.

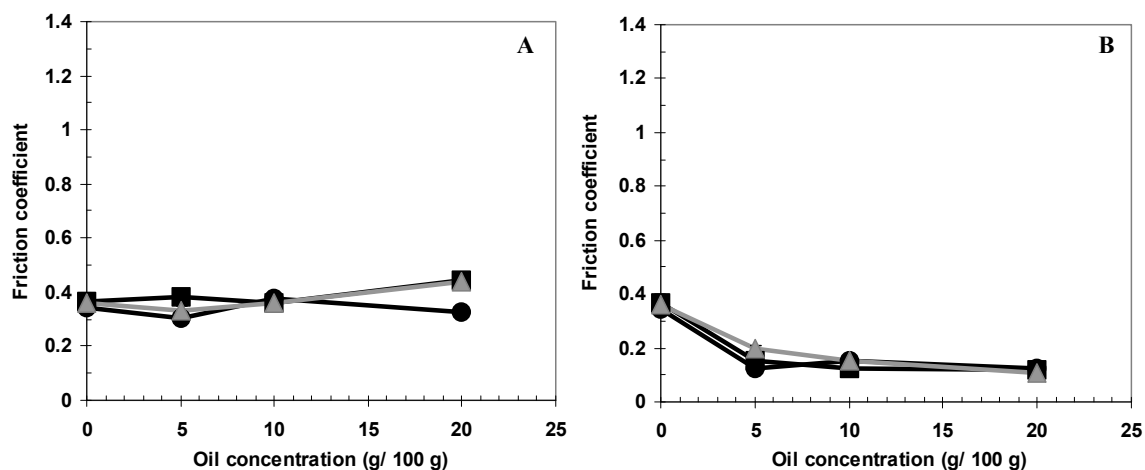


Figure 3.4 Friction coefficient vs. oil concentration for gelatine gels (■) with either bound (A) or unbound (B) droplets and for the same gels after addition of either 7 wt% water (●) or 7 wt% saliva (▲). Measurements temperature: 37°C. (Entrainment speed: 100 mm/s; Load: 3 N).

The observed results suggest that under these conditions the gelatine matrix determinates the lubrication. The molten gelatine, due to its very sticky properties, may form a film between the surface of the disc and that of the ring, masking the effect of the emulsion droplets. No effect of the water or saliva on friction was observed for gelatine gels. Friction measurements performed at 20°C showed a gradual decrease of the friction coefficient of gelatine gels containing the WPI-stabilised emulsion (bound droplets, Figure 3.5). For gelatine gels containing the Tween-stabilised emulsion (unbound droplets), no effect of temperature on friction was observed (Figure 3.5).

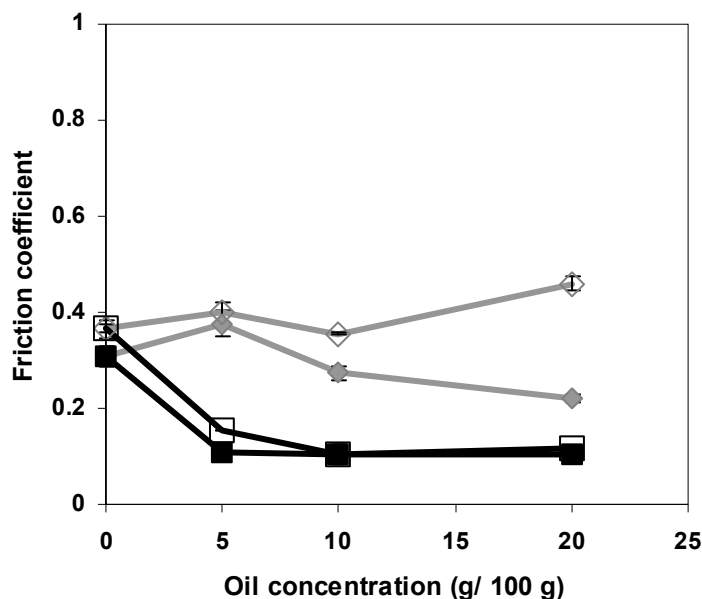


Figure 3.5 Friction coefficient vs. oil concentration for gelatine gels with either bound (♦) or unbound (■) droplets and at two different temperatures. (Open symbol: 37°C; filled symbol: 20°C) (Entrainment speed: 100 mm/s; Load: 3 N).

For κ -carrageenan gels, a significant decrease of the friction coefficient to about 0.15 was observed already at 5 wt% oil (Figure 3.6). Further increase of the oil concentration did not affect the friction coefficient. For these gels, the interactions between droplets and matrix do not have an effect on lubrication (therefore, in Figure 3.6 only the data for gels with bound droplets are shown). For both gels with bound and unbound droplets, no effect on friction was observed of dilution with 7% water or saliva. Both the emulsions stabilised by lactoferrin and WPI showed a friction coefficient below 0.1 already at 10 wt% oil (Figure 3.2). This value of the friction coefficient is comparable to that of the κ -carrageenan filled gels.

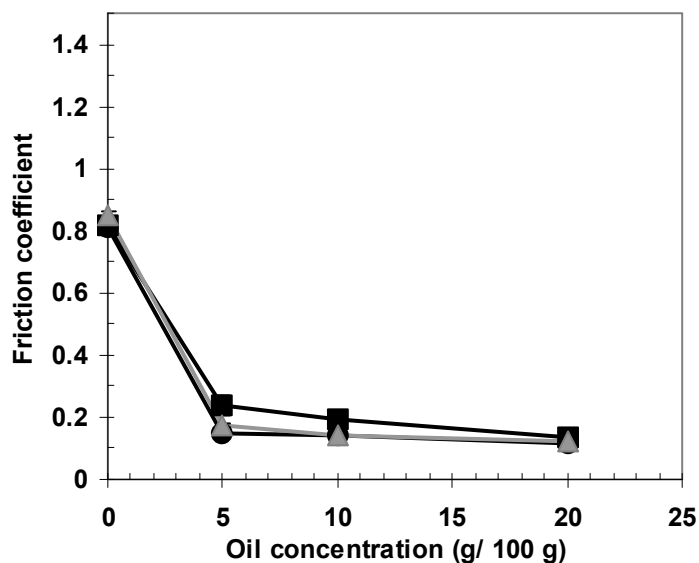


Figure 3.6 Friction coefficient vs. oil concentration for κ -carrageenan gels (■) with bound droplets and for the same gels after addition of either 7 wt% water (●) or 7 wt% saliva (▲). (Entrainment speed: 100 mm/s; Load: 3 N).

Figure 3.7 shows the effect of the oil concentration on the friction coefficient of WPI gels. These gels contain emulsions stabilised by WPI aggregates, which lead to oil droplets bound to the matrix. A small amount of oil (up to 5 wt%) present in the gel did not improve the lubrication properties significantly with respect to the gel matrix without the oil (~ 1.1). However, at oil concentrations above 5 wt% a gradual decrease of the friction coefficient was observed. At 20 wt% oil a friction coefficient of 0.2 was reached. For the emulsion stabilised by WPI aggregates, this value of the friction coefficient was obtained above 30 wt% of oil concentration (Figure 3.2). This suggests that a synergy between gel matrix and emulsion droplets may exist, lowering the lubrication properties of these gels with increasing oil concentration. As compared to gelatine and κ -carrageenan gels, the friction coefficient observed for WPI gels at any oil concentration below 20 wt% is higher.

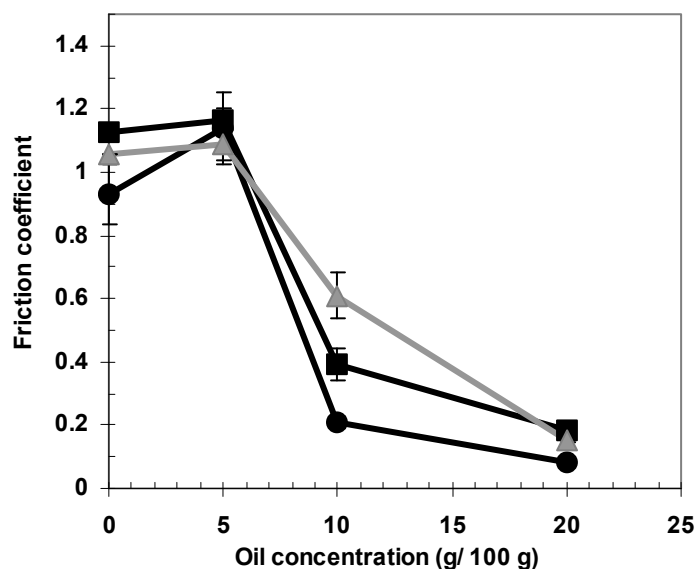


Figure 3.7 Friction coefficient vs. oil concentration for WPI gels with bound droplets (■) and for the same gels after addition of either 7 wt% water (●) or 7 wt% saliva (▲) (Entrainment speed: 100 mm/s; Load: 3 N).

3.3.4 Rheological properties of the sheared gels

The behaviour of lubricants in the mixed and hydrodynamic regime is known to be related to their viscosity. Higher viscosity values usually correspond to lower friction coefficients. In order to ascertain whether this holds also for sheared emulsion-filled gels, the ‘apparent viscosity’ of the sheared gels was measured with a rheometer using a vane geometry. A slight decrease of the ‘apparent viscosity’ in time was observed for all the gels (results not shown). This was attributed to the breakdown of the gel structure during measurement. To standardise the results, the ‘apparent viscosity’ values at a shear rate of 100 s^{-1} and at 100 seconds were therefore taken as measure. The relative differences in ‘apparent viscosity’ observed at 100 seconds between samples with different oil content remained constant in time.

The effect of the oil concentration on the ‘apparent viscosity’ of the sheared gel depended on the interactions between oil droplets and gel matrix. For κ -carrageenan and WPI gels with bound droplets, a gradual increase of the ‘apparent viscosity’ was observed with increasing oil concentration (Figure 3.8).

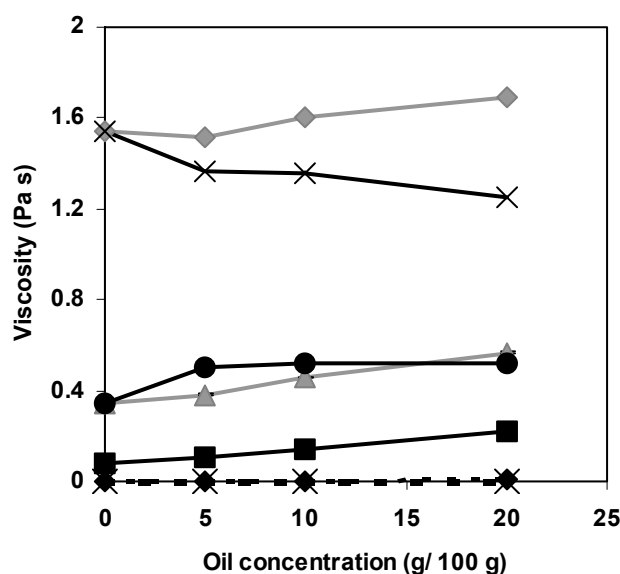


Figure 3.8 ‘Apparent viscosity’ of sheared gels vs. oil concentration. WPI gels with bound droplets (■), κ -carrageenan gels with bound (▲) and unbound (●) droplets, gelatine gels with bound (◆) and unbound (X) droplets. For gelatine gels the measurements were performed at 37°C (dotted line) and 20°C (solid line) (Shear rate 100 s⁻¹).

For κ -carrageenan gels with unbound droplets, the ‘apparent viscosity’ of the filled gels was higher than that of the gel without oil droplets and increasing the oil concentration above 5 wt% did not affect ‘apparent viscosity’. For gelatine gels, the effect of the oil concentration was temperature dependent. When the ‘apparent viscosity’ was measured at 37°C gelatine gels were molten. Under these experimental conditions very low viscosities and no effect of the oil concentration were observed (Figure 3.8). When the measurements were performed at 20°C, the ‘apparent viscosity’ of sheared gelatine gels with bound droplets increased with increasing oil concentration. For gelatine gels with unbound droplets, the ‘apparent viscosity’ of the filled gels was lower than that of the gel without oil droplets. For these gels, only a slight decrease of the ‘apparent viscosity’ was observed with increasing the oil concentration. This is possibly related to an increasing concentration of Tween in the gel. This emulsifier is likely to perform a lubricating action between the gel particles present in the mass of the sheared gel, decreasing the adhesion and cohesion forces.

3.3.5 Effect of shearing on microstructure of filled gels

The microstructure of the gels studied in this chapter has already been reported before [12,13]. In gelatine and WPI gels the oil droplets were non-aggregated, whereas in κ -

carrageenan gels, independently on the droplet-matrix interaction, the oil droplets were aggregated.

Possible changes in the microstructure of the gels as a result of the friction measurements, with particular attention to the coalescence of the oil droplets, were studied by CLSM microscopy. CLSM images were taken for each gel before and after friction measurements. Furthermore, the silicone discs used in the friction measurements were searched for traces of free oil, which could results from coalescence of the oil droplets during measurements. For gels with unbound droplets, migration of the oil droplets within the sheared gels occurred (Figure 3.9; results only shown for κ -carrageenan gels). For gels with bound droplets, the distribution of the oil droplets within the gels matrix did not change as a result of the friction measurements (results not shown). By CLSM microscopy no coalescence could be observed (Figure 3.9).

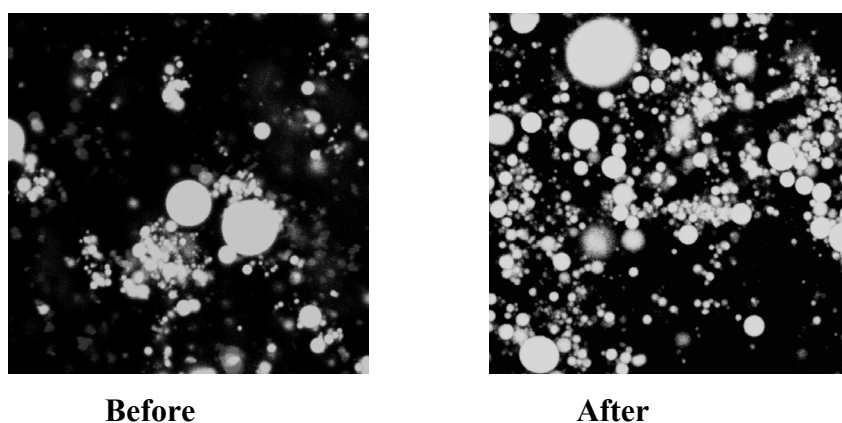


Figure 3.9 CLSM images of κ -carrageenan gels with unbound droplets before and after friction measurement (5 wt% oil; image size 39.7 X 39.7 μm).

3.4 Discussion

The lubrication properties of the oil in water emulsions used in this study are in agreement with the results of de Vicente et al [1] for oil in water emulsions. De Vicente et al. [1] studied the lubrication properties of oil-in-water emulsions in a steel-soft elastomer contact. They found that lubrication is determined by the ratio of the viscosities of the two phases. If the viscosity of the oil is at least 4 times larger than the viscosity of the continuous phase, the oil droplets enter the contact zone and dominate the lubrication properties, otherwise the friction is controlled by the continuous phase. The viscosity of

MCT oil is about 5 mPa s, i.e. about 5 times the viscosity of the water phase of the emulsions. The large decrease of the friction coefficient observed in this chapter already at an oil concentration of 1 wt% shows that also in the systems studied here the oil droplets enter the contact zone between the silicone disc and the neoprene ring, affecting the lubrication behaviour of the emulsions. The agreement between our results and those of de Vicente et al. [1] holds in spite of the difference in experimental conditions. In this chapter a silicone-neoprene contact was chosen, while Vicente et al. worked with a steel-soft elastomer contact.

The limited decrease of friction coefficient with increasing oil concentration above 10 wt% is in agreement with the results reported also by de Hoog et al. [20]. In this chapter a custom-made friction apparatus was used with materials with different surface properties like glass, rubber and pig's tongue. The authors showed that when mucosal surfaces were used and in the range of oil concentration between 10 and 40 wt% the friction coefficient of emulsions stabilised by WPI did not depend on the oil concentration. Furthermore, the surface characteristics were shown to have a large effect on friction.

The different emulsifying agents showed different lubrication behaviour. As compared to proteins, the friction coefficient of the 2 wt% Tween solution and of emulsions stabilised by this surfactant were in general lower (Figure 3.2). Tween is more active in decreasing the surface tensions of systems in which it is contained and might interact with the rubber surfaces and modify them through adsorption. Furthermore, Tween forms micelles already at concentrations above 0.007 wt% [21]. Therefore, at the concentration used in our work this surfactant is present as micelles. This could effectively lower friction for all Tween-stabilised emulsions within the whole range of speeds.

The lubrication properties of different gel matrices without oil droplets are likely to be governed by several factors, like the molecular properties of the gelling agent and the homogeneity of the sheared gel. For WPI gels (Figure 3.3), which show water phase exudation, the friction is high and is described by two different lubrication regimes. Up to a speed of 25 mm/s no effect of the speed on the friction coefficient is visible. This by definition implies that friction is in the boundary regime. At higher speed the friction coefficient starts to decrease with increasing speed, indicating the beginning of the mixed regime. For κ -carrageenan gels, which break down to a more homogeneous material, a continuous decrease of the friction coefficient with increasing speed is observed,

indicating a mixed regime over the whole range of speeds. The shape of the friction curve of gelatine gels as measured at 20°C indicates two lubrication regimes in the speed range studied, as described for WPI gels. The lower friction coefficient observed for gelatine gels as compared to WPI gels is probably due to the higher homogeneity, the fluid-like behaviour and the adhesiveness of sheared gelatine gels.

For all gel matrices, the mixed regime of lubrication was observed. Therefore, the bulk rheological properties of the lubricant will partly affect friction. For this reason, the relation between friction coefficient and ‘apparent viscosity’ of the sheared gels was studied. When comparing the results for the different matrices, it is clear that the ‘apparent viscosity’ of the sheared gel is not the only factor determining the lubrication properties (Figure 3.8). The ‘apparent viscosity’ of sheared gelatine gels is several times higher than that of WPI gels. Nevertheless, for gels with 20 wt% oil similar friction coefficients are observed.

When considering the effect of the oil concentration for each individual type of gel, the effect of ‘apparent viscosity’ on friction and the dependence of this effect on the interaction between oil droplet and gel matrix can be clearly observed (Figure 3.10). For gels with bound droplets, the ‘apparent viscosity’ increases with increasing oil concentration and the friction coefficient decreases with increasing ‘apparent viscosity’. For these gels, the observed increase in ‘apparent viscosity’ with increasing oil concentration is related to the increase in gel modulus (i.e. lower deformability of the particles) and to a different breakdown pattern [12,13]. With increasing oil concentration, the increase in modulus results in particles of the sheared gels with higher stiffness. Furthermore, with increasing oil concentration gels with bound droplets become more brittle and break down in smaller pieces, resulting in a more homogenous mass. For gels with unbound droplets, no effect of the oil concentration above 5 wt% on ‘apparent viscosity’ was observed (Figure 3.8). Furthermore, for these gels no relationship was observed between friction coefficient and ‘apparent viscosity’ (Figure 3.10). This is likely related to the effect of oil concentration on gel modulus and breakdown properties. For these gels, increasing the oil concentration results in a decrease of the gel modulus and has only a minor effect on gel brittleness [12,13]. Therefore, increasing oil concentration is likely to only slightly affect the homogeneity of the broken mass.

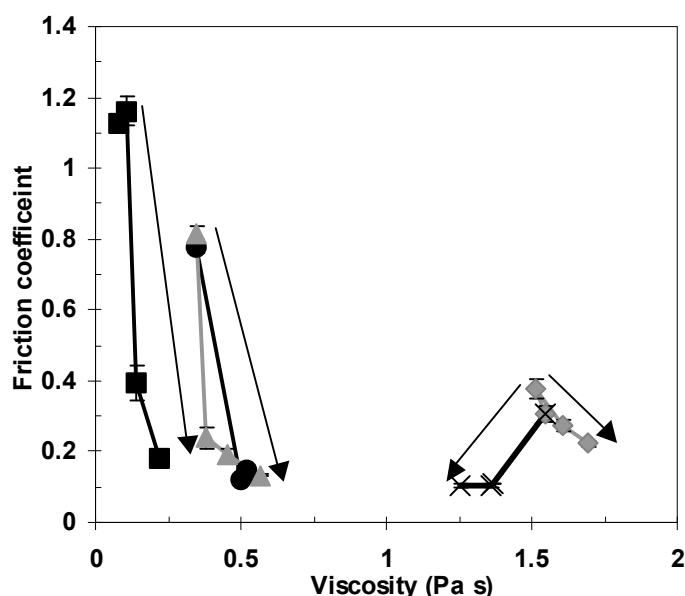


Figure 3.10 Friction coefficient vs. ‘apparent viscosity’ of sheared gels (◆: gelatine gels with bound droplets; X: gelatine gels with unbound droplets; ▲: κ -carrageenan gels with bound droplets; ●: κ -carrageenan gels with unbound droplets; ■: WPI gels with bound droplets. For gelatine gels both ‘apparent viscosity’ and friction coefficient were measured at 20°C, whereas for κ -carrageenan and WPI gels these measurements were carried out at 37°C. The arrows indicate the increase of the oil concentration. (Entrainment speed 100 mm/s; Load: 3 N; Shear rate 100 s⁻¹).

The effect of the oil concentration on ‘apparent viscosity’ is not the only factor explaining the large decrease in friction coefficient observed for gels containing oil droplets, as compared to the gels without oil. For gels with bound droplets, oil droplets present in the smallest gel pieces will affect friction like it happens for emulsions. Anyway, for systems like WPI gels, in which the matrix shows poor lubrication properties and the droplets are bound to the matrix, the ‘apparent viscosity’ of the broken gels plays a relatively larger role on lubrication. This results in a gradual decrease of the friction coefficient with increasing oil concentration. For κ -carrageenan gels, in which the oil droplets are extensively aggregated and, therefore, a larger number of oil droplets are present at the surface of the particles of the broken gels, the emulsion plays a relatively larger role. This results in a limited decrease of the friction coefficient of the broken gel at oil concentrations higher than 5 wt%, as observed for the emulsions. For gels with unbound droplets and in general for molten gelatine gels, also free droplets will be present in the mass of broken gel [12,16]. These droplets can affect friction directly. The lubrication properties of gels with unbound droplets are likely to be determined by the individual contribution of gel matrix and released oil droplets. The overall effect of the oil droplets

on friction does not appear different between gels with bound droplets and gels with unbound droplets. The lower friction coefficient of gelatine gels with unbound droplets as compared to gelatine gels with bound droplets is likely to be related to the effect of Tween.

Previous study [15] showed that the scores for mouth-feel attributes related to the presence of oil droplets in the gel matrix (e.g. *creamy* and *fatty*) increase with increasing oil concentration for gels with both bound and unbound droplets. The similarity of the lubrication properties of gels with bound and unbound droplets is in agreement with these findings. A relationship between the lubrication properties of sheared gels and the perception of sensory attributes related to the presence of oil droplets in the gel matrix can be hypothesised.

3.5 Conclusions

The lubrication behaviour of gels is largely determined by the molecular and functional properties of the gelling agent and the breakdown properties of the gel matrix. The inclusion of oil droplets in the gel matrix remarkably changes the lubrication properties of the gels. These changes depend on the interactions between oil droplets and gel matrix. The changes observed for gels with bound droplets are related to the increase in ‘apparent viscosity’ of the sheared gel mass. For gels with unbound droplets the decrease of the friction coefficient is likely to be the result of the individual contribution of gel matrix and released oil droplets. In spite of the two different mechanisms, the overall effect of the oil droplets on friction does not remarkably differ between gels with bound droplets and gels with unbound droplets. This is in agreement with findings of sensory studies on this type of systems.

References

- 1 De Vicente, J., Spikes, H. A. & Stokes, J. R. (2006). Viscosity ratio effect in the emulsion lubrication of soft EHL contact. *Journal of Tribology-Transactions of The Asme*, 128(4), 795-800.
- 2 Cassin, G., Heinrich, E. & Spikes, H. A. (2001). The influence of surface roughness on the lubrication properties of adsorbing and non-adsorbing biopolymers. *Tribology Letters*, 11(2), 95-102.
- 3 Weenen, H., Terpstra, M., Janssen, A., Jellema, R. H., De Wijk, R., Prinz, J., De Jongh, H. & Van der Linden, E. (2003a). Creaminess in mayonnaises: Rheology and oral coating. Abstracts of Papers of The American Chemical Society, 226, U77-U77.

- 4 Weenen, H., Van Gemert, L. J., Van Doorn, J. M., Dijksterhuis, G. B. & De Wijk, R. A. (2003b). Texture and mouthfeel of semisolid foods: Commercial mayonnaises, dressings, custard desserts and warm sauces. *Journal of Texture Studies*, 34(2), 159-179.
- 5 Jellema, R. H., Janssen, A. M., Terpstra, M. E. J., de Wijk, R. A. & Smilde, A. K. (2005). Relating the sensory sensation 'creamy mouthfeel' in custards to rheological measurements. *Journal of Chemometrics*, 19(3), 191-200.
- 6 De Wijk, R. A. & Prinz, J. F. (2005). The role of friction in perceived oral texture. *Food Quality and Preference*, 16(2), 121-129.
- 7 Malone, M. E., Appelqvist, I. A. M. & Norton, I. T. (2003). Oral behaviour of food hydrocolloids and emulsions. Part 1. Lubrication and deposition considerations. *Food Hydrocolloids*, 17, 763-773.
- 8 Chen, J. S., Moschakis, T. & Nelson, P. (2004). Application of surface friction measurements for surface characterization of heat-set whey protein gels. *Journal of Texture Studies*, 35(5), 493-510.
- 9 Aguilera, J. M. & Kinsella, J. E. (1991). Compression strength of dairy gels and microstructural interpretation. *Journal of Food Science*, 56(5), 1224-1228.
- 10 Kim, K.-H., Renkema, J.M.S., Vliet, T. Van (2001). Rheological properties of soybean protein isolate gels containing emulsion droplets. *Food Hydrocolloids*, 15, 295-302.
- 11 Kim, K.-H., Gohrani, S. & Yamano, Y. (1996). Effects of oil droplets in physical and sensory properties of o/w emulsion agar gels. *Journal of Texture Studies*, 27, 655-670.
- 12 Sala, G., van Aken, G. A., Cohen Stuart, M. A. & van de Velde, F. (2007). Effect of droplet-matrix interactions on large deformation properties of emulsion-filled gels. *Journal of Texture Studies*, 38 (4), 511-535.
- 13 Sala, G., van Vliet, T., Cohen Stuart, M. A., van Aken, G. A. & van de Velde, F. (Submitted-a). Deformation and fracture of emulsion-filled gels. Effect of oil content and deformation speed.
- 14 Sala, G., van Vliet, T., Cohen Stuart, M. A., van de Velde, F. & van Aken, G. A. (Submitted-b). Deformation and fracture of emulsion-filled gels. Effect of gelling agent concentration and oil droplet size.
- 15 Sala, G., De Wijk, R. A., van de Velde, F. & van Aken, G. A. (2008). Matrix properties affect the sensory perception of emulsion-filled gels. *Food Hydrocolloids*, 22 353-363.
- 16 Sala, G., van de Velde, F., Cohen Stuart, M. A. & van Aken, G. A. (2007). Oil droplet release from emulsion-filled gels in relation to sensory perception. *Food Hydrocolloids*, 21, 977-985.
- 17 Van de Velde, F., Pereira, L. & Rollema, H. S. (2004). The revised chemical NMR shift data of carrageenans. *Carbohydrate Research*, 339(13), 2309-2313.
- 18 Chojnicka, A., Visschers, R. W. & de Kruif, C. G. (Submitted). Lubrication properties of protein aggregates dispersion in a soft contact.).
- 19 Silletti, E., Vingerhoeds, M. H., Norde, W. & Van Aken, G. A. (2007). The role of electrostatics in saliva-induced emulsion flocculation. *Food Hydrocolloids*, 21(4), 596-606.
- 20 De Hoog, E. H. A., Prinz, J. F., Huntjens, L., Dresselhuis, D. M. & van Aken, G. A. (2006). Lubrication of oral surfaces by food emulsions: the importance of surface characteristics. *Journal of Food Science*, 71(7), E337-E341.
- 21 Malik, W. U. & Jhamb, O. P. (1970). Critical Micelle Concentration of Some Polyoxyethylated Non-Ionic Surfactants and Effect of Additives. *Kolloid-Zeitschrift and Zeitschrift Fur Polymere*, 242(1-2).

Chapter 4

Lubrication, rheology and adsorption of polysaccharide solutions

Abstract

In this chapter three sets of physical properties of polysaccharide solutions are characterized: the friction coefficient as a function of load and entrainment speed is obtained using a commercial tribometer employed with soft hydrophobic poly(dimethylsiloxane) (PDMS) substrates; shear viscosity and non-linear viscoelasticity (normal stress differences) are determined up to shear rates of 10^5 s^{-1} using a narrow gap parallel plate rheometry; adsorption and interfacial film properties onto hydrophobic (PDMS) substrates using Surface Plasmon Resonance (SPR) and Quartz Crystal Microbalance-Dissipation (QCM-D). This combined experimental approach generated a comprehensive picture on thin film formation, layer deposition and layer stability. Polysaccharide solutions studied in this chapter are commonly used in the food industry and their molecular characteristics are clearly reflected in the obtained data. For example, we find that the rheological measurements reflect the rigid-like nature of polysaccharides with the normal stress difference well described by a rigid dumbbell model at high shear rates.

A novel finding from the study is that the thickness of the hydrated adsorbed polysaccharide film, obtained from QCM-D, is directly related to the predicted film thickness between rubbing substrates at the transition between hydrodynamic and mixed lubrication regimes, obtained from friction measurements. While this transition zone is only dependent on the polymer's film thickness and the viscosity at shear rates around 10^4 s^{-1} , adsorption studies indicate that the boundary regime is likely to be controlled by the physical nature of the adsorbed film in terms of viscoelasticity, adsorbed mass density and hydration. In this regime, the polysaccharides that adsorbed the least were the least effective which we ascribe to their inability to retain water in the contact zone. Films that were highly viscoelastic and hydrated displayed the lowest boundary friction coefficient since the adsorbed mass of polymers is able to sustain a load and retain water in the film; pectin was the superior boundary lubricant while LBG was the least effective. This study shows that to understand the lubrication and enlighten different functional characteristics of food constituents, a combined insight of diverse techniques is necessary.

4.1 Introduction

Water soluble hydrocolloids, like polysaccharides, have a wide range of applications and are of great interest to the food industry and consumer products in general, including cosmetic and pharmaceutical products where they are used extensively as thickeners, gelling agents and stabilizers. The presence of polysaccharides has a profound role on the texture of a product, and has been particularly useful in creating structured low-fat foods with acceptable sensory properties. For example, in protein/polysaccharides mixed gel systems [1] it was found that mouth-feel attributes of ‘watery’ and ‘crumbliness’ of gels correlated with the amount of exuded phase during oral processing. Neutral polysaccharides tend to appear in the serum after compression of these mixed gels. It was noted that the release of these biopolymers influences the mouth-feel perception through direct contact with the oral tissue. Therefore, the interaction of polysaccharides (e.g. adsorption, adhesion, lubricity) with oral surfaces is thus relevant to study. Understanding these fundamental properties contributes to the long term goal of providing a link between physiological responses and physical characteristics of complex food systems.

In considering how fluids behave between the tongue and palate, it is clear that the lubrication process (at different speeds) is involved where a load is applied on the tongue as it shears the lubricant (i.e. food, beverage). In general lubrication processes, such as a ball sliding and/or rolling against a plate at high speeds, hydrodynamic lubrication appears when there is enough pressure in the lubricant film from the motion to sustain the load and keep the surfaces separated. The friction and fluid lubricant film thickness between the surfaces is primarily determined by the viscosity (rheology) of the fluid at the high shear rates present in the lubricant film. At low speeds however, there is not enough pressure developed to keep the surfaces separated and the friction increases accordingly [2]. This effect can be mitigated by altering the surface properties and/or the formation of a relatively immobile layer (adsorbed boundary film) that is capable of sustaining the load. The response of a lubricant for a particular tribopair is typically presented in the form of a Stribeck curve, where the friction coefficient ($\mu = F/W$) is given as a function of entrainment speed (U) or other speed dependent factors such as ηU , where η is the viscosity of the fluid at the shear rate present within the contact zone while F is the tangential friction force under an applied load (W). Three different lubrication regimes can usually be distinguished. At low entrainment speeds, the *boundary regime* occurs where the rotating surfaces are in direct physical contact; the friction coefficient is approximately

constant with speed and its value, which is generally high, depends on the properties of both surfaces (including roughness, elasticity and surface energy) and the thin layer of material deposited or confined between the surfaces. At higher entrainment speeds, the friction coefficient decreases with increasing speed indicating that fluid is being entrained into the contact region to separate the surfaces; in this intermediate regime (the *mixed* regime), both the rheological behavior of the solution in the contact region and the properties of the surfaces that are in partial contact contribute to the friction coefficient. At high speeds, hydrodynamics dominates such that both surfaces are fully separated; the friction coefficient increases with increasing entrainment speed and it largely depends on the viscosity of the lubricant. This is the so-called *hydrodynamic* regime of lubrication. In oral lubrication, the contacting substrates are highly compliant and the pressure in the contact region causes deformation of the substrate rather than affecting the viscosity of the lubricant, which is contrary to traditional studies in tribology involving hard surfaces; this is referred to as *iso-viscous elastohydrodynamic* lubrication [3-5].

There are only a few studies that focus on the influence of polysaccharides on the lubrication properties of aqueous solutions in soft-tribological contacts. In steel ball-hydrophobic elastomer disc tribopair, [6] showed that increasing concentrations of pig gastric mucin (PGM) and guar decreased the friction coefficient in the mixed regime due to adsorption and viscous effects. The measured friction coefficient was correlated to the adsorption properties of the polymers investigated with evanescent wave spectroscopy. Their study showed that for the adsorbing polymers (PGM) the boundary friction coefficient was lower compared to water. This was attributed to the formation of thin, adsorbed layer. In addition, non-adsorbing polymer (guar) showed similar boundary lubrication to water meaning that it did not contribute to the formation of molecular film. However, in the mixed regime of lubrication guar reduced the friction [6]. De Vicente et al. [7] observed a decrease in friction for polyethylene oxide (PEO), xanthan gum and guar solutions with increasing concentration in the mixed regime, caused primarily by hydrodynamic and viscous forces and used an effective viscosity to collapse the data to a single curve. Furthermore, de Vicente et al. [7] determined the shear rates presents in the contact gap to be between 10^4 - 10^6 s⁻¹. Both studies of Cassin et al. [6] and de Vicente et al. [7] demonstrated that high-shear viscosity plays an important role in determining the dynamics in the soft-tribological contact within the mixed regime, but neither study measured the actual viscosity at shear rates relevant to tribological studies of beyond 1000

s⁻¹. Malone et al. [8] considered that ‘oral slipperiness’ perception was related to the mixed-regime friction coefficient for guar solutions between a steel ball and rough-elastomeric plate. However, to truly rationalize this in terms of fluid (lubricant) material properties, it becomes necessary to decouple the relevant roles of the high-shear viscosity and adsorbed film properties on the friction coefficient measured within the mixed regime.

Recent studies have begun to elucidate the role of adsorbed polymers films on boundary aqueous lubrication. In summary, when a polymer is strongly bound through electrostatics or covalent bonding, the degree of hydration of the polymer as well as the presence of hydrated ions has been found to determine the boundary friction coefficient for aqueous systems [9-13].

The objective of the present study is to probe various dilute polysaccharide solutions under conditions similar to those present in tongue-palate interactions. This primarily involves characterization of their lubrication properties using soft elastomeric sphere and a flat disc in a mixed sliding/rolling contact mimicking oral substrates and processes. The tribological studies are presented in relation to full rheological characterization including viscosity and normal stress differences up to shear rates in order of 10⁵ s⁻¹ and characterization of the films adsorbed at polysaccharide solution/elastomer interface in terms of their thickness, hydration and viscoelastic properties. This is a first comprehensive study of polysaccharide solutions relating their adsorption and rheological properties to lubrication. The approach taken here is based on the prospect of performing future studies on the mouth-feel perception of the biopolymer solutions. With this in mind, we considered a common basis for comparison was to characterize different biopolymers with the same characteristic shear viscosity at a shear rates of around 50 s⁻¹ that is commonly regarded as most representative to ‘oral thickness’ perception [14-18]. We chose a range of biopolymers that varied in charge density, molecular weight, and conformation, as listed in Table 4.1. In this way we anticipated to obtain an understanding on how commonly used biopolymers will affect the rheology, lubrication and adsorbed film properties that may subsequently affect mouth-feel and other sensory percepts of food products.

4.2 Materials and Methods

4.2.1 Materials

Sugar syrup (67 Brix) was kindly provided by Cosun (Roosendaal, The Netherlands). Low acryl gellan gum (KelcogelTM F), xanthan gum (KeltrolTM T), GSK-carrageenan (C-122, κ/ι -hybrid carrageenan extracted from *Gigartina skottsbergii*), locust bean gum (C-130, LBG) and high methyl ester (HM) pectin (H-6) were kindly donated by CP Kelco Inc. (Lille Skensved, Denmark). Guar gum (OP 3309) was obtained from SKW Biosystems (Boulogne Billancourt, France) and tara gum (Ferwotar) from Caldic Ingredients b.v. (Oudewater, The Netherlands). Chemical composition of these polysaccharides was previously reported by de Jong and van de Velde [19]. All ingredients were used without further purification and without correction for their moisture content. The molecular weight and charge density of the biopolymers used in this chapter are listed in Table 4.1.

4.2.2 Sample preparation

Two types of solutions were used in this chapter:

- *Newtonian solution.* The lubricants consist of aqueous sugar syrup or glycerol solutions. Newtonian fluids at various concentrations were obtained at ambient temperature by mixing the solutions with demineralised and filtered (Millipore) water.
- *Shear thinning polysaccharide solution.* All polymers solutions were prepared at ambient temperature, by hydrating the appropriate amount of the material in demineralised and filtered (Millipore) water for approximately 3 hours. Subsequently, solutions were heated at 80 °C for 45 min under continuous stirring. After heating, the polysaccharides solutions were cooled to room temperature, stored at 4 °C and used within 2 days after preparation. Table 4.1 lists the polysaccharides and their concentration used in this chapter. These concentrations were chosen based on a previous rheological study that considered them to possess the same viscosity at 50 s⁻¹ at 20°C (Anke Janssen, Personal Communication).

Table 4.1 Description of the polysaccharides used in this chapter. ^a Charge density in mol/mol monosaccharide; all charged polysaccharides given in this table carry negative charges, from de Jong and van de Velde, [19]. ^b Weight average molecular weight distribution as determined by SEC-MALLS from de Jong and van de Velde, [19].

Polysaccharide	Charge density ^a	Mw (kDa) ^b	Concentrations (%)	Characteristic / application
Pectin	0.29	170	1.27	from fruit and vegetables, used in food as a gelling agents, thickener, water binder, stabilizer
Xanthan gum	0.25	4200	1	bacterial polysaccharide, used in bakery products, beverages, sauces, emulgator, dressings-thickener, stabilizer, provides 'fat-feel' in low/no-fat dairy products
Locust Bean Gum	0	1500	0.48	galactomannan, extracted from the seed of the tree used in dressing, desserts cream, instant products, ketchup, pet food, cream filling, cream cheese
Gellan gum	0.25	1400	0.54	bacterial polysaccharide, used as a emulsifier and stabilizer, thickener, in the jelly desserts, fruit preparations, dairy products
κ/ι-Carrageenan	0.7	580	0.91	from the seaweeds, used as a gelling agent for jellies and puddings, thickening agent for soups and sauces, as stabiliser in the ice crème, whipped cream etc.

Tara gum (0.48%) and guar gum (0.57%) were also investigated, but they were later found to contain microgel-like clusters in solution. Since this complicated our interpretation of measurements, the results were excluded. All other solutions were optically inspected using microscopy and found to contain no non-dissolved materials or microgels.

4.2.3 Rheological measurements

Experimental method

The rheological properties of all solutions investigated in this chapter were recorded at 25 °C using a standard rheometer (AR 2000, TA Instruments, Leatherhead, UK). Aluminum parallel-plate geometry with 40 mm diameter was used to measure the viscosity and normal stress differences (i.e. fluid non-linear elasticity) of the solutions at gap heights of 30 μ m and 50 μ m from low to high shear rates (beyond 10^5 s⁻¹). Parallel plate geometry was chosen because Davies and Stokes [20] have previously shown that it can be used to obtain flow curves up to extremely high shear rates with a similar accuracy to the more usually preferred cone-and-plate geometry. The procedures of Davies and Stokes [20] are followed here, including corrections for the gap error that is apparent when performing parallel plate measurements; these are briefly detailed in the following section.

Data analysis for parallel plate rheometry

Davies and Stokes [21] highlighted that there are several sources of error in the gap measurement when using parallel plate geometry. A correction to the gap setting has to be carried out in order to eliminate an observed decrease in the apparent viscosity with reduction of the gap height. This gap error arises primarily due to the non-parallelism between two plates and confinement of air during zeroing [21]. To reduce the impact of air confinement, the gap is zeroed at a load of 5 N. The gap error is assessed by measuring the apparent viscosity of a Newtonian fluid (e.g. silicon oil) at different gap heights. The gap error (ε) was determined by plotting δ/η_M against the commanded gap δ ; this gives a line of gradient $1/\eta$ and intercept of ε/η (Davies and Stokes, [20]). The true gap is $h = \varepsilon + \delta$, and the actual apparent viscosity η_{actual} is given by:

$$\eta_{\text{actual}} = \eta_M \frac{\delta + \varepsilon}{\delta} \quad (4.1)$$

η_M corresponds to the measured (or uncorrected) apparent viscosity. The gap error for this set of experiments was typically around 10 μm . In the parallel plate geometry, both shear stress and shear rate are functions of the geometry radius. These parameters are equal to zero at the center and reach the maximum at the edge of the plates. The viscosity (η) and normal stresses (N_1 - N_2) at the rim of the plates in terms of measured torque (M), normal force and angular velocity (Ω) can be derived from a force balance on the plates and were calculated using equations described in Davies and Stokes [20]. We evaluated $\frac{d \ln M}{d \ln \Omega}$ by fitting a Cross model to the raw data following Davies and Stokes [20] and a similar high level of accuracy was found. Corrections to the normal force measurements for inertial effects were included while the normal force gradient was evaluated using a power law model following Davies and Stokes [20].

4.2.4 Tribological measurements

The lubrication properties of all aqueous solutions used in this chapter were measured at 25 °C with a Mini Traction Machine (MTM, PCS Instruments Ltd., UK). This instrument consists of two rotating steel elements: a ball and a disc. During measurements the ball is loaded on the disc that is immersed in the lubricant. Following Bongaerts et al. [22], the MTM was modified using a compliant poly(dimethylsiloxane) (PDMS) ball and flat PDMS disc in order to assure a lower contact pressure that is relevant to contact pressures between tongue and palate in the oral cavity. The radius of the PDMS sphere and disc was

9.5 mm and 23 mm, respectively, with the thickness of the latter element of 4 mm. The Young's modulus (E) of the PDMS material was 2.4 MPa [22]. In order to investigate the effect of the surface roughness on the lubrication properties of polysaccharide solutions, two types of the PDMS discs were used that differed in roughness. The root-mean-square (r.m.s.) of asperities was equal to 8.6 nm and 382 nm for smooth and rough PDMS disc, respectively.

Prior to the experiments the PDMS surfaces were cleaned in an ultrasonic bath with isopropanol, followed by rinsing with demineralised filtered water (Millipore). After such treatment the surface of the PDMS elements retained its natural, hydrophobic characteristic. New PDMS surfaces were used for each measurement. The friction was determined as a function of the applied entrainment speed (U) in a range between 1 and 750 mm/s, while the applied load was set to 1 N. Friction coefficient (μ) was measured at least three times for every speed and averaged. While data were measured starting from high-to-low speeds and followed by low-to-high speeds, only data obtained from decreasing speed are discussed here, since curves showed negligible hysteresis. Each experimental point was recorded at an average constant slide-to-roll ratio of 50 %. Detailed information about the experimental technique and preparation of the PDMS substrates are reported elsewhere [22].

So-called Stribeck master curves for aqueous Newtonian lubricants were obtained using water, corn syrup-water and glycerol-water, and these are found to be similar to those previously obtained by [22]. This is obtained by plotting the friction coefficient as a function of $U\eta$, and fitting the following equation to the data [22]:

$$\mu_{tot} = g(U\eta_{eff})^n + \left(\frac{h(U\eta_{eff})^l - g(U\eta_{eff})^n}{1 + (U\eta_{eff} / B)^d} \right) \quad (4.2)$$

h and l are the boundary friction coefficient and power law index, respectively; g and n are the elastohydrodynamic (EHL) friction coefficient and power law index, respectively; B is effectively the transition value of $U\eta$ between the boundary and mixed regimes and d is another power-law index; η_{eff} is the 'effective' viscosity in the contact zone, which is for Newtonian fluid independent on shear rate and thus, well defined. Using U in mm/s, the fitting values found for the smooth surface are: $n=0.46$, $g=0.0027$, $h=4.73$, $l=0.19$, $B=0.035$, and $d=2.06$; and for the rough surface: $n=0.46$, $g=0.0028$, $h=1.26$, $l=0.0044$, $B=0.24$, and $d=2.35$. These were similar to the values obtained by Bongaerts et al. [22] for the same smooth and 'medium-rough' surfaces, and hence the data has not been shown for

brevity. These master curves are included as a line on all subsequent plots of friction coefficient against the product of speed and viscosity.

4.2.5 Determination of the properties of the adsorbed boundary films

The properties of the adsorbed boundary films were determined using a combination of Quartz Crystal Microbalance with Dissipation function and Surface Plasmon Resonance techniques. In order to mimic a surface chemistry that reflects the MTM experiments, PDMS was spin coated from its 5% solution in toluene onto the gold working electrode of the Q-sense crystal or onto substrate of the SPR chip. After coating for 15 s at 3000 rpm, the substrates were left to cure overnight in the oven set to 120°C and then cleaned in isopropanol and de-ionised water in the same way as MTM discs and spheres. The polysaccharides were allowed to adsorb at the substrate from their solutions for 25 minutes. This time equals the time between the introducing solutions into the MTM measuring chamber (i.e. starting the experiment) and reaching the boundary lubrication regime.

Quartz Crystal Microbalance with Dissipation Monitoring (QCM-D)

The viscoelastic properties of the adsorbed film were probed by the Quartz Crystal Microbalance with Dissipation monitoring technique (QCM-D) using a Q-Sense™ instrument, model E4 (Q-Sense, Vastra Frolunda, Sweden) with a peristaltic pump maintaining the flow of the liquids through the measurement chamber. In this study a gold coated AT cut quartz sensors (Q-sense, QSX 301-standard gold) was used with a nominal resonance frequency of 5 MHz, which were spin coated by a thin hydrophobic layer of PDMS. The experimental set up and basic principles are explained in detail elsewhere [23]. The QCM-D signal was recorded in the form of changes of a resonance frequency and a dissipation of the oscillation energy of the piezoelectric quartz resonator. Baseline corresponds to the values recorded in deionised water. The temperature of the measuring chamber was stabilized at 25 °C, with the solution flow rate of 50 µl/min. The polysaccharide solution was left in contact with the substrate for 25 minutes, then excess polymer was rinsed with deionised water.

The relation between the change of detected signal and the properties of the adsorbed film is not straight forward and a theoretical model has to be applied in order to resolve them. In an approach developed by [24], the quartz resonator is assumed to be purely

elastic and the adsorbed film is modelled as a Voigt viscoelastic element with a complex elasticity modulus G_f defined as:

$$G_f = \mu_f + i2\pi f \eta_f = G_f' + iG_f'' \quad (4.3)$$

where μ_f is the film shear elasticity modulus, f is the sensing frequency, η_f is the film viscosity, G_f' is the apparent film storage modulus and G_f'' is the apparent film loss modulus. Beside the basic resonance frequency, odd overtones were also detected (3rd, 5th, 7th, 9th, and 11th). The data were numerically fitted to obtain the film thickness, shear elasticity modulus and viscosity assuming a film density of $\rho_f = 1100 \text{ kg/m}^3$, using a commercially available program, Q-tools™. The adsorbed mass was obtained as:

$$m_{\text{Voight}} = h_f \rho_f \quad (4.4)$$

where h_f is the thickness obtained from the fit to Voigt model and ρ_f is the input density. The Voigt mass and the adsorbed film's shear elasticity modulus and viscosity are nearly independent of the choice of input density (in reasonable limits, e.g. between 1010-1500 kg/m^3), however, the fitted film thickness is inversely proportional to the chosen density [24, 25].

Surface Plasmon Resonance (SPR)

The Biacore™ 2000 (Biacore AB, Uppsala, Sweden) was used, which is an SPR instrument operating in Kretschman configuration. The gold coated sensor chips were purchased from GE Healthcare (SIA kit Au). The main principles of SPR are explained in detail elsewhere [26, 27]. In brief: At the chip's surface, the light is reflected under total internal reflection conditions. The angle of a minimum reflection, the SPR angle θ , is detected, which changes upon adsorption at the interface or change of the bulk solvent. The baseline was recorded in deionised water. During SPR experiments, the temperature was set to 25 °C and the flow rate to 10 $\mu\text{l/min}$. The flow was stopped 5 minutes after polysaccharide solutions were introduced into the measuring chamber (when the onset of the adsorption plateau was observed) and was resumed during rinsing by deionised water after allowing 25 minutes for adsorption.

Hydration of the adsorbed film

While SPR is sensitive to “dry” mass of the film related to refractive index changes, QCM-D is sensitive to hydrated “wet” mass of the film, since the water trapped within the film affects its viscoelastic properties. This water can be attributed to the “bound water”

involved in hydration shells associated with the adsorbed molecules as well as to the “mechanically trapped water” within the topological irregularities of the film [28-30].

The relative solvent content in the film was calculated as:

$$w = 100\% \frac{(m_{Voigt} - m_{SPR})}{m_{Voigt}} \quad (4.5)$$

4.3 Results and Discussion

4.3.1 Rheology

Figure 4.1 shows the flow curves of polysaccharide solutions that include data obtained using the parallel plate geometry at a gap of 50 microns. The shear rate and viscosity data were corrected for a gap error of $\varepsilon = 9.5 \mu\text{m}$. Data for sugar syrup (97%) is included as a reference constant viscosity Newtonian fluid. All polysaccharide solutions investigated show non-Newtonian behavior, where the viscosity decreased with shear rate, indicating shear-thinning or pseudo-plastic behavior. This type of flow behavior typically arises due to alignment and disentanglements of the long polymer chains by applying a shear force to the solution. While all solutions were chosen to have essentially the same viscosity at shear rates of around 50 to 200 s^{-1} ($\eta \sim 0.11 \pm 0.03 \text{ Pas}$ at 100 s^{-1}), differences are observed at lower and higher shear rates.

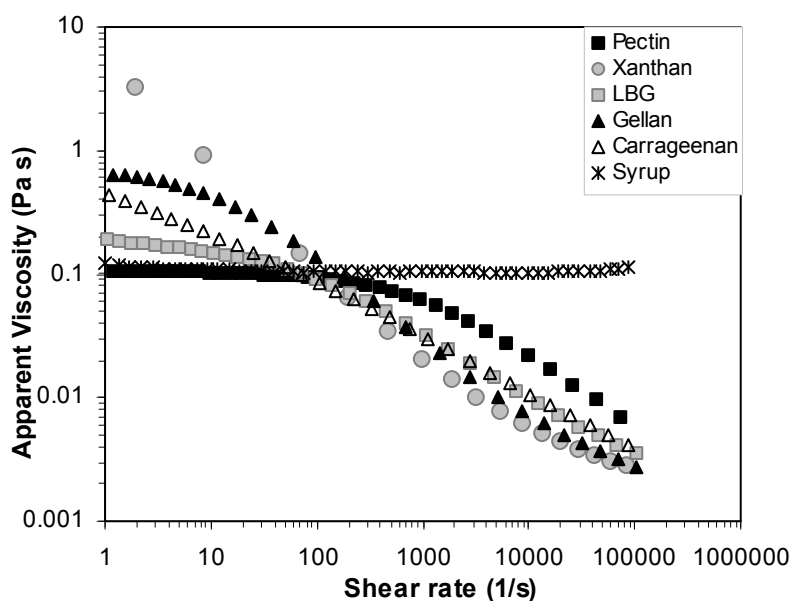


Figure 4.1 Flow curve of polysaccharide solution and 97% corn syrup at 25°C measured with parallel-plate geometry at gap height of 50 μm . Polymer concentrations are listed in Table 4.1.

Figure 4.2 shows the elasticity of the polymer solutions in the form of normal stress differences ($N_1 - N_2$) obtained at high shear rates; note that N_2 is generally regarded as zero for polymer solutions so that ($N_1 - N_2$) can be considered as equivalent to N_1 (see Davies and Stokes, [20]). The normal stresses were also measured for the Newtonian syrup and found to give scattered values about zero, thus providing confidence that the normal stresses for the polymer solutions are free from methodological or instrumental artifacts.

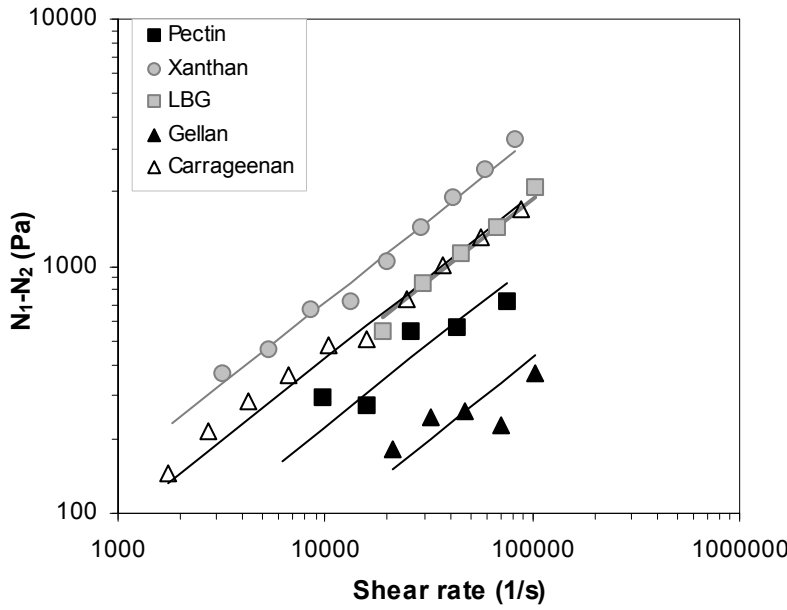


Figure 4.2 Non-linear viscoelastic measurements of polysaccharide solutions measured at 25°C with parallel plate geometry at gap height of 50 μm , showing normal stress differences ($N_1 - N_2$). The lines are fits to rigid dumbbell model assuming $N_2 = 0$ and fitting relaxation times λ_D (see listed relaxation times in Table 4.2).

All show power law behavior with relatively low power law indices that are characteristic of rigid-rod like molecules. Therefore, a dumbbell model [31-33] suitable for high shear rates was fitted to the data: $N_1 = 1.2nkT(\lambda_D \dot{\gamma})^{2/3}$, where relaxation time λ_D is the free parameter and n, k, T are the number density of molecules, Boltzmann's constant, and temperature, respectively. The model follows the data points reasonably accurately, with the fits shown in Figure 4.2. The relaxation times are listed in Table 4.2 and there is a large span between different samples. The highest relaxation times, and hence elasticity, was obtained for xanthan gum solutions although it also had the lowest viscosity at high shear rates. Three distinct groups are apparent in terms of non-linear elastic properties: xanthan > LBG >> carrageenan, gellan >> pectin.

Table 4.2 Relaxation time (λ_D) of the polysaccharide solutions calculated from Dumbbell model.

Polysaccharide	λ_D (ms)
Pectin	0.10
Xanthan	101.28
Lbg	27.53
Gellan	2.26
Carrageenan	2.72

4.3.2 Tribology

Figure 4.3(A) displays the friction coefficient of the polysaccharide solution as a function of the entrainment speed measured using the smooth PDMS disc. The data show clear differences in measured friction, and the system generally reflects a mixed and hydrodynamic lubrication regimes. At increasing values of entrainment speed, the friction coefficient decreases to a minimum and then increases with increasing speed; this is indicative of the mixed and hydrodynamic regimes respectively. At the lowest speed, LBG is the least lubricating while pectin is the most lubricating. However, at the highest speeds, the polysaccharides are difficult to distinguish.

To decouple the influence of viscosity and surface effects, the data is re-plotted in Figure 4.3(B) to show the friction coefficient as a function of $U\eta_{eff}$. η_{eff} was determined by fitting the hydrodynamic portion of the Stribeck curves to that for the Newtonian solutions (i.e. the master curve). This is necessary because the exact shear rate in the contact is unknown due to the current inability to measure film thickness directly in soft-contacts. According to EHL theory and observations from the previous studies, the friction coefficient in hydrodynamic regime depends solely on the product of the entrainment speed and the viscosity for constant load and substrate elasticity, and regardless of wetting or roughness [22]. This provides a convenient method to determine the effective viscosity in the contact, with the values obtained for the polysaccharides listed in Table 4.3. One can now observe that pectin, gellan, and carrageenan all exhibit similar friction curves when an effective viscosity is considered (see Figure 4.3(B)).

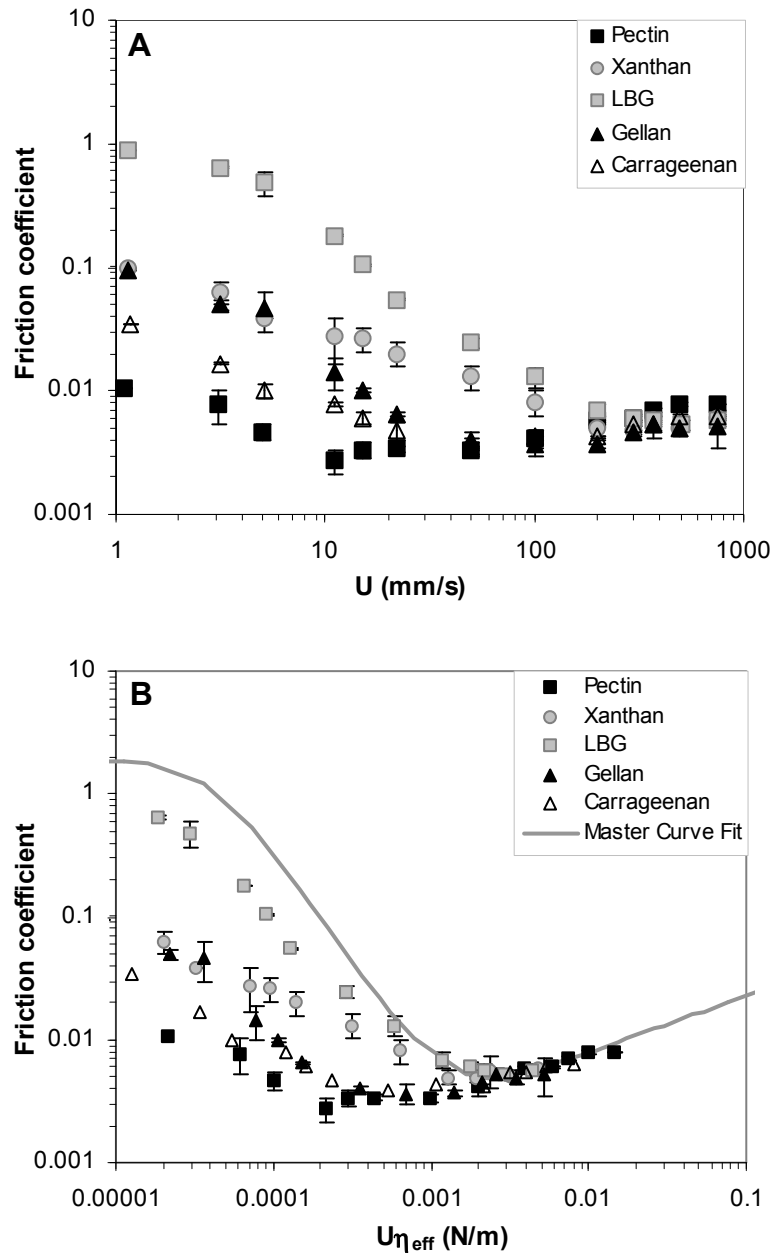


Figure 4.3 Tribological properties of polysaccharide solutions between *smooth* hydrophobic PDMS tribopairs, showing apparent friction coefficient as (A) a function of entrainment speed, and (B) as a function of $U\eta_{eff}$, the product of entrainment speed and an effective viscosity. The line is the Newtonian master curve (equation 4.2) for smooth PDMS surfaces. The effective viscosity is determined for the polysaccharide solutions by overlaying the data in hydrodynamic regime to that of the master curve. The error bars are indicated.

Table 4.3 Effective viscosity (η_{eff}) of the polysaccharides solutions in the hydrodynamic regime between smooth PDMS tribopairs. The effective shear rate $\dot{\gamma}_{(\eta_{eff})}$ is obtained from the corresponding viscosity in Figure 4.1. The estimated error for the viscosity is 0.0005. $\min(U\eta_{eff})$ corresponds to the transition between the mixed and EHL regimes. The minimum (h_m) and central (h_c) film thickness were predicted at the values of $\min(U\eta_{eff})$ using the model of the de Vicente et al. [4].

Polysaccharide	Smooth PDMS		$\min(U\eta_{eff})$	h_m	h_c
	η_{eff} (Pa s)	$\dot{\gamma}_{(\eta_{eff})}$ (1/s)	(N/m)	(nm)	(nm)
Pectin	0.0197	14008.80	$9.8 \cdot 10^{-4}$	613	1261
Xanthan	0.0064	11236.39	$2.4 \cdot 10^{-3}$	1101	2149
LBG	0.0059	32303.65	$2.9 \cdot 10^{-3}$	1262	2431
Gellan	0.0070	9824.63	$1.4 \cdot 10^{-3}$	776	1562
Carrageenan	0.0107	10392.06	$2.1 \cdot 10^{-3}$	1028	2018

Figure 4.3(B) also shows more clearly that there is shift in the transition between the mixed and EHL regimes due to the polysaccharides; this is most pronounced for pectin, gellan and carrageenan that promote full film lubrication at significantly lower values of $U\eta_{eff}$ than xanthan gum and LBG. A similar result was previously observed for aqueous surfactant solutions (see Graca et al. [34]) that was considered to be a surface wetting effect. The transition point for each polymer is listed in Table 4.3 in terms of $\min(U\eta_{eff})$. Also shown is the effective shear rate from the viscosity flow curves (Figure 4.1), whereby a shear rate of around 10^4 s^{-1} is required in order to obtain the values observed for η_{eff} . In addition, Table 4.3 presents the predicted ‘minimum’ (h_m) and ‘central’ (h_c) film thickness at the junction between the mixed and elastohydrodynamic regime based on $U\eta_{eff}$ and calculated using the model of Vicente et al. [4]. For further discussion on this data, see section 4.3.4.

Figure 4.4 shows the friction coefficient as a function of speed for the rough PDMS tribopair. The results indicate that only the boundary and mixed lubrication regime is observed for all samples. The friction data is approaching a plateau at low entrainment speeds, which is indicative of boundary lubrication; the hydrodynamic pressure is not enough to prevent contact between asperities of the rubber in the measured range of entrainment speeds. At low speeds, LBG and gellan are the poorest lubricants while carrageenan and pectin are the most lubricating; this largely mirrors the results for the smooth surface except that gellan is a poorer lubricant for the rougher contact. Since there is no hydrodynamic regime, there is no anchor in which to normalize the data and hence an effective viscosity has not been determined.

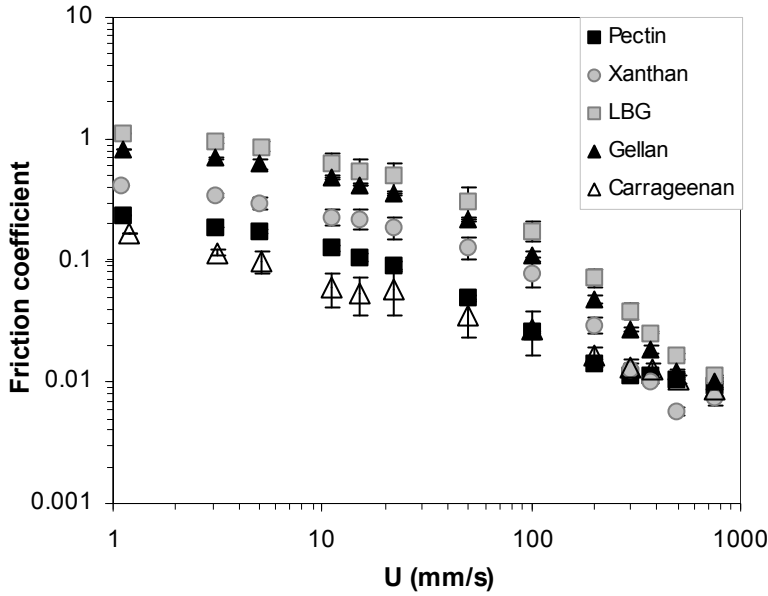


Figure 4.4 Tribological properties of polysaccharide solutions between *rough* hydrophobic PDMS tribopairs, showing apparent friction coefficient as a function of entrainment speed. The error bars are indicated.

The boundary regime was probed for rough substrates by measuring the friction force as a function of applied load, as presented in Figure 4.5. A non-linear response is observed for water and several samples, which is characteristic of a Hertzian contact for compliant rough substrates whereby the area of contact is proportional to $\sim W^{2/3}$ [35-37]. Subsequently, the influence of contact area is demonstrated by accurately fitting $F = kW^{2/3} + A_1$ to the data at low loads (<1 N) (k is a coefficient while A_1 is a constant to account for a slight offset at zero load). This fits water, LBG and xanthan across the full data range, but it is only accurate at low loads for the other samples; deviation may arise due to film wear at high loads resulting in a higher than expected friction force. Linear fits at low loads, $F = \mu W + A_2$, which is effectively Amonton's law (μ is an effective boundary friction coefficient) with the addition of A_2 as a constant, describe most of the data reasonably well at loads below 1 N. It provides an accurate fit across the whole load range for carrageenan and pectin that are effective boundary lubricants. All fitted parameters are listed in Table 4.4, and in most cases $k \sim \mu$. The constants A_1 and A_2 relate to adhesion between the substrates since their value decreases with decreasing boundary friction coefficient.

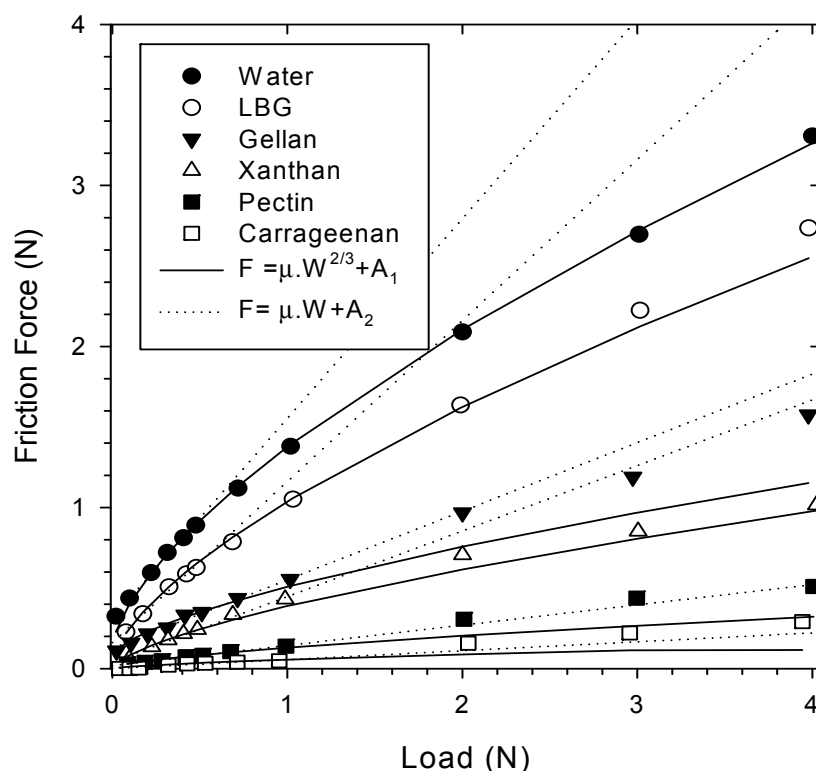


Figure 4.5 Friction force versus load for polysaccharide solutions and water between rough PDMS surfaces.

Table 4.4 Parameters obtained from fitting the friction force as a function of load.

Sample	A_1	μ	A_2	μ
Water	0.14	1.15	0.31	1.24
Pectin	0.00	0.13	0.02	0.13
Xanthan	0	0.41	0.04	0.41
LBG	0.04	1	0.16	1
Gellan	0.08	0.43	0.13	0.43
Carrageenan	0	0.05	0	0.06

4.3.3 Adsorption, hydration and viscoelasticity of interfacial films

To provide more insight in the origin of the lubrication of the polysaccharide solutions, SPR and QCM-D were employed to determine the effective thickness, hydration and viscoelastic properties of the adsorbed interfacial films. The combination of these two techniques allows the ‘dry’ mass and ‘wet’ mass of the adsorbed film to be determined, and thus the degree of film hydration that has previously been considered influential to boundary lubrication [12]. This is anticipated to be directly related to the properties of the thin film that contributes to the boundary and mixed lubrication in the contact zone. In this

series of measurements four polymer solutions were examined: pectin, LBG, xanthan and gellan gum.

Figure 4.6 shows the adsorbed ‘dry’ mass from SPR measurements. The data shows that a majority of the polymer is adsorbed within 5 minutes. The adsorbed mass can only be determined following rinsing, since the bulk refractive index contributes to the response. The samples were rinsed 25 minutes after the beginning of the measurement. This revealed the adsorbed amount of polymers that follows a sequence: pectin >> xanthan > LBG, gellan, as listed in Table 4.5.

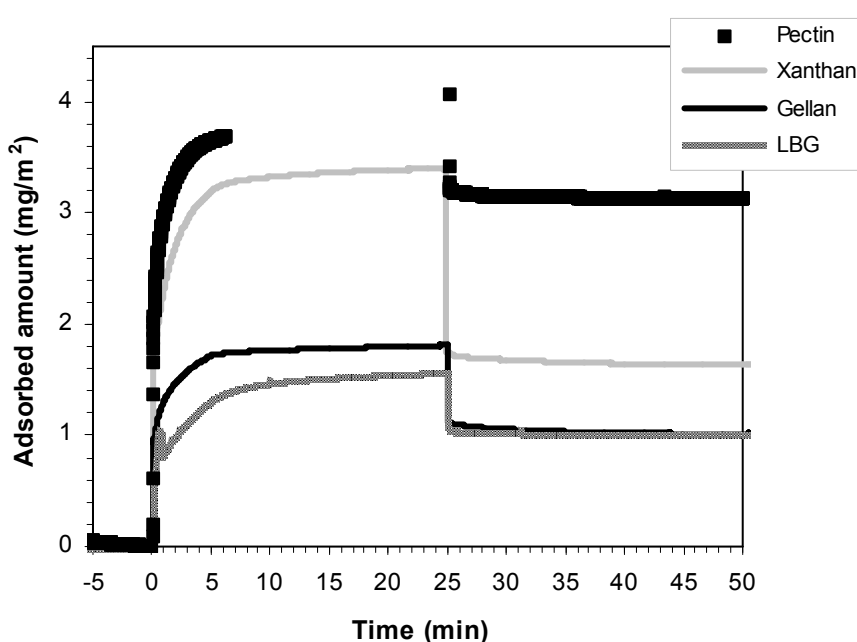


Figure 4.6 The adsorbed ‘dry’ mass from SPR measurements.

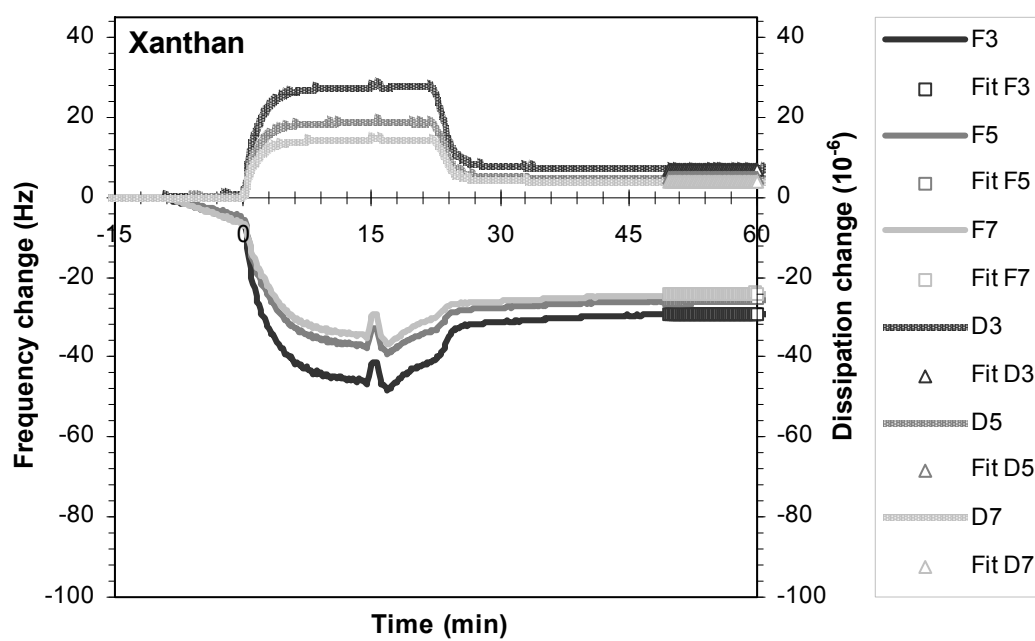
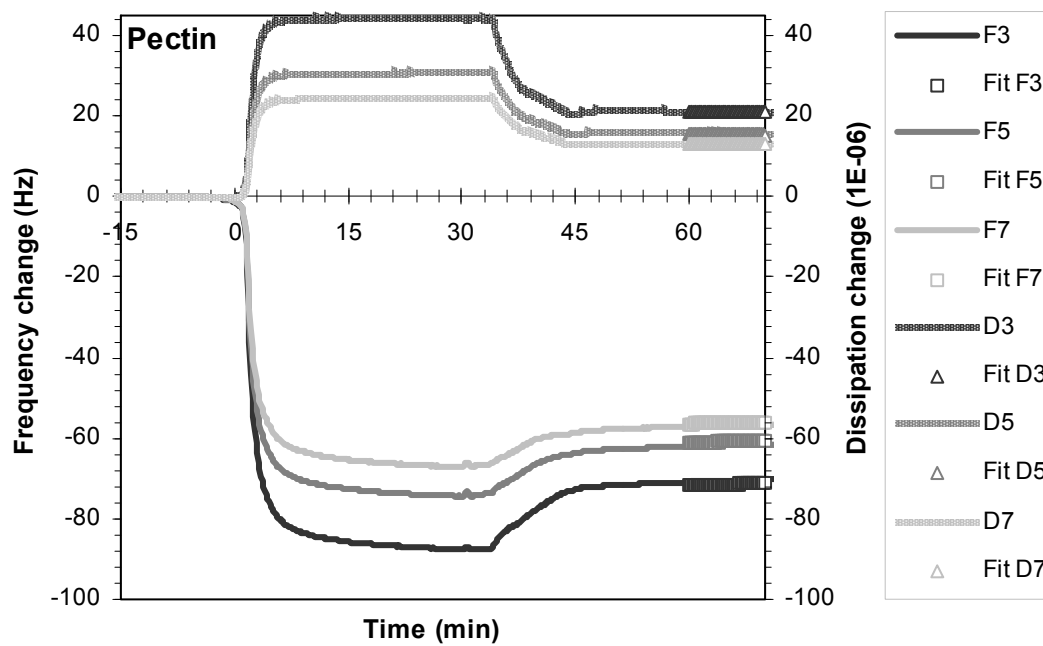
Table 4.5 Properties of the adsorbed polysaccharide films from SPR and QCM-D measurements.

Polysaccharide	QCM (wet) mass (mg/m ²)	SPR (dry) mass (mg/m ²)	Viscosity (mPa.s)	Shear modulus (kPa)	Hydration (%)	Solvent /polymer mass ratio	Adsorbed film thickness (nm)
Pectin	38.67 ± 0.39	3.12 ± 0.31	1.38 ± 0.02	34.2 ± 7.2	92 ± 1	11.39	38.6
Xanthan	14.59 ± 1.36	1.63 ± 0.16	1.36 ± 0.02	44.4 ± 1.3	89 ± 2	7.95	14.6
LBG	4.85 ± 0.02	1.01 ± 0.10	2.08 ± 0.02	105.1 ± 4.1	79 ± 2	3.8	4.9
Gellan	30.25 ± 0.44	1.01 ± 0.10	1.07 ± 0.01	22.6 ± 0.12	97 ± 1	28.85	30.2

The ‘viscoelastic’ properties of the adsorbed polysaccharide films are reflected in the QCM-D results (see Figure 4.7). The baseline corresponds to resonance frequency and dissipation of the clean PDMS modified sensor crystal immersed into deionised water, and

rinsing was typically performed at 25 minutes time point, removing non-adsorbed polymers. Pectin displays a large variation in the frequency change between different overtones and large dissipation. This illustrates an adsorption of a highly viscoelastic, non-rigid layer. In contrast, the frequency changes sensed for different overtones are similar in the case of LBG sample. Moreover dissipation of energy by the film is low, indicating that the adsorbed layer is rigid. While film properties were compared for films rinsed by water, it is also interesting to compare the results obtained for substrate in contact with bulk polymer solutions. An initial rapid increase in the dissipation of the oscillation energy is caused mainly by the exchange of the water to polysaccharide solution in the measurement chamber and it is caused by an increase in the bulk liquid viscosity, elasticity and density. In the case of gellan and LBG the actual adsorbed film formation is a much slower process. Even after 25 minutes of contact between solution and film the measured values do not reach any plateau. On the other hand, the layer formation is rapid for pectin and xanthan and takes place on the same time scale as the exchange of water to polysaccharide solution in the QCM-D chamber.

Table 4.5 summaries the properties of the adsorbed film determined by combining the SPR and QCM-D results: the ‘wet’ mass, ‘dry’ mass, % hydration, and solvent/polymer mass ratio. These results show that the adsorbed polysaccharide films are highly hydrated, comprising more than 70% of water and the effective density of hydrated films is very close to that of water. Thus, an “effective” thickness of the adsorbed films can be approximated as a ratio between wet mass and density of the water, and follows the order: pectin (38.6 nm) > gellan (30.2 nm) > xanthan (14.6 nm) >> LBG (4.9 nm). However, while gellan forms a relatively thick film, it is the most fluid-like of all samples with the lowest apparent film viscosity and shear modulus as it contains 97 % water.



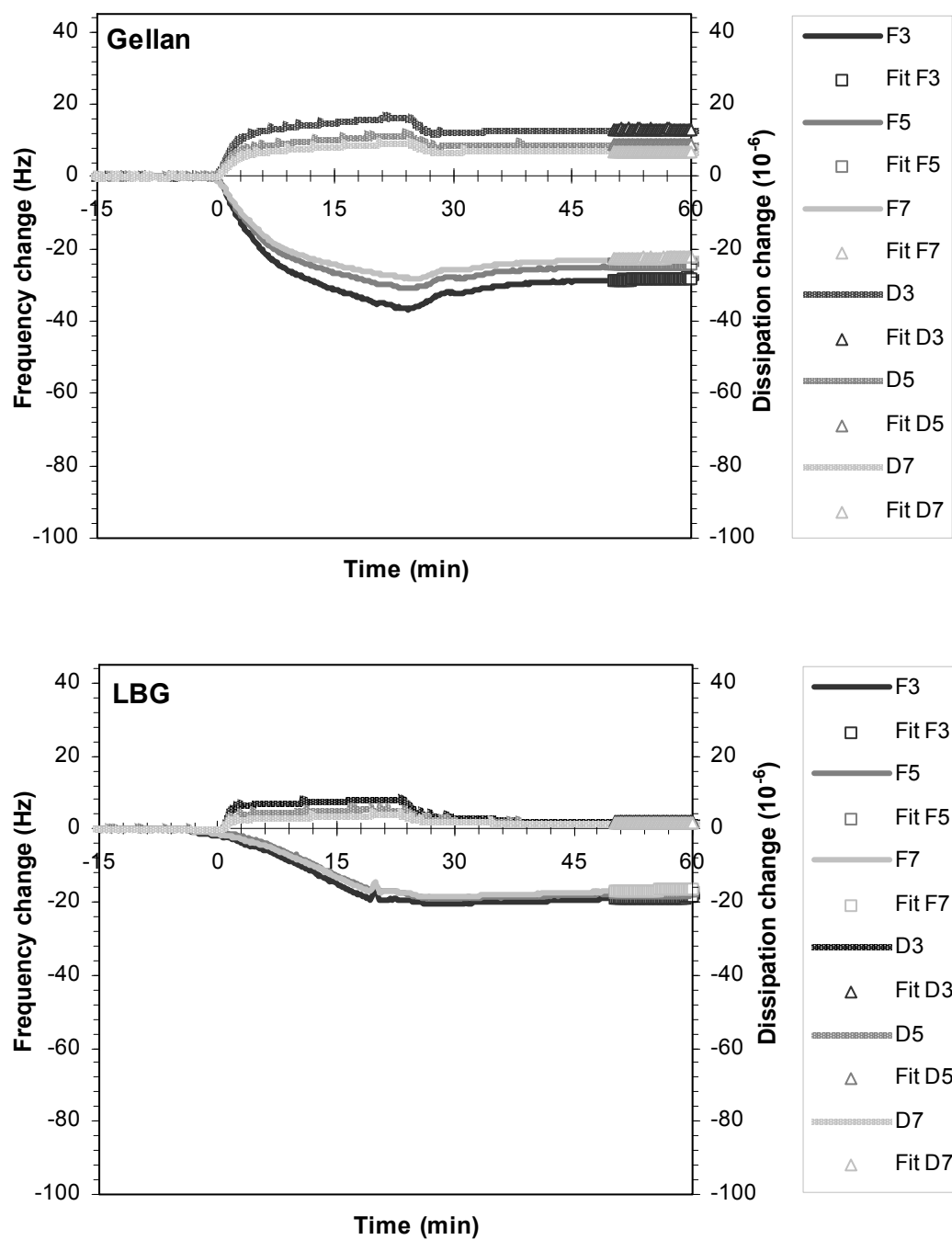


Figure 4.7 Change in frequency and dissipation as measured using the QCM-D technique. Different graphs correspond to four specimens: pectin, xanthan, Gellan and LBG.

4.3.4 Relating Interfacial film properties to lubrication

We show here the novel finding that there is a direct relationship between the tribological properties and the effective hydrated film thickness of the adsorbed polymers obtained from QCM-D. The adsorbed film thickness linearly correlate (negatively) with both the minimum and central film thickness predicted from the ($U\eta_{eff}$) values when the friction coefficient is a minimum at the junction between the EHL and mixed regimes for the smooth surfaces, as shown in Figure 4.8; the correlation coefficient for the linear fits is $r^2=0.998$ (it should be noted that the adsorbed film thickness is directly proportional to the wet mass of adsorbed polymer). This is a significant outcome, as it indicates that the QCM-D measurements are indeed related to the observed tribological properties of the polysaccharides, and that increasing the thickness of the hydrated polymer layer promotes full film entrainment at lower entrainment speeds and thus to smaller distances between rubbing surfaces. This is seemingly independent of the nature of the adsorbed film, at least in the context of the polysaccharides examined and where the adsorbed hydrated film thickness is of similar order to the roughness length scale ($\sim 10\text{nm}$). Since it is independent of polysaccharide type, we currently consider that this to be due to the hydrated polymer film reducing the effective roughness of the substrate.

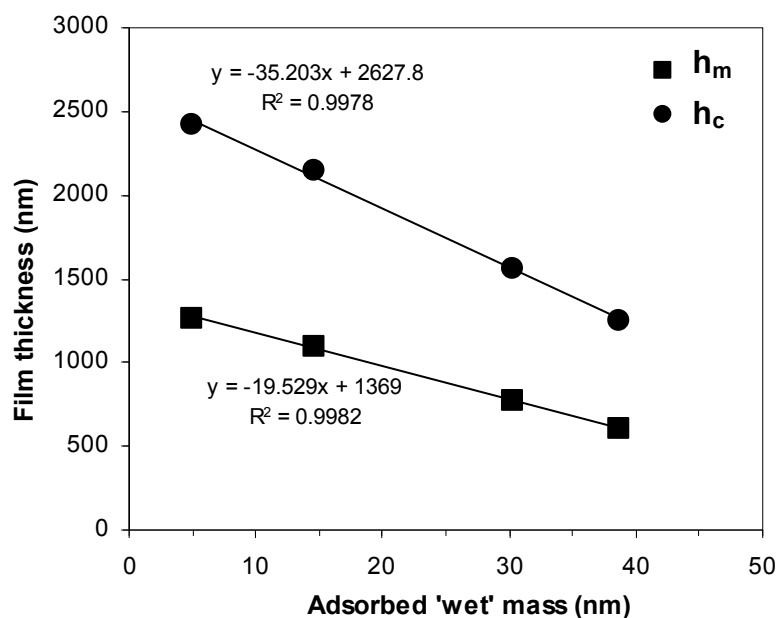


Figure 4.8 Minimum (h_m) and central (h_c) film thickness versus adsorbed hydrated film thickness. The lines correspond to fits.

Further correlations were investigated between the friction measurements and the adsorbed film parameters obtained from QCM-D and SPR, although only relatively weak correlations are found (not shown for brevity). For smooth surfaces, it is found that films of low elasticity and large thickness are more lubricating; the friction coefficients in the speed range of 1 – 100 mm/s correlate positively with the film modulus ($r^2 = 0.94$, linear correlation) and negatively with the hydrated film thickness (wet mass) in the speed range of 10-100 mm/s ($r^2 = 0.94$, power law correlation). In contrast, for rough surfaces, lubrication (in the boundary regime) is governed by the dry mass of adsorbed polymer; the friction coefficients in the speed range of 1 – 100 mm/s ($r^2 = 0.95$, linear correlation) correlate reasonably well with the dry mass of adsorbed polysaccharide and with the *so-called* adhesion parameters A_1 and A_2 ($r^2 = 0.93$ & 0.96 respectively, power-law correlation). However, whilst these correlation coefficients are reasonable, with only 4 samples it is difficult to prove whether it is causal at this stage.

We conclude that the viscoelasticity, hydrated mass and film thickness, and quantity of adsorbed polymer are all very important for setting the lubrication properties of a polysaccharide solution during the transition in the mixed regime to the boundary regime.

4.4 Concluding Remarks

Lubrication has received recent attention as a means to understand the complexity of mouth-feel and other sensory attributes. However, tribological measurements are difficult to interpret and comprehensive model studies on the lubrication properties of food components in soft tribological contacts, mimicking the pressures in tongue-palate / tongue-teeth interactions, are required to form a basis of understanding. We have endeavored to provide such a basis using several polysaccharide thickeners and constructing solutions so that their viscosity at around $50 - 200 \text{ s}^{-1}$ are essentially the same ($\eta \sim 100 \text{ mPas}$), such that they could all be considered to have a similar oral ‘thickness’. The polysaccharides studied include pectin, xanthan gum, carrageenan, and gellan. Three sets of physical properties are characterized: shear viscosity and non-linear viscoelasticity (normal stress differences) are measured up to shear rates of 10^5 s^{-1} using a narrow gap parallel plate rheometry; the lubricated friction coefficient as a function of load and entrainment speed is obtained using a commercial tribometer with soft hydrophobic (PDMS) substrates; adsorption and interfacial film properties onto hydrophobic (PDMS)

substrates using SPR and QCM-D. This combined experimental approach generated a comprehensive picture on thin film formation, layer deposition and layer stability in relation to lubrication properties.

Our experiments have demonstrated that while all the polysaccharides tested had a similar viscosity at moderate shear rates, distinct differences are observed at low and high shear rates and in their non-linear viscoelasticity. A rigid dumbbell model accurately described their apparent normal stress differences such that the polysaccharide solutions could each be characterized by a single characteristic relaxation time. The friction measurements on smooth surfaces demonstrated that many of the differences in friction coefficient in the mixed and hydrodynamic regime arise due to differences in the viscosity at shear rates of order 10^4 s^{-1} . However, polymers that adsorbed to form films that had a larger thickness than the surface roughness were also found to promote full film lubrication at lower speeds compared to non-adsorbing Newtonian fluids.

In this work the novel finding is reported that the total lubricant film thickness at the junction between the mixed and EHL regime, where the friction coefficient is a minimum, directly correlates with the hydrated film thickness of adsorbed polymer or ‘wet mass’ obtained from QCM-D. Overall, the friction coefficient in the mixed regime between smooth tribopairs seem to depend mainly on the hydrated adsorbed polymer mass and film modulus, while for the rough tribopair the friction coefficient in the boundary regime was more dependent on the overall amount of adsorbed polymer. Pectin was found to be the most effective lubricant: its high viscosity at high shear rates led to a lower friction coefficient in the mixed-regime, and it adsorb to the surfaces in high amounts to form films that were highly hydrated and viscoelastic. In contrast, Locust bean gum only adsorbed as a very thin rigid film and it subsequently had very little influence on the friction coefficient on rough or smooth surfaces.

Since these polymer solutions have been constructed to have essentially the same ‘oral thickness’, anticipated differences in mouth-feel perception would probably arise due to the differences in their physical properties and interaction with oral substrates. We have characterized their rheology, lubrication and adsorption to model substrates, but another factor not considered in this work is the interaction of the polymers with the salivary film coating oral surfaces; this will be the subject of future work. This was thus far not considered due to the complexity of salivary films, although recent studies by Stokes and Davies [38], Koliandris et al. [39], Rossetti et al. [40 and 41], Davies et al. [42], and

Vingerhoeds et al. [43], are starting to unravel this complexity to determine the response of saliva and salivary films to food components as well as their affect on sensory perception.

In conclusion, this study shows that there are many differences in physical properties between polysaccharide solutions that are designed to have a similar ‘oral thickness’; such differences include the rheology, adsorption, and lubrication properties. The study has particularly highlighted that the lubrication properties of measured polysaccharides depend on both their rheology and adsorption properties. Therefore, to understand the lubrication as effectuated by consumption of, for example food, and to enlighten different functional characteristics of food constituents, a combined insight of diverse techniques is necessary.

Acknowledgement

The authors would like to thank Georgina Davies (Unilever) for help with rheological measurements. Anne van de Pijpekamp and Anke Janssen are acknowledged for advice on formulating the polysaccharide solutions. Special thanks to Jeroen Bongaerts (Unilever) for his advice on tribology. The authors also wish to thanks Thomas Branfield (Unilever) for his help with PDMS preparation. All tribological, rheological and surface adsorption measurements were made at Unilever Corporate Research. Agnieszka Chojnicka-Paszun thanks Unilever for allowing use of their facilities to perform tribological and rheological studies. Lubica Macakova thanks the EU TOK Marie Curie Program for financial support of the project ‘Oral Biolubrication and Bioadsorption from Multiphased Complex Fluids’ MTKD-CT-2006-042779. We are grateful to Unilever Corporate Research for permission to publish these results.

References

- 1 van den Berg, L., van Vliet, T., van der Linden, E., van Boekel, M. A. J. S., van de Velde, F. (2007). *Food Hydrocolloids*, 21:961-979.
- 2 Butt, H. J., Graf, K. & Kappl, M., (2003). *Physics and Chemistry of interfaces*. Weinheim: WILEY-VCH Verlag, p.225.
- 3 Esfahanian M. & Hamrock, B. J. (1991). *Tribology Trans.*, 34, 628.
- 4 de Vicente, J., Stokes, J. R. & Spikes, H. A. (2005a). *Tribology Letter*, 20:273-86.
- 5 de Vicente, J., Stokes, J. R. & Spikes, H. A. (2006). *Food Hydrocolloids*, 20:483-91.
- 6 Cassin, G., Heinrich, E. & Spikes, H. A. (2001). *Tribology Letters*, 11:95-102.

- 7 de Vicente, J., Stokes, J. R. & Spikes, H. A. (2005b). *Tribology International*, 38:515-26.
- 8 Malone, M. E., Appelqvist, I. A. M., Norton, I. T. (2003). *Food Hydrocolloids*, 17: 763-773.
- 9 Klein, J., Kumacheva, E., Perahia, D., Mahalu, D. & Warburg, S. (1994a). *Faraday Discuss.*, 98, 173-188.
- 10 Klein, J., Kumacheva, E., Mahalu, D., Perahia, D. & Fetters, L. (1994b). *Journal of Nature (London)*, 370, 634-636.
- 11 Lee, S. and Spencer N. D. (2005). *Tribology International*, 38(11-12), 922-930.
- 12 Muller, M. T., Yan, X., Lee, S., Perry, S. S. & Spencer, N. D. (2005). *Macromolecules*, 38, 5706-5713.
- 13 Bongaerts, J. H. H., Cooper-White, J. J. & Stokes, J. R. (2009). Low Biofouling Chitosan-Hyaluronic Acid Multilayers with Ultra-Low Friction Coefficients. *Biomacromolecules*, 10, 1287-1294.
- 14 Wood, F. W. (1968). Psychophysical studies on the consistency of liquid foods. Rheology and texture of foods. London: Society of Chemical Industry, Monograph 27, 40-49.
- 15 Shama, F., & Sherman, P. (1973). *Journal of Texture Studies* 4(1), 111-118.
- 16 Cutler, A. N., Morris, E. R., & Taylor, L. J. (1983). *Journal of Texture Studies* 14(4), 377-395.
- 17 Dickie, A. M., & Kokini, J. L. (1983). *Journal of Food Science*, 48(1), 57-61.
- 18 Stanley, N. L. & Taylor, L. J. (1993). *Acta Psychologica* 84, 79-92.
- 19 de Jong, S. & van de Velde, F. (2007). *Food Hydrocolloids*, 21 1172-1187.
- 20 Davies, G. A. & Stokes, J. R. (2008). *Journal of Non-Newtonian Fluid Mechanics*, 148:73-87.
- 21 Davies, G. A. & Stokes, J. R. (2005). The Society of Rheology, Inc. *Journal of Rheology*, 49(4), 919-922.
- 22 Bongaerts, J. H. H., Fourtouni, K., Stokes, J. R. (2007a). *Tribology International*, 40:1531-42.
- 23 Rodahl M., Hook, F., Krozer, A., Brzezinski, P. & Kasemo, B. (1995). Review of Scientific Instruments, 66 (7), 3924-3930.
- 24 Voinova, M. V., Rodahl, M., Jonson, M. & Kasemo, B. (1999). *Physica Scripta*, 59(5), 391-396.
- 25 Larsson, C., Rodahl, M. & Hook, F. (2003). *Analytical Chemistry*, 75(19), 5080-5087.
- 26 Lofas, S., Malmqvist M., Ronnberg, I., Stenberg, E., Liedberg, B. & Lundstrom, I. (1991). *Sensors and Actuators B*, 4, 79-84.
- 27 Nagata, N. & Handa, H. (2000). *Real-Time Analysis of Biomolecular Interactions*; Springer-Verlag: Tokyo.
- 28 Macakova, L., Blomberg, E. & Claesson, P. M. (2007). *Langmuir*, 23, 12436-12444. (Supporting Information).
- 29 Hook, F., Voros, J., Rodahl, M., Kurrat, R., Boni, P., Ramsden, J. J., Textor, M., Spencer, N. D., Tengvall, P., Gold, J. & Kasemo, B. (2002). *Colloids and Surfaces B-Biointerfaces*, 24(2), 155-170.
- 30 Reimhult, E., Larsson, C., Kasemo, B. & Hook, F. (2004). *Analytical Chemistry*, 76(24), 7211-7220.
- 31 Stewart, W.E. & Sorensen, J.P. (1972). Hydrodynamic interaction effects in rigid dumbbell suspensions. II. Computations for steady shear flow. *Trans. Soc. Rheol.* 16, 1-13.
- 32 Bird, R. B., Armstrong, R. C. & Hassanger, O. (1987). *Dynamics of Polymeric Liquids. Volume 1: Fluid Mechanics*, (2nd edn.) John Wiley Interscience, 142.
- 33 Stokes, J. R., Graham, L. J. W., Lawson, N. J. & Boger, D. V. (2001). Part 2, *Journal of Fluid Mechanics* 429, 117-153.
- 34 Graca, M., Bongaerts, J. H. H., Stokes, J. R. & Granick, S. (2007). Friction and adsorption of aqueous polyoxyethylene (Tween) surfactants at hydrophobic surfaces. *Journal of Colloid and Interface Science*, 315, 662-670.
- 35 Archard, J.F. (1957). *Proc. Roy. Soc. Lond. Series A – Mathematical and Physical Sciences*, 243 (1233) 190-205.
- 36 Myant, C., Spikes, H. A. & Stokes, J. R. (2009). Influence of load and elastic properties on the rolling and sliding friction of lubricated compliant contacts. *Tribology International*, In Press, Corrected Proof.
- 37 Mo, Y.F., Turner, K.T. & Szlufarska, I. (2009). Friction laws at the nanoscale, *Nature*, 457(7233), 1116-1119.

- 38 Stokes, J. R. & Davies, G. A. (2007). *Biorheology*, 44(3), 141-160.
- 39 Koliandris, A., Lee, A., Ferry, A. L., Hill, S. & Mitchell, J. (2008). Relationship between structure of hydrocolloid gels and solutions and flavour release. *Food Hydrocolloids*, 22, 623-630.
- 40 Rossetti, D., Yakubov, G. E., Stokes, J. R., Williamson A. M. & Fuller G. G. (2009a). *Food Hydrocolloids*, 22(6), 1068-1078.
- 41 Rossetti, D., Bongaerts, J. H. H., Wantling, E., Stokes J. R. & Williamson A. M. (2009b). *Food Hydrocolloids*, 23(7), 1984-1992.
- 42 Davies, G.A., Wantling, E. & Stokes, J.R. The Influence of Beverages on the Stimulation and Viscoelasticity of Saliva: Relationship to Mouthfeel ? *Food Hydrocolloids*, In Press.
- 43 Vingerhoeds, M. H., Silletti, E., Groot, J. D., Schipper, R. G. & Van Aken, G. A. (2009). Relating the effect of saliva-induced emulsion flocculation on rheological properties and retention on the tongue surface with sensory perception. *Food Hydrocolloids*, 23, 773-785.

Chapter 5

Sensorial analysis of polysaccharide-protein gel particle dispersions in relation to lubrication and viscosity properties

Abstract

In this chapter polysaccharide-protein gel particle dispersions were investigated for their sensorial relation to their bulk rheological and tribological properties. Sensory analysis was performed by a QDA panel to evaluate distinct mouth-feel perception. Attributes such as powdery, slipperiness, stickiness, and filmy were then correlated to tribological and rheological data of these dispersions. Since thickness perception masked scores of other attributes, all samples were tuned to obtain the same score in sensorial thickness to minimize its influence.

The experimental survey presented in this chapter revealed an interesting set of correlations. The friction coefficient showed a negative correlation with slipperiness, while with other attributes the established relation was below a significant level. Attributes, such as stickiness, sliminess and filmy, correlated with viscosity data of the dispersions within a wide range of shear rates. In addition, a direct relation was found between the powdery attribute and the size of particles present in the dispersions. Moreover, the hardness of these particles seemed to have a strong influence on the steepness of this latter relation.

5.1 Introduction

The perception of particles in the food system can vary with their type (e.g. protein aggregates, fat droplet or starch granules), shape (e.g. round vs irregular), size, hardness, and depends on the medium that they are dispersed in. In some of the products the particles are hardly sensed (e.g. fat droplets in the mayonnaise or starch granules), whereas in others the clear evidence of them can be distinguished (e.g. groats or porridge in the puddings or fragments of fruits in yogurts).

The effect of particles on the perceived texture and lubrication properties of semi-solid food was studied by de Wijk and Prinz [1]. Higher friction was obtained for large or irregular particles than for small or round ones. It was found that higher friction typically was associated with a decreasing sensation of creaminess, fattiness, stickiness or smoothness and increasing sensation of attribute such as roughness. Interestingly, their study showed that sharp-edged particles, which increased the friction, reduced astringency perception. Another study relating the particles with oral perception [2] showed strong correlation between the presence of the particles and texture perception of the semi-solid custard dessert. This relation was explained by the lubricative properties of the food relative to the oral tissue. It was shown that upon particles addition, the attributes associated with poor lubrication (e.g. roughness) increased, while the attributes associated with good lubrication (e.g. creaminess or fattiness) decreased.

Other study revealed, that rather soft chocolate particles that are below 25 μm in size and have irregular shapes (but not hard edges) are perceived as smooth [3]. On the other hand, a gritty effect was observed even for small (around 10 μm), irregular aluminum oxide particles [4]. Imai et al. [5] found that an increase of the particle concentration (different types of microcrystalline cellulose) and their size lead to an increase of grittiness perception. On the other hand, a decrease of this attribute was observed as the viscosity of the dispersion medium increased. Other study of Tyle [6] showed that oral texture of model particles (garnet, polyethylene and mica) depends on their size, shape, and hardness in aqueous suspensions. He found, that grittiness perception was more apparent for small hard and sharp particles than for large, soft, and round ones. Furthermore, the particle size and concentration in the soft model systems were related to creamy attribute by Kilcast and Clegg [7]. They found that larger particle size and higher concentration reduce creaminess.

Van Vliet and Walstra [8] pointed that food products containing particles may become inhomogeneous during the storage. Thus processes such as sedimentation or creaming of particles in food systems may affect their perception. They gave an example of the cocoa particles that may sediment forming a bitter dark-brown layer on the bottom and light-brown upper layer with bland taste. Also, in some beverages particles may settle at the bottom forming hardly dissolved layer during shaking.

The correlation between friction coefficients measured at different speeds and slippery perception was investigated by Malone et al. [9]. A significant level of correlation between lubrication properties of the fluids and slippery perception was obtained at entrainment speed between 10 and 100 mm/s. Therefore, authors concluded that the mixed regime of lubrication is relevant to study the in-mouth processing associated with the slippery perception. As the entrainment speed between 10 and 100 mm/s corresponds to estimated film thickness of the order to 1.5 – 25 μm , most of the particles found in food system falls into this range.

In some of the product uncontrolled and undesired sensory responses due to e.g. sedimentation, creaming of particles, or too obvious occurrence of particles may have a discouraging effect on a consumer. Therefore, a deep understanding of the behavior of particles in the suspension is of importance. Lately, new type of particles called protein particles (spheres or beads) were developed (work carried out in our research group). These spherical particles were generated by harvesting and washing from protein-polysaccharide gel (obtained via cold-set gelation [10]). The advantages of these spherical particles are: theoretically they can be generated from any type of protein and it is easy to modify them e.g. different size of particles might be obtained by varying the polysaccharide concentration [11]. The size of particles is of importance during mastication of a food product [2,8]. Therefore, in the current work the impact of these spherical protein agglomerates (with radii of about 8 to 56 μm) on lubrication properties of different polysaccharide solution was studied. These polysaccharide solutions were of our interest as they are widely applied in the industry. In addition, to compare the protein particles with different systems, degraded protein gel particles mixed with polysaccharide solutions were investigated. Their size varied between 48 and 57 μm and was comparable to the largest protein spheres. Thus a relation of particles to sensory properties was investigated to study the impact of different sizes and types of particles on the perception [12].

The protein beads have been prepared in different ways in order to control their sizes and were modified to control hardness. The native small and large protein particles were cross linked with transglutaminase (TGase), which led to an increase of their hardness (work carried out in our research group). The largest protein beads were swollen as a result of an increase of pH to 8. This process led to a decrease of the firmness of large swollen beads. The aim of this chapter is to investigate the relation between sensory properties of mixed polysaccharide/protein particle dispersions and their rheological and tribological properties.

5.2 Materials and Methods

5.2.1 Materials

Whey protein isolate (WPI) BiproTM was purchased from Davisco Foods International Inc. (La Sueur, MN). Xanthan gum (KeltrolTM T), locust bean gum (C-130, LBG), and high methyl ester pectin (H-6) were kindly donated by CP Kelco Inc. (Lille Skensved, Denmark). All polysaccharides were of unstandardised quality and, therefore, without additives. Chemical composition of these polysaccharides was reported by de Jong et al. [13]. Glucono- δ -lactone (GluconalTM, GDL) was kindly provided by Purac Biochem (Gorichem, The Netherlands). Transglutaminase (Activa WM) was obtained from Ajinomoto Foods Europe S.A.S. (Paris, France). All ingredients were used without further purification and without correction for their moisture content. Reverse osmosis water was used in all cases.

5.2.2 Sample preparation

Polysaccharide solutions

Stock solutions of LBG (1.7 % w/w), xanthan (4% w/w) and pectin (3% w/w) were prepared by sprinkling the powder over a sieve into the appropriate amount of water under continuous stirring. Solutions were hydrated for at least 2 hours. Subsequently, the solutions were filtered to remove possible non-dissolved material and heated at 80 °C for 45 minutes. The pectin sample was filtered after heating. The solution was cooled using running tap water. LBG stock solution was diluted to 0.8, 1.0, 1.2 and 1.5% (w/w), xanthan to 1.5, 2, 2.75 and 3.25% (w/w) and HM-pectin solution to 1.5, 2.0, 2.25 and 2.5% (w/w). These samples, including the stock solutions, were used for sensory analysis

as well as for the tribological and rheological experiments. The solutions were used for measurements within two days after preparation.

Protein particles

Protein particles (beads) were obtained using the phase separation property of a whey protein isolate/ locust bean gum mixed gel. WPI 9% (w/w) was dissolved in water under continuous stirring, for at least 2 hours at room temperature. Soluble WPI aggregates were obtained by incubating the WPI solution in portions of 400 ml at 68.5 °C in a water bath for 2.5 hours [14]. The properties of these WPI aggregates dispersions were described in Chapter 2 [15]. After heating, the dispersions were cooled to ambient temperature using running tap water. Subsequently, the dispersions of WPI aggregates were diluted with de-ionized water to a concentration of 3% (w/w). Next, LBG stock solution of 1.7% w/w was prepared as described above. Mixtures of WPI aggregates dispersion and locust bean gum stock solutions were made and WPI/LBG mixed protein system were prepared by the so-called acid-induced cold gelation process [16]. The gelation of the mixed WPI/LBG solution was induced by the addition of 0.25% (w/w) of glucono- δ -lactone (GDL) to achieve a pH value of 4.8 ± 0.1 after 20 h of incubation at 25 °C. To isolate the protein beads from the LBG-containing solution, the acidified mixed system was washed three times with de-ionized water. In order to obtain the best sedimentation of the protein particles different speeds of centrifugation in each of the steps were used. First, the system was diluted with water (1:1.5 ratio) in 1 liter centrifuge bottles and centrifuged (Sorvall RC3C, Sorvall Instruments, Waltham, USA) during 15 minutes at 4000 rpm and at 2000 rpm for the small and large sized protein particles, respectively. The second time, the pellet after centrifugation was thoroughly mixed using a spoon to form one homogeneous mass which was dispersed with water (1:1.5 ratio) in 1 liter centrifuge bottles. Small and large beads were centrifuged at 2500 rpm and at 1500 rpm, respectively for 15 minutes. The third time, the pellet was processed and dispersed with water similarly to the second time. In this step the mixture system was centrifuged during 15 minutes at 2000 rpm and at 1500 rpm for the small and large sized protein particles. After these three centrifugation steps, the pH value of the pellet containing beads was 4.50 ± 0.05 . Subsequently, the protein beads were isolated from this polysaccharide-continuous WPI/LBG system. By adjusting the LBG concentration during the gelation procedure, different sizes of protein particles were prepared [11]. Protein particle at small and large size were obtained by preparing WPI 9-3/0.7% and WPI 9-3/0.53% gels, respectively. The

abbreviation indicates that gels were prepared from a 9 % (w/w) of WPI aggregate dispersion which was diluted to 3 % (w/w) of protein and mixed with 0.7 or 0.53% (w/w) LBG that was previously diluted from the prepared 1.7% LBG stock solution. Protein beads were always made in portions of 900 ml. To determine the amount of protein in the obtained pellet of protein beads, 1 g of pellet was dispersed in 20 ml of 6M urea/ 1% (w/w) sodiumdodecylsulphate (SDS) solution, after which water was added until a volume of 200 ml. Absorbance at 280nm was measured using a Cary 4000 spectrophotometer (Varian, Inc., California, USA). For the different protein beads (small and large, before and after transglutaminase treatment, see below) A280 values were calibrated using Kjeldhal analysis (ref given), to calculate protein content of the pellet. In this way a factor could be estimated to quickly calculate protein content based on a simple measurement of A280.

To increase firmness of the protein beads (small and large), the above-described protein particles could be cross-linked with transglutaminase (TGase) [17]. This was done prior to the washing and isolation step of the beads. Transglutaminase was added at a ratio of 1:10, by sprinkling the TGase powder over a sieve into the acidified mixed system under continuous stirring. After 30 minutes of stirring, the solution was filtered to remove possible non-dissolved TGase and incubated during 3 hours at 50 °C without stirring [11]. Enzymatic activity was stopped by incubation at 68.5°C during 30 min, after which the beads were washed as describe above and isolated.

Raising the pH, using 1M NaOH, of the suspended protein particles to 7.8-8.0 an increase of the size of the large beads (obtained from WPI9-3/0.53% system) could be obtained [11]. Prior to adjusting the pH, the protein bead pellet (of known protein content) was diluted 1:1 with water to be able to magnetically stir easily and mix in the NaOH solution. The viscosity of the solution increased tremendously upon addition of the NaOH, therefore a manual and careful mixing procedure was done when approaching the final pH value.

All samples were stored in the fridge. Prior to the experiments protein beads were mixed with polysaccharide solution (LBG, pectin and xanthan) in a concentration of 3 % (w/w). In order to simplify the designation of the samples used in this chapter, Table 5.1 shows their abbreviations.

Table 5.1 Lists of samples used in this chapter with their codes, abbreviations and their particle sizes. Note that the actual size of the small gel particles (WPI9-6SM/2) is bigger than gel particles (e.g WPI9-6/2) due to their aggregation.

Particles	Codes	Abbreviation	Size (μm)*
Small beads	WPI9-3/LBG 0.7%	SM	15
Small beads crosslinked with TGase	WPI9-3/LBG 0.7%/TGase	SMTg	8
Large beads	WPI9-3/LBG 0.53%	LA	21
Large beads crosslinked with TGase	WPI9-3/LBG 0.53%/TGase	LATg	14
Large beads prepared at pH8	WPI9-3/LBG 0.53%/pH8	LA8	56
Gel particles	WPI9-9/3	9-9/3	52
Gel particles	WPI9-6/3	9-6/3	48
Gel particles	WPI9-6/2	9-6/2	51
Small gel particles	WPI9-6SM/2	9-6S/2	57

* average values obtained from Mastersizer 2000, Malvern Instruments D[3,2] [average values taken from 11, 12 to be published].

Degraded protein gel particles

The fragmented gel particles were obtained by the mechanical breakdown of WPI gels. Initially, dispersions of the 9% (w/w) WPI aggregates were prepared as described above. Subsequently, the WPI aggregates were diluted with de-ionized water to a concentration of 6% (w/w) or were used non-diluted (abbreviation WPI9-6% and WPI9-9%, respectively). Gelation of the protein aggregates dispersions was induced by addition of 0.44 or 0.66% (w/w) GDL for WPI gels which 6 and 9 % (w/w) protein respectively, to reach a final pH value of 4.8 ± 0.1 after 20 hours of incubation at 25 °C. The gels were pre-homogenised with demineralised water (75% (w/w) gel, 25% (w/w) water) in a blender. A colloid mill (RD3 N60, Probst & Class Maschinenfabrik, Rastatt Germany) was used to mechanically breakdown the gels into particles of about 35-40 μm size. In order to remove the excess of water after colloid mill treatment, the samples were centrifuged at 3000 rpm for 15 minutes in a RC3C Sorvall centrifuge with a H6000A rotor. The supernatant was carefully removed from the sediment to avoid loss of gel particles. In order to determine the final protein concentration of the sediment containing the gel particles, the water removed by centrifugation was accurately weighed. Finally, particles of fragmented gel were mixed with polysaccharide solutions (LBG, pectin and xanthan) in two different concentrations: 2 and 3% (w/w) (abbreviated WPI9-6/2 and WPI9-6/3, respectively; see Table 5.1).

5.2.3 Quantitative descriptive analysis (QDA)

The sensory characteristics of the polysaccharide/particle dispersions were investigated using a sensory panel trained in Quantitative Descriptive Analysis (QDA) [18]. The sensory evaluation is an established method to measure, analyze, and interpret the responses given by panelists about products and perceived through human senses. Therefore, during training sessions eleven panelists (judges) were asked to identify and define mouth attributes (see Table 5.2). The first four attributes listed in Table 5.2 correspond to mouth-feel sensation, while the last one (filmy) describes the after-feel perception. The samples were evaluated at room temperature and were presented to each assessor randomly. The bottle with the solution containing particles was gently shaken in order to get a homogeneous distribution in the sample. Subsequently, each sample was served in a small plastic test cup. Prior to the testing the panelists were asked to gently stir the samples. In order to prevent mixing of saliva with the samples multiple spoons were used by the judges (one for stirring and taking out the sample from the test cup, the second one was subsequently used for putting the sample in the mouth). The samples were evaluated in duplicate during six profiling sessions. In each profiling session, three different polysaccharides (LBG, pectin and xanthan) with or without particles were tested. Each profiling starts with 1% (w/w) LBG in order to score the reference for all defined attributes. These scores were used as calibration points for each attribute. In order to mask possible differences between solutions, 2 µl/ml of an artificial sweetener (Natrena) and 0.4 µl/ml of a 5% (w/w) ethyl butyrate (citrus fruit flavor) solution in propyleneglycol were added to the polysaccharide solutions. The sensory characteristics of the polysaccharide/particle dispersions were described in more detail by Janssen et al. [12].

Table 5.2 Definitions of selected attributes generated by quantitative descriptive sensory analysis.

Attributes	Definitions
Slippery	The samples slips away in the mounth (no grip)
Sliminess	Thick liquid that stays in the mouth
Stickyness	A sticky sensation on palate and between the teeth (sticky threads sensed by tongue, palate and throat)
Powdery	The sensation of small particles like e.g. flour
Filmy	Staying behind of the layer in the mouth

5.2.4 Rheological measurements

The viscosity data of the polysaccharides solutions were recorded at 30 °C using a standard rheometer (AR 2000, TA Instruments, Leatherhead, UK) with double concentric cylinder geometry. Flow curves were obtained by measuring the apparent viscosity as a function of increasing shear rate (from 0.1 and 1000 s⁻¹). The measurement consisted of two steps: a 5 minutes conditioning step where the system was temperature equilibrated, followed by continuous ramp with exponentially increasing shear rate lasting for 15 minutes. All measurements were performed at least in duplicate and average values were presented. All polysaccharide/particles solutions showed non-Newtonian behavior and results were previously reported by van de Pijpekamp et al. and Janssen et al. [11, 12].

5.2.5 Thickness tuned viscosity profile for the polysaccharide solutions

Thickness often masks or dominates the sensation of other mouth-feel attributes (e.g. stickiness) [19]. Therefore in the current study, the experimental panel was asked to choose the concentration of different polysaccharides (out of five concentrations for each polysaccharide), such that the thickness attributes of these solutions were the same. As described above, three different polysaccharides were used in this chapter: LBG, pectin and xanthan solution. The panelists were asked to match the thickness attribute for all polysaccharides according to a reference sample, which was 2.25 % (w/w) pectin. Similar mouth-feel thickness as perceived for a 2.25% (w/w) pectin solutions were obtained for a LBG and xanthan solution at a concentration of 1 and 2 % (w/w), respectively [12].

In general, the thickness attribute of a solution is known to be described to large extend by apparent viscosity (see Stanley and Taylor [20] and references therein). Therefore, in the current work, the viscosity of the thickness tuned polysaccharide solutions were treated as a reference for the solutions to which particles were added. As described in section 2.2 all protein beads were added to LBG, xanthan and pectin solution in concentration of 3 % (w/w), while gel degraded particles were added in a concentration of 2 and 3% (w/w). It is evident that addition of protein beads with different sizes and hardness as well as fragmented gel particles affected the viscosity of the solutions and so thickness perception. Therefore, all the polysaccharide/particles mixed dispersion were adjusted to match the reference viscosity of the solutions tuned for thickness attribute (i.e. 1, 2.25 and 2% (w/w) for LBG, pectin and xanthan, respectively). This was done by adjusting the concentration of the polysaccharides in the polysaccharide protein particle mixtures to achieve viscosity

profile the thickness tuned polysaccharide solutions without particles. For more detailed information about the sample preparation see van de Pijpekamp et al. and Janssen et al. [11, 12].

5.2.6 Particle size

The size of the protein and fragmented gel particles were determined by Malvern 21 Mastersizer 2000 (Malvern Instruments Ltd., Malvern, UK) providing the volume-surface average or Sauter diameter ($d_{3,2}$) (see also [11]). The samples were analyzed in triplicate. The values in micrometers for all particles used in this chapter are listed in Table 5.1 .

5.2.7 Tribological measurements

A Mini Traction Machine (MTM) (PCS Instrument) with compliant rotating neoprene rubber surfaces (purchased from Eriks company, Arnhem, The Netherlands) was used to measure friction coefficient (μ). The friction coefficient was plotted as a function of the entrainment speed (U), which provided so called Stribeck curve described in a previous study (in Chapter 2 and Chapter 4 [15, 22]). The contact was between the neoprene O-ring and a neoprene disc. For each measurement a new rubber was used and cleaned with ethanol and reverse osmosis water and subsequently dried to the air. The experimental conditions are described in Chapter 2 [15] and were done at a temperature of 30°C ($\pm 1^\circ\text{C}$), with 2 and 5N load, slide-to-roll ratio of 50% and speed from 500mm/s to 5mm/s. All measurements were performed at least three times and averaged (each presented point corresponds to a mean value). The standard deviation in all the measurements was below $\sigma=\pm 0.1$. Please note that the actual load applied in the tribometer for soft surfaces is not calibrated. However the relative values are valid.

5.2.8 Confocal Laser Scanning Microscopy

For imaging a LEICA TCS SP Confocal Laser Scanning Microscope (CLSM) equipped with an inverted microscope (model Leica DM IRBE) and Ar, DPSS and HeNe visible light lasers (Leica Microsystems (CMS) GmbH, Mannheim, Germany) was used. Objective lenses of 20x magnification (HC PL APO 20x/0.70 CS) and 63x magnification (HCX PL APO 63x/1.20 W CORR CS) were used. Solutions were stained with an aqueous solution of Rhodamine B (20 μL of a 0.2% (w/w) Rhodamine B added to 1 ml of sample). Excitation was performed at 561 nm and emission of Rhodamine B was recorded

between 580 and 700 nm. Reported digital images were recorded at a penetration depth of 15 μm and image files were acquired in 1024x1024 pixel resolution.

5.3 Results

In this chapter three polysaccharides (LBG, pectin, and xanthan) mixed with protein particles of different type, size and hardness, were used as food models. These hydrocolloid mixtures exhibit different characteristics (both physical and chemical, see Chapter 4 and [13]) that were reflected in sensorial, tribological and rheological measurements. The aim of this work was to study the impact of different protein particles mixed with polysaccharide solutions on human perception by linking sensory to physical data. For instance the different rheological characteristics of the hydrocolloids affect their thickness perception. The apparent viscosity was an important parameter in determining this thickness attribute and contributed also to other sensory characteristics. Previous work (Janssen et al. [12]), however, showed that viscosity-tuned polysaccharide solutions exhibit a different perception of thickness. These polysaccharide solutions had a common interception in the flow curve at shear rate of 50 s^{-1} , generally believed as a relevant oral processing condition (see Chapter 1, Chapter2 [15] and Chapter 4 [22] references therein). In this chapter an alternative approach was chosen to minimize the effect of the thickness attribute from the sensory analysis. To do so, the judges (assessors) were asked to pick the solution with similar perception of this attribute from several concentrations of the different polysaccharide solutions (see section 2.5 in materials and methods). As a results a 2.25% of pectin, 1% of LBG and 2 % (w/w) of xanthan were chosen to have similar thickness attribute. This approach showed that a sample with similar thickness attribute, had different bulk rheological behavior (data not shown, see [12, 23]). The obtained viscosities were used to construct reference flow curves. Next, the protein particles were added into the polysaccharide system. Figure 5.1 shows an example of the reference viscosity curve for the xanthan solution (2 % (w/w)) and the flow curves after addition of protein spheres and degraded gel particles followed by appropriate dilution of the xanthan solution. It can be concluded that the apparent viscosity of the particles/polysaccharide solution was adjusted in such a way that viscosity effectively matched the reference polysaccharide solution.

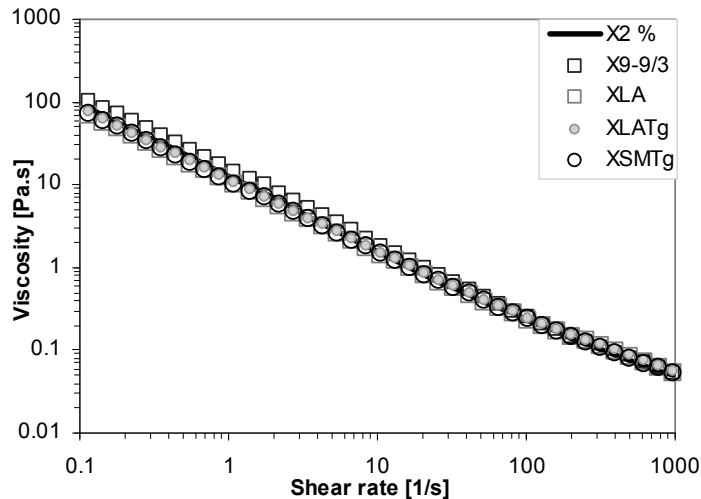


Figure 5.1 Viscosity as a function of the shear rate for xanthan solutions with and without different particles.

5.3.1 Influence of protein beads and degraded protein gel particles on the tribological properties of polysaccharide solutions

Effect of polysaccharide type

The lubrication properties of reference polysaccharides (LBG 1%, pectin 2.25 % and xanthan 2 % (w/w)) are shown in Figure 5.2 in so-called Stribeck curves. For all samples the hydrodynamic lubrication regime was inaccessible due to speed limitations. The shape of the Stribeck curves differed for the different polysaccharides. The boundary regime was observed only in the case of LBG. LBG indicated the highest friction and a clear boundary regime below about 20 mm/s. The Stribeck curve in this regime was flat and independent of speed. The boundary regime changed into the mixed regime instantaneously at speeds of about 20 mm/s. A steep decrease was followed by a shallower decline of friction at speeds above ~ 40 mm/s. At the highest measured speed the friction reached $\mu=0.3$. Pectin also reached this friction value for high speed, although, it does not show the boundary regime. At the lowest speed pectin lubricated relatively well and was already in the mixed regime starting at $\mu=0.4$. The friction coefficient of xanthan was lower by about 0.15 than pectin in the entire range of speeds and showed the most efficient lubrication within all three samples. Similarly to pectin the boundary regime was not observed and the friction decreased slowly at all measured speeds indicating the mixed lubrication regime.

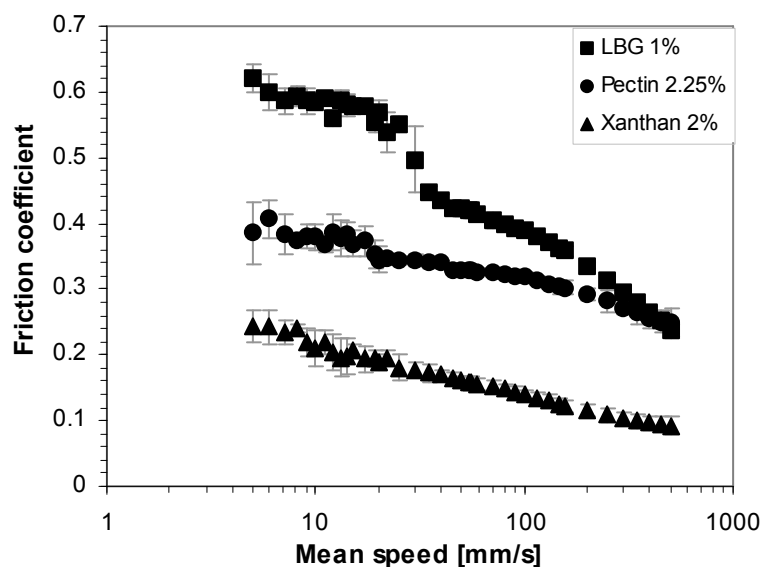


Figure 5.2 The lubrication properties of reference polysaccharide solutions: LBG 1%, pectin 2.25% and xanthan 2%, (w/w). These concentrations were tuned to have the same thickness perception.

Effect of polysaccharide concentration

Although a single concentration were selected because of its thickness perception, it is still good to know how various concentrations influence friction. To evaluate the influence of the polysaccharide concentration on its tribological performance, four different concentrations were used for each polysaccharide. In Figure 5.3, the friction of xanthan samples was strongly influenced by the concentration (the friction decreases by over 30% when the concentration was doubled and by about 60% when it increased by a factor of 2.7). At the lowest concentration the friction coefficient decreased from about 0.3 at low speeds to about 0.1 at the highest speeds, while at the higher concentrations the Stribeck curve was shifted downwards. At a concentration of 4% (w/w) the friction decreased from about 0.15 down to below 0.05. The lower the friction, the better the lubricant performs. For pectin the effect of concentration was relatively weak. Higher concentrations seemed to provide better lubrication. Interestingly an increase of concentration beyond 2.25% seemed to have no effect at low speeds and enhanced lubrication only at high speeds. Both xanthan and pectin showed no sign of the boundary regime even at their lowest concentration. This indicated that even such a low concentrations of this polysaccharide prevent the surface to be in contact.

In the case of LBG the Stribeck curve showed the boundary regime at low speeds. Regardless of the concentration the friction in this regime remained similar (oscillates

within the range of about $\Delta\mu = \pm 0.05$). Similar behavior was observed at higher speeds, for concentrations below 1.7%. This demonstrates that in the case of LBG the concentration did not influence the boundary lubrication. Moreover, a concentration of about 1.7% was required to affect the friction coefficient at high speeds. The friction coefficient at 500 mm/s changed from about $\mu=0.25$ for concentration of 0.8% to about $\mu=0.22$ for 1.2% and to $\mu=0.08$ at concentration of 1.7%.

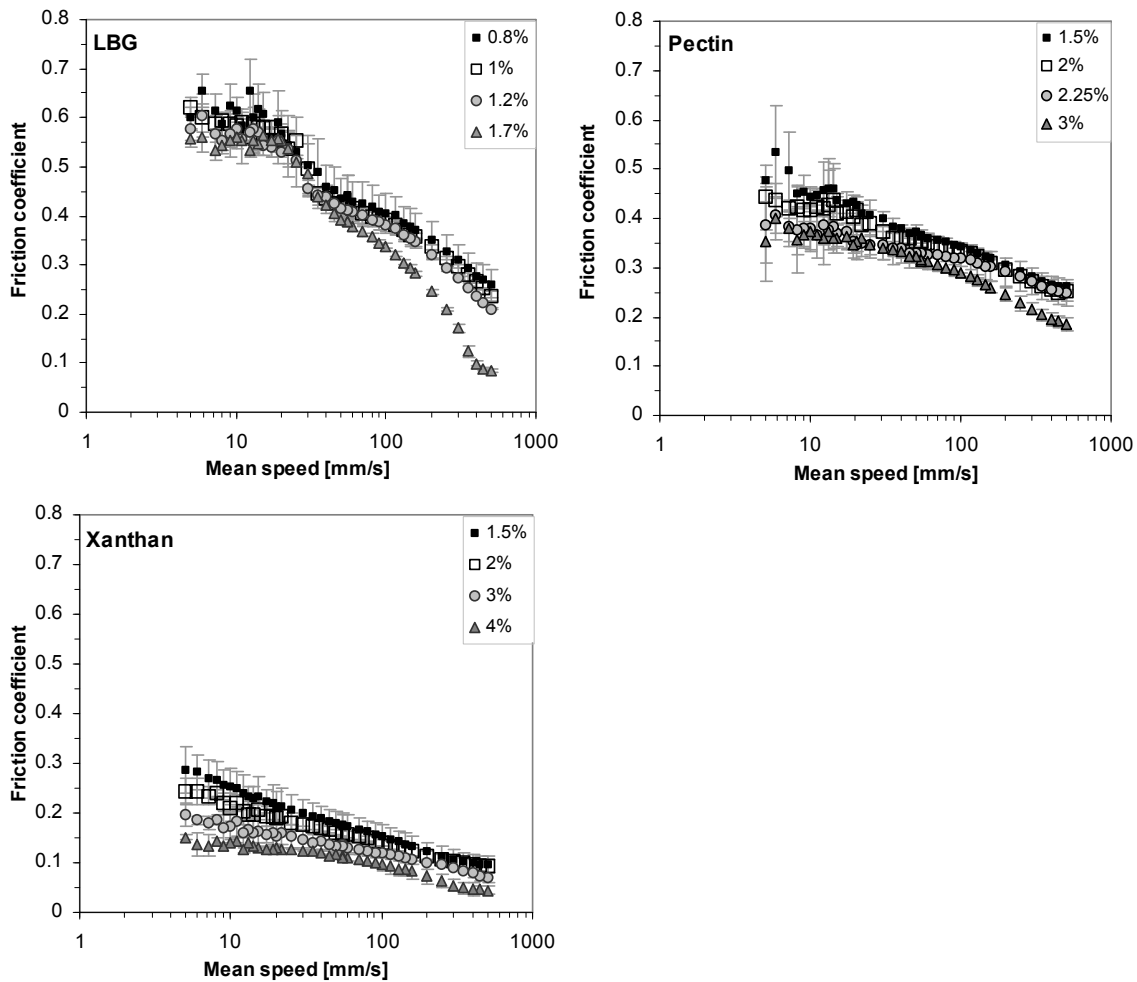


Figure 5.3 Stribeck curves: friction coefficient as a function of mean entrainment speed for three different polysaccharides with various concentrations as indicated. From the bottom left clockwise: xanthan, LBG, and pectin.

Effect of particles

Beads. The effect of beads on friction depended strongly on conditions such as type of lubricant (polysaccharide) or applied load. To understand the influence of particles the change of the lubrication properties of polysaccharides was studied upon an introduction of different beads and at two different loads. Figure 5.4 shows the Stribeck

curves for three polysaccharides at two loads (2 and 5 N). Each panel presents the frictional data for a polysaccharide mixed with particles. In addition, for a reference a data of a solution without beads was included.

Particles introduced into the contact zone generally increased the friction coefficient. In the case of LBG the relative increase of the friction coefficient was stronger for the normal load of 5 N. Almost all types of beads resulted in an increase of the friction by about 15% compared to LBG alone. An exception (relative decrease in friction) was observed for the largest beads. These latter particles were prepared at pH=8 and were swollen, which probably made them easily deformable. These soft beads also caused a decrease of friction at low normal load (2 N). In this case, however, the effect was much stronger (the friction coefficient decreased about 30% relative to the case of LBG alone). Other particles at this load showed a much weaker increase or no increase at all. Moreover, it seemed that the smaller the particles, the larger the increase of the friction coefficient was. Large beads showed a very similar Stribeck curve to LBG without particles, while small and cross-linked with TGase beads caused an increase of the friction.

For pectin the effect of beads on the friction was similar to that observed with LBG. For pectin beads caused an increase of the friction coefficient by about 30% for both normal loads. This polysaccharide was characterized by more effective lubrication properties resulting in friction lower than for LBG. Interestingly, the increase of the friction was observed only at low speeds (below about 100 mm/s). For low normal load and above 100 mm/s almost all particles caused a decrease of the friction coefficient. Only the largest beads (cross-linked with TGase) showed the same Stribeck curve as for pectin alone. The lowest friction was obtained for small beads. Even at low speeds they improved lubrication and resulted in friction lower than that of pectin alone. At higher load (5 N) the effect of beads was similar. Most of particle types caused an increase of friction (by up to about 30%) at lower speeds. Only small beads showed a decrease below about 200 mm/s. Above that speed all Stribeck curves seemed to overlap and to follow the one of pectin alone.

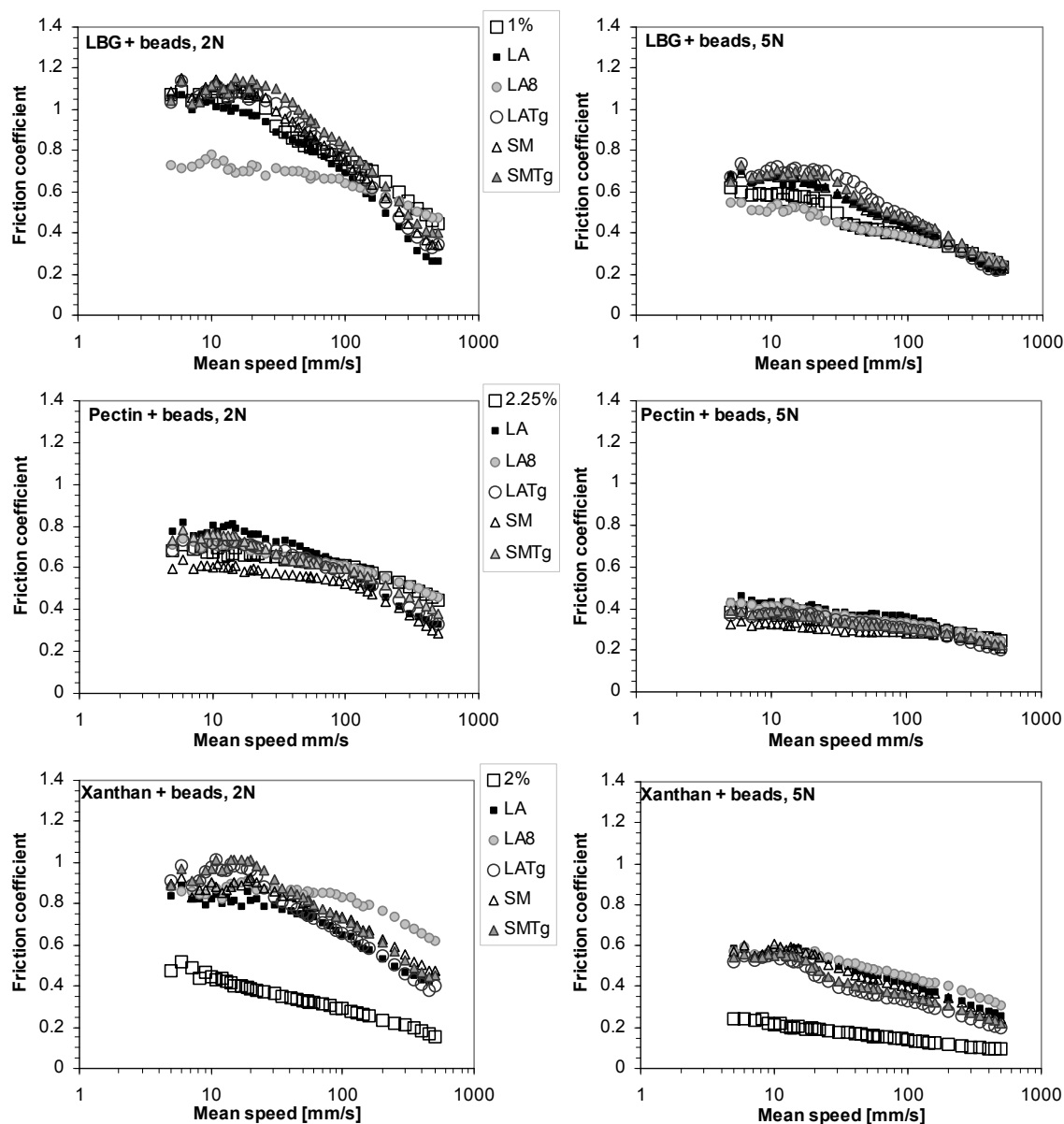


Figure 5.4 Stribeck curves: the effect of beads on friction at two loads. Each panel presents the frictional data for a polysaccharide mixed with particles. For reference, data for a solution without beads are also included.

The strongest effect of beads was observed for xanthan solutions. The Stribeck curve changed dramatically upon addition of beads regardless of their size or elasticity (deformability). The friction coefficient increased in this case by a factor of 2 (by 100%) for both normal loads. When particles were introduced to the xanthan solution, the Stribeck curve resembled that of LBG. In the case of lower normal load, large, soft beads (prepared at pH=8) seemed to have an extensive boundary regime up to 100 mm/s unlike at higher load, where the transition to the mixed regime occurred at about 10 mm/s. Moreover, at high normal load (5 N) the effect of beads seemed to be related to the

hardness of particles. The lowest friction was observed for the hardest beads (cross-linked with TGase) and the highest friction occurred for the softest, large particles (prepared at pH=8).

Degraded protein gel particles. Interestingly, gel particles showed rather similar behavior to large beads prepared at pH=8 (data not shown). For LBG and pectin at a low normal load they induced a decrease of the friction coefficient, while at high load they seemed not to affect the Stribeck curve at all. Also in the case of xanthan, gel particles caused a similar effect as large swollen beads. The friction coefficient was significantly increased by the presence of these gel particles. This behavior was most likely a result of similar size of gel particles and large beads (prepared at pH=8). Therefore it seemed that the main factor in shaping the Stribeck curve by not dissolved, or gel particles was their size. In general, particles can influence the lubrication by changing the environment for a lubricant. Possibly it resulted from the interaction of particles with surfaces (locking or filling asperities) and thickness of the film between surfaces.

Micro-images of the protein particles before and after MTM measurements.

To obtain better understanding of the influence of particles on frictional properties of polysaccharide solutions the influence of the MTM analysis on the integrity of the particles was investigated. A comparison was made of pre-processed particles to post-processed particles. Van de Pijpekamp et al. and Janssen et al. [11, 12] already reported the micro-image of the intact samples by CLSM images. In the present chapter images of the polysaccharide/protein solutions were made before and after MTM experiments (see Figure 5.5). This comparison revealed no visible changes in the system. The beads seemed to have a round shape and the same distribution of sizes as prior to the MTM experiment. Gel particles also preserved their initial sizes and irregular shapes. As all the particles (protein spears and gels) seemed to be unchanged after the tribological measurements, only few representative images are shown.

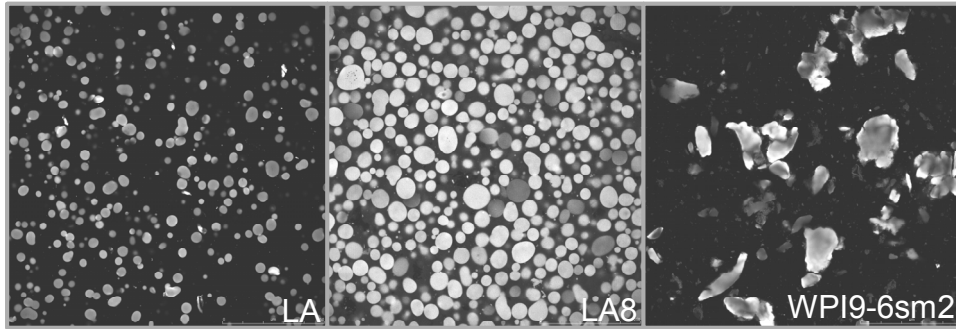


Figure 5.5 Microstructure of the large protein spheres (LA), swollen beads treated at pH=8 (LA8) and gel particles (WPI9-6sm2) after MTM experiment. Dimensions 158 μ m*158 μ m.

5.3.2 Influence of protein beads and degraded protein gel particles on perception of sensory attributes.

To relate the tribological data to sensory study it was necessary to investigate attributes that could be linked to lubrication properties. Since all the samples were tuned to have similar perceived thickness, the current work was focused on the remaining 5 attributes (see Table 5.2).

Powdery

Figure 5.6 shows the scores for all 5 attributes for the most representative samples. The data in each diagram was sorted by particle size, i.e. the particle size increased from left to right (note that large particles cross-linked with TGase were smaller than small particles). The influence of particles on oral perception was stressed in the case of the powdery attribute. These results are, however, counter intuitive. Although the presence of particles enabled the powdery sensation, the largest particles scored very low. Additionally, only xanthan samples demonstrated a clear dependence of the powdery attribute score with particle size (with the exception of the large swollen beads). It seems thus that powdery correlates to particle size, but is diminished for soft particles.

Slippery

For this attribute it was striking that xanthan, being a much better lubricant than LBG and pectin, scored only slightly higher for slippery attribute (see Figure 5.6). Moreover, the presence of particles resulted in a very small decrease of the score, contrary to the MTM data, where the friction coefficient increased significantly. Also for other samples the relative sensory scores were not reflecting findings of the MTM study. Pectin appeared here to be a worse lubricant than LBG, while the situation was in fact the opposite. Thus,

the correlation expected for slippery and friction coefficient very likely is influenced by some other property of the food dispersion, e.g. the film forming capacity.

Stickiness and filmy

Stickiness and filmy attributes are related. They described the ability of a sample to stick to the surface and form a lubricating film. Interestingly large particles (gels and swollen beads) seemed to work against film formation. For xanthan and LBG the effect of large particles was relatively strong. Xanthan seemed to be ineffective in film formation regardless of the presence of particles in the solution. Pectin on the other hand formed a film very well (compared to other samples) and seemed not to be affected by any particles. This was in agreement with friction data, where pectin was the second best lubricant and its lubrication properties were very weakly changed when particles were introduced. The other two polysaccharides, however, showed different behavior with and without particles and it could be reflected in the study of stickiness and filmy attributes. In conclusion for stickiness and filmy attributes small particles have weak effect on polysaccharides while large particles affect LBG and xanthan, but not pectin.

Sliminess

All three polysaccharides had high score for this attribute. However, the effect of particles seemed to be identical to the case of stickiness and filmy attributes. For LBG and xanthan large particles (gels and swollen beads) caused a decrease of the score while for pectin the difference was small.

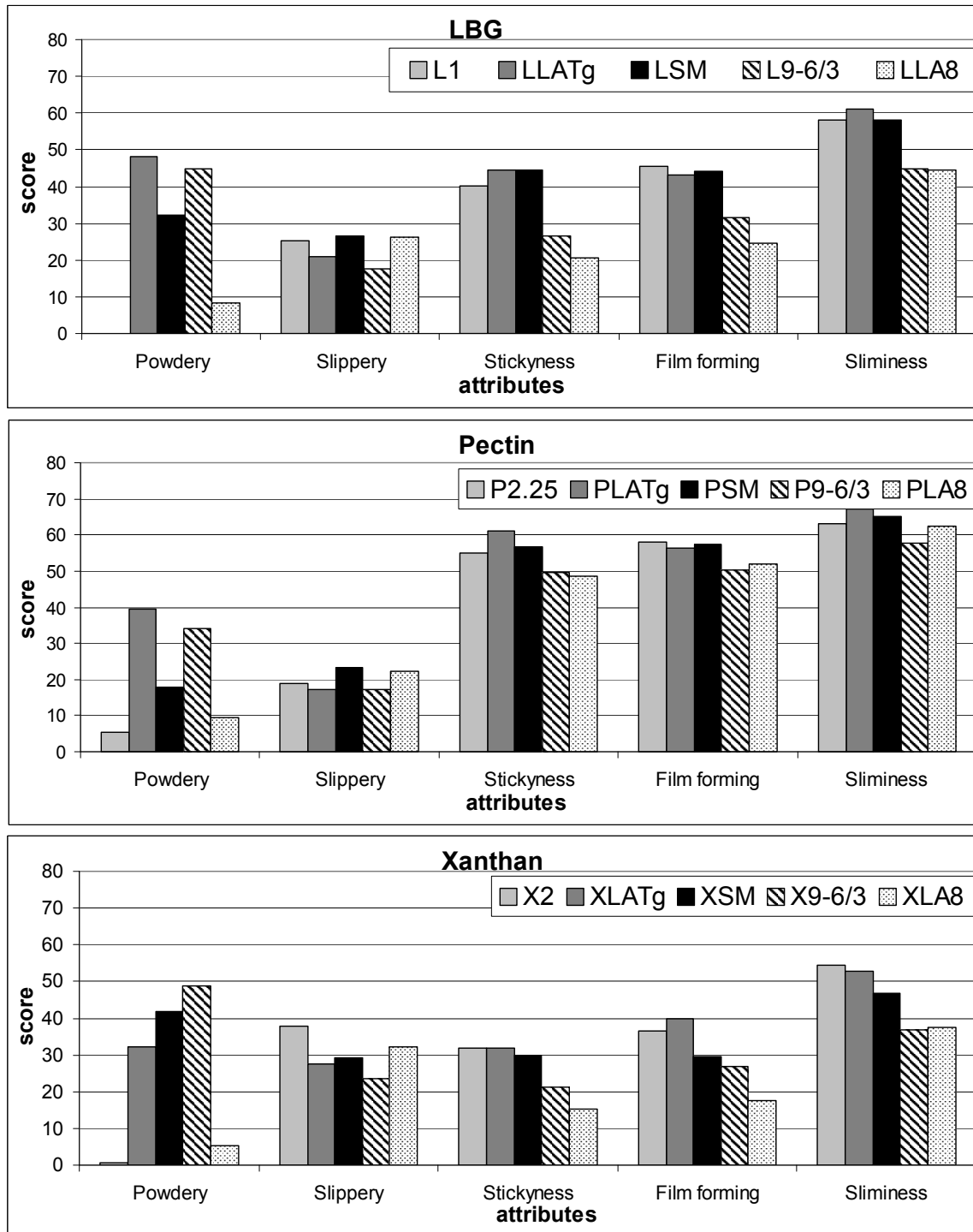


Figure 5.6 Attributes score for LBG, pectin and xanthan mixed with particles. Note that in each diagram the particle size increases to the right. One sample without particles was added to each diagram for reference.

5.4 Discussion

5.4.1 General schematic picture of contact lubrication

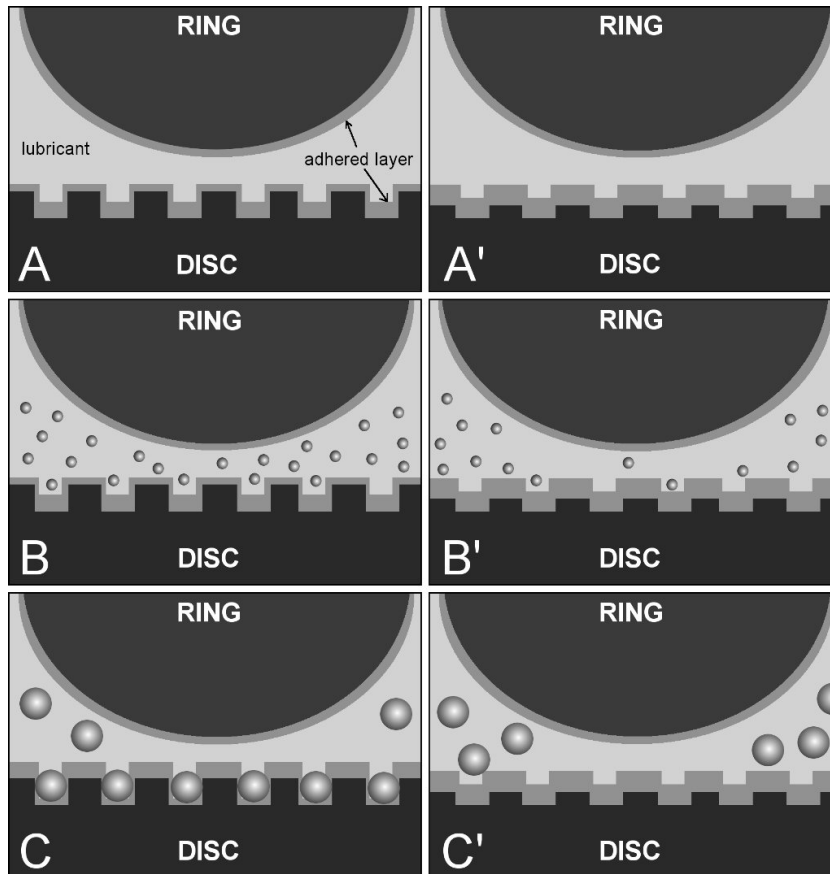
A hypothetical scheme of the lubrication processes of the three polysaccharides with and without beads is presented in Figure 5.7. Left panels correspond to a low applied load, while the right panels represent higher normal load. LBG was characterized by rather poor lubrication properties (e.g. Figure 5.2, Figure 5.3), although it was hydrophobic and could form a thin boundary film on the rubbing surfaces. In the case of low normal load, particles could enter the contact zone. Protein beads smaller than asperities size (below about 50 μm) had a weak effect and caused only a small increase of the friction coefficient where the lubrication was dominated by LBG. Large swollen particles (prepared at pH=8) were of comparable size as the surface roughness. As they were pushed into the asperities by the applied load, the lubricant was pushed out of the asperities. This caused a decrease of effective surface roughness and lower friction coefficient. The scheme was different for larger load. The thin film formed at the surfaces and smaller gap prevented large beads from entering in the contact zone. Therefore, lubrication was dominated by LBG and was unaffected by the presence of large swollen particles. Beads smaller than the asperity size, on the other hand, did influence the friction, as the asperities were compressed by the higher normal load. Surfaces were pushed closer together and particles could provide more friction by "locking" inside the surface roughness.

Similar effects were observed for pectin. The hydrophobic nature of this polysaccharide allowed the formation of a thick boundary film at also hydrophobic surfaces, as shown in Chapter 4 [22]. Moreover this sample was characterized by better lubrication properties than LBG that possibly resulted from a thicker boundary film. In the case of a low applied load, particles smaller than the surface roughness weakly affected the friction. They entered into large asperities and polysaccharide dominates the lubrication with a thick boundary film that very well covered both surfaces. Large swollen beads (produced at pH=8) could not enter the contact zone even at this low load. Well lubricated surfaces could not provide sufficient friction to pull the particles into the gap between the disc and the ring. Therefore the Stribeck curve was nearly identical to the situation without beads (see pectin in Figure 5.7). In the case of a large load, large swollen particles were also prevented from entering the contact area resulting in very similar friction coefficient to the one obtained for pectin alone. Smaller beads at high load had also a very weak effect on lubrication. Although they possibly could enter the gap between

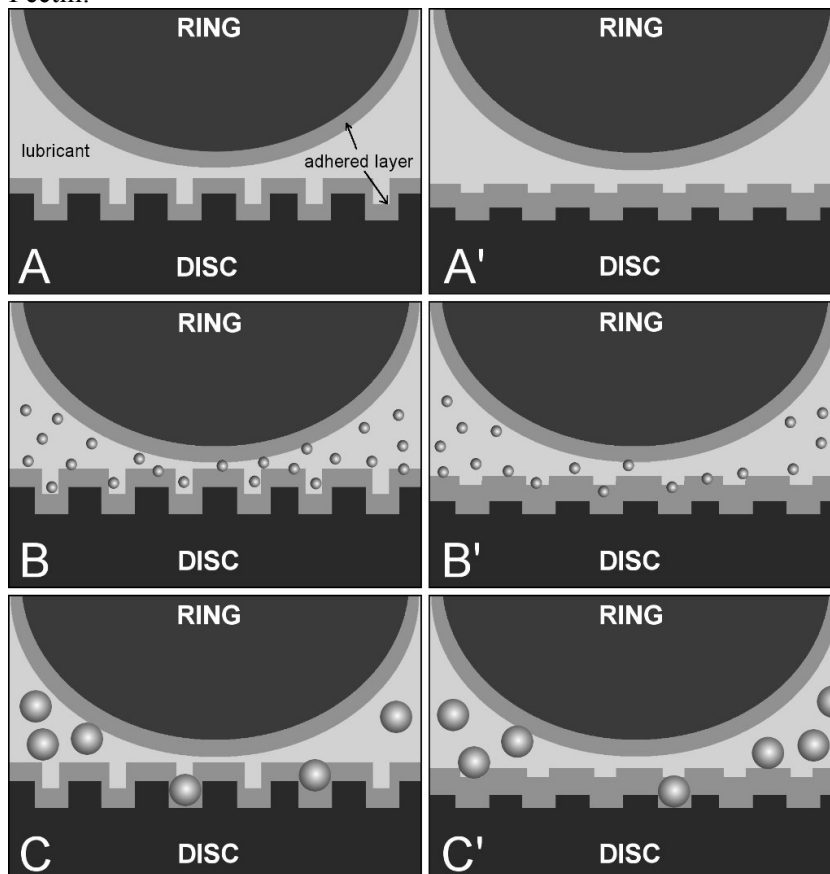
two rubbing surfaces, the thick boundary film of pectin provided a very good lubrication. With higher load the asperities were suppressed and could release more lubricant into the contact zone resulting in significantly lower friction.

As in the case of pectin, xanthan also forms a thick film. For xanthan, however, the friction coefficient is lower, which suggests that the formed film is thicker and thus separates the rubbing surfaces better. This indicates that xanthan adheres to neoprene rubber more efficiently than pectin. Interestingly, unlike in the case of other polysaccharides, introduction of beads into the solution dramatically changes the lubrication properties (see xanthan in Figure 5.7). Regardless of particles size or hardness the friction coefficient after introduction of beads increases significantly. This behavior possibly results from an interaction between polysaccharide and protein beads leading to degradation of adhesion properties of the solution. Therefore, xanthan mixed with beads forms much thinner film and the friction becomes dominated by the particles and/or surface roughness. Although all beads cause a significant increase of the friction coefficient, hard and compact particles (cross-linked with TGase) enhance the friction by a factor of 2 compared to an increase by a factor of 3 for the largest beads (prepared at pH=8). This suggests that particles may effectively increase surface roughness as larger beads result in worse lubrication.

LBG:



Pectin:



Xanthan:

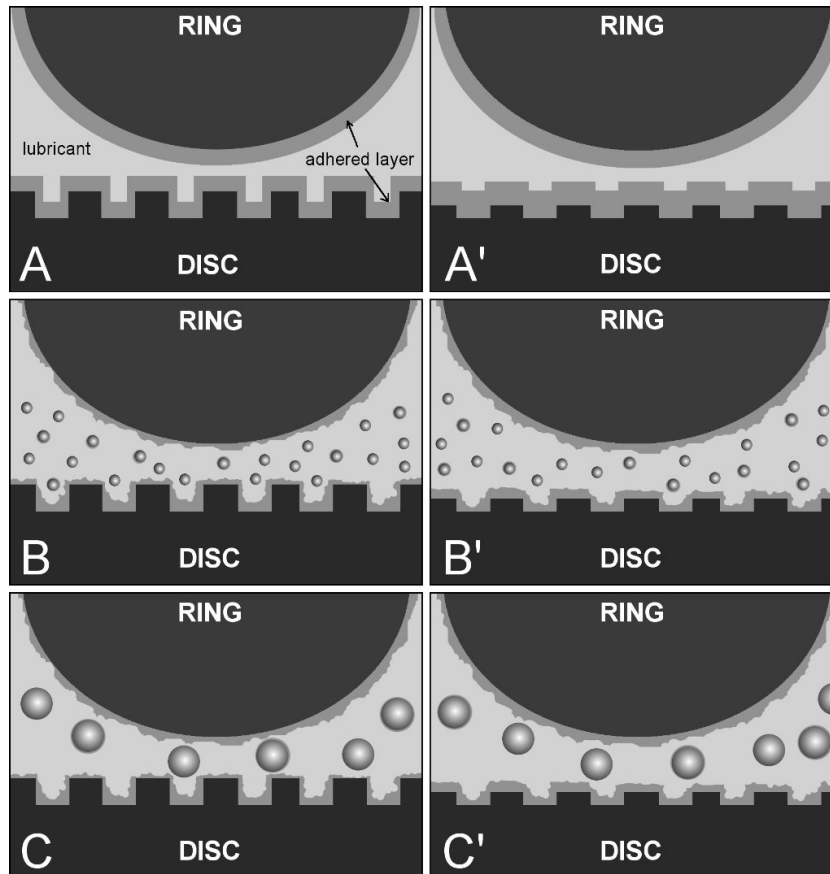


Figure 5.7 Hypothetical scheme of the lubrication processes of the three polysaccharides with and without protein beads. Left panels correspond to a low load (of 2N), while the right panels represent a higher normal load (of 5 N). A, B, and C correspond to cases of pure polysaccharide, polysaccharide with small and with large particles, respectively.

5.4.2 Correlation between the experimental data and sensory attribute

In this chapter a link between sensory perception and laboratory experiments was investigated to obtain a better understanding of complex food systems. It is of interest to find a relation between tribological or rheological properties and attributes describing oral processing. In this section the correlation between these data will be reviewed.

Tribological data

Intuitively, frictional data should be compared to attributes related to lubrication processes in the mouth. The relevant sensory attributes were: slipperiness, filmy, stickiness, and sliminess. Since the speed between tongue and palate is usually rather low, friction data used in this correlation corresponded to low speeds (50 mm/s) also. Figure 5.8 shows attribute scores for these four attributes as a function of the friction coefficient at 50 mm/s.

Although, the slippery score remained rather low for all samples it showed a relation with the friction data. As expected the higher scores obtained in the panel study corresponded to low friction and thus good lubrication properties. Other attributes, however, showed much weaker correlation if any. Although, efficient film forming would result in low friction, xanthan samples without particles showed very good lubrication properties without filmy after-feel. The same result was observed for stickiness, where correlation could not be established. Sliminess just like in the case of other attributes show no correlation. Interestingly, samples of pure xanthan showed a decreasing trend for all these attributes but shifted towards low friction coefficient in respect to all other samples.

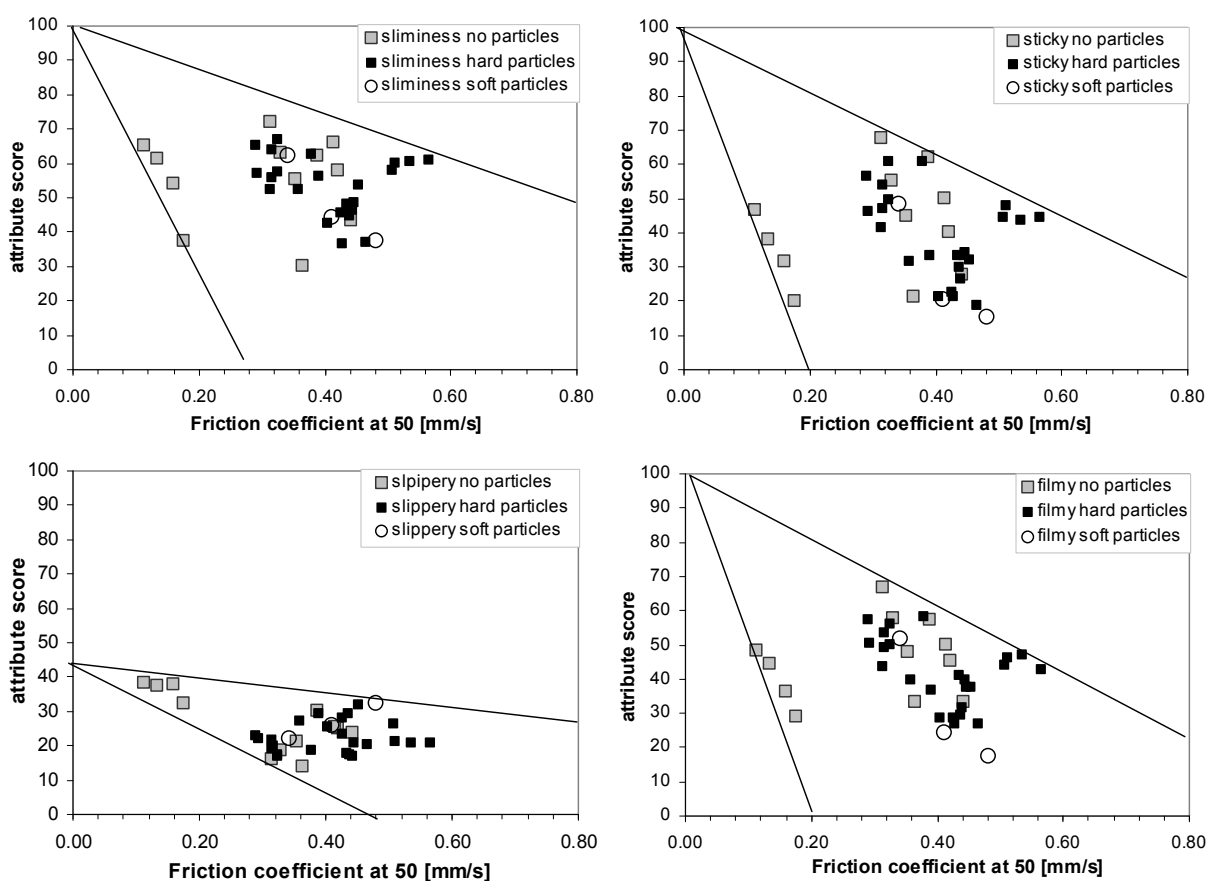


Figure 5.8 Correlations between attributes and the friction coefficient at 50 [mm/s]. Lines are used to show that the data points seem to follow negative correlation, although, they present large spread.

To determine whether any link existed between friction and sensory panel data the correlation coefficient was calculated with significance level of 0.576 for polysaccharides without particles and 0.325 for the case with and without particles (for $\alpha=0.05$). The results presented in Table 5.3 showed that a significant negative correlation was

established for slipperiness, while the correlation coefficient for other attributes was below significance. Interestingly, the correlation with slippery attribute was slightly better for polysaccharides alone than for the case with particles. On the other hand, the three remaining attributes showed poor correlation for the case without particles (likely due to poorer statistics), although the decreasing trend was observed. Furthermore, it seemed that xanthan (without particles) formed a sub-population detached from the rest of the sample. Possibly it was an effect of polysaccharide properties like hydrophobicity or adhesion. Xanthan being hydrophilic contrary to other tested polysaccharides was repelled by the rubber surfaces. In the oral environment the tongue and palate are covered with a mucosa layer. It is therefore not very clear to what extent the interaction specificity as observed in tribology reflects the in-mouth condition.

Table 5.3 Correlation coefficient calculated between experimental data and sensory attributes. The values in bold emphasize a significant correlation for a given attribute.

Attribute	without particles		complete set of sample	
	Friction	Viscosity	Friction	Viscosity
	at [50mm/s]	at 1000 [1/s]	at [50mm/s]	at 1000 [1/s]
Slippery	-0.719	-0.404	-0.400	-0.464
Sliminess	-0.075	0.619	-0.237	0.708
Sticky	0.194	0.896	-0.195	0.897
Filmy	0.179	0.884	-0.273	0.866
Significance level for $\alpha=0.05$	0.576		0.325	

Since each type of polysaccharide behaves differently in the MTM, possible correlations with sensory attributes need to be classified. The samples were divided in three groups according to the type of polysaccharide (LBG, pectin, and xanthan). It was observed that filmy attribute correlated with friction data only for polysaccharide dispersion not mixed with particles. Figure 5.9 shows the relation between all samples studied in this chapter with the filmy attribute and friction coefficient. For each polysaccharide without particles a negative correlation was observed. Thus, a higher perception of filmy attributes occurred for samples with better lubrication properties (lower friction). Once particles were added into the system the correlation was diminished or lost suggesting that the particles inhibit film formation.

Although the slippery attribute was correlated with friction for most polysaccharide-solutions with and without particles, the correlation coefficient for

individual species was below significance level (data not shown). This was most likely the effect of the narrow range of sampled friction coefficients and small differences in attribute scores. Only in the case of xanthan, where particles increased the friction significantly, a correlation was established. Additionally, for LBG samples without particles the slippery attribute showed negative correlation with friction.

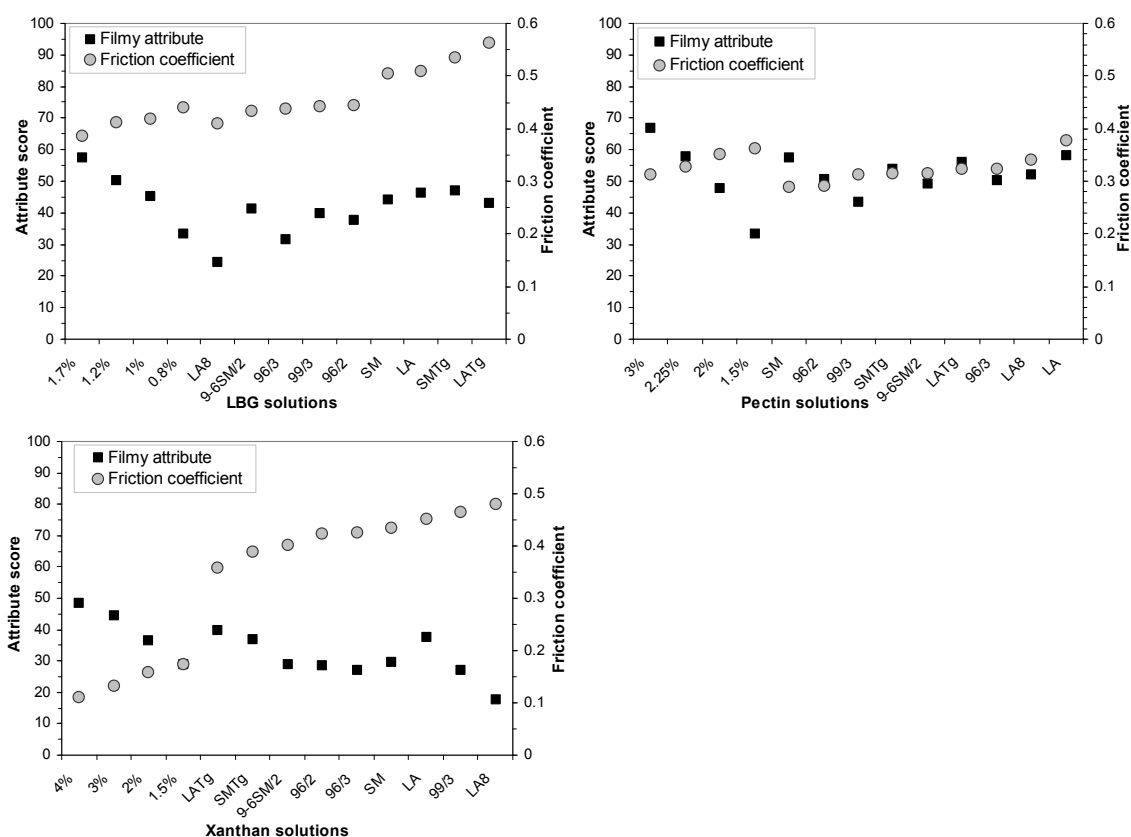


Figure 5.9 Filmy attribute (black squares) and friction coefficient (taken at 50mm/s) (gray circles) for different solutions.

In this chapter all polysaccharide-particle dispersions were tuned to have the same perceived thickness as the reference sample, and consequently the concentrations of polysaccharide in these samples were different (see Janssen et al. [12]). Figure 5.10 showed sticky attribute as a function of the polysaccharide concentrations. For better visual presentation the concentrations have been normalized. A clear positive correlation between the sticky attribute and polysaccharide concentration was observed (higher amount of polysaccharide in the solution corresponded to higher attribute score). Interestingly, the correlation between stickiness and concentration was disturbed by particles, although it seemed that the presence of particles shifted the relation to higher

attribute scores preserving the slope. This resulted in lower correlation coefficient when samples with and without particles were considered altogether. Other attributes that were influenced by concentration of the polysaccharide were slimy and filmy (data not shown). In general, these attributes gave the same dependence on the concentration as observed for stickiness in Figure 5.10. This is correct for all samples with and without particles. However, in the case of polysaccharide alone the statistical population was much lower resulting in very high significance level (0.995 for $\alpha=0.05$). Thus relatively high correlation coefficients obtained for sliminess of studied samples (0.68 for LBG, 0.93 for pectin and 0.90 for xanthan) still remained below the significance level. Also a positive correlation between concentration and filmy attribute was below significance level in the case of LBG without particles. This might also be caused by a spread in relatively small statistical population. The concentration of the polysaccharide also influenced their lubrication properties as was shown in Figure 5.3. However, once particles were introduced in the systems the correlation was not apparent anymore (Figure 5.4 e.g. LBG and pectin).

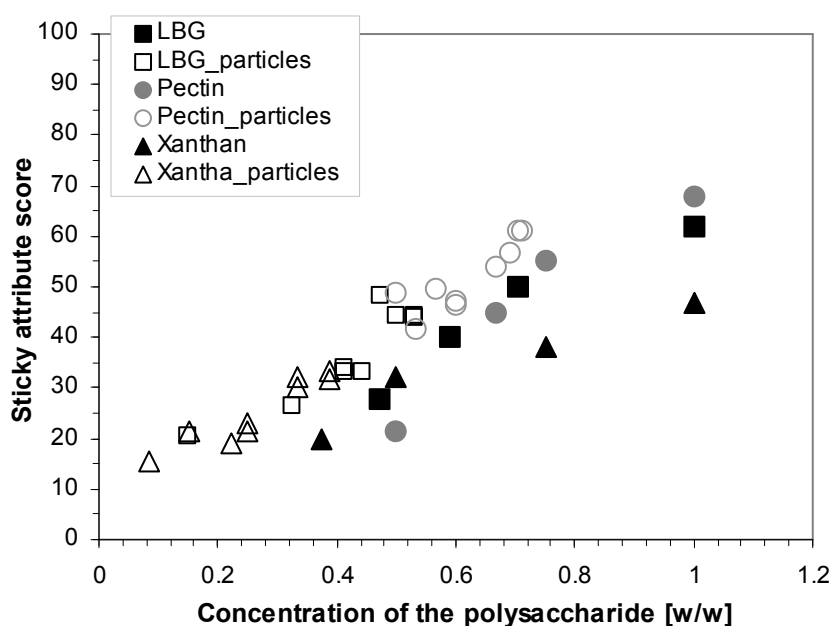


Figure 5.10 Sticky attribute for all samples (with and without particles) as a function of polysaccharide concentration. Black squares and triangles correspond to LBG and xanthan, respectively, whereas gray data points correspond to the pectin solutions. Filled symbols belong to pure polysaccharide solutions (without particles), whereas open symbols correspond to the polysaccharide solution mixed with particles. The concentration range was normalized to the highest polysaccharide concentration (LBG 1.7%, pectin 3% and xanthan 4% (w/w)).

To elucidate possible correlations for stickiness, sliminess and filmy attributes, it is beneficial to include the evaluation of rheological properties of the systems as well.

Viscosity data

Stickiness, sliminess and filmy were expected to be related to the bulk shear viscosity. Indeed these three attributes showed a significant correlation with viscosity at shear rate above 50 s^{-1} . The correlation coefficients calculated for viscosity at 1000 s^{-1} are shown in Table 5.3 and are much higher than the significance level. The samples without particles suffered from a poorer statistics, but still show a significant correlation. In Figure 5.11 the scores of these three attributes are plotted against viscosity at 1000 s^{-1} .

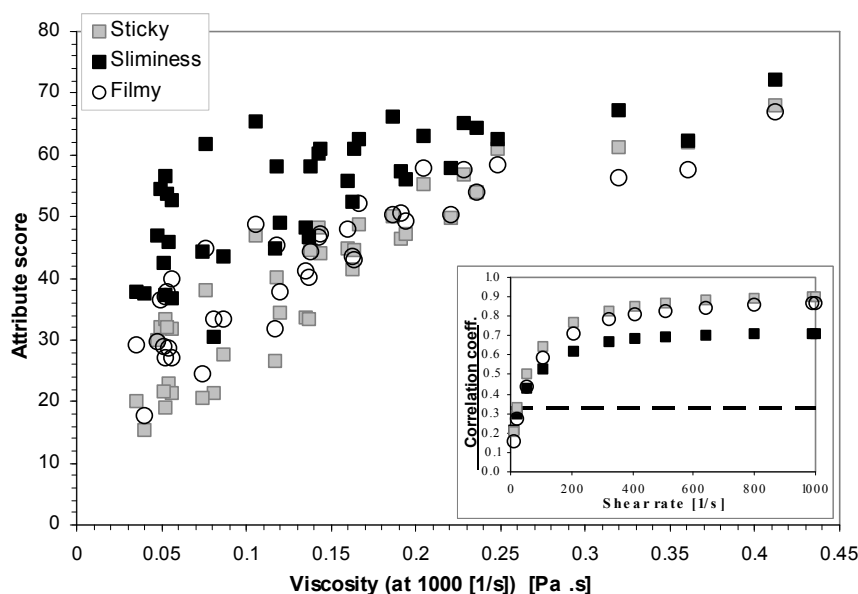


Figure 5.11 Correlations between attributes and the viscosity data measured at 1000 s^{-1} . Inset figure corresponds to the calculated correlation coefficient for the viscosity at different shear rates. A dotted line corresponds to the significance level of 0.344 for $\alpha=0.05$.

Although sliminess showed somewhat larger spread of data points its correlation coefficient was still high (~ 0.71). The sticky and filmy attributes denoted practically the same sensory property but assessed during and after the consumption, respectively. The data almost overlap in the plot and show a high and comparable correlation coefficient of 0.87 for filmy sensation and 0.9 for sticky attribute. Although the viscosity used to calculate the correlation coefficient was taken at high shear rate, it showed very similar result also at lower shear rates. The inset in Figure 5.11 shows the correlation coefficient for the three attributes as a function of shear rate. The correlation coefficient was significant for shear rates above $\sim 20 \text{ s}^{-1}$, although, its significance increased with

increasing shear rate. Our results were in good agreement with previous study, where texture attributes (thickness, stickiness and sliminess) for different food and model systems were correlated with their flow behavior [20,23 -30].

Particles properties

The last attribute investigated in this study was powdery. Although frictional data showed a dependence on particle's properties, it was more intuitive to compare the powdery attribute to particle properties directly rather than to friction data. The presence of particles might induce powdery perception and intuitively particle size should influence the score of this attribute, as larger particles should be more perceivable than smaller ones. Figure 5.12 shows indeed this relation. Larger particles corresponded to a higher score of the powdery attribute. Although for native particles (not treated with TGase nor exposed to high pH) this relation was clear, when all studied particles are taken into account, a slightly different picture emerges. The reason was that size was not the only factor that mattered. Softer, swollen particles (produced at pH=8) seemed to have weaker influence on the powdery perception (possibly due to lower density and thus relatively softer structure), while harder particles (treated with TGase) caused stronger powdery feeling. This was most likely related to the deformability of particles and could result in weaker perception of these particles. Although, correlation coefficient for these sample populations was below significance level, it resulted from low number statistics. It was thus interesting to pursue this issue further in a follow up study, where hardness of particles was quantified and larger sample was investigated.

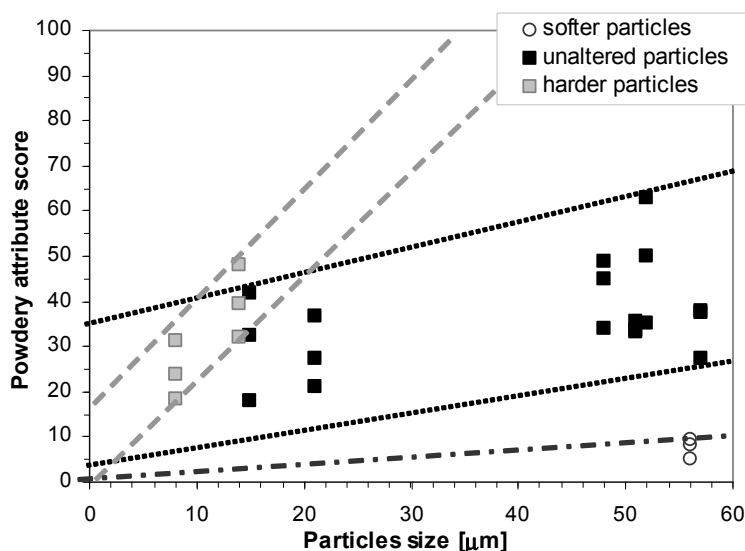


Figure 5.12 Correlations between powdery attribute and particle size. Lines show a decreasing slope of relation between attributes score and article size for decreasing hardness of particles.

5.5 Conclusions

This chapter presented a comprehensive study of the influence of particles (protein spheres and gel particles) on tribological and rheological properties of different type of polysaccharide solutions. Laboratory experiments were complemented by QDA panel study in order to establish a relation between friction data and sensory perception in the oral cavity.

The most important findings in this chapter revealed the relation between the experimentally measured data and perception of attributes sensed by the panelist. It was found that slippery perception correlated well with the friction coefficient. The samples with high score for this attribute provided good lubrication properties. Other attributes showed correlation with friction that was below a significance level. Interestingly particles seemed not to affect the correlation between slippery and the friction coefficient, as significant coefficients were obtained for both populations (with and without particles). Missing correlations between the friction coefficient and other attributes (filmy, sticky, and slimy) might be caused by an influence of other parameters like e.g. adhesion that can be affected by the properties of the surface.

A very good correlation of viscosity with viscosity-related attributes in a wide range of shear rate (from 50 to $>1000\text{ s}^{-1}$) was established. Correlation coefficients well above significant level were obtained for stickiness, sliminess and filmy attributes.

It was shown that not only a particle size, but also particle hardness related with powdery perception. Small beads provided weaker powdery sensation, while larger resulted in higher attribute score. Harder particles, however, were characterized by stronger size dependence than softer particles. However, this finding required further study on larger statistical population and with quantified hardness parameter.

Established correlations between sensory attributes and tribological and rheological data give a significant opportunity for the industry to program oral perception of food products in laboratory without necessity of oral evaluation. Additionally new analytical methods can be developed to provide absolute quantities describing sensory attributes instead of relative scores that are difficult to translate into physical characteristics.

Acknowledgement

The authors would like to thank to Jan Klok for his assistance through microscopy and CLSM images.

References

- 1 De Wijk R.A. and Prinz, J.F. "The role of friction in perceived oral texture". *Food Quality Preference*, (2005), 16, 121-129
- 2 Engelen L., de Wijk R.A., van der Bilt A., Prinz J.F., Janssen A.M. and Bosman F., "Relating particles and texture perception". *Physiology & Behavior*, 86, (2005) 111-117.
- 3 Minifie BW, Chocolate, cocoa and confectionery: science and technology. AVI Publishing Co.,Inc., Westport, CT: (1980).
- 4 Utz K-H. The interocclusal tactile fine sensitivity of the natural teeth as studied by aluminium oxide particles. *Dtsch Zahnarztl Z* (1986); 41:313-315
- 5 Imai E., Hatae K., Shimada A. Oral perception of grittiness. *J Text Stud* (1995); 26:561-576
- 6 Tyle P. Effects of size, shape and hardness of particles in suspension on oral texture and palatability. *Acta Physiologica North-Holland* (1993); 84:111-118
- 7 Kilcast D, Clegg S. Sensory perception of creaminess and its relationship with food structure. *Food Qual Prefer* (2002); 13:609-623
- 8 Van Vliet T. and Walstra P. Weak particle network, in *Food Colloids*, (Eds. R.D. Bee, P.Richmond and J. Mingins). Special publ. No 75, Royal Society of Chemistry, Cambridge, 206-217
- 9 Malone ME., Apperlqvist, I. A. M. and Norton I. T. Oral behaviour of food hydrocolloids and emulsions. Part 1. Lubrication and deposition considerations, *Food Hydrocolloids* , (2003), 17, 763-773
- 10 Alting, A. C., de Jongh, H. H. J., Visschers, R. W., & Simons, J. W. F. (2002). Physical and chemical interactions in cold gelation of food proteins. *Journal of Agricultural and Food Chemistry*, 50, 4682-4689
- 11 Van de Pijpekamp, A. M., Janssen, A. M. and de Jongh, H.H.J., (2008) Functionality of protein-based particles; Potentials for food applications. Submitted to *Food Biophysics*.
- 12 Janssen, A.M., van de Pijpekamp, A.M., Chojnicka, A., Zinoviadou, K.G., Sala, G., "Oral adhesion: Relavance of bulk rheological properties and presence of particles". In preparation.
- 13 De Jong, S. and van de Velde, F., "Charge density of polysaccharide controls microstructure and large deformation properties of mixed gels" *Food Hydrocolloids* 21 (2007) 1172-1187.
- 14 Alting, A. C.; Hamer, R. J.; de Kruif, C. G.; Visschers, R. W. "Formation of disulphide bonds in acid-induced gels of preheated whey protein isolate" *Journal of Agricultural and Food Chemistry*, (2000), 48, 5001-5007.
- 15 Chojnicka, A., de Jong, S., de Kruif, C.G. and Visschers, R.W., "Lubrication properties of protein aggregate dispersions in a soft contact". *Journal of Agricultural and Food Chemistry*, (2008), 56,1274-82
- 16 Alting, A. C., Hamer, R. J., de Kruif, C. G., Paques, M., & Visschers, R. W. (2003). Number of thiol groups rather than the size of the aggregates determines the hardness of cold set whey protein gels. *Food Hydrocolloids*, 17 (4), 469-479
- 17 Jaros, D., Parschefeld, C., Henle, T., & Rohm, H. (2006). Transglutaminase in dairy products: chemistry, physics, applications. *Journal of Texture Studies*, 37,113-155.
- 18 Stone, H. and Sidel, J.L. (1985). *Sensory Evaluation Practices*. Academic Press, Orlando, FL.
- 19 De Wijk, R. A., van Gemert, L. J., Terpstra, M. E. J., & Wilkinson, C. L. (2003). Texture of semi-solids: Sensory and instrumental measurements on vanilla custard desserts. *Food Quality and Preference*, 14, 35-317.

- 20 Stanley N.L. and Taylor, L.J. (1993). Rheological basis of oral characteristics of fluid and semi-solid foods: A review. *Acta Psychologica* 84, 79-92.
- 21 Chojnicka-Paszun A., Doussinault S., de Kruif C.G. and de Jongh H.H.J. "Frictional behavior of diverse oral surface analogs and their interaction with complex polysaccharide/MCC particle dispersions". Submitted.
- 22 Chojnicka-Paszun A., Macakova L., Stokes J.R., de Kruif C.G. and de Jongh H.H.J. "Lubrication, rheology and adsorption of polysaccharide solutions". Submitted.
- 23 Cutler, A.N., E.R. Morris and L.J. Taylor, (1983). Oral perception of viscosity in fluid foods and model systems. *Journal of Texture Studies* 14, 377-395.
- 24 Richardson, R.K., E.R. Morris, S.B. Ross-Murphy, L.J. Taylor and I.C.M. Dea, (1989). Characterisation of the perceived texture of thickened systems by dynamic viscosity measurements. *Food Hydrocolloids* 3, 175-191.
- 25 Wood, F.W., (1968). Psychophysical studies on the consistency of liquid foods. S.C.I. Monograph 27, 40-49.
- 26 Szczesniak, A.S. and E. Farkas, (1962). Objective characterisation of the mouthfeel of gum solutions. *Journal of Food Science* 27, 381-385.
- 27 Christensen, C.M., (1979). Oral perception of solution viscosity. *Journal of Texture Studies* 10, 153-164.
- 28 Hill, M.A., (1991). Dynamic rheology: Application to the formulation of a real food product. *Food Science and Technology Today* 5, 29-31.
- 29 Morris, E.R. and L.J. Taylor, (1982). Oral perception of fluid viscosity. *Progress in Food and Nutrition Science* 6, 285-296.
- 30 Morris, E.R., R.K. Richardson and L.J. Taylor, (1984). Correlation of the perceived texture of random coil polysaccharide solutions with objective parameters. *Carbohydrate Polymers* 4, 175-191.

Chapter 6

Friction properties of oral surface analogs and their interaction with polysaccharide/MCC particle dispersions

Abstract

To further improve food products and to fully satisfy the end consumer it is necessary to gain an in depth picture of the process that occur during mastication in the oral cavity. Especially a physical description (both in a qualitatively and quantitatively sense) of the oral food processing would be beneficial for a more effective prediction in product reformulation and new development. For this purpose a tribological and rheological study of polysaccharide solutions was employed. In this chapter we investigate their tribological properties using a set of different rubbers. These rubbers simulate soft, oral surfaces and may indicate how measurements are related to material properties. The properties of the different surfaces are characterized using a number of techniques, including stereomicroscopy, confocal laser scanning microscopy, contact angle and elasticity measurements.

Soft neoprene rubbers undergo wearing, which causes a significant increase of the surface roughness. The differences between the surfaces tested occur predominantly in the boundary lubrication regime. Our results show clearly that the properties of the surface are important only in the case of lubricants that cannot efficiently form boundary film. This lubrication layer eliminates to a great extent the influence of the surface on the lubrication.

6.1 Introduction

Food consumption of products that comply to more strict safety and health aspects requires a strongly increasing understanding of food structuring and breakdown. To aid food product development, it is necessary to understand the oral processing and the perception of food. To keep in pace, many sophisticated investigation techniques have been developed more recently, but they require a continuous improvement to provide the necessary insights. Food processing in the mouth can be simulated in tribological experiments [1], while food integrity can be studied using rheology. Where the first aspect (friction science) is focused on the interaction between a specimen and processing surfaces, the latter methodology is used to determine the visco-elastic properties of a sample product that responds to applied stresses by the surfaces. Ideally, these surfaces perfectly mimic the characteristics of the oral cavity (palate and tongue), but its complexity currently prohibits straightforward analysis. Therefore, it is relevant to investigate to what degree surface properties do affect and oral perception to set the contours of to what extent mouth properties must be simulated to get a adequate understanding.

The tongue surface consists of an epithelial layer (e.g. mucosa) and different muscular layers [2]. The surface of the tongue is highly heterogeneous due to the presence of a variety of papillae that differ in size and function [3]. Papillae cover the surface of the tongue and are responsible for the roughness of this surface [4]. Among the various papillae the most common are cone-shaped filiform papillae [3] with an approximate roughness of about 100 μm [4]. On the other hand, the palate does not have papillae and therefore is much smoother.

The wetting properties of the oral surfaces are important as well. The measurement of a contact angle of a water droplet on a dry tongue surface revealed its hydrophobic nature [5]. However, the oral cavity is lubricated by a mucus layer, which consists mostly of mucins (glycoproteins) and water [6]. This provides a good lubrication in the oral cavity, as the mucins consists of the molecules with a high water binding capacity [7]. Therefore, once the oral surfaces are lubricated with saliva, a more hydrophilic nature is revealed [8-11].

The tongue under compression is highly deformable, as it consists of a complex network of fibers [12, 13]. The orientation of these fibers varies within the tongue, giving rise to differences in a muscular deformability. This results in different elastic moduli depending

on the position on the tongue. For example Pouderoux and Kahrilas [14] showed the differences in contact pressure depending on the location on the tongue: at the anterior part the pressure of about 19 kPa was reported, in the middle it was about 20 kPa and at the posterior area about 11 kPa. A study by Tsuga et al. [15] reveals the differences in pressure during the swallowing of water at the anterior part of the tongue to be 36 kPa and at the posterior to be 24 kPa. The tongue velocity for the swallowing was estimated in these studies at 68 mm/s. The estimated tongue pressures based on a balloon type sensor were reported by Hayashi et al. [16] to be between 3 and 27 kPa during swallowing.

Oral surfaces have been simulated in tribological studies in several ways. The basic setup consists of two very hard, steel surfaces. Cassin et al. [17] and later Vicente et al. [18] introduced one soft surface to emulate realistic physical parameters for soft bio-tribological contacts. The presence of one hard surface, however, results in pressures much higher than present in the oral cavity. To comply to this criterion Bongaerts et al. [19] and later Chojnicka et al. [20] introduced a setup with two soft surfaces. This further reduced the contact pressure and allowed for better simulation of the oral conditions.

Moreover, in other study, human mouth environment was mimicked in the optical tribological configuration setup where the contact between pig oral tissue and glass plate occurred [9] and in the custom-made friction apparatus where 2 musocal surfaces were used [21,22]. The work of Dresselhuis et al. [9] and de Hoog et al. [21, 22] showed the importance of the surface roughness, hydrophobicity and deformability as well as the applied physical parameter (e.g. load) during the measurements.

In the current work, several techniques were applied to evaluate how important the choice of surface properties was to evaluate or predict the lubrication of a food product in the oral cavity. Surface roughness was studied using CLSM and microscopy techniques, hydrophobicity was determined with the goniometer that measures the contact angle, the elasticity of the rubbers was investigated using large-deformation rheology, whereas the viscosity of the solutions was examined with small deformation rheometer. The lubrication properties of a solution under shear were measured using a tribometer. In this case due to the pressure applied during the measurements (between rotating O-ring and disc) rubbers underwent wearing process that varied between different materials and could significantly affected the structure of the surface in the contact area. In this chapter we continued using the setup that consisted of two soft elements. However, we concentrated our efforts on determination of the tribological properties of several surface materials.

They were chosen by their difference in elasticity and surface roughness that cover a wide parameter space. Therefore, the link between these properties and frictional properties could be established. This parameter study determines how sensitive the tribological measurements are on the properties of the applied surface. Moreover, the lubrication properties of three different commercial polysaccharide solutions (locust bean gum, xanthan and pectin) are studied on several types of materials. These hydrocolloids are commonly used in the food industry and their physical and chemical characteristics are well described in Chapter 4 [23]. Furthermore, to observe the effect of hard microscopic particles on the lubrication properties, a phenomenon that is often encountered in food products, the polysaccharide solutions are mixed with microcrystalline cellulose particles.

6.2 Materials and Methods

6.2.1 Materials

Samples. Xanthan gum (Keltrol™ T), locust bean gum (C-130, LBG), and high methyl ester pectin (H-6) were kindly donated by CP Kelco Inc. (Lille Skensved, Denmark). Chemical composition of these polysaccharides was previously reported by de Jong et al. [24]. Microcrystalline cellulose (MCC) particles were obtained from JRS Pharma (Rosenberg, Germany). All ingredients were used without further purification and without correction of their moisture content. Reverse osmosis water was used in all cases to obtain the solutions.

Rubbers. Silicone, neoprene, and Teflon sheets were purchased from Eriks company (Arnhem, The Netherlands). The supportive discs were carved from these sheets using a molder. Before use the discs were washed with ethanol, reverse osmosis water and dried with air.

6.2.2 Sample preparation

Polysaccharides. Stock solutions of LBG (1.7 % w/w), xanthan (4% w/w) and pectin (3% w/w) were prepared by sprinkling the powder using a sieve into the vortex of a beaker containing the appropriate amount of water. The polysaccharide powder was hydrated for at least 2 hours. The solution was filtered to remove possible lumps and followed by heating at 80 °C for 30 minutes, except for the pectin solution that was filtered after heating. This sample was the thinnest and, thus sieving was easier. LBG stock solution was diluted to 1.0 (w/w), xanthan to 1.8 (w/w), and pectin solution to 2.25

(w/w). These concentrations were used in previous study (see Chapter 5 [25]) and were characterized by similar thickness perception in the mouth. Note that sensory attributes are out of the scope of this chapter. The solutions were stored in the fridge and were used for measurements within two days after preparation.

MCC particles. To study the influence of hard particles on friction, microcrystalline cellulose (MCC) particles are added to the LBG, pectin, and xanthan solutions. The MCC particles (3.2% (w/w) of final weight) are dissolved in water and added to the polysaccharide solution. The MCC particles are hard and irregular and have more elongated shape with a length in the range between 10 and 100 μm .

Rubbers. In the current chapter several materials (silicone, neoprene, and Teflon) are investigated. These materials are supposed to mimic the mouth environment in the tribometer by differing properties like roughness, elasticity and hydrophobicity. For neoprene and silicone rubbers, three different values of elasticity are selected. In order to simplify the description of different rubbers throughout this chapter, abbreviations composed of the first letter of the rubber with the symbols: S (soft), M (medium) and H (hard) are assigned (according to their elasticity, with S being the most elastic, and H the least elastic, i.e. SS for the softest silicone).

6.2.3 Rheological measurements

The viscosity data of the polysaccharides solutions are recorded at 30°C using a standard rheometer (AR 2000, TA Instruments, Leatherhead, UK) with double concentric cylinder geometry. Flow curves are obtained by measuring the viscosity as a function of increasing shear rate. The measurement consists of three steps (15 minutes each): a conditioning step where the system is temperature equilibrated, followed by continuous forward and backward ramp steps with the shear rate increased from 0.006 to 1000 and back to 0.006 s^{-1} . Each point was measured at a fixed shear rate with a duration time of 12-18 s. Brookfield oils (Viscosity Standard, Benelux Scientific, Scientific Instrument & Lab Equipment) with 10, 50 and 100 mPa are used to calibrate the equipment.

6.2.4 Tribological measurements

A Mini Traction Machine (MTM) (PCS Instrument) is used to measure friction between two rotating surfaces (ball and disc). In order to study low contact pressure the compliant rubber surfaces are used in this MTM set-up. This is done by introduction of a steel

cylinder with an attached neoprene O-ring. In addition a 3 mm thick disc (made of silicone, neoprene or Teflon) is fixed on top of the steel disc. This experimental technique was reported previously in Chapter 2 and 3 [20, 26]. The rotating speed of the disc and the ring as well as the normal load (W) (the force applied to press the ring against the disc) can be adjusted using the instrument software. The friction force (F_f) arises from the ring-disc interaction at the applied speed and is measured through a force transducer attached to the ball motor. This yields the friction coefficient: $\mu = F_f / W$, determined as a function of the applied entrainment speed. The rubber-rubber contact caused a strong vibration of the ring-ball shaft at high speeds ($>600\text{mm/s}$). This engenders resonance and then the jump of the O-ring. For this reason the upper limit of the speed is set to 500 mm/s . A lower limit of 5 mm/s is chosen due to large data scatter below this speed (most likely caused by non-continuous drag). Each experimental point is recorded at average constant slide-to-roll ratio (SRR) equal to 50 %. It is obtained from the average relative motion of the ring in respect of the disc. The slide-to-roll ratio is defined as the difference in surface speed between the disc and the ball divided by their entrainment speed (U) (the mean tangential velocity at the point of contact). The SRR equal to 50% corresponds to a combination of rolling and sliding contact similar to the contact between tongue and palate. All measurements were performed at a temperature of 30°C ($\pm 1^\circ\text{C}$) that is kept constant using the thermostat of the MTM. After a few minutes of measurement, especially for neoprene rubbers, a track becomes visible on top of the rubber (the thin top layer of the disc becomes damaged). To obtain more coherent results, the measurements consist of 5 consecutive steps: first step stabilizes the temperature to 30°C , two pre-steps are made at a normal load of 5N , one step at 2N , and the last step at 5N again. Each measuring step is composed of 39 points recorded at speeds from 500mm/s to 5mm/s . Prior to the experiments the rubber surfaces are cleaned with ethanol, reverse osmosis water and dried with air before launching the experiment. New rubbers are used for each measurement. All measurements are performed four times and subsequently averaged (each presented point corresponds to a mean value).

6.2.5 Instron: large deformation measurements to establish the elasticity of the rubbers

Different disc material (vary in the elasticity) was selected in the tribological experiments to evaluate the effect of the surface properties. To estimate the elasticity of the silicone, neoprene, and Teflon the Instron 5543 (Instron Int., Edegem, Belgium) is used. The

rubbers are placed between a steel plate and a 5 mm diameter steel stick that are then pressed towards each other. Knowing the contact area and the thickness of the rubber the Young's modulus is calculated from the slope of the initial linear relation of the stress versus strain curve. The Young's modulus for each rubber is a mean value obtained in five independent measurements.

6.2.6 Confocal Laser Scanning Microscopy

The microstructure of the solutions of polysaccharide with MCC particles, and the external aspect of the rubber are visualized with confocal laser scanning microscopy (CLSM). CLSM-images were recorded on a LEICA TCS SP Confocal Laser Scanning Microscope (Leica Microsystems CMS GmbH., Mannheim, Germany), equipped with an inverted microscope (model Leica DM IRBE). Leica objective lenses (magnification 5x, 10x, and 63x water immersion) are used. Digital image files are acquired in a tagged image file format at 1024x1024 pixels resolution.

To visualize the MCC particles, the polysaccharide is stained with Rhodamine B (0.2 wt% solution; 10 μ L per mL sample). The single photon mode is used with an Ar/Kr visible light laser. The excitation wavelength is set at 568 nm for Rhodamine B.

In order to better evaluate the roughness that is induced during the MTM measurements, CLSM images at magnification of 10x are quantified using software available with the setup. The rubber surfaces are observed in the reflection mode, with an Argon visible light laser (at 488nm excitation wavelength). Successive images are taken by the microscope at different depths and are collected by the experimental software. Positioning of the cursor on the image allows one to see the two sections of the rubber (vertical and horizontal – indicated with the stripes on the right and at the bottom in Figure 6.3- see description of this figure below). It is also possible to move the line in a section in order to determine the depths of an asperity. Therefore, this method enables one to determine the spatial dimensions of the asperities.

6.2.7 Stereomicroscopy

Stereomicroscopy (Leica Microsystems MZ16 with optical zoom 16) is used to evaluate the surface of the rubbers. The objective lens used is a PL APO type with a numerical aperture of 0.20 and 1.7 μ m resolving power.

6.2.8 Contact angles measurements

The contact angle measurement is done using a conventional goniometer (ERMA contact angle meter G-1). A symmetrical drop is deposited on the surface material using a syringe with a constant solution volume of 10 μ l. All rubbers are cleaned with an ethanol, reverse osmosis water, and dried with air. The contact angles are determined visually at room temperature at both sides of the drop (within one minute after the drop is applied). Reported contact angles are the average of 5 measurements.

6.3 Results and Discussion

The frictional properties of the polysaccharide solutions are strongly influenced by parameters such as surface roughness, hydrophobicity and material elasticity. In the oral cavity, these parameters can vary from person to person, especially with age. Sensory perception of samples may depend on the characteristics of the surfaces in the oral cavity (tongue and palate). In order to study food processing under oral processing conditions the influence of the surface during the mastication has to be evaluated. In this chapter the relations between different surface characteristics and lubrication properties of polysaccharide solutions are investigated. Therefore, several materials (silicone, neoprene and Teflon) of different elasticity and roughness are examined. In addition, the rheological characteristics of the solution and its interaction with the surfaces play an important role in lubrication properties of the solution. Therefore, in the current work, three hydrocolloids (LBG, pectin and xanthan) that are commonly used in the industrial application and that exhibit different lubrication properties (see also Chapter 5 [25]) are investigated. These three hydrocolloids behave as non-Newtonian solutions that differ in shear thinning behavior and properties like molecular weight and charge density (see Chapter 4 [23]).

The aim of this work is to characterize the influence of the surface properties on the lubrication behavior of polysaccharide solutions. In addition, we study the influence of hard and elongated MCC particles mixed with the polysaccharide solutions. These particles are used to investigate influence of solid grains on frictional characteristics of polysaccharide solution in which they are suspended.

6.3.1 Surface properties of the rubbers

Seven different materials were studied (Teflon, three different neoprene (N) and three different silicone (S) discs). These materials were expected to vary in surface

roughness and in elasticity. Figure 6.1 presents the Young modulus (E) of different rubbers determined using large deformation experiments with the Instron. Silicone rubbers show relatively small differences in elasticity. Their Young's modulus varies from 4 MPa for silicone S to 9 and 10 MPa for silicone M and H, respectively. Neoprene rubbers show much greater variation in the Young's modulus. The highest elasticity (i.e. the lowest Young's modulus) was determined for neoprene S ($E=5$ MPa). Neoprene M and H are harder with Young's moduli of about 11 MPa and 21 MPa, respectively. The lowest elasticity was obtained for Teflon ($E \approx 30$ MPa).

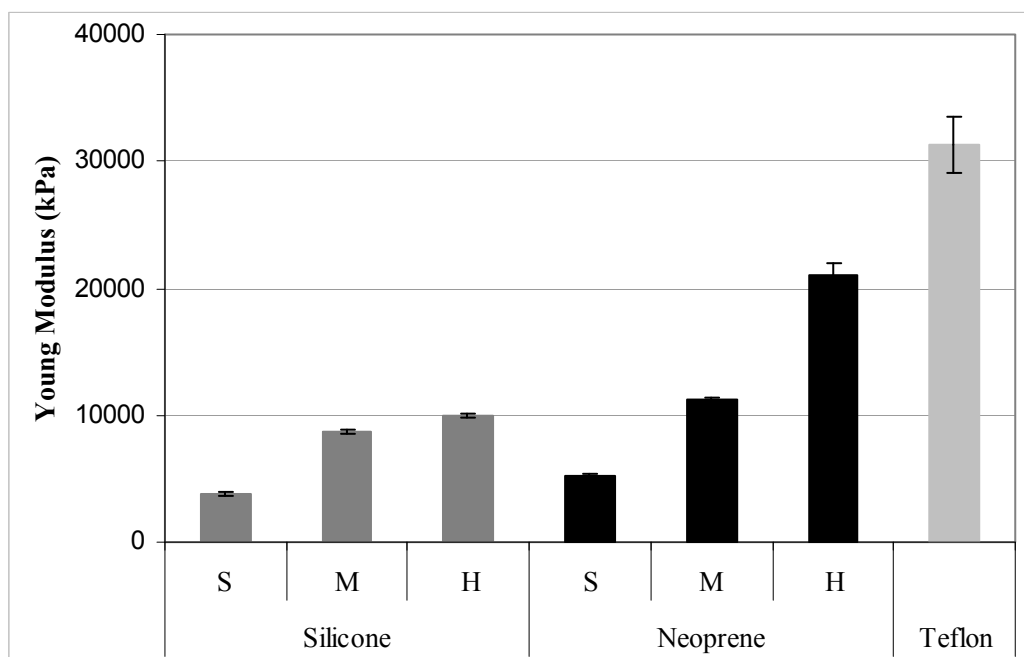


Figure 6.1 Young modulus of the silicone, neoprene and Teflon discs measured with Instron.

Small differences in the surface roughness are observed for all of the rubbers before the start of tribological measurements. During the MTM experiment, a different evolution of the roughness (wear) is noticeable caused by the applied normal load and friction and depends on the elasticity of the material. Consequently, the top layer of the disc is damaged (wear off) by the O-ring due to tensile stress in the contact between two surfaces. This forms a pattern further referred to as track. Figure 6.2 shows microscopic pictures of the material surfaces after the tribological measurements with the polysaccharide solution. Teflon is not shown in the Figure 6.2 as the track evolution during the tribological measurements was small, and thus hardly visible. Due to the differences in elasticity of used materials discs undergo a wearing process leading to the

development of different tracks. The experimental conditions in this figure (e.g. the physical parameters or the lubricant) are kept constant for all materials tested. In addition, the track usually shows two areas of different roughness. The first one is smooth and results from the contact between the disc and the O-ring. The second is rougher and most likely results from an imperfect junction of the O-ring that locally exerts higher pressure causing stronger wear and tear.

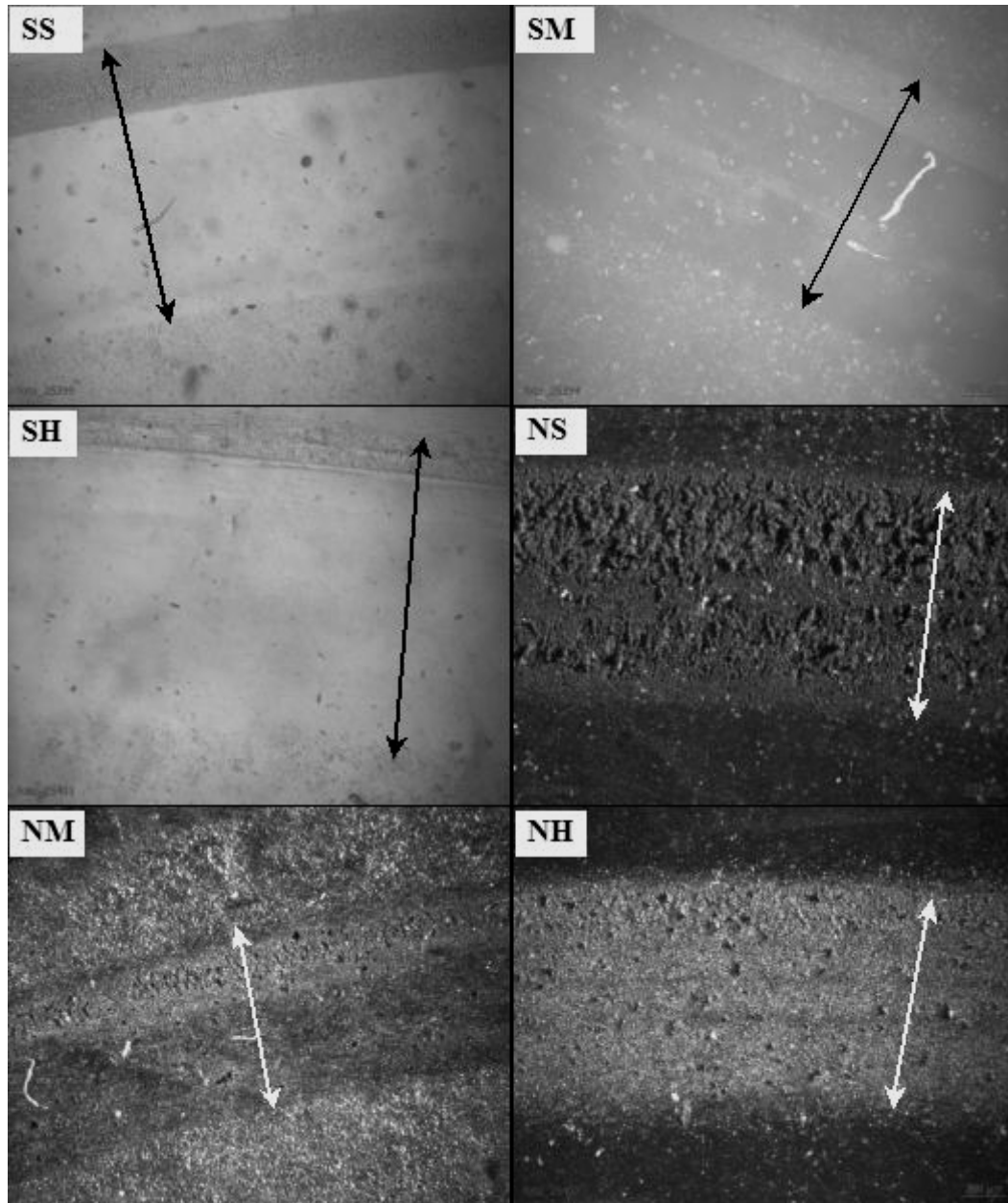


Figure 6.2 Stereomicroscope pictures of silicone (S) and neoprene rubbers (N) with different values of elasticity (S, M, H). The arrow indicates width of the track. Please note the differences in scale for some of the pictures.

Generally the silicone tracks are smoother than neoprene tracks. The MTM measurements form large asperities in the track of the neoprene. This explains the need for the two pre-steps in the experimental settings that prevent significant roughness evolution during the measurement.

To quantify the structure of the surfaces and to determine the size of asperities CLSM images of the discs are obtained. Both the width and the depth of the surface roughness were established.

Figure 6.3 shows as an example of two extremes CLSM images of soft silicone (SS) and hard neoprene (NH) rubbers. The left panel corresponds to the silicone S that is evidently smoother than the neoprene H in the right panel of Figure 6.3. An elevation of the surface element is color-coded, where brighter means higher level and darker corresponds to lower level. The track can be easily distinguished in both cases and its width is almost the same for all of rubbers (approximately 900 μ m). For the silicone disc the track is smooth and contains a small number of rather small asperities (10-20 microns, see Table 6.1), while neoprene is characterized by a more rough landscape. Large asperities (20-80 microns) are engraved in the surface forming a network of valleys. Two different parts of the track are also clearly visible. In the case of Teflon the track was hardly visible, since the rubber was very hard ($E \approx 30$ MPa) and smooth. Consequently, very small asperities (if any) are created, which are smaller than the detection-limit of the microscopes. This sets the upper limit for the Teflon asperities at 1 μ m. The depth of asperities is determined from the cross-section of the disc obtained by the CLSM technique. These corss-sections are shown below and next to each image. The established spatial properties are listed in Table 6.1. For silicone rubbers the surface is slightly affected. The asperities seem to be shallower as if the thin surface layer of the disc was uniformly removed. Note that the depth of the track is of the order of the asperities, meaning that the wearing process removes the surface material as well as forms new, shallower, asperities. In the case of neoprene the surface roughness evolution depends on the material properties of the rubber. Asperities of neoprene S and M are enhanced by a factor of about four during a measurement, while in the case of neoprene H the roughness increases only marginally.

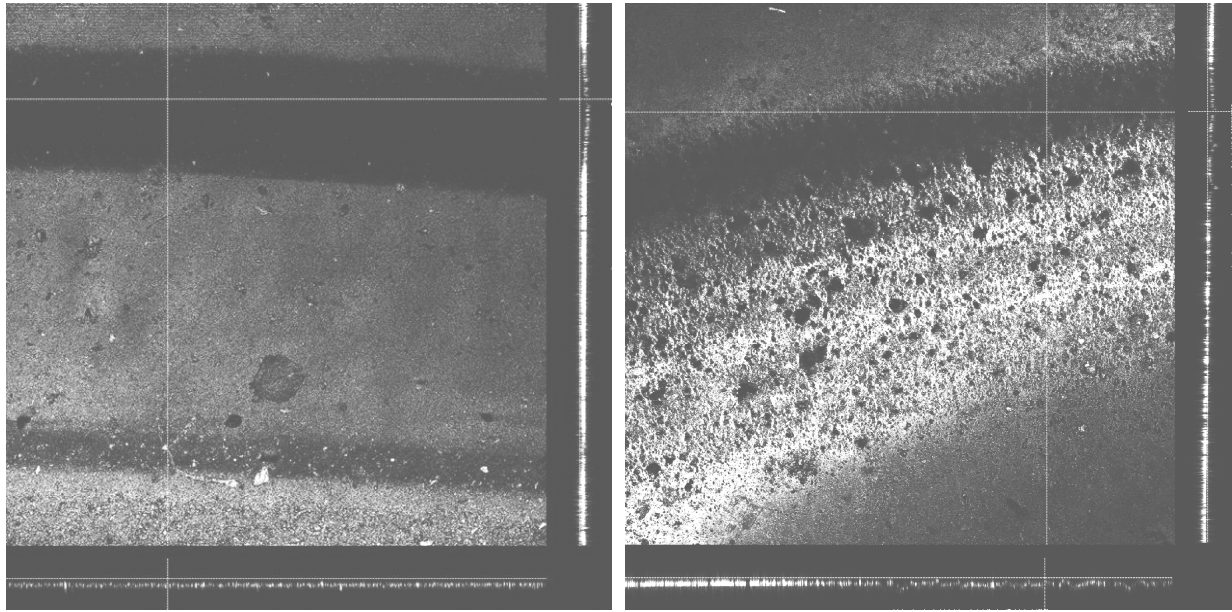


Figure 6.3 Images of two different rubbers obtained by CLSM method. Left panel shows silicone S and right panel shows neoprene H. Color coding indicate depth. Bright areas correspond to bumps while dark spots show holes in the surface. Stripes on the right side and below each panel show the cross-section obtained along lines drawn in both images.

Table 6.1 Characteristics of the silicone and neoprene rubbers obtained by CLSM orthogonal tool. The depth of the track is not really observable, it corresponds to the depth of the asperities.

Rubber		Depth asperities in track (μm)	Width asperities (roughness) (μm)	Depth of the track (μm)	Depth asperiteis outside the track (μm)
Silicone	S	10	< 5	5-10	15
	M	15		25	20
	H	15-20		25	30
Neoprene	S	50-80	~ 50	50-80	10-15
	M	50		50	10-20
	H	20		30	10-15

6.3.2 Contact angles

To determine the adhesive properties of the surfaces and different polysaccharides solutions (with and without MCC particles), the contact angles between samples and materials were performed with the goniometer (Table 6.2). It is valuable to characterize the ability of the solutions to coat a surface, as it might influence the lubrication properties in the tribometer. A low contact angle indicates strong, adhesive, interactions between the droplet solution and the disc. The contact angle in the case of water provides information

about hydrophobicity of the surface. Thus contact angle below 90° indicates hydrophilic surface and means that polar molecules will spread on such surface fast forming a lubrication layer. On the other hand, large angle indicates hydrophobic nature that results in spreading of non-polar solutions on such surface. Droplets try to remain in a minimum energy state by minimizing the surface area (approaching a spherical shape).

Table 6.2 Mean contact angles values in degrees, for the polysaccharide solutions with and without MCC particles on different materials: silicone, neoprene and Teflon. Measurements were performed using a goniometer. Each contact angle was measured at least four times. The uncertainty is $\sigma = \pm 2^\circ$.

Sample	Silicone	Neoprene	Teflon
Water	102	98	97
LBG	102	102	90
LBGMCC	103	101	105
Pectin	99	96	82
PectinMCC	95	94	93
Xanthan	98	95	89
XanthanMCC	105	97	71

It can be observed that for water all rubbers showed hydrophobic behavior (contact angle higher than 90°). Although the contact angle for silicone is the highest (102°), for neoprene and Teflon it is only slightly lower (98° and 97° respectively). Similar results are obtained for all samples. However, this might be influenced by a high viscosity of these solutions that could prevent easy spreading of a droplet on the surface.

In the case of silicone all solutions are characterized by contact angle very similar to that of water (within a range between 98° and 102°). Neoprene shows also small differences. LBG is characterized by the contact angle 4° larger than for water, while pectin and xanthan show decrease in the contact angle by 2° and 3° , respectively. Only in the case of Teflon slightly larger differences are observed. Although all polysaccharides show a decrease in the contact angle compared to water, LBG and xanthan are very similar (90° and 89° , respectively). For pectin decrease is stronger, as the contact angle drops to 82° .

These results show outstanding behavior of Teflon rubber that recorded the strongest variation for different solutions. Although all rubbers show hydrophobic response, silicone has clearly the strongest hydrophobic nature.

In the case of polysaccharides, pectin and xanthan seem to adhere slightly better than LBG and water. Interestingly, these results do not fully translate into friction data. LBG that has identical contact angle to water shows very different Stribeck curve. This results most

likely from polymers that are introduced into the solution and form thin film. However, once polymers are in the solutions the contact angle can give an indication for the friction coefficient. LBG with the highest contact angle is also characterized by the weakest lubrication properties of all polysaccharides, especially for the neoprene rubber.

When MCC particles are introduced, the contact angle deviations strongly depend on the rubber. The smallest differences were reported for neoprene and the largest for Teflon. In the case of neoprene the contact angle changed upon addition of MCC particles by up to 2° only. For LBG and pectin a decrease was observed by 1° and 2°, respectively. For xanthan a 2° increase was observed, which means that the adhesion properties of all samples to neoprene were not affected by the presence of MCC particles. Larger changes were observed for silicone, although in the case of LBG, the contact angle increased by only 1°. For pectin it decreased by 4° and the biggest difference was observed for xanthan where MCC particles caused an increase of the contact angle by 7°. In the case of Teflon MCC particles caused the most significant changes. For LBG and pectin the contact angle increased by 15° and 11°, respectively, while for xanthan it decreased by 18°.

Again these results show very specific behavior of Teflon. MCC particles seem not to have a big influence on the contact angle for silicone and neoprene, but cause strong variation in the case of Teflon. Interestingly the friction data also show very small differences between the cases with and without MCC particles. Thus small variation in the contact angle observed for silicone and neoprene after addition of particles are similar to the changes in lubrication properties. However, significant change in the adhesion properties of polysaccharide solutions after introduction of MCC particles are not reflected in the lubrication data.

6.3.3 Lubrication properties of polysaccharide solutions without particles

Tribological measurements are made to evaluate the ability of different polysaccharide solutions to lubricate various surfaces (Figure 6.4 A-C). In addition, water is used as a lubricant to well illustrate effects of polysaccharides, and different surfaces on friction properties (Figure 6.4 D). MTM measurements produce a Stribeck curve that provides the friction coefficient as a function of the entrainment speed. Soft materials undergo surface modification during the friction measurements that can enhance surface roughness. Moreover strong wearing of the neoprene rubbers results in a large uncertainty in the

measurements (the error bars for Teflon is about $\sigma=\pm 0.01$, for silicone $\sigma=\pm 0.03$ whereas for neoprene $\sigma=\pm 0.05$).

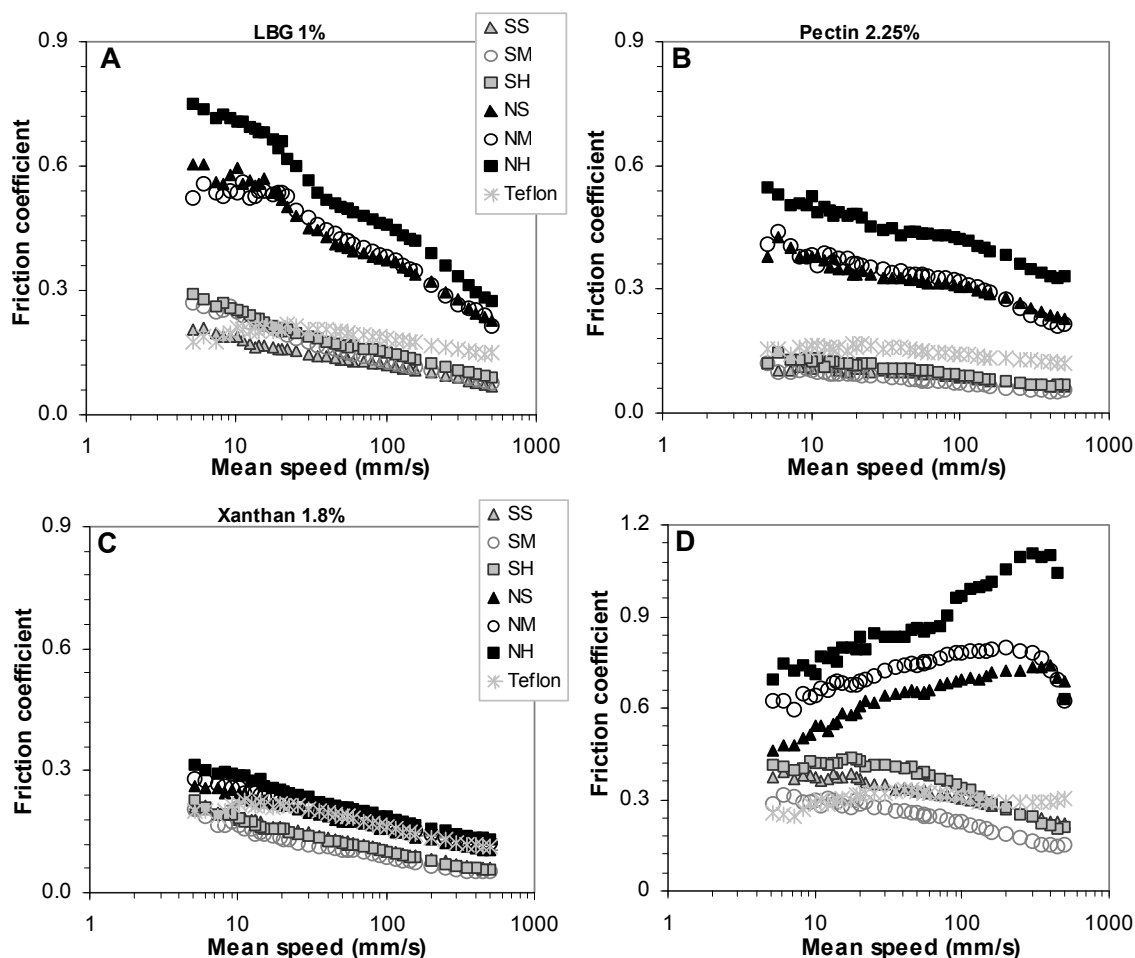


Figure 6.4 Friction coefficient as a function of the entrainment speed for polysaccharide solutions and for water measured at different materials. A: LBG, B: pectin, C: xanthan solution, D: water. Load: 5N. The standard deviation for Teflon is about $\sigma=\pm 0.01$, for silicone $\sigma=\pm 0.03$ whereas for neoprene $\sigma=\pm 0.05$. Note different scale on y-axis in graph D.

In the case of neoprene the lubrication properties of type S and M are generally almost indistinguishable. The neoprene H, however, is significantly higher for pectin and LBG. In the case of xanthan-solutions, however, the friction coefficient measured with NH is only slightly higher. The poorest lubrication is provided by LBG solution, where on neoprene S and M the boundary regime appears at speeds below about 20 mm/s. Neoprene H, however, seems to be already in the mixed regime although its friction coefficient is significantly higher. Pectin provides much better lubrication than LBG. It shows only mixed regime indicating good surface separation already at low speeds. Significant differences in measured friction on different surfaces were observed for pectin meaning

that its lubrication properties are linked to the surface properties. Xanthan seems to lubricate all surfaces the most effectively, as it shows the lowest friction coefficient of all polysaccharides in the entire speed range. For this solution the differences in Stribeck curves between all neoprene rubbers are very small.

The neoprene showed notably higher friction compared to the silicone rubbers (Figure 6.4). Although the general shape of the Stribeck-curve for all polysaccharides was similar between neoprene and silicone (the friction decreased gradually with increasing speed), in the case of water (Figure 6.4 D) the friction coefficient for the silicone rubber decreases with an increasing speed, contrary to the neoprene rubbers. For all three neoprene discs the mixed regime seems to begin at high speed, but only in the case of neoprene M the decrease of the friction is clear (well above 100mm/s). This results from a very extended boundary regime for the neoprene. Although surface roughness is usually believed to be responsible for the presence of a boundary lubrication regime, here the major role is most likely played by the surface-surface interaction. Two neoprene rubbers can better adhere to each other causing higher friction as they have similar hydrophobicity. This also results in damage of the surface of the disc and stronger wearing effect for neoprene rubbers. Thus the onset of the mixed regime for neoprene M may occur due to weaker interaction between the disc and the ring.

All silicone discs have very similar lubrication characteristics, as they show little difference in the friction coefficient. The Stribeck curve changes slightly between different polysaccharides, but for each sample all silicone discs produce a comparable result. This results most likely from similar material properties. All silicone rubbers undergo weak wearing effect that keeps asperities small, and have similar elasticity. Differences in elasticity and roughness (factor of 2) between silicone S and H are not reflected in their friction data. Their Stribeck curves almost overlap for pectin and xanthan. The difference can be observed only for LBG, where the shape of the Stribeck curve is different for the two discs. Moreover silicone M shows higher friction than silicone S only in case of LBG, although the difference occurs only at speeds up to around 100mm/s. Once pectin or xanthan is used as a lubricant, silicone M has lower friction than silicone S.

In the case of Teflon the friction coefficient is of the same order as silicone, but it has a slightly different shape (Figure 6.4). For water Teflon has a friction coefficient of about 0.3 and its Stribeck curve remains relatively flat at higher speeds. In all the cases (water and polysaccharides) Teflon shows higher friction than silicone rubbers for higher speeds.

The boundary regime and the onset of the mixed lubrication regime usually remains at the level similar to or even lower than silicone rubbers. The only exception is pectin that causes the friction coefficient to be higher at all speeds than for any silicone disc at all speeds. Moreover, Teflon shows the presence of the boundary regime for all samples. This may be a result of the very high Young modulus of non-deformable disc surface. A high pressure in the contact area of Teflon and O-ring makes it more difficult for a lubricant to enter resulting in the boundary regime.

Although material of a disc plays a major role in shaping the Stribeck curve, lubricants are equally important. Water provides very poor lubrication resulting in a much extended boundary regime especially in the case of, very rough, neoprene rubbers (see Figure 6.4 D). Interestingly, LBG seems to also be a rather ineffective lubricant, although the boundary regime is in this case significantly smaller or is not observed at all (Figure 6.4). For all polysaccharides the Stribeck curve shows if any a limited boundary regimes with the exception of Teflon. This may also result from different surface evolution during the experiment (wearing effect) under different lubrication regimes. The wearing process produces a similar surface for all solutions (see Table 6.1) but the asperities are larger in the case of lubrication by water. The best lubrication properties are provided by xanthan. In this case the difference between neoprene and silicone rubbers are the smallest. Pectin also provides very good lubrication but only at silicone and Teflon discs. Neoprene rubbers, however, show the friction coefficient lower than for LBG but still significantly higher than for xanthan. This suggests that pectin does not lubricate well irregular surfaces in contrast to xanthan that due to its hydrophilic nature might separate two hydrophobic surfaces. Pectin, on the other hand, forms a thin film that provides an efficient lubrication at low speeds for smoother surfaces (e.g. silicone or Teflon).

Clearly, from the above it has to be concluded that the good lubricants can compensate “negative” effects of surfaces on friction. For instance large difference in surface roughness in the case of Xanthan still lead to very similar Stribeck curves.

6.3.4 Lubrication properties of polysaccharide solutions with MCC particles

In order to understand the effect of the particles on the surface properties MCC particles are added to the polysaccharide solutions mentioned above. Figure 6.5 shows the friction coefficient measured for these samples with different discs. With the exception of xanthan solutions, the boundary regime is characterized by a higher friction coefficient when MCC

particles are present in the solution (cf. Figure 6.4). In the case of LBG the Stribeck curves show significantly higher friction in the boundary regime, when MCC particles are added to the solution. The difference between samples with and without MCC particles generally decreases with increasing speed. Therefore, MCC particles have a strong influence on the boundary regime and weakly affect the hydrodynamic regime. However, for all discs friction measured with LBG solution mixed with particles is higher than without particles. In general, for pectin friction measured with and without MCC particles is very comparable. This is the case for the silicone discs, where the impact of particles on friction appears to be limited. The only difference was observed for NM at low speeds and NH at high speeds. In the latter case, friction for pectin without particles is higher for NH at high speed and similar at low speeds. The friction coefficient on the NS, NH and Teflon rubbers is constant for speeds up to ~ 100 mm/s. This means that boundary regime for pectin is strengthened by introduction of the MCC particles. In the case of neoprene H boundary regime was shifted to higher value of the friction coefficient.

The size range of the MCC particles is extensive. The smallest grains are about $10\mu\text{m}$ in size, while the largest are an order of magnitude larger. Some of them can easily fit in the asperities of the rubber discs affecting the friction. These hard and elongated whiskers can stick out of asperities effectively increasing the surface roughness or causing a locking effect. Additionally the formation of the thin film separating the two surfaces in the boundary regime can be disturbed by the presence of hard grains in the contact zone. The other option is that the particles can accumulate in front of the contact zone preventing the entrainment of the lubricant, which causes an increase of the friction.

Generally, particles influence friction in the boundary regime. The strongest effect is observed at rather low entrainment speed below about 30 mm/s.

Although for pure polysaccharides influence of the surface properties on friction plays a minor role, particles introduced to lubricant enhance surface effects. Possibly particles influence interaction of a lubricant with surfaces affecting lubrication efficiency. Therefore, neoprene rubbers characterized by large surface roughness might be influenced stronger than smooth silicone as observed in Figure 6.5.

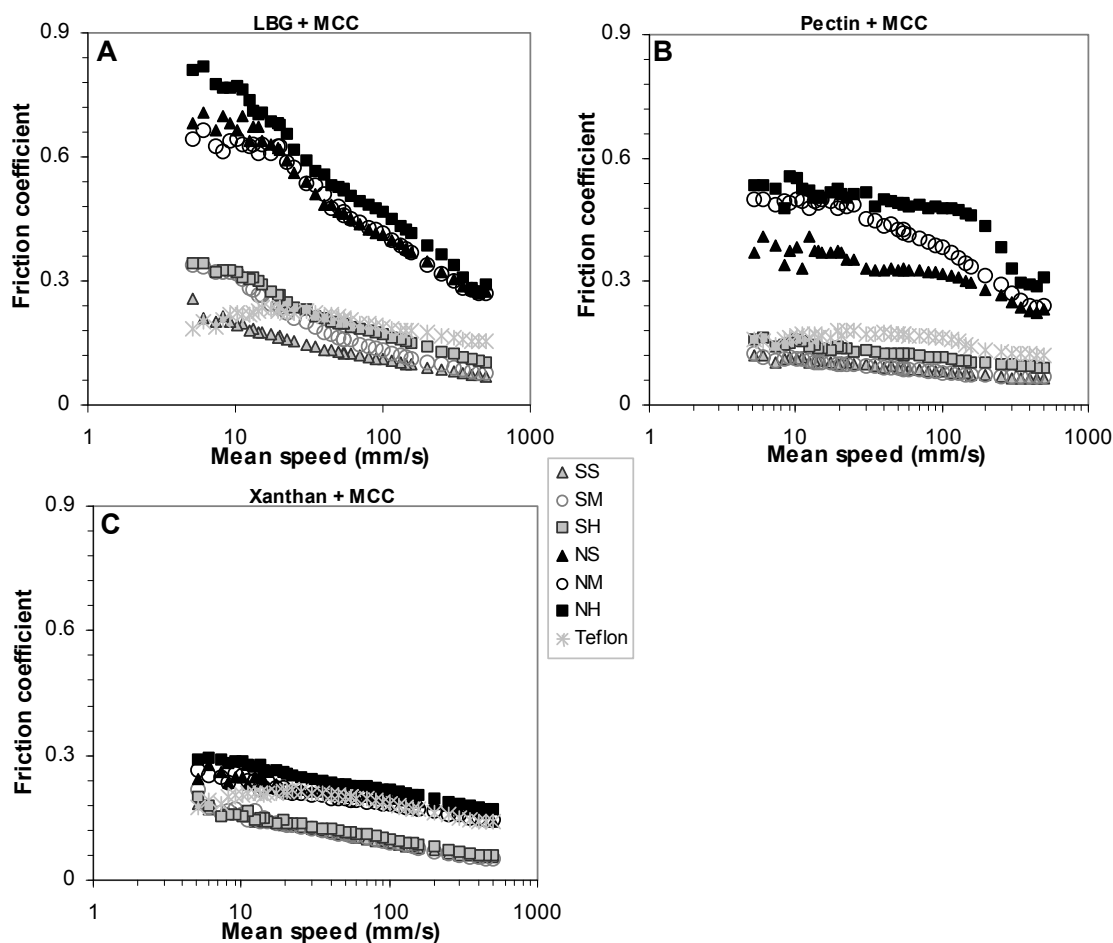


Figure 6.5 Friction coefficient as a function of the entrainment speed for polysaccharide solutions mixed with MCC particles measured at different materials. A: LBG, B: pectin, C: xanthan solution. Load: 5N. The standard deviation for Teflon is about $\sigma=\pm 0.01$, for silicone $\sigma=\pm 0.01$ whereas for neoprene $\sigma=\pm 0.04$.

6.3.5 Rheological properties of polysaccharide solution with and without MCC particles

Figure 6.6 shows the flow deformation curves for the polysaccharide solutions with and without MCC particles. All solutions show the non-Newtonian (shear thinning) behavior, where the viscosity decreases with an increasing shear rate. For the polysaccharide solutions with MCC particles, a slight decrease of the viscosity is observed for LBG and pectin samples. In the case of the xanthan solution, which shows the strongest shear-thinning behavior, presence of MCC particles cause a minor increase of the viscosity. This might be related to possible interaction between xanthan and MCC particles and could be further investigated in a future study.

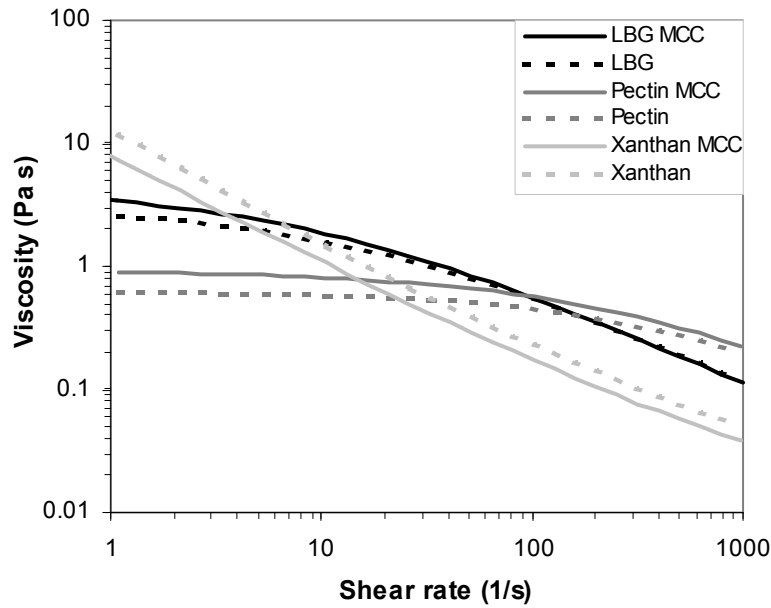


Figure 6.6 Viscosity as a function of the shear rate for polysaccharide solution with and without MCC particles.

6.3.6 Master curves for Newtonian solution on each of the rubber

Above results showed the importance of the lubrication properties over the disc characteristics. For that reason it appears to be very important to match the bulk rheological properties of the lubricant (only valid in the mixed and hydrodynamic regime). When the lubricant is introduced in between the surfaces in the MTM, the friction is governed mostly by the lubricant properties (like the ability to create the adhered layer on the surfaces or its behavior under the shear). Since the studied polysaccharides are non-Newtonian solutions, their rheological properties change during the experiment and can influence the measured friction. The influence of viscosity in the mixed and hydrodynamic regimes can be eliminated by construction of the master Stribeck curve. This allows to match the rheological properties of all samples and to bring more focus to the properties of the surfaces. To construct the master Stribeck curve several Newtonian solutions (water and different concentration of glycerol) are measured in the tribometer. Their viscosity evolution effect is eliminated from the frictional data by plotting the Stribeck curves as a function of $U\eta$. This leads to superposition of the friction curves for all Newtonian solutions. Consequently, general frictional behavior of the Newtonian solutions on each of the disc might be expressed by constructing so called master Stribeck curve ([19] and Chapter 4 [23]) by fitting the Newtonian Stribeck curves presented in terms of $U\eta$. The values obtained from this fitting procedure for each of the materials are listed in Table 6.3.

Figure 6.7 shows the master Stribeck curves for different materials studied in the current work.

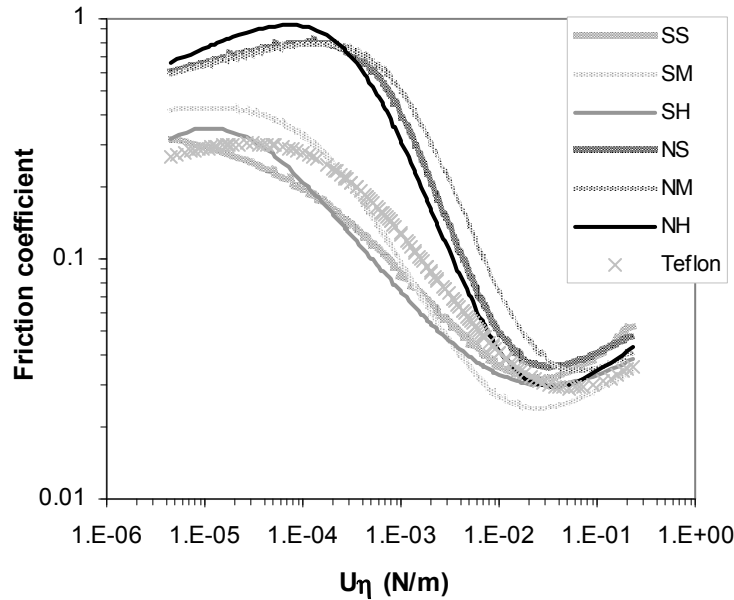


Figure 6.7 Master Stribeck curves from Newtonian solutions (water and different concentrations of the glycerol) for all the discs used in the tribometer. The master curves are obtained by plotting the friction coefficient as a function of the $U\eta$ product. Mater curves were obtained using the equation from Bongaerts et al. [19]. Load: 5N.

Table 6.3 The values obtained from the fitted Stribeck curve of the Newtonian solution, which generated master curve for particular material used in the tribometer. As reported previously [19, and in Chapter 4: 23] the friction coefficient in the elastohydrodynamic lubrication regime (μ_{EHL}) is given by a power-law of the product of the entrainment speed and the viscosity: $\mu_{EHL} = g(U\eta)^n$, with a slope n and index g . The master fitting function generated curve: $\mu_{tot} = \mu_{EHL} + \frac{h(U\eta)^l - \mu_{EHL}}{1 + (U\eta / B)^d}$, to the Newtonian data points. The h and l are the boundary power-law coefficient and index, respectively.

Fitted values	SS	SM	SH	NS	NM	NH	TEFLON
n	0.48	0.27	0.28	0.24	0.27	0.33	0.35
g	0.00	0.01	0.01	0.01	0.01	0.01	0.00
h	0.36	0.61	4.24	1.10	1.06	1.72	0.61
l	0.00	0.07	0.43	0.11	0.11	0.18	0.14
B	0.14	0.16	0.01	0.65	0.90	0.31	0.19
d	0.59	0.97	0.98	1.45	1.30	1.30	0.83

In the case of the silicone S , no boundary regime and a shallow decrease of the friction coefficient with $U\eta$ was observed. Silicone M showed higher friction coefficient in the

boundary regime and the onset of the mixed regime at low $U\eta$. In this case a steep decrease and the lowest friction coefficient in the minimum of $U\eta$ (among all samples) was observed. For silicone H very short boundary regime was visible. Although it was higher than for silicone S, the Stribeck curve decreased to the same level at the friction minimum. Neoprene M enters mixed and hydrodynamic regime of lubrication at the highest $U\eta$. On the other hand, neoprene H enters mixed regime at relatively low and hydrodynamic regime at relatively high $U\eta$. The master curve of neoprene S lies in between the NM and NH. It enters mixed regime relatively late, while the hydrodynamic regime relatively early. Teflon material showed extended boundary regime. Consequently the onset of the mixed regime is observed at $U\eta$ of around 0.1. The onset of the hydrodynamic regime is observed relatively late (at high $U\eta$).

All neoprene rubbers have very long boundary regime and show high friction coefficient at the onset of the mixed regime. This results from large surface roughness. In the case of silicone smaller asperities cause shorter boundary regime with lower friction coefficient. Therefore the master curve is lower compared to neoprene. Silicone rubbers enter mixed and hydrodynamic regime at low $U\eta$. For both neoprene and Teflon disc, the onset of the hydrodynamic regime was observed at high $U\eta$. The low Stribeck curve for Teflon resulted from a very smooth surface of this material. Despite the smallest asperities, relatively long boundary regime was observed for Teflon which most likely results from high Young's modulus and thus high contact pressure.

master curves expose surface influence on the lubrication process. In the hydrodynamic regime, all curves overlap showing that surface does not influence friction, but boundary and mixed regime show strong variation between different rubbers. Surface roughness seems to be the most influencing factor, as neoprene rubbers with the largest asperities show the longest boundary regime and the highest friction coefficient. However, Teflon that has the lowest asperities show also relatively long boundary regime but with lower friction coefficient. Thus the hardness of the material seems to be second important property that can influence the lubrication process.

6.4 Conclusions

In this chapter we explore the influence of different surfaces (rubbers) on the tribological measurements for a number of food-relevant liquid systems that differ in lubrication. Seven rubbers of different properties are used for this purpose. Their characteristic is

established using a number of techniques. From this study one can see that a softer and smoother material allows better lubrication. The Stribeck curves obtained for different surfaces also depend very much on applied polysaccharide. For weak lubricant (e.g. LBG) a strong wearing effect significantly increases the friction coefficient compared to a good lubricant (e.g. xanthan).

We have shown that the influence of the surface under good lubrication conditions is not significant. Therefore, in developing new food products it may be of prime importance to control their lubrication properties rather than focus on the surface characteristics. For instance, other substances may be used to mimic fat, that frequently is employed solely to improve lubrication.

The investigation of the influence of particles on tribological measurements shows that the main effect is also observed at relatively low speeds (below about 50 mm/s). Large particles cannot fit in asperities entirely and enhance the surface roughness, which results in extended boundary regime. Thus particles present in a solution can relatively easily be detected by tribological investigation. This provides good sensitivity in the process of food programming. In the case of good lubrication, however, the particles influence becomes weaker. Thus the better the lubricant the more difficult the detection of particles is. Thus possibly food products characterized by low friction coefficient might be mixed with elongated particles without large influence on their lubrication properties.

Acknowledgement

The authors would like to thank Anne van de Pijpekamp and Anke Janssen for advice on concentrations of used polysaccharides.

References

- 1 Malone ME., Apperlqvist, I. A. M. and Norton I. T. Oral behaviour of food hydrocolloids and emulsions. Part 1. Lubrication and deposition considerations, *Food Hydrocolloids*, (2003), 17, 763-773
- 2 Keeton W.T., McFadden C.H., Elements of biological science (1979) New York, W. W. Norton & Company
- 3 Toyoda, M., Sakita, S., Kagoura, M., Morohashi, M. (1998). "Electron microscopic characterization of filiform papillae in the normal human tongue". *Archives Of Histology And Cytology*, 61(3), 253- 268.

- 4 G.A. van Aken "Relating food microstructure to sensory quality", in: D.J. McClements (ed.) "Understanding and controlling the microstructure of complex foods" Woodhead Publishing Limited, year Cambridge, CB21 6AH, England
- 5 Mei van der, H. C., White, D. J., Busscher, H. J. (2004). On the wettability of soft tissues in the human oral cavity. *Archives of Oral Biology*, 49(8), 671-673.
- 6 Schipper, R. G., Silletti, E., Vingerhoeds, M. H. (2007). Saliva as research material: Biochemical, physicochemical and practical aspects. *Archives of Oral Biology*, 52 (12), 1113-1214.
- 7 Amerongen, A. V. N., Veerman, E. C. I. (2002). Saliva - the defender of the oral cavity. *Oral Diseases*, 8(1), 12-22.
- 8 G.A. van Aken, M.H. Vingerhoeds, E.H.A. de Hoog (2005) "Colloidal behaviour of food emulsions under oral conditions" in Dickinson E., *Food Colloids 2004: Interactions, microstructure and processing*. Cambridge, The Royal Society of Chemistry, 356-366
- 9 D. M. Dresselhuys, E.H.A. de Hoog, M.A. Cohen Stuart, G.A. van Aken, "Application of oral tissue in tribological measurements in an emulsion perception context" *Food Hydrocolloids*, 22(2), 323-335 (2008).
- 10 Ranc, H., Elkhyat, A., Servais, C., Mac-Mary, S., Launay, B., Humbert, P., (2006). Friction coefficient and wettability of oral mucosal tissue: Changes induced by a salivary layer. *Colloids and Surfaces A: Physicochemical and Engineering Aspects* 276 (1-3), 155.).
- 11 J.H.H. Bongaerts, D. Rosetti and J.R. Stokes, "The Lubricating Properties of Human Whole Saliva", *Tribology Letters* vol 27, Nr 3, (2007): 277-287
- 12 Napadow, V. J., Chen, Q., Wedeen, V. J., Gilbert, R. J. (1999). Intramural mechanics of the human tongue in association with physiological deformations. *Journal of Biomechanics*, 32(1), 1-12
- 13 Gilbert, R. J., Napadow, V. J. (2005). Three-dimensional muscular architecture of the human tongue determined in vivo with diffusion tensor magnetic resonance imaging. *Dysphagia*, 20(1), 1-7
- 14 P. Poudrouc and P.J. Kahrilas, (1995). Deglutitive tongue force modulation by volition, volume, and viscosity in humans. *Gastroenterology* 108, 1418-1426.
- 15 K. Tsuga, R. Hayashi, Y. Sato and Y. Akgawa, (2003). Handy measurement for tongue motion and coordination with laryngeal elevation at swallowing. *J. Oral Rehabil.* 30, 985-989.
- 16 Hayashi R., Tsuga, K., Hosokawa, R., Yoshida M., Sato, Y., Akagawa, Y. (2002) A novel handy probe for tongue pressure measurements. *Int. J. Prosthodont.* 15: 385-388
- 17 G. Cassin, E. Heinrich, H.A. Spikes, *Tribology Letters* (2001) 11:95-102
- 18 J. de Vicente, J.R. Stokes, H.A. Spikes, *Tribology International* (2005);38:515-26
- 19 J.H.H. Bongaerts, K. Fourtouni, J.R. Stokes, *Tribology international* (2007); 40:1531-42
- 20 Chojnicka, A., Visschers, R. W. & de Kruif, C. G., Lubrication properties of protein aggregates dispersion in a soft contact, *Journal of Agricultural and Food Chemistry*, (2008) 27;56(4):1274-82.
- 21 de Hoog, E. H. A., Prinz, J. F., Huntjens, L., Dresselhuys, D. M., van Aken, G. A. (2006). Lubrication of oral surfaces by food emulsions: the importance of surface characteristics. *Journal of Food Science*, 71(7), E337-E341.
- 22 Prinz, J.F., de Wijk, R.A., Huntjens, L., Load dependency of the coefficient of friction of oral mucosa. *Food Hydrocolloids*, (2007), vol.21(3), 402-408.
- 23 Chojnicka-Paszun A., Macakova L., Stokes J.R., de Kruif C.G. and de Jongh H.H.J. "Lubrication, rheology and adsorption of polysaccharide solutions" (submitted).
- 24 S. de Jong, F. van de Velde, *Food Hydrocolloids* 21 (2007) 1172-1187
- 25 Chojnicka-Paszun A., A.M. Janssen, A.M. van de Pijpekamp, S. Doussinault, G. Sala, H.H.J. de Jongh and C.G. de Kruif. "Sensorial analysis of polysaccharide-protein gel particle dispersions in relation to lubrication and viscosity properties" (To be submitted).
- 26 A. Chojnicka & G. Sala, C.G. de Kruif, F. van de Velde *Food Hydrocolloids* 23 (2009) 1038-1046.

Chapter 7

Sensory perception and friction coefficient of milk with increasing fat content

Abstract

The ability to relate a physical property like the friction coefficient of a product to its sensory perception is of key importance for food industry. It may simplify the process of development of new or reformulation of existing products. In addition, it can provide a more absolute measure for programming sensory perception based on modification of tribological properties of a food product.

In this chapter a multi-approach study is applied to a set of milk-related emulsions in order to establish a correlation between sensory attributes scored by trained panelists and data obtained in laboratory. In the current work it was shown, that above a certain fat concentration threshold (different for silicone and neoprene rubbers) increase of the fat content in emulsion led to a decrease of the Stribeck curve in the boundary regime. This was associated with shear-induced coalescence that took place on rubber surfaces.

It is shown that for example creamy perception was perceived only when the friction coefficient was below 0.25 for silicone rubber at entrainment speeds lower than 200 mm/s. Under those conditions a gradual increase of perceived creaminess with friction was obtained above 1 % of fat content. This gradual increase of the creaminess and thus decrease of friction was attributed to the coalescence of fat globules on the surface of the tongue and rubber disc, respectively. This effect was more efficient at lower speeds and certain fat content. At higher speeds, however, fused fat droplets were broken into smaller droplets (reversing coalescence) due to the high shear, thereby eliminating the correlation. Additional correlations were found between mouth-feel attributes and viscosity. Most probably shear-induced coalescence of the fat droplets, which occurred in the tribometer and influenced experimentally measured friction coefficient is also responsible for sensory responses of milk samples.

7.1 Introduction

One of the most important sensory attributes for dairy products is the perceived creaminess or fat film formation. These attributes are associated with the amount of fat present [e.g. 1]. Creamy or fatty perception was previously related to the apparent viscosity of the product [2-4]. Since fat content and viscosity are one to one related according to the Einstein viscosity, fat content and viscosity are an expression of the same parameter. In addition, it was shown recently, that bulk rheology does not fully describe characteristics of the sensory properties of emulsions, hence the importance of the friction and sensory fat perception was highlighted [5-10]. During consumption, food is rubbed between tongue and palate, forming a thin film on the oral mucosa that experiences friction forces. The relation between thin film properties and food texture was investigated for chocolate [8] and mayonnaise [9]. These studies confirmed that tribology, thin-film morphology and wetting properties of the samples provide relevant insight that could not be obtained by bulk rheology alone. It was concluded that texture of the samples correlated better with thin film tribological properties rather than bulk characteristics [8,9]. Recently an extensive study was reported relating the creamy and fatty perception of emulsions to their lubrication properties [11-13]. Dresselhuis et al. showed that emulsions with higher efficiency towards coalescence were perceived as lower in friction and as more creamy/fatty. This was verified by physically measured friction, which decreases for lower perceived friction. Therefore the ability of emulsions to spread on oral and artificial surfaces was reported to be of significance [12,13]. The friction force was previously measured in the custom-made friction apparatus for emulsions with 10 to 40 % fat content [14]. That work showed that in the studied range of fat content no dependence between measured friction force and oil fraction between mucosal surfaces existed.

A number of studies investigated the relation between sensory attributes and composition or physical characteristics of the product. De Wijk et al. [16] suggested three dimensional sensory space for dairy custard desserts. The principal axis linking roughness to creaminess was related to the fat content; the melting to thick axis could be related to the starch content and the viscosity of the food, whereas principal axis describing airy to heterogeneous was related to the type of starch. A further study showed that the creamy attribute could be associated with bulk and surface properties of the oral food bolus [17]. In addition, sensory attributes e.g. stickiness perception correlated with the extensional viscosity, as a food product might stick between the tongue and palate and form filament

threads upon their spacial separation [18]. Moreover, it was shown that stickiness and sliminess correlated with small and large deformation rheological measurements [19].

The influence of fat on the sensory properties, viscosity and color of low-fat milk (0-2 %) was studied by Phillips et al. [20]. Their work showed that the mouth-feel attributes increased with fat content. However, the unambiguous interpretation of the results was argued because of difference in visual appearance. Similar results were obtained by Pangborn et al. [21] who showed that once the panelist were not able to see the milk emulsions they were not capable to discriminate the differences between 0 and 3.5 % of fat in the milk.

In this chapter homogenized and pasteurized milk with different fat content were studied under applied shear in the tribometer and rheometer. In addition, sensory evaluations of the samples were studied using the quantitative descriptive analysis (QDA). Next the correlation analysis between perceived attributes and measured physical properties was investigated. In addition confocal scanning laser microscopy was employed to detect fat coalescence and its influence on friction measurements. To our knowledge no systematic change in the creamy attribute and measured friction coefficient between two soft contacts was obtained before for such low fat concentrations. Moreover, the importance of the coalescence is discussed.

7.2 Materials and Methods

7.2.1 Materials

Samples. Homogenized and pasteurized semi skimmed milk with fat concentration of 0.06 % (w/w) and full fat milk with 8.68 % (w/w) of fat was standardized to the same protein content (3.3 % (w/w)) and supplied by Campina Innovation (Wageningen, The Netherlands).

Rubbers. Silicone, neoprene and Teflon materials were purchased from Eriks company (Arnhem, The Netherlands).

7.2.2 Sample preparation

Semi skimmed and full fat milk (0.06 and 8.68 % (w/w), respectively), were mixed in order to accomplish emulsions with the desired concentration of fat: 0.15, 0.3, 0.5, 0.7, 1, 2, 3, 4, 6.5 % (w/w)/ (g fat/100g milk). The samples were stored in the fridge at 5 °C, and used within two days. Freshly prepared emulsions were used in each experiment.

7.2.3 Quantitative descriptive analysis (QDA)

An expert panel (consisting of 10 persons) evaluated the sensory properties of the milk with different fat concentration. Due to limited number of samples (9) that could be tested by assessors in the QDA sensory panel, only milks with up to 4% of fat content was used. The panel was familiarized and trained to score on seventeen attributes common in the assessment of milk (see Table 7.1). These attributes belong to four different categories i.e. smell/taste, mouth-feel, mouth/after-feel and after-taste/feel sensation. The samples were presented to each assessor at 14 ± 2 °C degree in two different groups due to the large differences in fat content. The five lowest fat concentrations (from 0.06 to 0.7 % (w/w)) were presented in the first group, whereas second group consisted of the samples with the highest fat percentages (from 1 to 4% (w/w)). The reason for the grouping was to prevent cross-over effects (of especially fat) as much as possible. Each sample was served in a small plastic cup that was covered with aluminium foil to avoid the influence of light and to ensure that the head space, for the smell evaluation, was optimal. Within each group the samples were presented unmarked to assessors and in a randomized sequence. Assessors assigned a score on a scale from 0 – 100 for each attribute.

7.2.4 Rheological and tribological measurements

The viscosity data of the emulsion were recorded at 20 °C using a standard rheometer (AR 2000, TA Instruments, Leatherhead, UK) with double concentric cylinder geometry. Flow curves were obtained by measuring the apparent viscosity as a function of increasing shear rate (from 0.1 and 1000 s⁻¹). More detailed description of this method was presented in Chapters 2 or Chapter 6.

A Mini Traction Machine (MTM) (PCS Instrument) with the compliant rotating surfaces was used to measure friction coefficient (μ) as a function of the entrainment speed. Each measurement was taken at 20 °C with a new surface cleaned with ethanol, and reverse osmosis water and then dried with air. Further description of this method and the setup can be found in Chapter 2 and Chapter 6.

Table 7.1 Definitions of attributes generated by quantitative descriptive sensory analysis.

Attributes	
Smell/Taste (S/T)	Definitions
Creamy	Smell and taste associated with (whipped)cream
Flat/Watery	Lack of milk smell and taste
Sour	Taste of lactic acid
Sweet	Taste of milk sugar
Musty(muff)	Smell and taste associated with a cellar/old cupboard/cabinet
Metalic	Smell and taste associated with (blood)metal
Cardboard	Smell and taste associated with wet paper/cardboard
Mouth-feel (MF)	Definitions
Creamy	Mouthfeel associated with (whipped)cream
Powdery	The sensation of small particles like e.g. flour
Soft/Velvet	A soft sensation in the mouth
Watery	The sensation of water in the mouth (no body)
Sticky	A sticky sensation on palate and between the teeth
Mouth/after-feel (AF)	Definitions
Rough	A rough/coarse sensation in the mouth/on the tongue (after swallowing)
Fat film	The sensation of a fat-like layer in the mouth (after swallowing)
After-taste/feel (AT)	Definitions
Slimy	A slimy sensation in the throat after swallowing
Dry	A dry sensation on the tongue/mouth after swallowing
Sour	A sour taste left behind in the mouth after swallowing

7.2.5 Confocal Scanning Laser Microscopy

After MTM measurement the visualization on the micro scale level of the surfaces used was done with a LEICA TCS SP by Confocal Laser Scanning Microscope (CLSM) equipped with an inverted microscope (model Leica DM IRBE) and Ar, DPSS and HeNe or Ar/Kr visible light lasers (Leica Microsystems (CMS) GmbH, Mannheim, Germany). The objective lenses of 5x magnification and 20x magnification (HC PL APO 20x/0.70 CS) were used. In order to observe a possible coalescence of the fat on the discs, fluorescing isothiocyanate with Nile Red (FITC/NR) was used to stain the protein and oil phases of the milk, respectively. A 55 ml of emulsion with 1 ml of FITC/NR was mixed prior to the experiment. After the measurements the disc was investigated under the CLSM. The excitation was performed at 480 and 520 nm for FITC and Nile red, respectively. Reported digital images for silicone and Teflon disc were recorded at a penetration depth of 10 μm . Due to large asperities in the neoprene rubber a projection

(scan) of 30 μm inside the track was performed. Images were obtained in 1024x1024 pixel resolution.

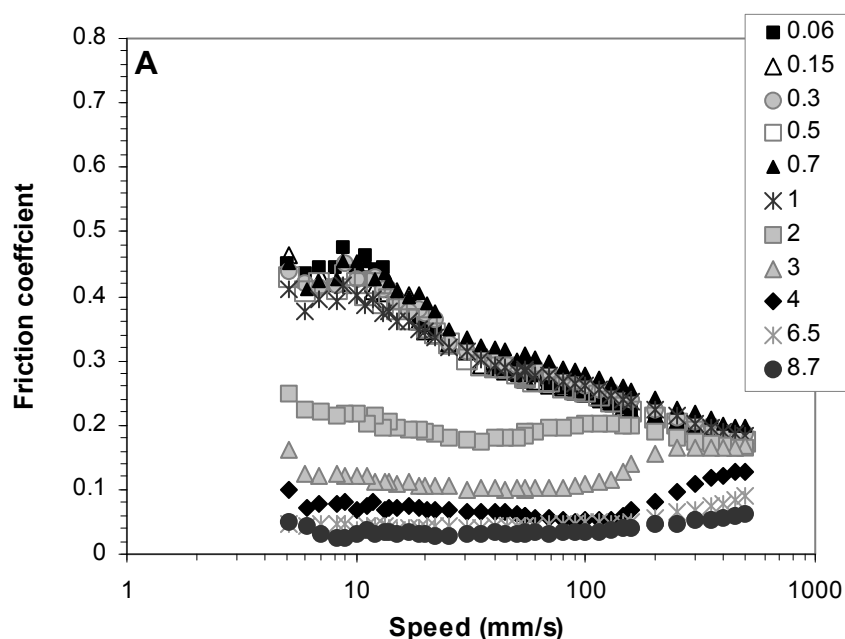
7.3 Results

7.3.1 Friction coefficient

In order to find the best match between oral surfaces and tribometer measurements 3 different rubbers were tested. This extends the parameter space and helps to select the most suitable oral surface analog which provides the best correlation with a sensory attribute. These rubbers differ in hardness and surface roughness. In a tribological measurement the friction is measured of a sample that can entrain between two surfaces as a function of the speed by which these two surfaces are displaced relative to each other. The resulting plot is the so-called Stribeck curve.

Silicone

The friction coefficient determined for all samples is shown in Figure 7.1A. Samples with the lowest fat content indicate boundary lubrication regime below a speed of about 10 mm/s. The mixed regime follows at higher speeds. Interestingly, all emulsions with a fat content below 1% exhibit similar behavior. Thus it is impossible to distinguish low fat content samples solely based on their Stribeck curves.



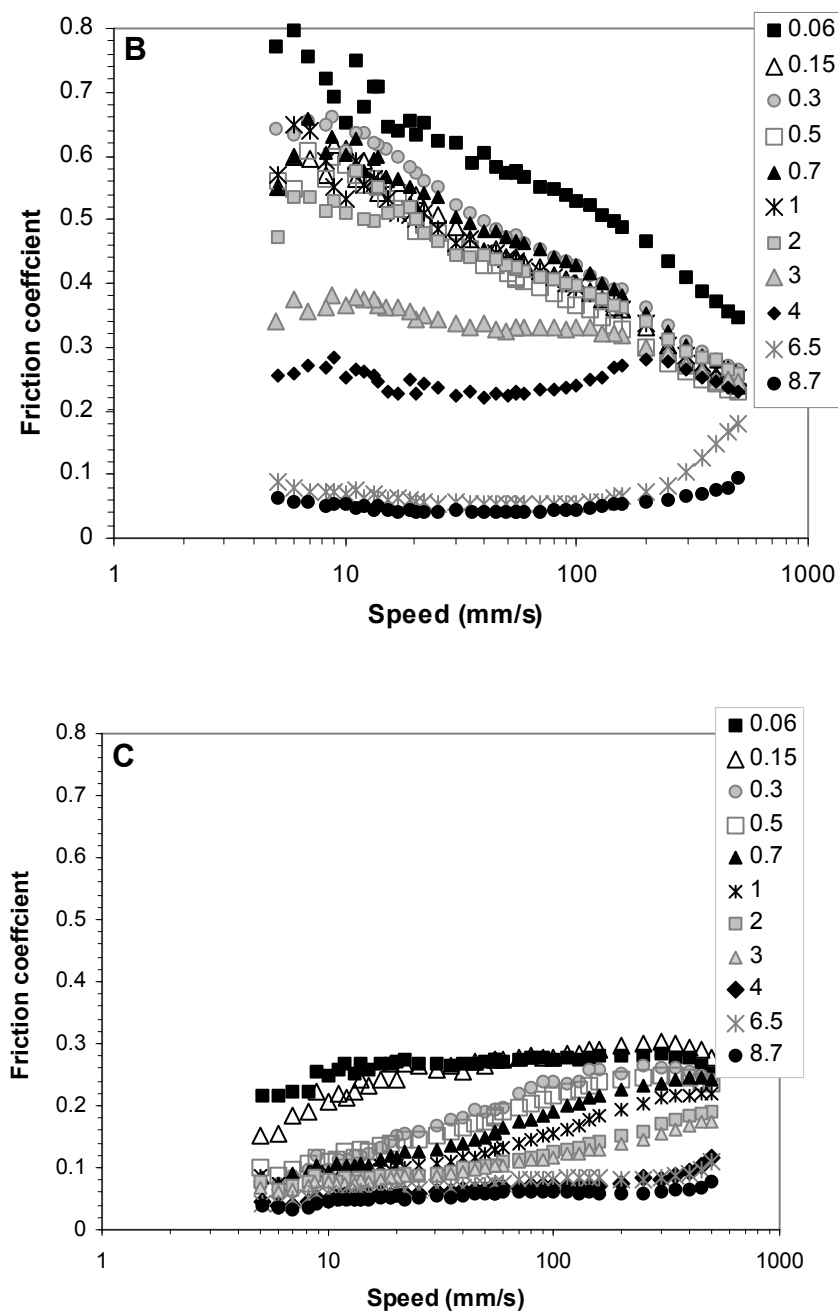


Figure 7.1 Friction coefficient for all samples measured with 3 different rubbers: A-silicone, B-neoprene, C-Teflon. Friction coefficient measured at $W=5\text{N}$ step 5.

Emulsions with a fat concentration above 1% show a decreasing friction coefficient with increasing concentration of fat. Interestingly, this behavior seems to saturate at fat contents of about 6.5%, as the decrease of the friction coefficient slows down. As the friction coefficient decreases with increasing fat concentration, the boundary regime extends as well to higher speeds. This behavior is most likely related to coalescence of fat droplets and subsequent adhesion of fat onto the surfaces. The higher

the fat concentration, the thicker or the more extended the boundary film becomes. Once sufficient film thickness is established the bulk fluid entrainment is suppressed. Initially (for low fat emulsion content) the friction may be governed by the bulk fluid and possibly lubrication is dominated by proteins at all entrainment speeds. On the other hand, for high fat content the fat forms the boundary film and dominates the lubrication, allowing the entrainment of bulk emulsion to be suppressed and causing an extended boundary regime with very low friction coefficient. High speed, however, most likely leads to breaking the adhered fat layer and emulsifying the fat. The friction increases then as a result of entrainment of bulk fluid and influence of proteins that provide poorer lubrication than fat. In addition, the high fat content samples exhibit a significant time dependence in their Stribeck curves. The longer the surfaces are processed and exposed to emulsions the lower the friction coefficient measured. Possibly this behavior results from a relatively slow process of film formation and/or coalescence of fat droplets. Emulsions with lower fat concentration require more time for fat to adsorb onto the surface compared to high fat content samples. Moreover, the coalescence may be partially suppressed at high speeds. Effects due to the rubber are most likely negligible as in the case of water (much poorer lubricant) the Stribeck curve show very little changes with time (see Figure 7.2).

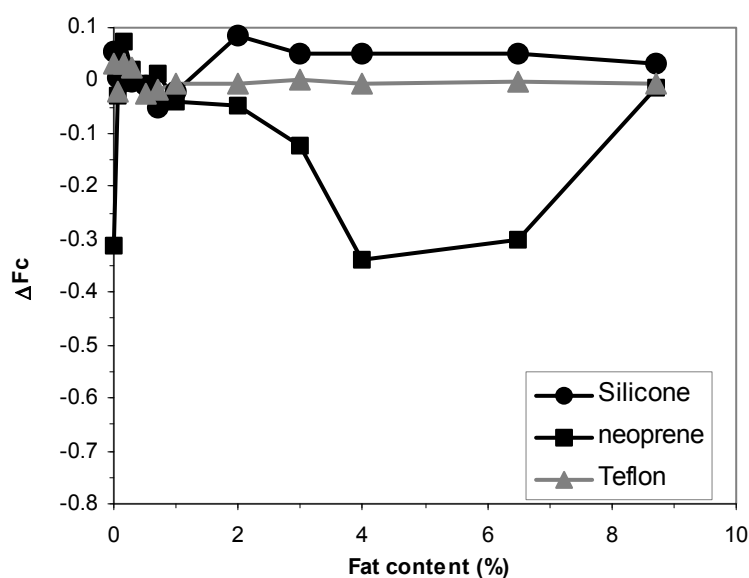


Figure 7.2 Change in the friction coefficient at 10mm/s for different samples after 3 experimental runs.

Neoprene

In the case of neoprene rubber the Stribeck curves show very similar shapes. Low fat content emulsions show similar lubrication characteristics with an exception of milk with 0.06% fat (the lowest concentration). The latter sample has a friction coefficient about 0.1 higher than other low fat content emulsions. Moreover its Stribeck curve is comparable to that of water. It suggests that for neoprene there are two thresholds. The first one requires some minimum fat content to show any change in lubrication characteristics. The second threshold is for fat content of about 2%. Below this concentration Stribeck curves are practically undistinguishable. Above that point an increasing fat concentration causes a decrease of the friction coefficient.

The value of the friction coefficient is for all samples higher in the case of neoprene rubber than for silicone. This is likely a consequence of the larger surface asperities of the neoprene rubber and was discussed previously in Chapter 2 and Chapter 6.

The time dependence in the case of neoprene is more prominent. Although this rubber is known to undergo wear during friction, it seems that the main cause of the decreasing friction coefficient with the number of experimental runs is the film formation or coalescence. In Figure 7.2 the change in friction coefficient (ΔF_c) is presented as a function of fat concentration in a sample. A very strong change in friction between runs for water is a direct result of the wear of the surface. However, introduction of fat in very small quantity results in a drastic reduction of the change in friction. The wear process seems to be suppressed. The further increase of the ΔF_c with increasing fat content is very unlikely to be caused by the wear as the lubrication efficiency increases, preventing a direct contact between the two rubbing surfaces. Coalescence or film formation is the most probable effect leading to a change in friction over time. Interestingly, this time dependence is different from the case of silicone, which must be a result of different material properties.

Teflon

In the case of Teflon the Stribeck curves are very different from the other two rubbers. The Teflon surface is very smooth and much harder than silicone or neoprene (see Chapter 6). This results in significantly lower friction in the low speed range (see Figure 7.1c). The boundary regime extends to very high speeds and the onset of the mixed regime is observed only for speeds above about 300 mm/s. Moreover all milk samples show unique characteristics and can be easily distinguished based on their frictional properties. An

increasing fat content causes a decrease of friction even for very small concentrations, unlike for the two other rubbers, where a certain threshold was needed in order to further decrease the friction coefficient.

The time dependence of the shape of the Stribeck curve was not observed in the case of Teflon (see Figure 7.2). The surface does not undergo a wearing process and is both hydrophobic and lipophobic meaning that the water and fat are repelled from the surface. Film formation is therefore unlikely to occur on Teflon and therefore there is no time dependence.

7.3.2 Viscosity

Bulk rheological analysis shows that the viscosity of all samples is comparable. The data is confined in the viscosity range between $1.5 \cdot 10^{-3}$ and $4 \cdot 10^{-3}$ (Pa.s) (see Figure 7.3). Thus over two orders of magnitude difference in fat concentration translates to only a factor of 2 in viscosity. Moreover, the milk samples with fat content below 1% are practically undistinguishable by the viscosity; their flow curves almost overlap. The systematic increase of the viscosity is observed most likely above a concentration of 1%. This is due to emulsion droplets that increased the viscosity as a function of the volume fraction of the droplets [22, 23]. A weak shear thinning behavior observed above 0.5 % of fat content is due to possible weak attractive interactions between fat globules in the milk. It can be observed, that between 0.5 % and 1 % of the fat content the viscosity decreases 10% over two orders of magnitude in shear rate. The shear thinning becomes slightly stronger with increasing fat content and for concentration of 8.5% the viscosity drops by 20% between shear rate of 10 1/s and 1000 1/s.

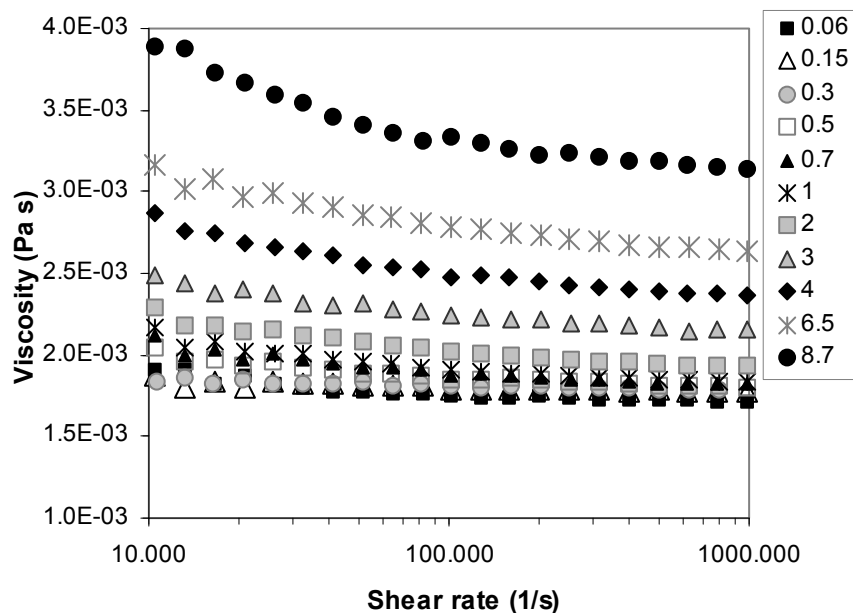


Figure 7.3 Viscosity data of all samples.

7.3.3 Confocal Laser Scanning Microscopy (CLSM)

CLSM imaging presented in Figure 7.4 revealed that indeed fat droplets coalesce at the surface, forming larger structures surrounded by bulk solution. In the case of silicone the surface is well covered by an adhered fat layer. The track formed during the tribological experiment is well visible as fat seems to be concentrated more towards the center of this track (light *gray color*), while protein is visible at the edges (dark *gray color*).

In the case of neoprene the fat seems to form a structure. This results from adhesion and coalescence of fat droplets within large asperities. The surface, however, is not covered with such a uniform layer. The distinction between protein and fat components is more visible than in the case of silicone.

Teflon rubber shows a different picture, with interesting structures formed by the coalescing fat. The lipophobic surface prevents adhesion and thus large droplets have a more confined shape. This results in sharper boundaries between the components.

The coalescence of fat is clearly visible for all rubbers and thus verifies the lubrication hypothesis.

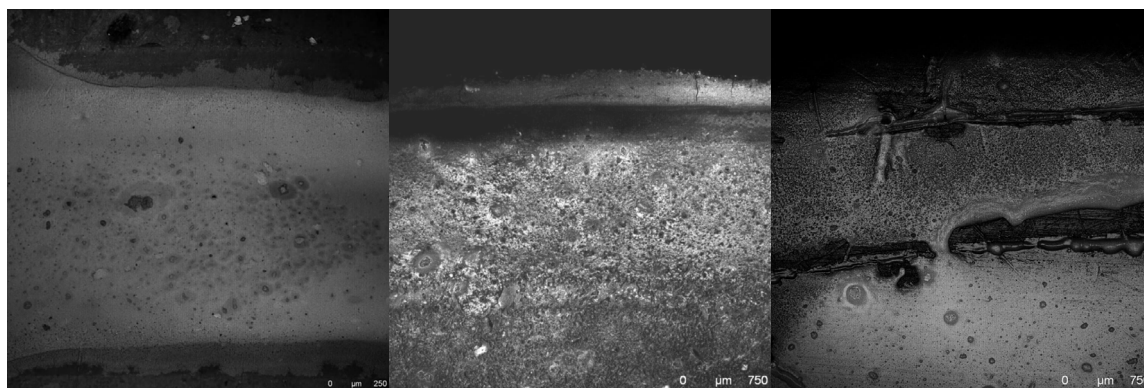


Figure 7.4 CLSM images of 3 different rubbers after processing 3.5% milk in MTM. Note different scale for silicone rubber. Light gray corresponds to fat.

7.3.4 Sensory attributes study

The panel analysis of milks with varying fat content between 0.06 and 4% are shown in Figure 7.5 for a number of sensory attributes. Just like in the case of friction and viscosity low fat content samples have no systematic trend. For all attributes the data points are scattered for samples below 1 % fat content. As reported before, the color of the milk is of great importance for the sensory perception. It was shown, that difficulties with perceived differences between low fat content up to even 2 % [20] or 3.5 % [21] was observed. In the current work, although the panelists were not able to see the samples prior testing, the differences in sensory attributes were perceived above 1 %.

Trends are only visible for samples with a concentration of fat above 1 %. Several attributes show a good correlation for fat content above 1 %, while others show no relation at all. Note that two groups of attributes can be distinguished: describing taste and describing texture perception. In the case of taste the creamy attribute increases with an increasing fat content. Similarly creamy texture shows the same trend, although, at lower score. A similar score to the creamy texture is obtained for the soft/velvet attribute. It increases with an increasing oil concentration. The watery attribute can be found in both taste and texture categories and it scores almost exactly the same in both categories (here only the texture attribute is presented). It follows a decreasing trend for an increasing fat concentration. Therefore, the higher the fat content is in milk the less watery it tastes and feels.

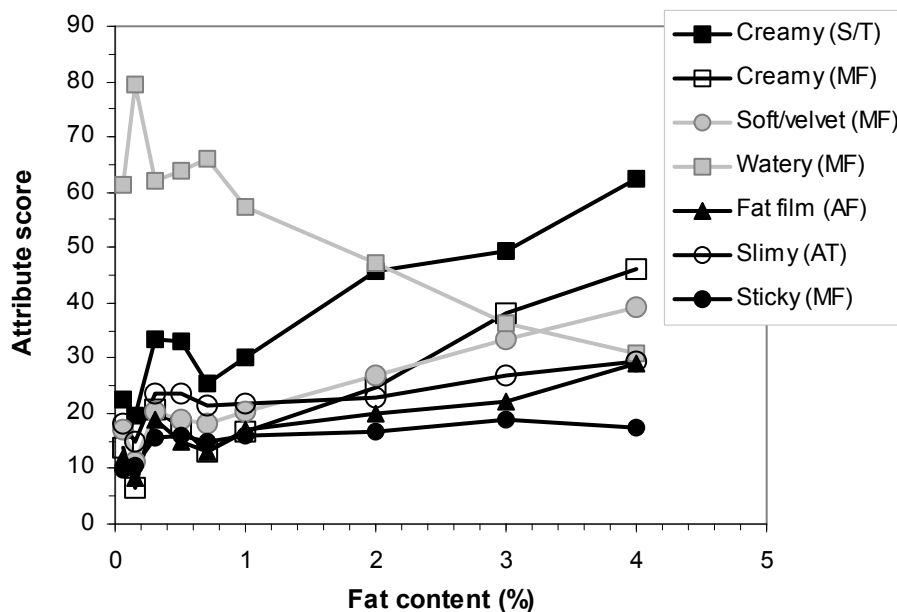


Figure 7.5 Score of attributes as a function of fat content in milk sample.

Interesting results are obtained for perception of stickiness. All samples, regardless of fat content, show very similar and low score and thus no relation is observed in this case. This is in agreement with previous findings, where low perception of stickiness was associated with high creamy perception for custard products [24]. On the other hand, the fat film attribute shows an increasing trend with an increasing concentration of oil.

7.4 Discussion

In this chapter three different techniques are applied to milk samples. The applied methods are analyzed to establish possible links between oral perception of taste and texture and friction coefficient or viscosity of a sample. To establish an absolute link between friction and sensory, first the viscosity influence on the tribological data has to be eliminated. This is commonly done by construction of a so-called master Stribeck curve, in which the entrainment speed is multiplied by the (shear rate dependent) viscosity. Thus eliminating the fluid viscosity from the friction measurement.

7.4.1 Master Stribeck curve

The investigated milk samples have relatively flat viscosity flow curves (Figure 7.3) that indicate Newtonian behavior. Although for higher fat content emulsions (above 0.5%) a shear thinning is observed, it is relatively moderate. It can be observed that viscosity increases only by about 40% while the fat concentration increases by a factor of almost 9.

This shows that the viscosity corrected (master) Stribeck curve (data not shown) is very similar to the curve presented in Figure 7.1. The difference occurs only for high fat content samples where the viscosity is slightly higher. Low fat content emulsions, however, behave like Newtonian solutions and have almost identical viscosity. Their master curve is only shifted by a factor of about $2 \cdot 10^{-3} \text{ Pa s}$ with respect to the friction data in Figure 7.1.

7.4.2 Correlation of different methods

Testing oral perception is commonly performed by trained assessors that assign relative scores to certain attributes. Other methods like tribology or rheology provide more absolute values of parameters that are not easily transformable to attributes of oral perception. This work is focused on versatile methods and correlation of results between them to calibrate panel studies and to derive the basis for further study, where tribology and rheology can replace or support the QDA panel approach.

Although the panel study involves a number of attributes, some of them have no obvious link to frictional data. For instance taste is determined by molecular composition, while texture depends very much on mechanical friction, viscosity and structure of the sample. This work focuses on the attributes describing texture and mouth-feel perception like *creamy*, *watery*, *soft*, *fat film*, and *slimy*.

Viscosity-QDA panel

Although the range of viscosity of the emulsions studied in this chapter is narrow, the viscosity increases systematically with an increasing fat concentration in milk samples. Initial increase, however, is very small. Figure 7.6 shows attribute scores (for different attributes perceptions) plotted against viscosity of different emulsions obtained at high shear rate. Below 1 % of fat no correlation is observed, and the data appear scattered. This might be due to the perception limit of about 1% fat content below which the sensory attributes show strong variation and no systematic trend. Only above that critical concentration a clear correlation is established. The correlation coefficient for presented attributes is well above significance level (see Table 7.2).

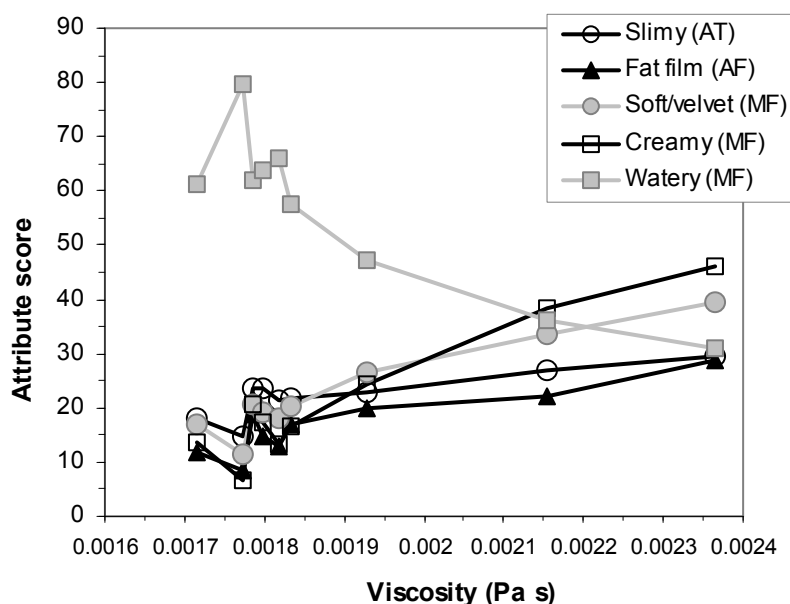


Figure 7.6 Different attribute scores plotted against viscosity (measured at high shear rate) of milk samples with different fat concentration.

Table 7.2 The correlation coefficient between sensory attributes and the friction coefficient and viscosity. The viscosity and friction coefficient of emulsions with different fat content was taken at high shear rate and 10 mm/s (with $W=1$ N), respectively. The significance level for studied population size and $\alpha=0.05$ is 0.666. In bold the watery attribute for Teflon disc is shown as the

Attributes	Viscosity (Pa.s)	Friction coefficient		
		silicone	neoprene	Teflon
Creamy (S/T)	0.93	-0.95	-0.929	-0.743
Creamy (MF)	0.949	-0.945	-0.944	-0.667
Soft/velvet (MF)	0.949	-0.957	-0.946	-0.705
Watery (MF)	-0.889	0.939	0.897	0.643
Fat film (AF)	0.885	-0.881	-0.891	-0.776
Slimy (AT)	0.81	-0.771	-0.812	-0.843

only one below the significance level.

Creamy and soft attributes show the best correlations where the relation with viscosity is very steep even in such a narrow viscosity range. The creamy and soft sensation becomes stronger with an increase of viscosity. It is remarkable that a minute change in viscosity can be clearly distinguished sensorically, given the fat concentration is above perception limit of about 1% fat concentration. It must be stressed and realized that viscosity and fat content correlate in a one to one manner according to the Einstein (Batchelor) equation. In other words in this respect fat content is synonymous to viscosity. Other attributes (slimy

and fat film after-feel) show slightly lower correlation. This indicates that fat film formation requires higher viscosity or fat concentration to obtain a higher score of sensory attribute. In addition film formation most likely determines the boundary lubrication properties and thus strong correlations can be expected (see the following section). The watery attribute shows negative correlation as expected. In this case the low fat content samples show variation as well due to mentioned above perception limit.

Friction-QDA panel

Friction data is obtained for a wide range of entrainment speeds. Therefore a specific speed needs to be chosen in order to determine the correlation coefficient. In this chapter four different speeds were selected from both the boundary and the mixed regime to evaluate correlations: 10, 50, 150, and 400 mm/s (data not shown). The highest correlations were expected at the lowest speeds, as they correspond to typical velocities in the oral environment ([1,5] and Chapter 1). Moreover, the friction depends on the type of the surface (rubber) used in the tribometer setup. The correlation analysis allows the determination of the most suitable oral surface analog among the three investigated rubbers (see also Chapter 6).

Figure 7.7 shows the friction coefficient measured at 10 mm/s for different milk samples as a function of fat content. Silicone and neoprene rubbers indicate a systematic friction decrease with an increasing fat concentration. This means that fat supports boundary film formation and provides better lubrication conditions. The data for neoprene rubber is shifted to higher values within respect to the silicone data, which results from significantly larger surface roughness. The third type of rubber, Teflon, shows almost no dependence of the friction coefficient on the fat concentration in the lubricating sample. This is a result most likely from the lipophobic nature of this surface. The boundary fat film cannot be formed on this surface and thus the friction coefficient remains constant regardless of the fat content in the lubricant. At higher speeds (data not shown, see Figure 7.1) silicone and neoprene rubbers show a much weaker dependence of the friction on the fat content as they are in the mixed regime; in those conditions the boundary film is of lower importance for the lubrication.

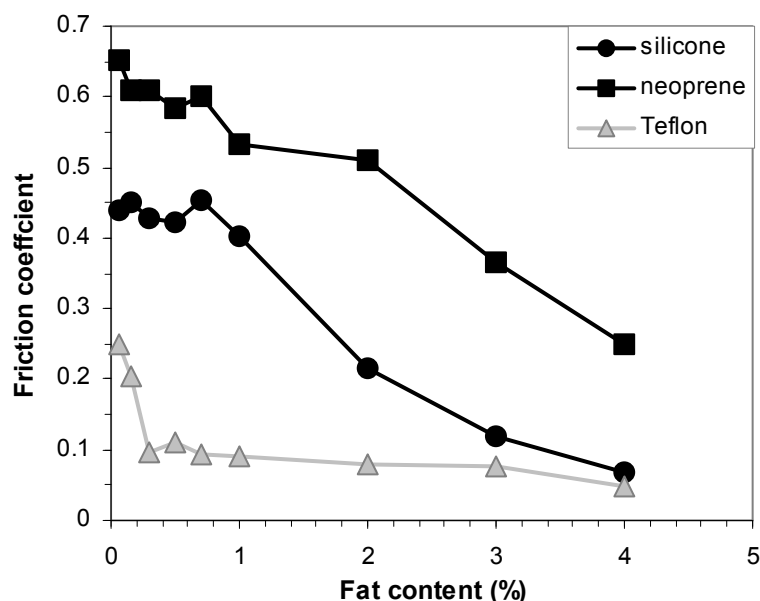


Figure 7.7 Friction coefficient as a function of fat content for a speed of 10 mm/s.

Figure 7.8 shows six different sensory attributes scores plotted against the friction coefficient for the various samples. Note two different creamy attributes that were determined for taste and for texture perceptions. Almost all presented attributes show negative correlation, except for the watery attribute. Fat film formation or creamy sensation implicates efficient lubrication in the boundary regime. Previous studies (e.g. [5,6,27]) showed that creaminess was associated with increase of the fat content in the product, which resulted in decreased friction and thus better lubrication properties of the product. Similarly to fat film and creamy attributes soft or slimy feeling could not occur when the lubrication was inefficient and friction coefficient was high. In such a case the perception is expected to be rough. The watery attribute, however, implies liquid lubricant that cannot adhere to the surface and thus cannot form a boundary film.

Although all attributes show a correlation with a physical property, the data did not show monotonic behavior. The friction coefficient decreased systematically with increasing fat content, but the attribute scores were scattered below a perception limit of about 1 % fat. This resulted in data variation at high friction coefficients (low fat content). In addition silicone and neoprene rubbers show very similar slopes but shifted in respect to each other. The neoprene rubber caused higher friction than silicone for the same samples. Interestingly, the Teflon showed an almost vertical slope indicating that the correlation may not be very good as different attribute scores resulted in a very similar friction coefficient.

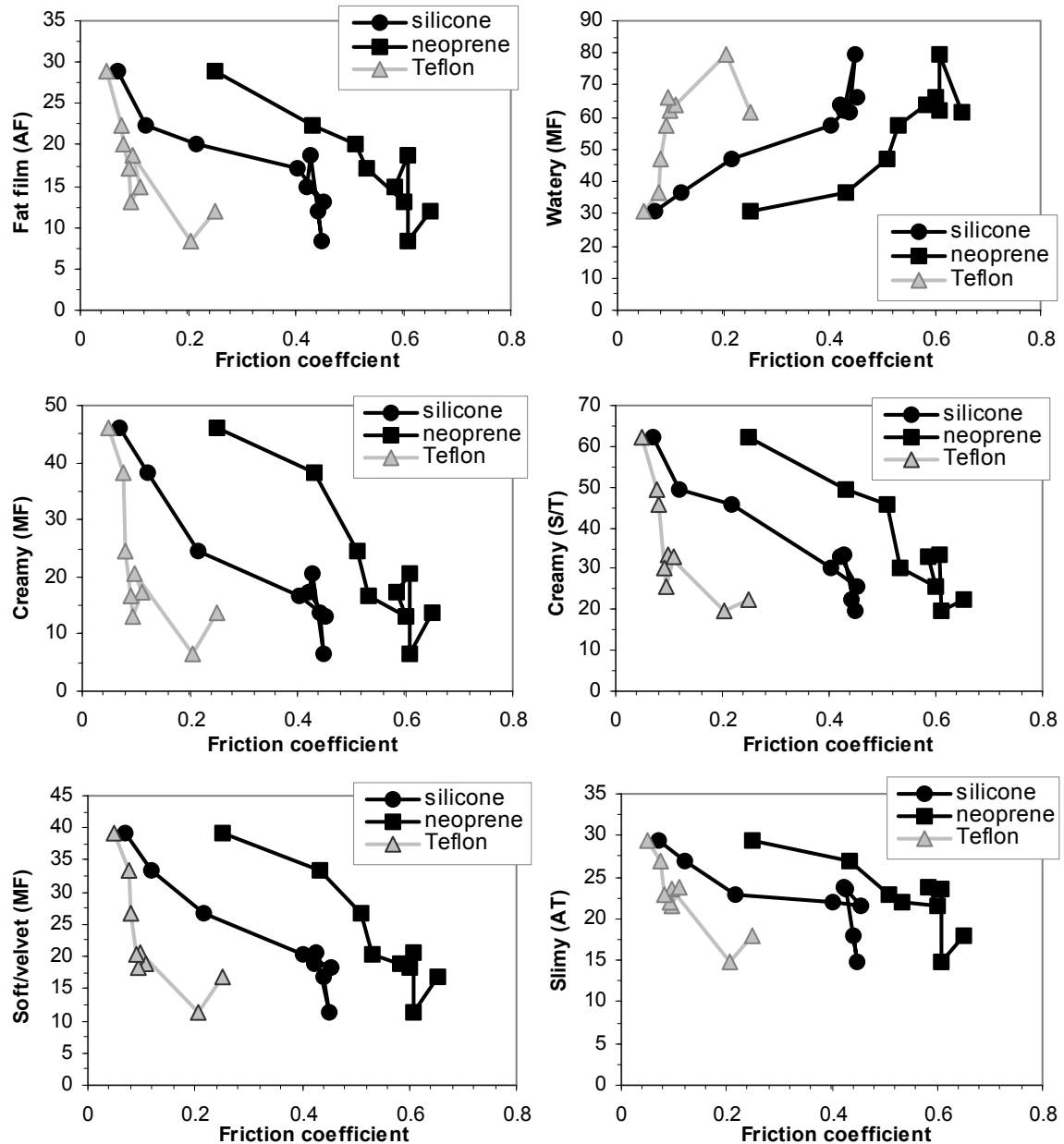


Figure 7.8 Different attributes as function of the friction coefficient at low speed (10 mm/s).

The correlation coefficients for relations presented in Figure 7.8 are summarized in Table 7.2. Data for silicone and neoprene was well above a significance level of 0.666. Only in the case of Teflon attribute watery is not significant and attribute creamy is at the significance level. This shows that a very good correlation was established between the sensory attributes and the friction coefficient. Besides fat film and slimy attributes silicone rubber shows a higher correlation coefficient and thus suggesting that this rubber may represent the oral environment better. In addition, neoprene rubber can undergo wearing process that changes the surface properties (see Chapter 6). Teflon shows the lowest

correlation coefficients for all attributes but slimy. Nevertheless significant correlation coefficients were obtained for all rubbers in almost all cases despite significant differences in material and surface properties of tested rubbers. This suggests that the friction data can be well related to the oral perception regardless of the applied setup.

Interestingly the choice of the speed at which the friction coefficient is selected for the correlation is of great importance. The oral processing occurs at speeds which range at about 10-50 mm/s (see Chapter 1). Therefore intuitively this would be the primary choice for the friction data selection. Indeed this range proved to be the best choice as the absolute value of the correlation coefficient increases with a decreasing speed. Figure 7.9 shows that result. This is expected as the speed observed in oral environment is of the order of 10-50 mm/s (see Chapter 1). For almost all attributes in the case of silicone the correlation coefficient remains significant (see dashed line in Figure 7.9) for all speeds. Only in the case of slimy the correlation becomes significant below 250 mm/s. In the case of neoprene the correlation was insignificant for friction coefficients taken at high speeds. The significance level was reached only below speeds of about 100 mm/s. Therefore the speed dependence of the correlation coefficient is much steeper for neoprene than for the silicone rubber. This shows that regardless of the rubber at low speeds the correlation is well established, while at high speeds it is not certain and surface properties may influence results. Interestingly, in the case of Teflon the correlation coefficient showed completely different behavior. It was increasing with the speed contrary to the other rubbers. Thus the best correlation was obtained at the highest speeds. Again in this case the surface and material characteristics are possible factors influencing the correlation between the friction coefficient and sensory attributes. Teflon is very hard and has very specific properties that make it a good theoretical study case. Results presented in this chapter show, however, that Teflon is not a good candidate for oral surface analog (see Chapter 6).

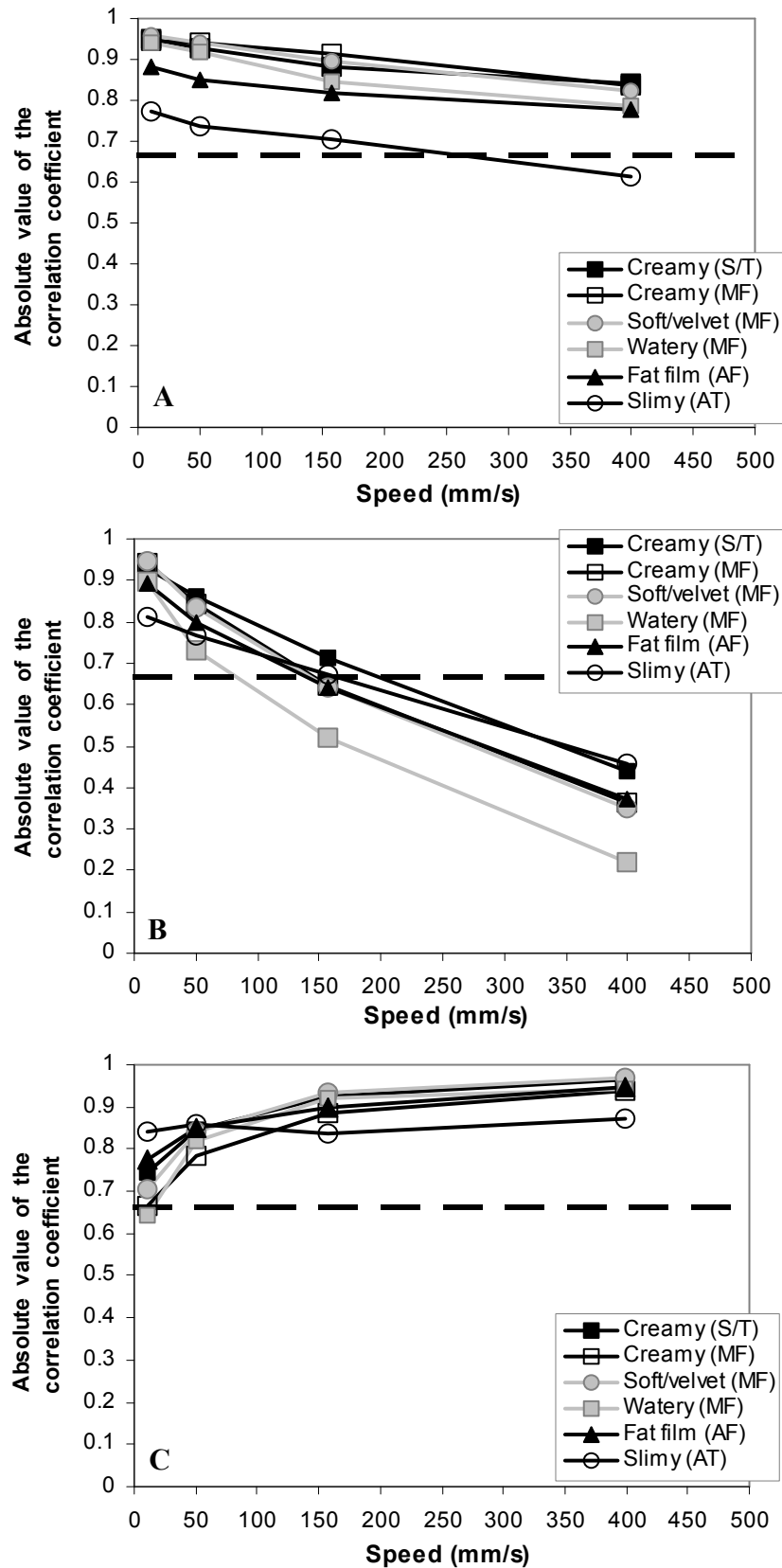


Figure 7.9 Correlation coefficient as a function of the entrainment speed. Dashed line indicates the significance limit for sample population presented in this chapter. Points above the dashed line are significant and points below are insignificant. Figures A, B and C correspond to friction coefficient data measured for silicone, neoprene, and Teflon, respectively.

7.4.3 Transition point

An interesting observation follows from evaluation of Figure 7.1. For silicone and neoprene rubbers friction curves at high speeds are similar for different fat content below certain threshold. In the case of silicone disc samples containing up to 3 % of fat show very similar friction curves above 300 mm/s. In fact, Stribeck curves for concentrations of 2% and 3% overlap above the entrainment speed of 350 mm/s. Higher concentrations, however, can be easily distinguished as their friction coefficients decrease with increasing fat content. For neoprene rubbers this effect is observable above 200 mm/s and up to 4% of the fat content. In this case samples containing 3% and 4% of fat also overlap, while higher concentrations show dependence of the friction coefficient on the fat content. This indicates similar lubrication characteristics of emulsions with fat concentration below some threshold at high speeds (mixed regime in this case). This might result from the entrainment of the bulk emulsion into the contact zone between two surfaces that have been already partly separated. High speed and shear disturb coalescent fat film and mix the fat droplets back into the emulsion. Therefore, the lubrication is governed by the bulk emulsion in all cases resulting in a similar friction coefficient.

Most likely the differences in threshold concentration of fat between silicone and neoprene rubbers are related to their differences in surface roughness. The rougher neoprene requires higher fat content to provide good lubrication as larger asperities result in more violent environment and thus easier distortion of the fat film. Consequently, for the neoprene rubber more fat is needed to discriminate the differences between low and high fat emulsions. For silicone rubber the threshold concentration is 4 %, whereas for rougher neoprene rubber this threshold is observed at higher oil concentration: 6.5 %. This effect might be due to either i) viscosity of the emulsion that is high enough to make a difference at these higher speeds or ii) a coalescence of the oil on the surfaces that is reversed at high speed and shear environment. An other explanation for the difference in threshold between silicone and neoprene might be their different hydrophobicity. As was shown in Chapter 2 and Chapter 6 the neoprene rubber showed more hydrophilic character than the silicone rubber. Therefore, the latter rubber has a more favorable surface for adhesion of the fat droplets, which would results in lower friction and lower fat threshold than neoprene. Most probably both the effect of the surface roughness and the hydrophobicity of the rubbers influenced the behavior of the studied emulsions. Although the latter parameter

probably is less important, as the differences between hydrophobicity of rubbers are minor (Chapter 2 and Chapter 6).

7.4.4 Coalescence of the emulsion droplets on the discs

The mean diameter of fat globules in homogenized milk was determined using a Mastersizer (data not shown) to be 0.27 μm . As shown in Figure 7.4 after the tribological measurements the coalescence of the emulsion droplets occurred on the rubber surfaces, e.g. in the case of silicone rubber the fat droplets size reached up to even 50 μm . This coalescence, most probably originated from the adhesion and subsequent spreading of the oil on the surface in the contact zone [11,12,14,25,26]. This is so called surface-induced coalescence. This process might be related to the affinity of the oil droplets to the surface, which leads to a cascade. Once the process has been initiated, more and more fat is deposited on the disc in the contact zone.

In the tribometer setup, where strong shear is applied, the emulsions in the contact zone are subjected to this shear in a very small gap. This might facilitate the surface-induced coalescence, and thus can be called shear-induced-surface coalescence. Moreover, deposition of the oil droplets might be facilitated by shear-induced coalescence in the bulk. However, the latter process is less probable as homogenized milk is known as a very stable emulsion. Surface-induced coalescence for a number of emulsions was observed, while no shear-induced coalescence in the bulk was observed [12]. Similarly, deposition and coalescence of the oil in the contact zone was observed [26] between two shearing surfaces, whereas no increase of the droplet size in the bulk of the emulsion was noted. In the current study the CLSM images of the oil for the neoprene disc (see Figure 7.4) seemed to form a structure, which is likely caused by the deposition of the emulsion droplets between large asperities inside the contact zone. It can be noticed that fat is deposited only in the contact zone, where shear occurred. The adhesion to the surface is very likely supported by large surface roughness (especially large cracks formed in the disc) that can physically entrap the emulsion. Similar observations were made by De Hoog et al. [26], where oil patches were visible only in the contact zone, after shearing of an oil in water emulsion between rubber ball and oscillating glass. A further study [13] showed that surface-induced coalescence of the emulsions lead to a decrease in oral friction measured in-vivo (human tongue) and ex-vivo (pig's tongue). This is in line with our study, even though different tribological methods and conditions were applied (e.g.

rotation instead of oscillation, different surfaces, speed, and load). Therefore we propose that in the oral environment the adhesion and coalescence of oil droplets between the papillae will lower the friction.

In the case of Teflon (Figure 7.4) fat seems to adopt large structures outside the track. Most likely the droplets were ejected from the contact zone where they underwent coalescence. As the surface is lipophobic fat cannot adhere to it.

7.5 Conclusions

In this chapter tribology, bulk rheology and sensory data were combined to evaluate possible correlations between them. In particular the panel study that provides relative scores of sensory attributes was complemented by tribological and rheological analysis of the samples to provide more absolute values of physical quantities. This work provides results that in future studies can aid to evaluate sensory perception of food products.

The sensory analysis of milk samples with different fat concentration showed that fat content below 1% cannot be distinguished and thus has little influence on the programming of the texture and/or taste of food products. Above this threshold concentration strong correlation is found between a number of attributes and the friction coefficient. This shows that tribology can be successfully used to evaluate the behavior and/or processing of food products in oral environments. The best correlations were obtained for low speeds that corresponded to the boundary lubrication regime. Although significant correlation was established also for the friction coefficient taken at higher speeds, material properties and surface characteristics seemed to have a stronger influence on the outcome of the analysis under those conditions.

Coalescence of fat droplets on the rubber discs occurred at low entrainment speed. This was attributed to the shear-surface-induced coalescence on the disc that had a significant effect on the lubrication properties of the emulsion enriched with milks. This effect was observed above a fat concentration of 1 % and 2 % for silicone and neoprene, respectively where a gradual decrease of the friction coefficients with fat content took place. At high speeds however, the coalescence was reversed (fused fat droplets were broken apart), hence an increase in friction.

Emulsions with fat content up to 3 % for silicone and 4 % for neoprene had similar lubrication properties at high speed. In spite of these high speeds, it is interesting to investigate further if these similarities can be translated to food developments.

Although, the choice of oral surface analog was shown to have a minor effect on correlation with sensory in the case of friction taken at low entrainment speeds, Teflon rubber showed very different behavior from other surfaces. This suggested that distinct characteristics of this rubber, in particular lipophobic nature and very smooth surface, disqualify Teflon as a potential industrial analog of oral surfaces. However its properties may be of great interests in other areas, where oral surfaces are not considered.

Finally, the data presented suggest that creaminess is perceived if the friction coefficient at low speed (below 100 mm/s) is below a threshold value (for silicone friction coefficient threshold ≤ 0.25). The creamy perception as well as lubrication properties of the milk increased gradually with fat content, above 1 % of fat for silicone rubber. This indicated a good correlation between creamy attributes and measured friction coefficient, a result that validates the use of tribology to better program specific sensory products in product development and reformulation.

Acknowledgement

The authors are grateful to Campina Innovation Company for a supply of the milk. We thank to Jan Klok for his help in obtaining the CLSM images, and Margreet Rippen for sensory evaluation. We thank Jan de Wit for the accurate determination of the content of fat, protein, and lactose in our emulsions.

Many thanks are directed to Els de Hoog and George van Aken for their inspiring discussion regarding the tribological data.

References

- 1 Van Aken, G.A., Vingerhoeds, M.H. & De Wijk, R.A. (in preparation for Food Hydrocolloids), Sensory perception of liquid emulsions: effect of oil viscosity and polysaccharides.
- 2 Kokini, J. L. (1987). The physical basis of liquid food texture and texture-taste interactions. *Journal of Food Engineering*, 6, 51-81.
- 3 Moore, P. B., Langley, K., Wilde, P. J., Fillery-Travis, A., Mela, D. J. (1998). Effect of emulsifier type on sensory properties of oil-in-water emulsions. *Journal of the Science of Food and Agriculture*, 76(3), 469-476.
- 4 Akhtar, M., Stenzel, J., Murray, B. S., Dickinson, E. (2005). Factors affecting the perception of creaminess of oil-in-water emulsions. *Food Hydrocolloids*, 19, 521-526.
- 5 Malone, M. E., Appelqvist, I. A. M., Norton, I. T. (2003). Oral behaviour of food hydrocolloids and emulsions. Part 1. Lubrication and deposition considerations. *Food Hydrocolloids*, 17(6), 763-773.

- 6 De Wijk, R. A., Prinz, J. F. (2005). The role of friction in perceived oral texture. *Food Quality and Preference*, 16(2), 121-129.
- 7 Lee, S., Heuberger, M., Rousset, P., Spencer, N. D. (2004). A Tribological model for chocolate in the mouth: General implications for slurry-lubricated hard/soft sliding counterfaces. *Tribology Letters*, 16(3), 239-249.
- 8 Luengo, G., Tsuchiya, M., Heuberger, M., Israelachvili, J. (1997). Thin film rheology and tribology of chocolate. *Journal of Food Science*, 62(4), 767-772.
- 9 Giasson, S., Israelachvili, J., Yoshizawa, H. (1997). Thin film morphology and tribology study of mayonnaise. *Journal of Food Science*, 62(4), 640-646.
- 10 Ranc, H., Servais, C., Chauvy, P. F., Debaud, S., Mischler, S. (2006). Effect of surface structure on frictional behaviour of a tongue/palate tribological system. *Tribology International*, 39(12), 1518-1526.
- 11 Dresselhuys, D.M., De Hoog, E. H. A, Cohen Stuart M. A., Vingerhoeds, M.H, Van Aken, G. A., "The occurrence of coalescence of emulsion droplets in relation to perception of fat" (2008) *Food Hydrocolloids*, 22(6), 1170-1183.
- 12 Dresselhuys, D.M., Klok, H. J., Cohen Stuart M. A., De Vries, R. J., Van Aken, G. A., De Hoog, E. H. A, "Tribology of o/w emulsions under mouth-like conditions: determinants of friction", (2007) *Food Biophysics*, 2(4), 158-171.
- 13 Dresselhuys, D.M, Cohen Stuart, M.A., Van Aken, G.A., Schipper, R.G., De Hoog E.H.A. "Fat retention at the tongue and the role of saliva: Adhesion and spreading of 'protein-poor' versus 'protein-rich' emulsions" (2008), *Journal of Colloid and Interface Science*, 321(1):21-9.
- 14 De Hoog, E. H. A., Prinz, J. F., Huntjens, L., Dresselhuys, D. M., van Aken, G. A. (2006). Lubrication of oral surfaces by food emulsions: the importance of surface characteristics. *Journal of Food Science*, 71(7), 337-341.
- 16 De Wijk, R.A., Prinz J.F. & Janssen A.M. (2006), Explaining perceived oral texture of starch-based custard desserts from standard and novel instrumental tests, *Food Hydrocolloids*, 20(1), 24-34.
- 17 De Wijk, R.A., Terpstra, M.E.J., Janssen, A.M., Prinz, J.F., "Perceived creaminess of semi-solid foods", (2006), *Trends in Food Science & Technology*, vol 17, issue 8, p 412-422.
- 18 Van Aken, G.A., Relating Food Microstructure to Sensory Quality, in: D.J. McClements (ed.) "Understanding and controlling the microstructure of complex foods" Woodhead Publishing Limited, year Cambridge, CB21 6AH, England
- 19 Stanley, N.L. and Taylor, L.J. (1993). Rheological basis of oral characteristics of fluid and semi-solid foods: A review. *Acta Psychologica* 84, 79-92.
- 20 Phillips, L.G., McGiff, M.L., Barbano, D.M. & Lawless, H.T. (1995), The influence of fat on the sensory properties, viscosity and color of lowfat milk, *J. Dairy Sci.*, 78, 1258-1266.
- 21 Pangborn, R. M, Bos, K.E.O. & Stern, J. S. (1985), Dietary fat intake and taste responses to fat in *milk* by under, normal. and overweight women. *Appetite* 6(25).
- 22 Van Aken, G.A., De Hoog, E. H. A., Nixdorf, R. R., Zoet, F.D., Vingerhoeds, M.H., Aspects of sensory perception of food emulsions thickened by polysaccharides, (2006) in Williams P. A. and Phillips G. O., *Gums and Stabilisers for the food industry*, Cambridge, The Royal Society of Chemistry. 13; *RSC special publication* 303:449-456.
- 23 Van Aken, G.A., M.H. Vingerhoeds, and E.H.A. De Hoog, (2005), Colloidal behaviour of food emulsions under oral conditions, in Dickinson, E., *Food Colloids* (2004): Interactions, Microstructure and Processing, The Royal Society of Chemistry: Cambridge. p. 356-366.
- 24 Kootstra, A.M.J., Holthuysen, N.T.E. & Mojet, J. (2007), Control of creaminess
- 25 Van Aken, G. A., Vingerhoeds, M.H, De Hoog, E. H. A., "Food colloids under oral conditions" (2007), *Current Opinion in Colloid & Interface Science*, 12, 251-262.
- 26 De Hoog, E. H. A., Dresselhuys, D.M., Van Aken, G. A., "Behaviour of food emulsions in thin films confined between two sliding surfaces" (2006), *Proc World Congr on Emulsions*.
- 27 De Wijk R.A. and Prinz, J.F. "Mechanisms underlying the role of friction in oral texture". *Journal of Texture Studies* 37, (2006) 413-427.

Chapter 8

Future prospects

8.1 This chapter

In this thesis mechanical processing of liquids and semi-solid food-related systems has been studied. In addition, the relation between experimentally measured friction and perceived sensory attributes was discussed. In order to obtain such relations, if any, one has to be in a good control of the experimental conditions and physically obtained friction data. Therefore a number of conditions was tested in the tribometer (e.g. different discs) with different physical parameters (e.g. load, speed, temperature) to provide the optimal experimental setup to obtain a good predictive measure for sensory attributes. The following parameters were investigated:

- The effect of the sliding to rolling ratio applied in the tribometer (MTM) with relation to a number of selected attributes.
- The influence of artificial saliva on lubrication properties of the dispersion.
- The effect of non-dissolved particles in the polysaccharide solution.
- The effect of size of the protein particles and aggregate dispersions on the film thickness in the MTM.
- The lubrication and rheological behavior of some commercial products.
- Programming sensory attributes based on physical parameters.

The lubrication and bulk rheological properties in this chapter were obtained according to the methods described in Chapter 1 unless stated otherwise.

8.2 The slide-to-roll-ratio in relation to sensory attributes

A preliminary study linking different relative motions between ring and disc (so called slide-to-roll-ratio) (SRR) in the tribometer with the sensory attributes was made. The effect of the SRR was shortly discussed in Chapter 2. However a different approach was chosen in this chapter by relating polysaccharides with different attribute scores (like sticky or slippery) to their lubrication properties. These attributes were selected due to their expected relation to the slide-to-roll-ratio. Therefore tribological measurements were all performed at low speeds for four different slide-to-roll-ratios. 0 % corresponds to the pure sliding motions where both speeds of the ring and disc are the same ($U_{disc} = U_{ring}$); 25 % where $U_{disc} = \frac{9}{7}U_{ring}$, 150 % where $U_{disc} = 7U_{ring}$, and 200 % which corresponds to the pure sliding motion with $U_{ring} = 0$. Here only two representative SRR are discussed

(i.e. 25 % and 150 %). The speed applied in the tribometer was kept low, only up to 35 mm/s, as in this case (different SRR) higher speeds would hide the possible relation between attribute and experimentally measured friction.

Figure 8.1 shows the stickiness and friction coefficient obtained at 25 and 150 % for four different dispersions. It appears that those two parameters correlate well, especially at low slide-to-roll-ratio, as decreased friction coefficients led to an increased stickiness attribute. Testing the stickiness attribute by the panelist was performed without rapid and strong sliding motion between tongue and palate. It seems thus reasonable that such a good correlation was obtained for lower sliding motion. At this point, however, the work is still at a preliminary stage and needs further investigation.

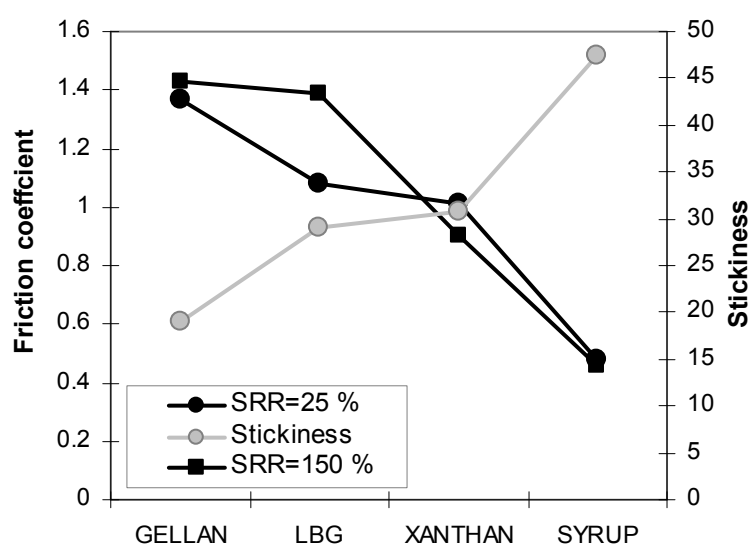


Figure 8.1 Friction coefficient for SRR 25 % (black circles) and 150 % (black squares) measured with the tribometer for four different dispersions and their stickiness perception (gray circles).

8.3 Artificial saliva study

Human saliva is a complex fluid consisting mainly of water, electrolytes, proteins and various enzymes [1]. Stress, vitamin deficiency, medication, smoking and even hormonal changes might influence the saliva composition, enzyme activity as well as the amount of the saliva production. Human saliva, once collected, needs careful handling as it is unstable. In this study, to eliminate these factors and to be in a good control of the system, the artificial saliva (based on pig mucins) is used as a “substitute” or model dispersion of

human saliva. Two commercial mouth-sprays are used in this work (BioXtra and Saliva Orthana). These mouth-sprays are generally used for individuals with dry mouth and were developed to restore the natural balance in the oral cavity. BioXtra contains oral enzymes and minerals, whereas Saliva Orthana is enzyme free with addition of (pig) mucin. Both dispersions contain electrolytes similar to these found in saliva.

Prior to tribological and rheological measurements the 9 % whey protein isolate (WPI) aggregate dispersion (WPI) was mixed with 7.5 % of artificial saliva. The bulk rheological properties of the dispersions were measured with a rheometer as described in Chapter 1 and were compared to pure water (Figure 8.2). Orthana mouth-spray had the lowest viscosity of all studied dispersions. Once added to the WPI-dispersion it lowers its viscosity (see Figure 8.2). The BioXtra shows a more viscous behavior which increased only slightly by addition of the protein aggregate dispersion. This is due to the low concentration of the saliva added to the WPI. Newtonian behavior at high shear rates was observed for most of the measured dispersions, except of the more viscous BioXtra.

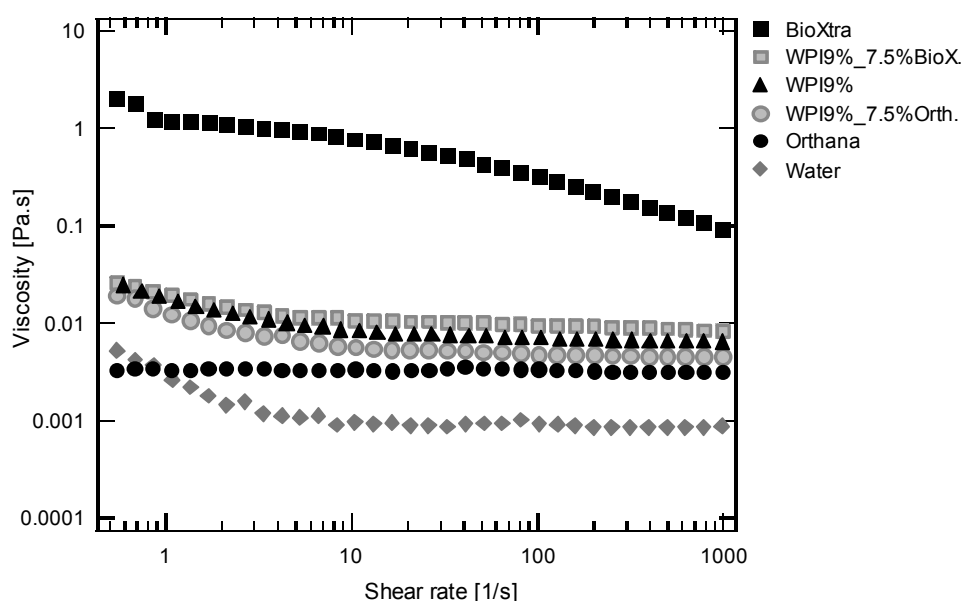


Figure 8.2 Viscosity measurements for protein aggregate dispersions and artificial saliva.

Lubrication properties of the dispersions were measured in the tribometer between a neoprene ring and silicone disc (Figure 8.3).

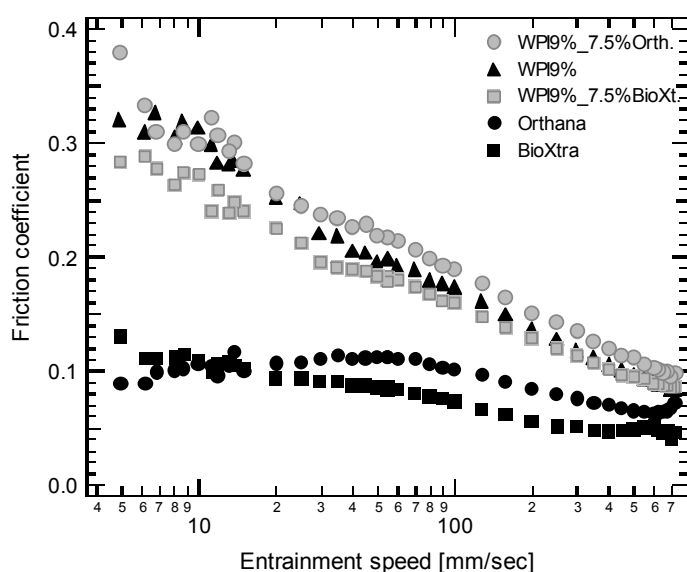


Figure 8.3 Tribological properties of the WPI protein aggregate dispersions mixed with artificial saliva.

The lubrication properties of the WPI mixed with two artificial saliva's are in line with the viscosity data (Figure 8.3). For these samples the occurrence of the mixed regime of lubrication only is observed (and no boundary regime). Therefore the friction coefficient is partly governed by the bulk rheological properties of the dispersion. Decrease of the friction coefficient for mixtures of WPI and BioXtra probably originated from the higher viscosity compared to protein alone (Figure 8.2). On the other hand, Orthana when added to WPI decreased its viscosity and so decreased the lubrication properties of the proteins. Very good lubrication properties of Orthana measured alone were observed. This is due to the adhesive interactions of mucin with the surface. Up to 100 mm/s the boundary regime of lubrication is visible for the Othana preparation. Recently it has been suggested that mucin facilitates lubrication between hydrophobic PDMS surfaces, which led to the reduction of friction in the boundary regime [2]. Yakubov et al. [2] suggested that for rough surfaces a viscous boundary lubrication occurs, so that the effective local viscosity of the adsorbed mucin acts as a viscous layer in between surfaces. BioXtra does not contain mucin, but the obtained friction coefficient is similar to the one measured for Othana. It seems that for this more viscous mouth-spray mixed lubrication occurred over the range of applied speeds.

The lubrication properties of the described dispersions were also measured on the disc surface only. Prior to the friction measurements the discs were pre-lubricated with 5 ml of saliva (data not shown). In the case of the BioXtra preparation, no differences were

observed between the pre-lubricated disc with saliva and mixture WPI-saliva system as presented above. This suggests that in this case the lubrication properties of the dispersions are governed by the WPI-aggregates and most likely mouth-spray Bioextra does not adsorb onto the surface. Better lubrication properties (compared to the one shown in Figure 8.3) were measured for Orthana when it was directly deposited onto the silicone disc before the tribological measurement. This again suggests that adsorption onto the surface of mucin as present in Orthana governs the lubrication properties, despite the relatively small concentrations used.

8.4 Non-dissolved particles in the polysaccharide dispersions

In Chapter 4 hydrocolloids well soluble in water were studied such as: LBG, pectin, xanthan, gellan and carrageenan. The presence of non-dissolved particles (often present in commercial products) in some of the biopolymers dispersions significantly affects their characteristics (e.g. sensory perception or instrumentally measured lubrication or rheological properties). Therefore in this section the influence of non-dissolved particles in polysaccharide dispersions (such as 0.57 % of guar and 0.48 % tara gum) was studied. Both these biopolymers are galactomanans and are extracted from plant seed. Guar gum is used as a binding agent and stabilizer in food, bread, cakes and pastries. Tara gum has applications nearly equivalent to guar gum. For further characteristics of guar gum (such as chemical composition) see reference [3].

This work was performed in collaboration with Unilever; measured friction and viscosity data were obtained at setups available at their research facilities. Tribology experiments were performed using the MTM with soft PDMS ball and disc contact, whereas viscosity was measured in a rheometer with parallel plate geometry reaching very high shear rates $\sim 10^5 \text{ s}^{-1}$. This allowed us to make a direct link with polysaccharide systems described in Chapter 4.

8.4.1 Microscopic images

Contrary to the dispersions described in Chapter 4, guar and tara gum dispersions showed in macroscopic images the presence of non-dissolved particles, even after a prolonged heating procedure. The microscopic images were obtained with stereomicroscopy (for the description of this technique see Chapter 2 and Chapter 6 in this thesis). Figure 8.4 A and Figure 8.4 B show images taken at 40x magnification of guar and tara gum dispersions,

respectively. It appears that for both dispersions non-dissolved particles can be observed, that tend to agglomerate, and that are locally surrounded by a gel network. This makes large irregular cluster of particles in the polysaccharide dispersions. A schematic drawing of such a structure is presented in Figure 8.4 C. The sizes of the non-dissolved particles for guar gum vary between 15 and 35 μm , whereas for tara gum they are between 13 and 31 μm . In the latter sample more regular (round) shaped particles are visible compared to guar gum, where particles of different shapes (both round and elongated) are present. It can be noticed that tara gum particles tend to accumulate into larger clusters compared to guar gum. Consequently, it appears that guar gum has less particles compared to tara gum. The size of a typical tara cluster varies between the 120 to 300 μm and between 60 to 270 μm for the guar sample. Moreover the microscopy images show that non-dissolved particles in tara dispersions are packed densely in clusters and are surrounded most probably with a thin gel layer. In the case of guar, the clusters tend to be smaller with fewer particles surrounded by extended gel networks.

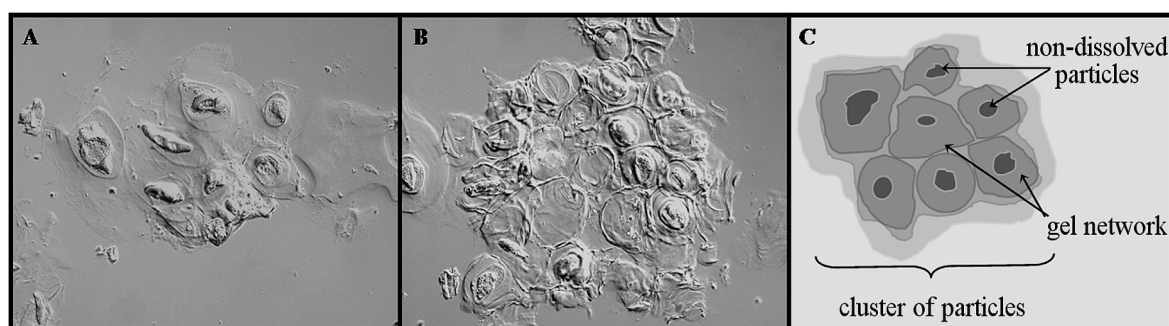


Figure 8.4 Microscopy images obtained for not fully dissolved dispersions of (A): guar gum, and (B): tara gum. (C): Schematic representation of the clusters particles in the polysaccharide dispersion.

8.4.2 Rheological and tribological properties of the polysaccharide dispersions

The non-dissolved particles might easily be trapped in surface asperities of the discs during the tribological measurements and thereby interfere with the measured friction. Additionally, they can be confined under shear in both the tribometer (between the two rotating elements) and rheometer, due to the applied narrow gap geometry.

The flow curves of the polysaccharide dispersions measured with parallel plate geometry are shown in Figure 8.5. As mentioned in Chapter 4, the apparent viscosity was obtained as a function of shear rate using two different gap heights: 30 and 50 microns. The

viscosity data shown in Chapter 4 (Figure 4.1) are plotted for a 50 micron gap only. In this chapter we show the difference between both gap heights. Clusters larger than the gap are squeezed and possibly broken into individual particles.

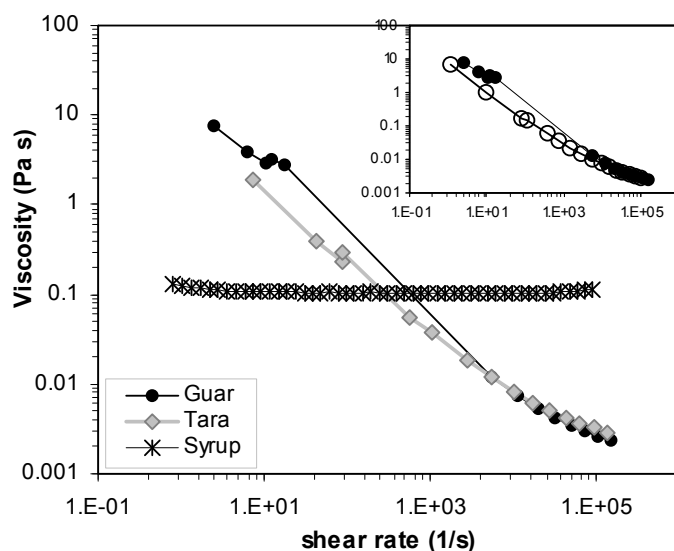


Figure 8.5 The shear and viscosity data were corrected for a gap error of $\varepsilon = 9.5\mu\text{m}$. Flow curve of 0.57 % guar and 0.48 % tara gum dispersion and 97% corn syrup at 25°C measured with parallel-plate geometry at gap height of 30 μm . , Inset: Flow curve for guar gum dispersion at two different gap heights: 30 and 50 μm closed and open symbols respectively

In Figure 8.5 , guar and tara gum dispersions show non-Newtonian behavior (viscosity decreased with shear rate) just like the polysaccharides discussed in Chapter 4. Figure 8.5 shows that guar and tara gum dispersions show even stronger shear-thinning effect than that of the xanthan dispersion (the most shear thinning polysaccharide used in Chapter 4). The viscosity decrease with the shear rate is steeper for guar gum, which might be related to the presence of particles of slightly larger size than in the case of tara gum. The effect of particle size for the narrow gap viscosity measurements were investigated by Davies and Stokes [4]. They found that confinement influences the rheological properties of suspensions and structured fluids when the gap is smaller than about five times the average characteristic dimension of the microstructure. The inset in Figure 8.5 shows guar gum viscosity measurements for the two gap sizes. Although the gap height in both cases is smaller than five times the average size of guar particles, a jamming effect seems to be absent. Similar result was obtained for the tara gum dispersion. Moreover, the rheological measurement indicates a decrease of viscosity with increasing gap size (see inset in Figure 8.5). This may result from a depletion effect, where particles are concentrated in the

central region between two plates and depleted in the vicinity of surfaces. This leads to a slipping effect and consequently an underestimation of the measured viscosity.

8.4.3 Behavior of the guar and tara gum dispersions under pressure in the tribometer

In this section the influence of microscopic particles on the friction force is discussed under different applied pressures (loads) in the tribometer and presented in Figure 8.6 . Both smooth and rough PDMS disc are used.

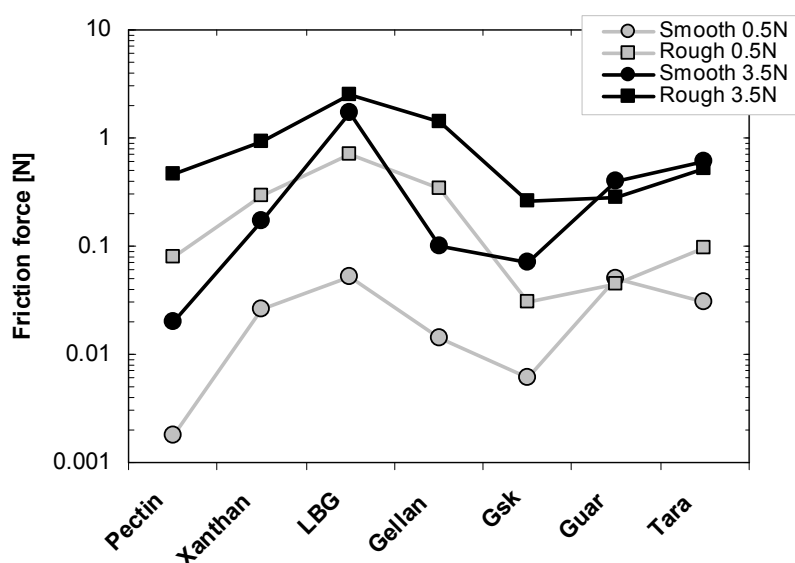


Figure 8.6 Friction force vs. polysaccharide measured at smooth (circle symbol) and rough (squares symbol) PDMS disc. Grey color: Load= 0.5 N; Black color: Load= 3.5 N. Entrainment speed: 5 mm/s.

Systematic differences between rough and smooth surfaces seem to indicate that the lubrication of the two types of surface is independent of the applied polysaccharides. It is mainly due to surface effects. A similar result is obtained for both low and high applied normal loads. In the latter case the LBG exhibits a much smaller difference between the two surfaces. This sample has a comparable friction force to water (data not shown) with an exception of the smooth surface at low load. Therefore, its lubrication properties are manifested only at small normal loads and smooth surfaces. Otherwise the lubrication is poor and comparable to the water case. A different behavior is observed for guar and tara gum. As these samples are characterized by the presence of microscopic (non-dissolved) particles in their dispersions this will affect the friction by filling the “valleys”/irregularities of the PDMS. At high loads the difference between the smooth and the rough surfaces is marginal. Depending on the size of the particles asperities in the

rough disc may be partially or fully filled, lowering the effect of irregularities of the surface. For both tara and guar gum the clusters of the particles most probably influence their frictional behavior. The aggregates are squeezed in the contact zone between two rotating surfaces. Possible destruction of the cluster under the pressure applied in the MTM might lead to a separation of the particles and gel network surrounding them. In the case of a low applied load no effect of the surface roughness is observed for the guar dispersion, whereas a small noticeable difference is visible for tara gum dispersions (Figure 8.6). This might be related to the stability of the clusters (they can be easily fragmented at high load and can survive at low load) or with the fact that under applied pressure different size distribution and type of the particles (both gel fragments and particles of different size) is produced. In the case of guar gum the clusters might be easily broken into the smaller parts due to the extended gel network and govern the lubrication properties at both surfaces.

In this paragraph the importance of the non-dissolved particles in the dispersion is highlighted. The lubrication properties of a product is a complex system that is related to the adsorption properties onto the disc (e.g. polymer–surface interactions, adhered layer of polymers), the bulk rheological properties (e.g. viscosity) as well as the particles present in dispersion.

8.5 Influence of particles on film formation

8.5.1 The elastohydrodynamic theory approach

A good lubricant is one that can efficiently separate two rubbing surfaces. In the boundary regime asperities overlap leading to high friction. In the mixed regime the surfaces are supported not only by their asperities but also by pressure of the lubricant enclosed in the contact zone. The elastohydrodynamic lubrication regime starts when the surfaces are fully pressure supported. Depending on bulk properties of the lubricant, load and entrainment speed the film separating surfaces has a thickness h_c given by equation 1.3 as described in Chapter 1. This equation was given by Esfahanian & Hamrock [5] for a ball-on-disc contact and is approximately 4/3 the minimum film thickness. The viscosity of non-Newtonian fluids changes with shear rate and thus depends on the applied entrainment speed. That relation can very well be described by a power-law and can be determined empirically by fitting $\eta = a\dot{\gamma}^b$ to the viscosity curve. In addition the shear rate

can be expressed as $\gamma = \frac{U}{h_c}$. Substituting these relations to equation 1.3 in Chapter 1, the film thickness as a function of entrainment speed alone is:

$$h_c = U^{1-\frac{0.34}{1+0.66b}} B^{\frac{1}{1+0.66b}} a^{\frac{0.66}{1+0.66b}} \quad (8.1)$$

$$\text{where: } B = 3.2R^{0.76}W^{-0.22}E^{*-0.45} \quad (8.2)$$

In the case of particles added to a dispersion the film thickness is affected directly for example by the presence of beads but also indirectly by changing the viscosity. Thus the film thickness can be expected to be:

$$\max(h_c, d), \quad (8.3)$$

where d is the particle size. If the dispersion cannot form a sufficiently thick film the lubrication may remain in the mixed or boundary regime at speeds where the hydrodynamic behavior is expected.

8.5.2 Modeling of the film thickness

The ability to separate rubbing surfaces determines at what speed dispersion can enter the hydrodynamic lubrication regime. Particles present in a dispersion can have a twofold effect. Depending on the environment they can help separating surfaces or they might lower friction by introducing rolling motion. In some situations, however, the particles can effectively enhance the surface roughness by e.g. locking in asperities. In addition, very high pressure in the contact between the particles and surfaces can induce additional roughness by pushing beads into the surfaces.

As the effect of particles on friction can be significant it is crucial to determine the film thickness to assess the possible influence of particles. Once the film is thicker than the particle size and surface roughness, the hydrodynamic regime is expected to start. Otherwise mixed or even boundary lubrication dominates the friction.

Firstly, the effect of the protein beads on the film thickness of the polysaccharide dispersion will be discussed. The characteristics, lubrication and rheological properties of these protein gel particles were elaborated in Chapter 5. Secondly, the influence of protein

aggregate dispersions on film formation will be presented. The effect of these biopolymers on measured friction and viscosity was partly already discussed in Chapter 2.

Xanthan gum

Xanthan shows good lubrication properties but it seems to form a rather thin film compared to other polysaccharides. At the highest considered speeds the film thickness is lower than the size of the smallest particles encountered (see Figure 8.7) and thus the lubrication is expected to be in the boundary or mixed regime. This is likely related to the strong shear thinning effect of xanthan that results in low viscosity at high speeds.

Xanthan dispersions without particles show that the film thickness remains below 1 micron for speeds below about 20 mm/s and go up to about 3 microns for speeds of about 500 mm/s. This is a relatively low thickness especially for rough surfaces with asperity size above a few microns.

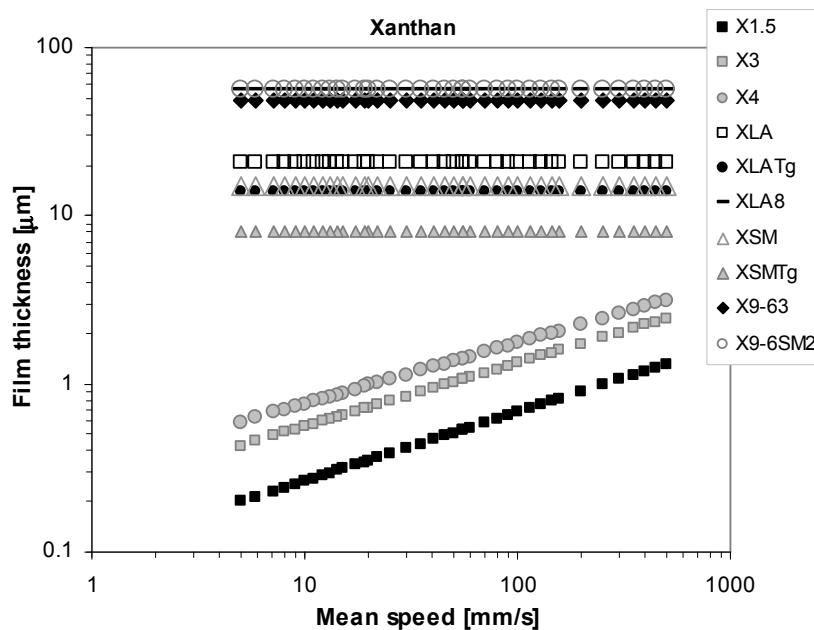


Figure 8.7 Film thickness of xanthan with different concentrations and protein particles obtained with equation 8.3.

Locust bean gum (LBG)

LBG is also characterized by the formation of a rather thin film in the contact zone. The thickness increases from about 1 micron at speeds below 10 mm/s up to about 5 microns at 500 mm/s. Therefore, even the smallest particles (8 microns in size) must dominate the lubrication in these dispersions, once they become entrapped in the contact zone. The Stribeck curve within the above range of entrainment speeds remains in the boundary or

mixed regime of lubrication. Figure 8.8 indicates that LBG dispersions without particles form films of thickness below 10 microns. When particles are introduced into the dispersion, the separation of the two surfaces is dominated by the beads. However, the film thickness approaches the particles size and thus slightly higher speeds may lead to a different picture, where the lubrication enters the hydrodynamic regime.

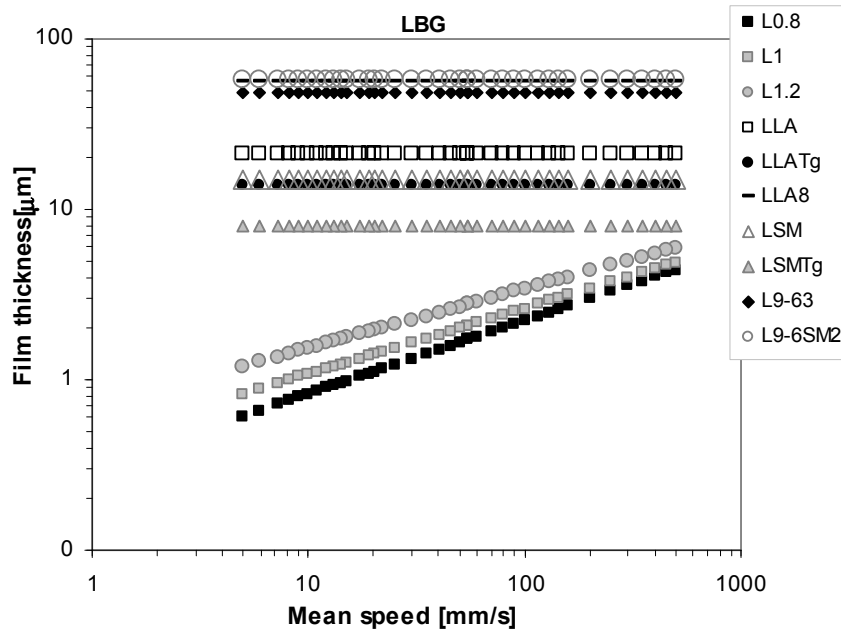


Figure 8.8 Film thickness of LBG with different concentrations and protein particles.

Pectin

The third polysaccharide (pectin) forms thicker films therewith exceeding particles size. Low speeds lead to a thin film of a few microns, the thickness increases up to about 40 microns at a speed of 500 mm/s. This is considerably larger than the smallest particles observed. Thus for these dispersions friction in the mixed or even hydrodynamic regime might be possible to observe for speeds above 200 mm/s. Figure 8.9 shows that the largest particles (swollen beads and gels) still dominate the surface separation and thus the lubrication remains in the boundary or mixed regime. This illustrates that pectin is characterized by a very good film formation ability and must be a very good lubricant. Even in the presence of relatively large asperities or particles it is expected to provide a thick films that at least partially supports the load and lowers the friction force.

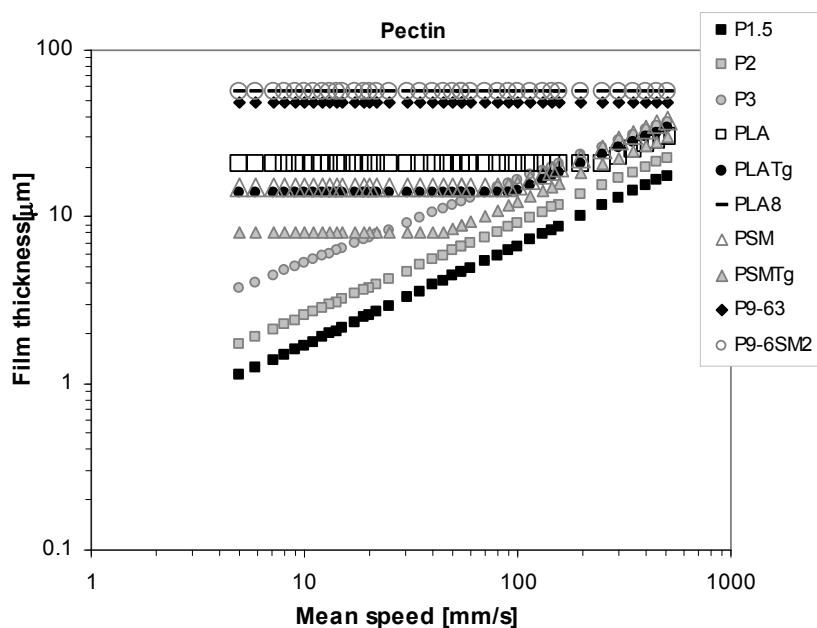


Figure 8.9 Film thickness of pectin with different concentrations and protein particles.

Protein aggregate dispersions

Protein aggregate dispersions form thin films, as shown in Figure 8.10. For lower concentration (2 % for ovalbumin and 3 % for WPI) the film is thinner than in the case of xanthan. It remains below 1 micron for speeds in the entire measured range (5 – 500 mm/s) and drop even below 0.1 micron thickness for speeds below about 10 mm/s (see Figure 8.10). The film thickness for higher concentrations is only about a factor of 3 thicker.

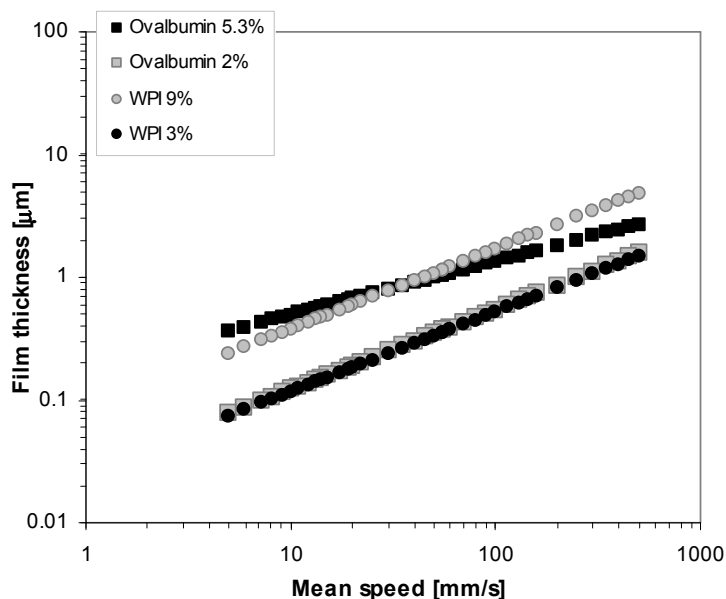


Figure 8.10 Film thickness of protein aggregate dispersions with different concentrations.

Protein particles are in most cases smaller than the film thickness. WPI particles are between 30 and 70 nm in size. Ovalbumin particles have a size comparable with exception of the highest concentration of 5.3% where particles are 0.7 micron in size. These aggregates are highly elongated (fibrillar) and if present in the contact zone they could adopt a preferred orientation parallel to the surface. In that way they are not able to dominate the separation of the surfaces.

8.6 Lubrication and bulk rheological properties of commercial dairy products

The purpose of this study was to investigate how large differences can be experimentally measured between products commonly found in the market. Figure 8.11 and Figure 8.12 show the bulk rheological and lubrication properties of different dairy products, respectively (milks, yoghurts and custards with different fat content). For comparison Newtonian solutions, such as water and olive oil are shown as well. The lowest viscosity corresponds to water which also gave the poorest lubrication properties compared to the other samples. Figure 8.11 shows that viscosity of skimmed milk ($\sim 0\%$ fat), compared to water, is higher by a factor of two. However, the friction coefficient differs only by about 30%. On the other hand, comparable lubrication properties (Figure 8.12) were observed for the full fat yoghurt ($\sim 3\%$ of fat), cream ($\sim 35\%$ of fat), custards ($\sim 2.6\%$ of fat) and olive oil. Although these products have different rheological properties, a friction coefficient of around 0.03 was measured below 200 mm/s. Low fat custards ($\sim 0\%$ of fat) were shown to have a high viscosity as the one obtained for full fat yoghurt and custard. Low fat custard shows high friction in the boundary and mixed regime whereas full fat custards exhibit a much lower boundary regime that extends up to 200 mm/s. As discussed in Chapter 7 the coalescence of the fat on the disc governs the lubrication properties of the product. The boundary lubrication shows the strongest dependence on fat content. Full fat products provide better lubrication. In addition viscosity seems to play a role as viscous samples may easier form the boundary film.

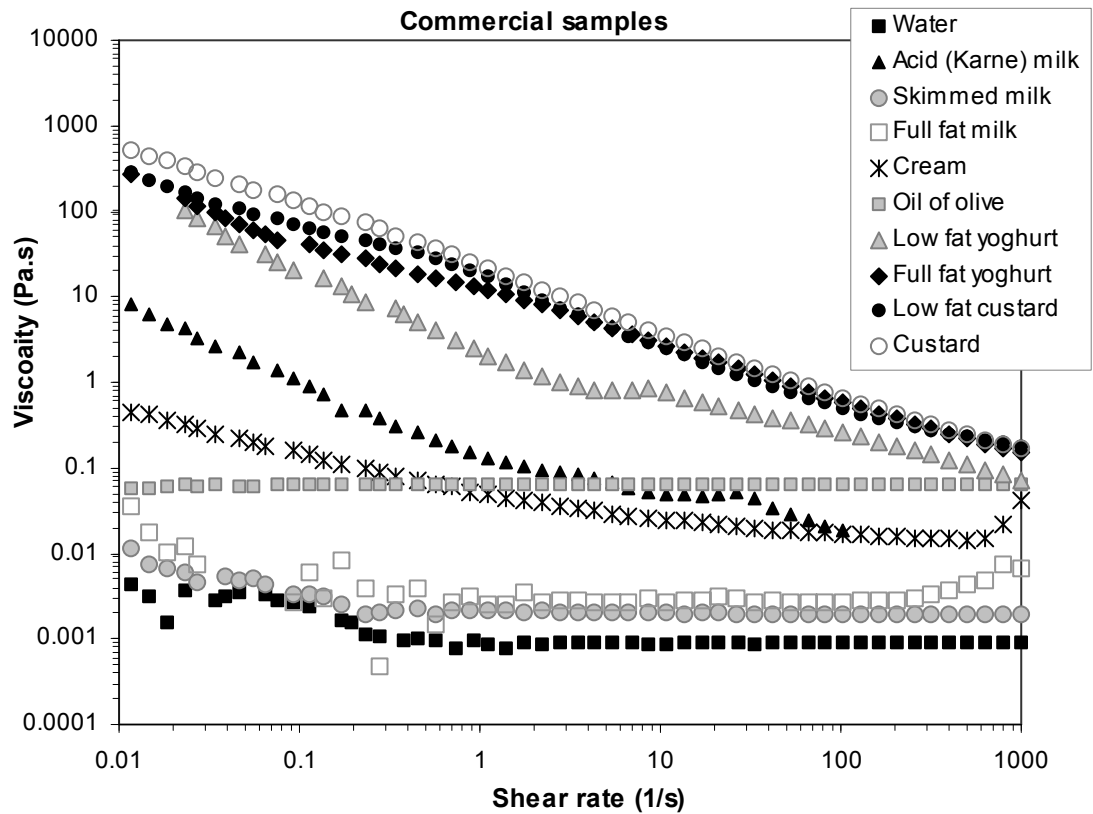


Figure 8.11 Apparent viscosity of the commercial dairy products, $T=30$ C. For comparison water and olive oil are presented as well.

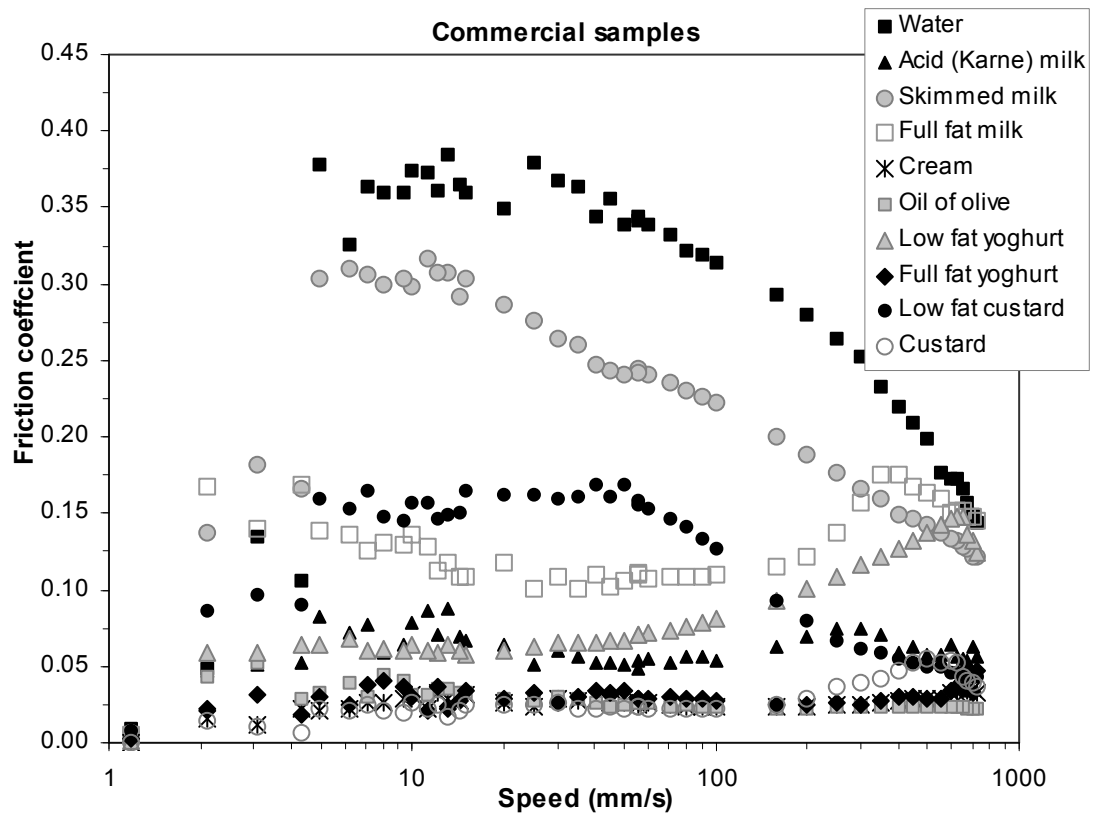


Figure 8.12 Friction coefficient of commercial dairy products. $SRR=50\%$, $W=5N$, $T=30$. For comparison water and olive oil are presented as well.

8.7 Programming sensory attributes based on physical parameters.

In this thesis food products are studied using multiple methods and covering a wide parameter space. The soft-soft contact has been studied for a number of different rubber surfaces with individual material properties like elasticity and surface roughness. As expected the best results in relating the sensory attributes to physical counterparts were obtained for silicone discs that are characterized by surface properties that resemble the oral environment the most, i.e. surface roughness, elasticity, wearing. Neoprene underwent significant wearing that strongly modified the surface during the measurement, while Teflon was characterized by very low elasticity and minimal surface roughness. Although correlation between sensory attributes and physical quantities was established on all surfaces, the best results were obtained for silicone. As the oral processing occurs at speeds between about 10-50 mm/s this speed range was found to be the most appropriate. In Chapter 7 it was shown that correlation between the sensory attributes and lubrication properties increases with decreasing speed.

References

- 1 Van Aken, G. A., Vingerhoeds, M.H, De Hoog, E. H. A., (2007), *Current Opinion in Colloid & Interface Science*, "Food colloids under oral conditions", 12, 251-262.
- 2 Yakubov G. E., McColl J., Bongaerts, J. H. H., & Ramsden J. J. (2009), *Langmuir*, "Viscous Boundary Lubrication of Hydrophobic Surfaces by Mucin," 25, 2313-2321
- 3 S. de Jong, F. van de Velde, (2007), *Food Hydrocolloids*, 21, 1172-1187.
- 4 Davies, G.A. & Stokes, J.R. (2008) *J. Non-Newtonian Fluid Mech.*, 148:73-87
- 5 Esfahanian M. & Hamrock, B.J. (1991), *Trib. Trans.*, Fluid-film lubrication regimes revisited, 34, 628.

Chapter 9

Concluding remarks and summary

9.1 Physical model

The broad and multidisciplinary study presented in this thesis allows to establish correlations between physical quantities obtained by different experimental methods. Tribology and bulk rheology are complemented by adhesion studies using Quartz Crystal Microbalance Dissipation and Surface Plasmon Resonance (see Chapter 4). These methods provide quantitative physical description of processes that are involved in oral food processing. In addition, Quantitative Descriptive Analysis is performed with panelists to quantify sensory attributes like e.g. slippery, creamy or filmy. In Chapter 5 and Chapter 7 correlations were established between these sensory attributes and physical quantities. Here, simple qualitative and quantitative models are formulated that describe sensory perception of food in terms of physical processes.

A number of correlations has been established between the friction coefficient or viscosity and sensory attribute scores, but some relations involve an interrelation between multiple quantities making the derivation of a model very complex. Therefore, a more conceptual model is presented first (see Figure 9.1). It shows which physical properties are relevant for texture, and how they must be adjusted in order to modify a sensory attribute to obtain a desired effect. For instance, the filmy perception of a product can be enhanced by increasing its viscosity. In addition, the friction coefficient is also well correlated with this attribute, meaning that enhancing its boundary lubrication properties will result in more filmy perception. This, however, results from the fact that boundary film formation is a feature of a good lubricant. Therefore, it is more likely that adhesive properties like polarity of the sample should be adjusted. This will further affect the filmy perception and lubrication characteristic of a product. Similarly, the powdery perception can be programmed by adjustment of added particles in the product. Increasing size of particles results in an increasing powdery perception. On the other hand, if large particles in the product cause unwanted powdery feeling, their hardness can be adjusted. Decreasing hardness of particles (even large ones) leads to a decrease of powdery perception, while small but hard particle can still provide powdery feeling. Therefore, in some cases there are a few ways to obtain the desired effect. This is very important, since physical quantities can affect multiple attributes, as well as attributes can influence or even mask each other (c.f. Chapter 5).

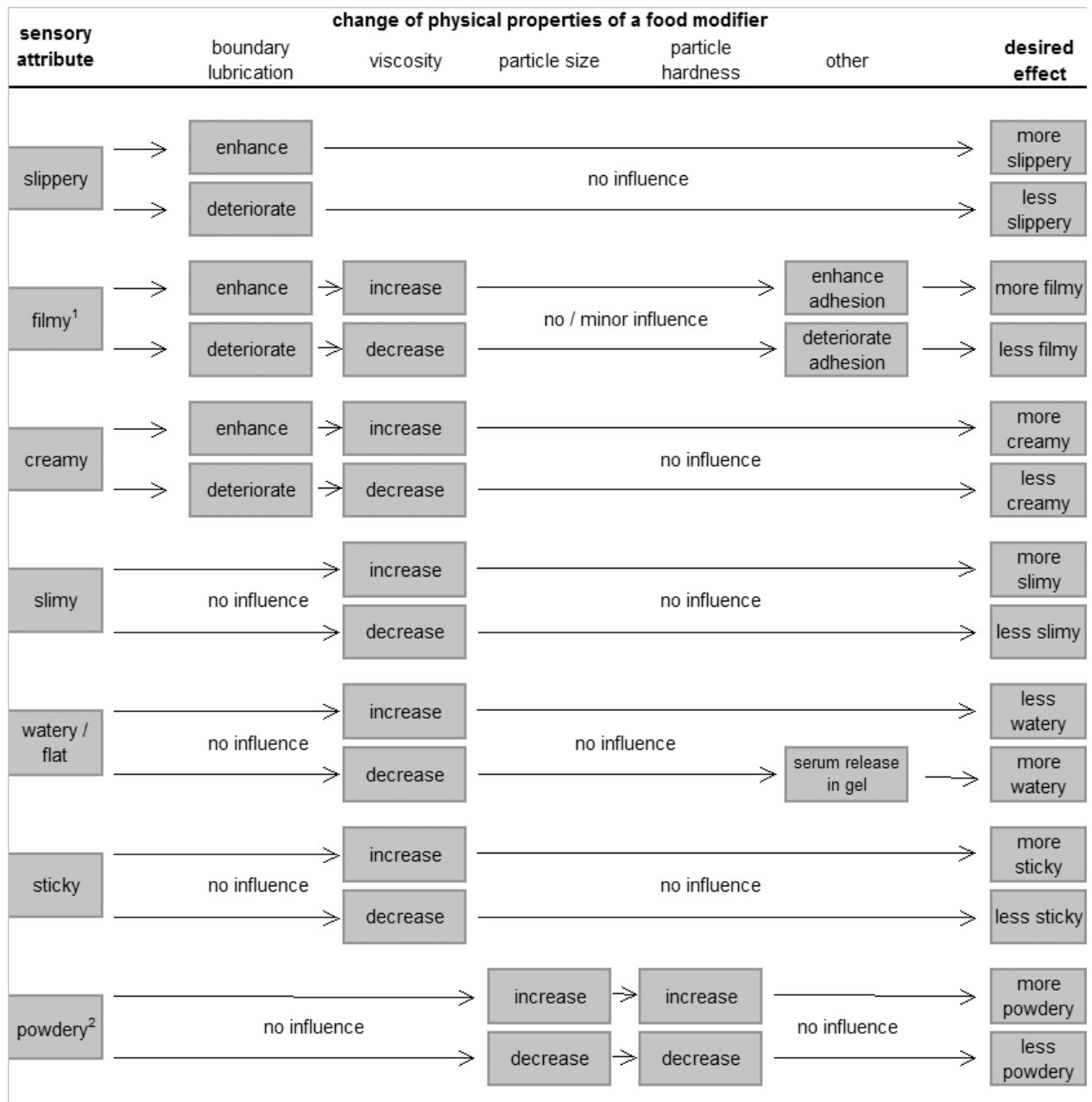


Figure 9.1 Conceptual model of programming sensory attributes by affecting physical quantities. The desired effect for a sensory attribute (last column) is obtained by modification of one or a combination of several physical properties of the product (middle columns).

¹The lubrication is affected by a modification of adhesion. Therefore it shows a correlation with the filmy attribute although the main effect is reached by changing adhesion properties.

²In the case of powdery attribute the size and hardness work against each other. This effect still requires additional study to confirm the hardness dependence.

9.2 Quantitative models

Most relations between sensory attributes and physical quantities are complex and show dependence on multiple parameters, some of them appear to be more straightforward. Quantitative models can be formulated for such cases.

Figure 9.2 shows that slippery and slimy attributes depend on only one quantity each: boundary lubrication and viscosity, respectively. The slippery attribute is intuitively related to lubrication. The more lubricious the product is the more slippery it is expected to be. This behavior is reflected in the tribological data. Figure 9.2 shows the slippery attribute score plotted against the friction coefficient (at 50 mm/s) obtained for over 30 different samples. Indeed, regardless of the presence of particles in a product and its viscosity, the slippery score A follows a power-law dependence on friction coefficient μ

$$A = \xi \mu^q \quad (9.1)$$

where $q = -0.24$ is the slope of the power-law and ξ is a vertical shift. Note that the attribute score is a relative measure and only the slope q carries valuable information. The dependence is rather shallow and thus, to lower the slippery by half, the friction coefficient must be increased almost 18 times.

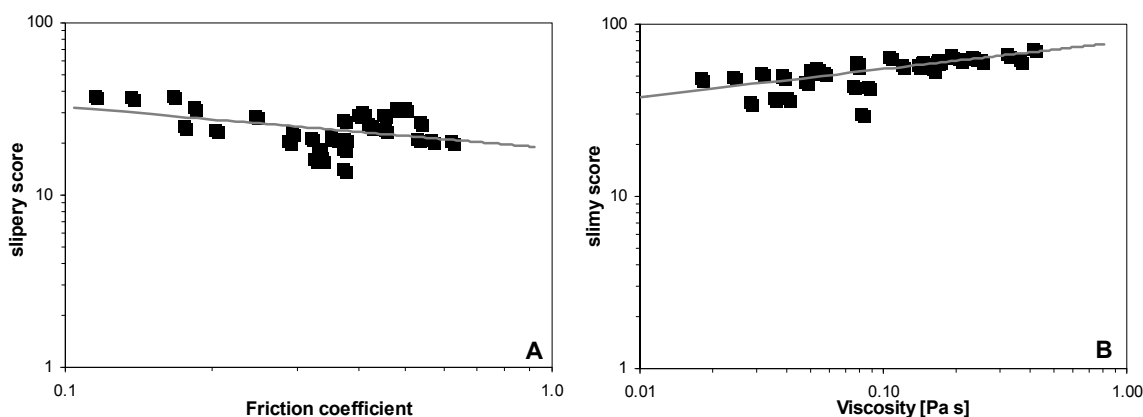


Figure 9.2 Least square fits to slippery attribute – friction (A) and slimy attribute – viscosity (B) data. Squares represent the measured data, while the solid line is the fitted power-law function.

A similar model was obtained for the slimy attribute. The viscosity is the only quantity that influences this attribute. Figure 9.2b shows the slimy attribute as a function of viscosity obtained for many samples. In this case the power-law function was fitted to the slimy-viscosity data. The slope is also shallow ($q = 0.16$). Thus to increase sliminess by a factor of 2 the viscosity must be lowered over 75 times.

An interesting relation was also obtained for the creamy attribute. In this case both viscosity and friction influence the perception and the viscosity variation in the studied sample is relatively small. Mainly the contribution of the lubrication properties needs to be taken into account. Figure 9.3 shows the creamy attribute as a function of the friction coefficient measured for emulsions with various fat content. The number of samples is limited, but the correlation is significant (c.f. Chapter 7). In this case the power-law slope is much steeper: $q=-0.77$. This shows that the creamy perception can be also controlled by modifying the lubrication properties of the product. Note that this relation is obtained with viscosity kept approximately constant. Although the contribution from the bulk rheology still needs to be revealed, the influence on the presented relation can be discussed qualitatively. Van Aken et al [1] showed that the creamy perception indicates positive correlation with viscosity meaning that increasing viscosity results in stronger perception of creaminess. In addition the components which increase viscosity are usually responsible for improving the lubrication as well, e.g. increase of polysaccharide concentration (note that viscosity itself has direct effect on friction only in the mixed and the hydrodynamic regimes of lubrication). Therefore, the fitted slope of $q=-0.77$ is expected to become steeper when the viscosity of a product remains a free parameter and can be increased.

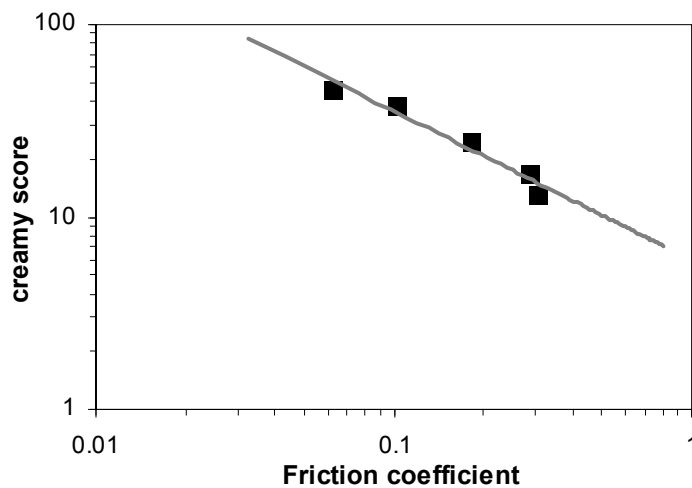


Figure 9.3 Least square fits to creamy attribute – friction data. Squares represent the measured data, while the solid line is the fitted power-law function.

9.3 Summary

In this thesis oral conditions are simulated in laboratory using various techniques and the mechanical processes involved in food processing are described quantitatively. This was achieved by modifying the commercial tribometer and the application of soft surfaces. A number of model food systems was investigated with respect to their lubrication and rheological properties. In addition the texture of semi-solid and liquid food (model) was studied using Quantitative Descriptive Analysis (QDA). Finally, the general link between the sensory attributes and physical quantities like friction and viscosity was established.

In **Chapter 2** a method for measuring friction between soft contacts was developed so that it resembles the mouth environment. It was shown that it is possible to mimic the oral conditions with a modified commercial tribometer. Moreover, the lubrication and rheological properties of different protein aggregates in an aqueous dispersion were studied. These were globular aggregates of whey protein isolate (WPI) and fibrillar aggregates of ovalbumin from egg white. Clear correlations between measured friction coefficient and specific properties of the lubricating fluid such as protein concentration, aggregate size, and aggregate shape were obtained. It was shown that higher concentration of aggregates as well as larger particle size provided better lubrication. In the boundary regime the micro-properties of the aggregate dispersions are of importance i.e., number of aggregates, their size, and sample-surface interactions. Better lubrication properties of the ovalbumin were explained by their fibrillar shape. In addition, deposition of protein material on the surfaces was discussed. The formation of thicker adhered layers of the proteins was related to the reduction of the friction coefficient in the boundary regime. Moreover, in this chapter the importance of the surface properties like elasticity, surface-surface interactions, and surface roughness is briefly discussed. Neoprene rubber is more elastic than silicone and therefore lower contact pressure for neoprene ring and neoprene disc was calculated. The rougher neoprene surface shifts the onset of the mixed regime to higher entrainment speeds compared to silicone. This effect was masked when highly concentrated and thus viscous ovalbumin dispersion was measured. It was suggested that protein aggregate particles could be trapped between large asperities, thus effectively smoothing out the roughness. Finally, the importance of the experimental conditions in the tribometer (e.g. load or slide-to-roll ratio) on measured friction was presented.

After developing a method for measuring the friction in soft contact and ability to well characterize protein aggregate dispersions, more complex system like the emulsion-filled

gels were investigated. The obtained results were presented in **Chapter 3**. These gels were studied under confined gap and applied shear and resembled broken down gels from oral processing. The increase of the oil content in the emulsions led to improvement of its lubrication properties. However, above 40 wt % oil emulsions reached the same friction coefficient as the pure oil. The lubrication properties of the gels strongly depended on the molecular properties of the gelling agent and on the breakdown behavior of the gel matrix. It was observed that the lubrication behavior for each type of emulsion-filled gel was affected by the interactions between oil droplets and matrix. For gels containing droplets bound to the matrix, the friction coefficient gradually decreased with increasing oil concentration. This was related to the increase in ‘apparent viscosity’ of the sheared gel mass. The friction coefficient of the emulsion filled gels with droplets non-bound to the matrix was lower than that of the same gel matrix without oil. No effect of the oil content on friction was observed. The decrease of the friction coefficient for gels with non-bound droplets was attributed to the individual contribution of gel matrix and released oil droplets. Both the emulsions and filled gels were studied under Confocal Laser Scanning Microscopy before and after applied shear in the tribometer. No coalescence of the oil droplets was observed. In addition no effect of saliva on the lubrication properties of emulsion-filled gels was noticed.

In **Chapter 4** various methods were applied to describe the lubrication, rheological and adhesive properties of number of polysaccharide solutions. The friction coefficient as a function of load and entrainment speed was obtained using a commercial tribometer with soft hydrophobic poly(dimethylsiloxane) (PDMS) substrates. High shear viscosity and non-linear viscoelasticity (normal stress differences) were determined up to shear rates of 10^5 s^{-1} using a narrow gap parallel plate geometry. Adhesive properties of different biopolymers were investigated using Surface Plasmon Resonance (SPR) and Quartz Crystal Microbalance-Dissipation (QCMD) methods. These techniques provided detailed insight into film formation on a surface (e.g. layer deposition and layer stability), thereby complementing friction measurements. Polymers forming thick, well hydrated and viscoelastic films showed better lubrication properties in the mixed lubrication and hydrodynamic regimes (for smooth PDMS disc). In the boundary regime samples that can sustain pressure in the contact zone and form thick films provided the best lubrication (for rough PDMS disc). This study showed that the lubrication properties of measured polysaccharides depend on a number of factors rather than on viscosity alone. Therefore,

to understand the lubrication phenomena occurring during consumption of food and to enlighten different functional characteristics of food constituents, a combined insight of diverse techniques is necessary.

Chapter 5 presents results obtained after introduction of different particles (protein spheres and gel particles) into the polysaccharide solutions. Their influence on sensory perception and on experimentally measured friction and viscosity were discussed. Moreover, correlations analysis between the sensory attributes and both the friction and the viscosity were established. Since thickness perception masked scores of other attributes, all samples were tuned to obtain the same score in sensorial thickness to minimize its influence. The most important findings in this work revealed the relation between the experimentally measured data and perception of attributes sensed by the panelist. It was found that the perception of the slippery attribute correlated well with the friction coefficient. The samples with high score for this attribute provided good lubrication properties. Other attributes showed no correlation with friction. Attributes such as stickiness, sliminess, and filmy correlated with viscosity data of the dispersions within a wide range of shear rates. In addition, a direct relation was found between the attribute powdery and the size of the particles present in the dispersions. Small beads provided a weaker powdery sensation, while larger beads resulted in higher attribute score. Harder particles were characterized by stronger size-dependence than softer particles.

The tribological properties of polysaccharide solutions (with and without microcrystalline cellulose particles) were investigated using a set of different rubbers in **Chapter 6**. Study of several rubbers with different properties can provide an indication of how measurements were influenced by material properties. It was shown that surface roughness, deformability and hydrophobicity of the discs influenced lubrication measured in the tribometer. Softer and smoother material allowed better lubrication. The differences between the surfaces tested occur predominantly in the boundary lubrication regime. This chapter showed that the properties of the surface are important only in the case of lubricants that cannot efficiently form boundary film. This lubrication layer eliminates to a great extent the influence of the surface on lubrication. Furthermore, the main effect of the particles on tribological measurements was noticed for low speed (below about 50 mm/s). Large particles could not fit in asperities entirely and enhanced the surface roughness, which resulted in extended boundary regime. Thus particles present in a solution could relatively easy be detected by tribological investigation. In the case of good lubrication,

however, the particles influence became weaker. Thus the better the lubricant the more difficult the detection of particles is.

Chapter 7 is focused on correlating sensory perception with physical quantities like friction coefficient or viscosity. Homogenized and pasteurized milk with different fat content was studied in this chapter. The correlation between perceived attributes and measured physical properties was obtained for mouth-feel attributes, although only above a threshold of about 1% fat content. Increase of the fat content in the milk up to 1 % was not perceived by panellist members nor experimentally measured friction. Above 1 % clear correlation was observed for attributes and friction measured at silicone disc for increasing fat content. This observation is slightly different for neoprene rubber where at a threshold of 2 % of fat the systematic change in the friction curves was noticed. This was attributed to the difference in surface roughness between two rubbers. For smoother silicone rubber, a thin fat film was created more effectively than in the case of rougher neoprene disc. The observation that the fat content in milk emulsions leads to a decrease of the Stribeck curve in the boundary regime (above a certain fat concentration threshold) was associated with shear-induced coalescence that took place on rubber surfaces. Most probably shear-induced coalescence of the fat droplets, that occurred in the tribometer and influenced experimentally measured friction coefficient is also responsible for sensory responses of milk samples.

In **Chapter 8** a few small and sometimes preliminary experiments are discussed supporting conclusions from previous chapters. The most interesting conclusion is that results from a low slide-to-roll-ratio correlate best with sensory and that mucin in artificial saliva contributes strongly to lubrication. The presence of small non-dissolved particles in the polysaccharide dispersions may influence friction. If asperities are large, particles may smooth out the irregularities and lower friction. The influence of particles also depends of the ability to form a film. A film thicker than particle size is expected to lubricate well regardless of the presence of particles. The film thickness was estimated using elastohydrodynamic theory and compared to the size of various particles. This showed at what speed the film thickness overcomes particle size and the full film lubrication can start. In addition several different commercial products were investigated and compared with respect to their tribological and rheological characteristics. Finally, conditions that allow the best correlation between physical quantities and sensory attributes are briefly

discussed. The best correlations are obtained for a set of parameters like speed, surface roughness and elasticity that is the closest to the oral conditions.

References

- 1 Van Aken, G.A., Vingerhoeds, M.H. & De Wijk, R.A. (In preparation for Food Hydrocolloids), Sensory perception of liquid emulsions: effect of oil viscosity and polysaccharides.

Samenvatting

Dit proefschrift beschrijft een aantal studies naar de simulatie van mondcondities in het laboratorium. De mechanische processen die deel uitmaken van de verwerking van voedsel in gesimuleerde mondcondities worden in het proefschrift kwantitatief beschreven. Het onderzoek werd mogelijk gemaakt door de toepassing van zachte materialen in een commerciële tribometer. De tribologische en rheologische eigenschappen van een aantal levensmiddelen en modelsystemen werden gemeten. Verder werd de textuur van dikvloeibare en vloeibare modelsystemen bestudeerd door middel van Quantitative Descriptive Analysis (QDA). Tot slot werd het verband tussen sensorische attributen en fysische parameters, als tribologische eigenschappen en viscositeit, vastgelegd.

In **hoofdstuk 2** wordt de ontwikkeling van een methode beschreven voor de meting van wrijving tussen oppervlakken van zachte materialen met behulp van een commerciële tribometer. De geoptimaliseerde experimentele condities worden beschouwd als een goede nabootsing van de wrijvingsfenomenen die tijdens voedselverwerking in de mond plaatsvinden. Door middel van de gepresenteerde methode werden de tribologische eigenschappen gemeten van waterige dispersies van bolvormige aggregaten van weiwitten en van fibrillen van ovalbumine. Van deze dispersies werden ook de rheologische eigenschappen gekarakteriseerd. Duidelijke correlaties werden vastgesteld tussen wrijvingscoëfficiënt en specifieke eigenschappen van de bestudeerde smeermiddelen, zoals eiwitconcentratie, en grootte en vorm van de aggregaten. Een toename van het eiwitgehalte en van de grootte van de aggregaten resulteerde in betere smeereigenschappen. In het grenssmering regime speelden het aantal en de grootte van de aggregaten en de monster-oppervlak interacties een grote rol in de smeereigenschappen van de dispersies. De relatief betere smeereigenschappen van de dispersies van ovalbumine werden verklaard door de fibrilstructuur van de aggregaten. Verder werd ook de depositie van eiwit op de oppervlakken bestudeerd. In het grenssmering regime resulteerde de vorming van dikke lagen eiwit in een lagere wrijvingscoëfficiënt. In dit hoofdstuk wordt ook het effect van oppervlakeigenschappen zoals veerkracht, oppervlak-oppervlak interacties en oppervlakruwheid op de gemeten waarden bediscussieerd. Neopreen rubber is stijver dan silicon rubber. Vervolgens, voor neopreen ring en neopreen schijf werd een lagere contactdruk berekend. Door de hogere ruwheid van neopreen verschoof het begin van het gemengde smeeregime naar hogere vloeistofmeesleuring snelheden in vergelijking met silicon rubber. Ovalbumine dispersies met een hoge

eiwitconcentratie en een hoge viscositeit maskeerden dit effect. Dit werd verklaard door de absorptie van eiwitaggregaten tussen de onregelmatigheden van het oppervlak, dat hierdoor vereffend zou worden. Tot slot wordt in dit hoofdstuk het effect gepresenteerd van de experimentele condities in de tribometer (bijvoorbeeld lading en verhouding tussen slippen en rollen) op de gemeten wrijvingscoëfficiënt.

Na een methode voor de meting van wrijving tussen oppervlakken van zachte materialen te hebben ontwikkeld en ervaring met de karakterisering van dispersies van eiwitaggregaten te hebben opgedaan, werden de smeereigenschappen van meer complexe systemen bestudeerd, zoals emulsiege vulde gelen. De resultaten van dit onderzoek worden in **hoofdstuk 3** gepresenteerd. In deze studie werden de gelen vermalen zodat ze op gelen verwerkt in de mond leken. Met betrekking tot de emulsies gebruikt voor de bereiding van de gevulde gelen gaf een toename van het oliegehalte een afname van de wrijvingscoëfficiënt. Emulsies met 40 gew.% olie hadden dezelfde wrijvingscoëfficiënt als de zuivere olie. De smeereigenschappen van de gelen hingen sterk af van de moleculaire eigenschappen en het breukgedrag van de matrix en van de druppel-matrix interacties. Voor gelen met gebonden druppels nam de wrijvingscoëfficiënt geleidelijk af bij een toename van het oliegehalte. Voor gelen met ongebonden druppels was de wrijvingscoëfficiënt lager dan die van de matrix zonder oliedruppels. Toch werd er voor deze gelen geen effect van het oliegehalte op wrijving waargenomen. De verschillende effecten van het oliegehalte op het smeergedrag van de verschillende gelen werden verklaard door de relatie tussen druppel-matrix interacties en ‘schijnbare viscositeit’ van de gebroken gelen. Voor gelen met gebonden druppels resulteerde een toename van het oliegehalte in een toename van de ‘schijnbare viscositeit’ van de gebroken gelen. Voor gelen met ongebonden druppels werd de afname van de wrijvingscoëfficiënt toegeschreven aan de individuele bijdrage van de matrix en van losse oliedruppels. Er werd geen effect van speekspel op de smeereigenschappen van emulsies en gelen waargenomen. Voor gelen met ongebonden druppels had het oliegehalte geen effect op viscositeit. Confocale Scanning Laser Microscopie (CSLM) opnamen van zowel de emulsies als de gevulde gelen lieten geen coalescentie zien van de oliedruppels als gevolg van de wrijvingmetingen.

In **hoofdstuk 4** worden een aantal methoden bediscussieerd voor de karakterisering van smeer-, rheologische en kleefeigenschappen van verschillende polymeeroplossingen. De wrijvingscoëfficiënt als functie van lading en vloeistofmeesleuring snelheid werd gemeten

door middel van een commerciële tribometer met zachte hydrofobische polydimethylsiloxaan (PDMS) substraten. Viscositeit bij hoge afschuiving en non-lineaire viscoelasticiteit werden gemeten tot een afschuivingsnelheid van 10^5 s^{-1} met een nauwe spleet parallelle platen geometrie. De kleefeigenschappen van verschillende biopolymeren werden onderzocht door middel van de Surface Plasmon Resonance en Quartz Crystal Microbalance-Dissipation methoden. Deze technieken leverden gedetailleerde informatie op over filmvorming aan een oppervlak (zoals laagdikte en laagstabiliteit). Deze informatie was complementair aan de wrijvingsmetingen. Polymeren die dikke, goed gehydrateerde viscoelastische films vormden vertonden betere smeereigenschappen in de gemengde en hydrodynamische regimes (voor gladde PDMS schijfjes). In het grenssmering regime leverden monsters die in het contactgebied drukbestendig waren en die dikke lagen vormden de beste smering (voor ruwe PDMS schijfjes). Deze studie heeft aangetoond dat de smeereigenschappen van de bestudeerde polymeren van verschillende factoren afhankelijk zijn, en niet alleen van de viscositeit. Vervolgens, om de smering geleverd door voedselproducten en de verschillende functionele eigenschappen van voedselbestanddelen te kunnen begrijpen, moet een combinatie van verschillende technieken worden gebruikt.

Voor het onderzoek beschreven in **hoofdstuk 5** werden verschillende deeltjes (eiwitbolletjes en fragmenten van eiwitgelen) toegevoegd aan oplossingen van polysacchariden. Het effect van deze deeltjes op de sensorische eigenschappen van de oplossingen en op hun smeereigenschappen en viscositeit worden in dit hoofdstuk bediscussieerd. Om de invloed van dikte op andere sensorische attributen uit te kunnen sluiten werd de samenstelling van de monsters aangepast zodat de sensorische diktewaarneming in alle gevallen gelijk was. Voor een aantal sensorische attributen werd een correlatie vastgesteld met fysische gegevens. Het attribuut glibberig was omgekeerd evenredig gecorreleerd aan de wrijvingscoëfficiënt. Andere attributen waren niet gecorreleerd aan de wrijvingscoëfficiënt. De attributen plakkerig, slijmerig en filmvormend waren gecorreleerd aan viscositeit data gemeten binnen een breed bereik van afschuifsnelheid. Verder werd een direct verband gevonden tussen het attribuut poederig en de grootte van de deeltjes toegevoegd aan de oplossingen van polysacchariden. De scores van dit attribuut waren lager voor monsters met kleine eiwitbolletjes. De relatie tussen dit attribuut en de grootte van de deeltjes was meer relevant voor harder deeltjes.

Om de relatie tussen gemeten waarden en materialen gebruikt in de tribometer te achterhalen werden de tribologische eigenschappen van oplossingen van polysacchariden (met en zonder deeltjes van microkristallijne cellulose) gekarakteriseerd met verschillende soorten rubbers (**hoofdstuk 6**). Er werd aangetoond dat de oppervlakte ruwheid, de vervormbaarheid en de hydrofobiciteit van de rubberschijfjes de wrijvingscoëfficiënt beïnvloeden. Met zachte en gladde schijfjes werden lagere wrijvingscoëfficiënten gemeten. De grootste verschillen werden in het grenssmering regime waargenomen. Het werk gepresenteerd in dit hoofdstuk heeft aangetoond dat de eigenschappen van het oppervlak alleen relevant zijn indien het smeermiddel geen effectieve grenssmering film kan vormen. Deze smeringslaag heft de invloed van het oppervlak op smering grotendeels op. Het grootste effect van deeltjes op smering werd bij lage snelheid (lager dan 50 mm/s) waargenomen. Grote deeltjes pasten niet tussen de onregelmatigheden van het oppervlak en verhoogden vervolgens de ruwheid daarvan. Dit resulteerde in een uitbreiding van het grenssmering regime. Deeltjes aanwezig in een oplossing konden dus door middel van tribologische metingen relatief goed opgespoord worden. Dit was echter moeilijker in het geval van goede smeringeigenschappen van het smeermiddel.

In **hoofdstuk 7** worden correlaties bediscussieerd tussen sensorische attributen en wrijvingscoëfficiënt van gehomogeniseerde en gepasteuriseerde melk met verschillende vetgehaltes. Goede correlaties konden alleen vastgesteld worden voor melkmonsters met een vetgehalte hoger dan 1 gew.%. Toenames van vetgehalte in het bereik 0-1 gew.% werden door de panelleden niet waargenomen en konden ook niet worden gemeten in de tribometer. Metingen met siliconen en neopreen leverden verschillende resultaten. Voor melkmonsters met vetgehaltes hoger dan 1 gew.% werd een duidelijke correlatie vastgesteld tussen wrijvingscoëfficiënt gemeten met een siliconen schijf en sensorische attributen. Met neopreen werden voor monsters met een vetgehalte van 2 gew.% en hoger wijzigingen in de wrijvingscurve waargenomen. Het verschil in het gedrag van siliconen en neopreen rubber werd toegekend aan verschillen in oppervlakruwheid tussen de twee rubbers. Het oppervlak van siliconen is gladder, en dit maakt de vorming van een effectieve vetfilm makkelijker. Het feit dat een toename van het vetgehalte (boven een bepaalde vetconcentratie) in lagere wrijvingscoëfficiënten in het grenssmering regime resulteerde, werd verklaard door coalescentie op het rubberoppervlak veroorzaakt door afschuiving. Coalescentie van vetbolletjes in de melk is waarschijnlijk ook verantwoordelijk voor de sensorische eigenschappen van de geteste monsters.

In **hoofdstuk 8** worden enkel kleine en oriënterende experimenten besproken welke voortbouwen op de conclusies van eerdere hoofdstukken. De meest interessante conclusie is dat de resultaten met een kleine slide-roll-ratio het best aansluiten bij de sensorisch waarnemingen en dat mucin sterk bijdraagt aan de smering. De invloed van deeltjes hangt sterk af van het filmvormend vermogen. Een film die dikker is dan de deeltjes grootte zal sterk bijdragen aan het smerend vermogen. Met behulp van elastohydrodynamische smeringstheorie werd de film dikte geschat en dat werd vergeleken met de deeltjes grootte. Ten slotte werd een aantal commerciële zuivel producten gekarakteriseerd ten aanzien van hun smerend vermogen en hun vet gehalte. Ook nu blijkt dat de beste correlaties worden verkregen als de condities in de mond het dichtst benaderd worden.

Acknowledgements

Thanks to all people of TI Food and Nutrition (TIFN), Nizo food research and Utrecht University for their contribution to this thesis.

First of all I would like to thank my supervisor Kees de Kruif for his great support during the past 4 years. Kees you shared with me an enormous scientific knowledge and stimulated many fascinating discussions. I learned a lot from you. Moreover, you supported me not only in my scientific endeavors, but also in a hectic and busy period of my personal life. Thank you very much for that.

I am also extremely grateful to my co-supervisor Harmen de Jongh for his scientific input to this thesis, interesting discussions, support, and of course great entertainment. Thank you also for making a good team out of B015.

I would like to thank Ronald Visschers for his patience and for introducing me to the fascinating world of food science. Your optimism in any situation was very supporting.

I would like to thank all the B015 members for the great time we shared together. Many thanks to Anne for her kindness, objectiveness, help in the lab, and with several experimental techniques. It was a pleasure to work with you. In addition I enjoyed our coffee breaks very much. Anke and Ladka were the greatest roommates I could ever ask. Anke, thanks for your enthusiasm, our frequent discussions, and your scientific contribution to this thesis. You have a great ability to make me laugh on any occasion. Ladka, thanks for your friendship and support during these years. I enjoyed very much our numerous talks. I would like to express my sincere gratitude to Guido, the most easygoing person I have ever met in my life. Thank you for being so optimistic every day, for bringing laughter to our office and most of all for being such a good friend over these years. Without you Chapter 3 would not be part of this thesis. Thank you for being so understanding and patient when working with me. Your input to this thesis can also be seen in the Dutch summary. In addition I would like to thank you for taking great care of Balbinka every time we went to Poland. Saskia, I had such a great time with you. We laughed a lot, especially during our trip to Italy. You are a great companion and a very sensitive person. Thank you for your help in many situations. I would also like to thank Fred for interesting, scientific discussions and help. I spent a very nice time with you and your family during several dinners. Kiki, how could I forget you? Although you were a part of the team only for one year, you surely left a part of yourself in all B015 hearts!

You were a great support for me over many months. Thank you for all the hours we spent in lab, working hard but also having great fun! It was a real pleasure to work with you!

Sophie, you were my student only for half a year and yet you carried out a lot of work, which resulted in the data discussed in Chapter 5 and Chapter 6 of this thesis. Thank you for your effort, optimism, interest in the subject and the delicious wafels!

Roelie I would like to thank you for your sympathy over these years, your optimism and great talks.

I thank Fred Beekmans for his effort over the years to connect the TIFN to the Nizo people, and his ability to help in any situation. Thank you for making NIZO a comfortable and simulating work place. I also want to thank Jan Klok for his help, especially with the CLSM images. I would like to express my gratitude to Hans Tromp. Hans, we were “lab colleagues” for almost half a year and, I had a really good time chatting with you. Thanks also for your help with a number of experiments. The first person, who welcomed me at the Nizo door was Els de Hoog. Els, I will never forget that! Thank you for many scientific discussions, especially on tribology. I would like to thank Franklin Zoet, who together with Guido were of great help during moving tribometer when I was unable to do it myself. I am grateful to Remco Fokkink for his guidance in the contact angle measurements.

I would also like to thank: George van Aken for interesting scientific discussions, Markus Stieger for helping me with the first steps with the MTM and introducing me to the rheology field, Jan de Wit and Thom Huppertz for their help with the milks enriched with emulsion, Ellie for the effort in preparing the shiny “beads” for me, Gerben-Jan for great technical support and all the people I met at Nizo for their contributing in making it such a nice place to work. It was pleasure to talk and work with you.

I would like to thank all TIFN people I met over these 4 years, on P2 meetings, seminars or discussions. I really appreciate the time spent with all of you and the great chats we had! I would like to express my gratitude to the people who work at headquarters of TIFN for the nice working atmosphere and for welcoming us with a smile. Thank you for your help with the ‘paper work’ during this research, especially at the end of my study.

I am also grateful to Carol Mosca, Diane Dresselhuis, Cathrine Heinzerling, Janine Knoop, Eva Castro-Prada, Cristina Primo, Neleke van Nieuwenhuijzen and Mary Smiddy. I would especially like to thank Carol for her open, Brazilian spirit, nice talks and extreme kindness.

Many thanks to Renate Ganzevles for her interest in my work and her great companionship, particularly at the conference in Aschaffenburg, I had such a fun with you!

I would like to thank Hans Meeldijk. Hans, without you the cover of this thesis would not be complete. Thank you for your effort and assistance during the Electron Microscopy images.

I am grateful to Unilever Corporate Research for the support and hospitality. Many thanks to all researchers I met there. In particular I would like to thank Jason Stokes for his guidance, great ideas, and scientific discussions. Many thanks go to Lubica Macakova for her efforts in the measurements and analysis of our data. Thank you very much for your concern and friendship. Jason and Luba thank you for your substantial contribution to Chapter 4, it was pleasure to work with both of you. I have learned a lot from you. In addition I would like to thank Georgina Davies who was my "lab coach" at Unilever.

Furthermore, I am extremely grateful to Celine Cluzel from PCS instrument for constant help via mail or telephone with the tribometer during the past years.

Moreover, I would like to express my gratitude to Matthias Eisner from Campina Innovation, who helped me with the emulsion enriched milk project, and Campina Innovation for providing milk with different fat contents for Chapter 7.

Thanks to all the colleagues of Utrecht University I met at the winter school in 2006 - that winter school with all of you was so great.

I would like to thank all the people I didn't mention, but I met during my stay in Holland.

I would also like to thank many colleagues of the Vrije Universiteit of Amsterdam. Without them I surely would have never been able to achieve this goal. In particular I would like to thank Rienk van Grondelle for his faith in me. Natalia, I will never forget the time we spent together laughing and talking for hours.

In addition I am very grateful to prof. Andrzej Dobek from the University of Adam Mickiewicz for support during my study in The Netherlands.

I would like to thank my dear friend Agnieszka Wencel for her interest in my research, and many interesting conversation.

Tomek Kopyciuk, my friend who has always supported me and believed in me even when I lost faith in myself, thank you for all our talks, for all your help over the past years and for the great time we shared during the short visit to Poland.

Most of all I would like to express my gratitude to my family. Moja najkochańska rodzinko na świecie: Mamo, Tato, Braciszku. Dziękuję Wam za wspieranie mnie przez te wszystkie lata, za dodawanie mi sił, za Waszą pomoc. Mamusiu i Tatusiu, dziękuję Wam za wiarę we mnie, nawet wtedy, kiedy sama w siebie nie wierzyłam. To dzięki Wam szłam do przodu, choć czasem było pod górkę. Zawsze mogłam na Was liczyć, dziękuję za słowa otuchy i za mobilizowanie mnie do pracy. Przede wszystkim dziękuję za Waszą bezgraniczną miłość, jesteście najlepszymi rodzicami jakich mogłam sobie wymarzyć na całym świecie. Tomciu, zawsze byłeś obok mnie, jesteś nie tylko moim ukochanym Braciszkiem ale i najlepszym przyjacielem, wiem że mogę na Ciebie liczyć w każdej sytuacji. Dziękuję Tobie za Twój optymizm, którym mnie 'częstujesz' podczas konwersacji, za twoją szczerość, za to, że potrafisz mnie rozweselić w każdej chwili i za to, że jesteś. Dziękuję Tobie za pomoc przy projektowaniu okładki do tej pracy.

Chciałabym również wspomnieć o moich niesamowitych drugich rodzicach (Mama Hanka i Tata Marek). Dziękuję Wam za przyjęcie mnie do rodziny z otwartymi ramionami, oraz za nieocenioną pomoc przez te wszystkie lata, a także za przepyszne smakołyki przesyłane do Holandii.

Mój kochany mężu, Dominiku, z całego serca chciałabym Tobie podziękować za te wszystkie lata spędzone razem. Za Twoją miłość i Twój niesamowity charakter. Dodawałeś mi sił, wspierałeś mnie i pocieszałeś w trudnych momentach. Twoja pomoc na końcu mojego doktoratu była niezastąpiona. Od niedawna nie opiekujesz się tylko mną, ale i naszą kochaną córeczką Zuzinką. Dziękuję Ci za to, że jesteś tak wspaniałym mężem i tatą. Dziękuję również za przygotowanie okładki tej pracy.

Kochana moja córeczko, choć jesteś taka malutka, dajesz mi tyle radości. Twój pierwszy uśmiech, pierwsze słowo i uścisk Twojej rączki, dodały mi wiele energii i siły dokładnie wtedy, kiedy potrzebowałam tego najbardziej. Jeszcze przed Tobą wiele ciekawych i nowych rzeczy, które będziemy wspólnie odkrywać.

Agnieszka

List of publications

R. Croce, T. Morosinotto, J.A. Ihalainen, A. Chojnicka, J. Breton, J.P. Dekker, R. van Grondelle and R. Bassi, (2004). Origin of the 701 nm fluorescence emission of the Lhca2 subunit of higher plant photosystem I. *Journal of Biological Chemistry*, 279, 48543-48549.

E.G. Andrizhiyevskaya, A. Chojnicka, J.A. Bautista, B.A. Diner, R. van Grondelle and J.P. Dekker, (2005). Origin of the F685 and F695 fluorescence in photosystem II. *Photosynthesis Research*, 84, 173-180.

R. Croce, A. Chojnicka, T. Morosinotto, J.A. Ihalainen, F. van Mourik, J.P. Dekker, R. Bassi and R. van Grondelle, (2007). The low-energy forms of Photosystem I light-harvesting complexes: spectroscopic properties and pigment-pigment interaction characteristics. *Biophysical Journal*, 93, 2418-2428.

A. Chojnicka, S. de Jong, C.G. de Kruif, and R.W. Visschers (2008). Lubrication properties of protein aggregate dispersions in a soft contact. *Journal of Agricultural and Food Chemistry*, 56, 1274-1282.

A. Chojnicka & G. Sala, C.G. de Kruif and Fred van de Velde (2009). The interactions between oil droplets and gel matrix affect the lubrication properties of sheared emulsion-filled gels. *Food Hydrocolloids*, 23, 1038-1046.

A. Chojnicka-Paszun, L. Macakova, J.R. Stokes, C.G. de Kruif and H.H.J. de Jongh, Lubrication, rheology and adsorption of polysaccharide solutions. Submitted.

A. Chojnicka-Paszun, S. Doussinault, H.J. Klok, C.G. de Kruif and H.H.J. de Jongh. Friction properties of oral surface analogs and their interaction with polysaccharide/MCC particle dispersions. Submitted.

A. Chojnicka-Paszun, H.H.J. de Jongh and C.G. de Kruif, Sensory perception and friction coefficient of milk with increasing fat content. Submitted.

A. Chojnicka-Paszun, A.M. Janssen, A.M. van de Pijpekamp, S. Doussinault, G. Sala, H.H.J. de Jongh and C.G. de Kruif, Sensorial analysis of polysaccharide-protein gel particle dispersions in relation to lubrication and viscosity properties. To be submitted.

Curriculum vitae

Agnieszka Chojnicka-Paszun was born on 24th of January 1979 in Poznań, Poland. In 1999 she started her Biophysics study at the Adam Mickiewicz University in Poznań at the faculty of Physics and Astronomy. After she acquired a bachelor degree she started a master study at Vrije Universiteit in Amsterdam as an exchange student of the Socrates – Erasmus program. In 2003 she was granted scholarship from the Vrije Universiteit to continue with her study. Agnieszka obtained Master degree in Physics, specialization Biophysics on the 23rd of August 2004, with a thesis entitled “Steady-state spectroscopic study of reconstituted Lhca Polypeptides”.

In February 2005 she started to work as a Ph.D. fellow at the TI Food and Nutrition (formerly known as Wageningen Center for Food Science) and was affiliated to the Universiteit Utrecht, Department of Physical and Colloid Chemistry, Debye Institute. Her Ph.D. was part of a project “Dynamics of biopolymer networks and textures” financed by TI Food and Nutrition. This thesis presents the result of research aiming to relate oral sensing of food to physical quantities like friction and viscosity.

Overview of completed training activities

Discipline specific activities

Courses and conferences

- 11th European Conference on the Spectroscopy of Biological Molecules (ECSBM), 2005, Aschaffenburg, Germany
- 6th Liquid Matter Conference (of the European Physical Society), 2005, Utrecht University, The Netherlands
- Gordon Research Conference on Tribology, 2006, Colby College, Waterville, Maine, USA
- Soft Condensed Matter and Advanced Colloid Science, 2005, Utrecht University, The Netherlands
- Debye Winter School 2006, High Tech Systems and Materials, Arnhem, The Netherlands
- 'Making Sense of Food Programme' WCFS food summit, 2005, Wageningen, The Netherlands
- Seminar on food microstructure, 2005, Wageningen University, Wageningen, The Netherlands

Visits

- Guest researcher, 2007, Unilever Corporate Research, Colworth Science Park, Sharnbrook, United Kingdom
- University of Twente, Surface Technology and Tribology group, Department of Engineering Technology, 2006, Twente, The Netherlands

Meetings

- Work meetings project 'Dynamics of biopolymer networks and textures', TI Food and Nutrition (TIFN), 2005-2008, Ede, The Netherlands
- Program meetings 'Structure and Functionality', TIFN, 2005-2008, Wageningen, The Netherlands
- Tribology meeting 2005- 2006, Ede/Wageningen, The Netherlands
- 'Oral physiology group' TIFN, 2005, Wageningen, The Netherlands

General courses

- NWO- Talent Classes : *Write it Right*, 2005, The Hague, The Netherlands
- Writing in English for Publication, 2006, James Boswell Institute, Utrecht University, The Netherlands

